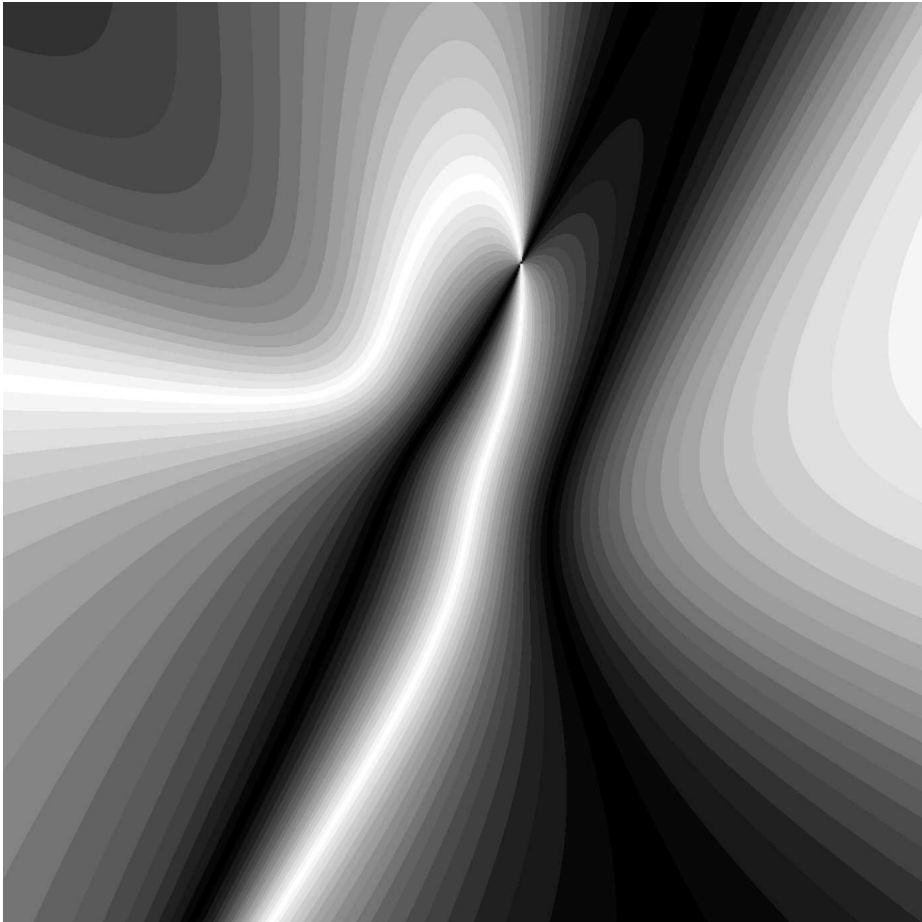
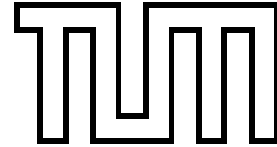


The Running of Neutrino Masses, Lepton Mixings and CP Phases



Stefan Antusch

Technische Universität München
Physik Department
Institut für Theoretische Physik T30d
Univ.-Prof. Dr. Manfred Lindner



The Running of Neutrino Masses, Lepton Mixings and CP Phases

Dipl.-Phys. Univ. Stefan Antusch

Vollständiger Abdruck der von der Fakultät für Physik der Technischen Universität München zur Erlangung des akademischen Grades eines

Doktors der Naturwissenschaften (Dr. rer. nat.)

genehmigten Dissertation.

Vorsitzender: Univ.-Prof. Dr. Eckehart Nolte

Prüfer der Dissertation:

1. Univ.-Prof. Dr. Manfred Lindner
2. Univ.-Prof. Dr. Andrzej J. Buras

Die Dissertation wurde am 15.7.2003 bei der Technischen Universität München eingereicht und durch die Fakultät für Physik am 1.9.2003 angenommen.

Abstract

In this thesis, the running of neutrino masses, lepton mixing angles and CP phases is investigated, using the description of neutrino masses by the lowest dimensional effective operator and its realization within see-saw scenarios. In the effective approach, the β -functions which govern the running of the parameters below the lowest see-saw scale in the Standard Model, in Two-Higgs-Doublet Models and in the Minimal Supersymmetric Standard Model are calculated. Analytical formulae, which allow to understand the running qualitatively and to a good approximation also quantitatively, are derived and compared to numerical results. In minimal see-saw scenarios, where only heavy singlets are added to the particle spectrum, the β -functions and matching conditions for the various effective theories, which arise from successively integrating out the heavy particles, are calculated in the above-named models. Characteristic properties of the running in these scenarios are discussed analytically and illustrated by numerical examples.

Zusammenfassung

In dieser Arbeit wird das Laufen von Neutrinomassen, leptonischen Mischungswinkeln und CP-Phasen untersucht. Dabei wird die Beschreibung von Neutrinomassen durch den niedrigst-dimensionalen effektiven Operator und dessen Realisierung in Seesaw-Modellen verwendet. In der effektiven Herangehensweise werden die β -Funktionen berechnet, die das Laufen der Parameter im Standardmodell, in Zwei-Higgs-Modellen und im minimalen supersymmetrischen Standardmodell bestimmen. Analytische Formeln, die ein qualitatives und in guter Näherung auch quantitatives Verständnis des Laufens erlauben, werden hergeleitet und mit den numerischen Resultaten verglichen. In minimalen Seesaw-Szenarien, in denen ausschließlich schwere Singlets zum Teilchenspektrum hinzugefügt werden, werden die β -Funktionen und Matching-Bedingungen für die verschiedenen effektiven Theorien berechnet, die durch das schrittweise Ausintegrieren der schweren Teilchen in den oben genannten Modellen entstehen. Charakteristische Eigenschaften des Laufens in diesen Szenarien werden analytisch diskutiert und durch numerische Beispiele verdeutlicht.

Contents

Abstract	5
Introduction	v
1 Origin and Description of Neutrino Masses	1
1.1 Fermion Masses in the Standard Model	1
1.1.1 Electroweak Symmetry Breaking	1
1.1.2 Fermion Masses	2
1.1.3 Experimental Results for Fermion Masses and Mixings	3
1.2 Extensions of the Standard Model Particle Content	5
1.2.1 Additional Higgs Triplet	5
1.2.2 Additional Fermion Singlets	6
1.2.3 The See-Saw Mechanism	8
1.3 Neutrino Masses in an Effective Theory Approach	9
1.3.1 The Lowest Dimensional Effective Neutrino Mass Operator	9
1.3.2 Tree-Level Realizations of the Neutrino Mass Operator	10
1.3.3 Loop Realizations of the Neutrino Mass Operator	10
1.3.4 Higher Dimensional Operators for Neutrino Masses	11
1.4 Neutrino Masses in Left-Right Symmetric Extensions of the SM	13
1.4.1 Minimal Left-Right Symmetric Models	13
1.4.2 The Pati-Salam Model	15
1.4.3 SO(10)-Unification	16
1.5 Dynamical Electroweak Symmetry Breaking by a Neutrino Condensate	19
1.5.1 Mass Eigenbasis for the Dynamical See-Saw Mechanism	20
1.5.2 The Coupled Dirac-Majorana Gap Equations	20
1.5.3 Implications for Neutrino Masses	22
2 The β-Functions for the Effective Neutrino Mass Matrix	23
2.1 Preliminaries on Renormalization	24
2.1.1 Renormalization Group Equations	25
2.1.2 Calculating RGEs from Tensor-Valued Counterterms	27
2.2 The Neutrino Mass Operator in Non-Supersymmetric Theories	30

2.2.1	Calculation of the RGE in the SM	30
2.2.2	Calculation of the RGEs in 2HDMs	36
2.3	The Neutrino Mass Operator in the MSSM	40
2.3.1	Preliminaries on $N=1$ Supersymmetric Theories	40
2.3.2	Component-Field Calculation of the RGE	42
2.3.3	Calculation of the 2-Loop RGE using Supergraphs	49
2.4	The Effective Theories of Minimal See-Saw Scenarios	54
2.4.1	Tree-Level Matching in Type I See-Saw Scenarios	54
2.4.2	Tree-Level Matching in Type II See-Saw Scenarios	56
2.4.3	The Effective Theories	57
2.4.4	Component-Field Calculation of the RGEs	58
2.4.5	Calculation of the RGEs at 2-Loop using Supergraphs	63
3	Analysis of Running Neutrino Masses, Mixings and CP Phases	67
3.1	Analytical Results in the Neutrino Mass Operator Approach	68
3.1.1	Derivation of Analytical Formulae for the Running Parameters	68
3.1.2	The Running of the Lepton Mixing Angles	71
3.1.3	The Running of the Neutrino Masses	73
3.1.4	The Running of the Dirac CP Phase	78
3.1.5	The Running of the Majorana Phases	79
3.1.6	Estimating the Generic Size of the RG Effects	80
3.2	RG Corrections Compared to Sensitivities of Future Experiments . .	82
3.2.1	Radiative Corrections for the Mixing Angle θ_{13}	82
3.2.2	Radiative Corrections for the Mixing Angle θ_{23}	83
3.3	The Running in Type I See-Saw Models	86
3.3.1	Solving the RGEs for Non-Degenerate See-Saw Scales	86
3.3.2	The Running of the Effective Neutrino Mass Matrix	87
3.3.3	Analytical Results for the Running of the Mixing Angles . . .	88
3.3.4	The Running Between the Thresholds	90
3.4	Radiative Generation of the LMA Solution in Type I See-Saw Models	92
3.4.1	The LMA solution from Bimaximal Lepton Mixing	92
3.4.2	The LMA Solution from Vanishing Solar Neutrino Mixing . .	98
	Conclusions	101
	A Appendix	103
A.1	The Mixing Parameters of Quarks and Leptons	105
A.1.1	Definition of the Mixing Parameters	105
A.1.2	Extraction of Mixing Angles and CP Phases	108
A.2	Useful Formulae and Notations	110
A.2.1	Weyl, Dirac and Majorana Spinors	110
A.2.2	Clifford Algebra in d Dimensions	111

A.2.3	Passarino Veltman Functions	111
A.3	Summary of Feynman Rules	115
A.3.1	Feynman Rules in the Extended SM	115
A.3.2	Feynman Rules in Extended 2HDMs	123
A.3.3	Feynman Rules in the MSSM Extended by Heavy Singlets . .	125
A.4	Results for Relevant Vertex Corrections and Self-Energy Diagrams . .	130
A.4.1	Summary of Results in the SM	130
A.4.2	Summary of Results in the 2HDMs	132
A.4.3	Summary of Results in the MSSM	134
A.5	Summary of the RGEs for the Minimal See-Saw Scenarios	136
A.5.1	The RGEs in the Extended SM	136
A.5.2	The RGEs in Extended 2HDMs	137
A.5.3	The RGEs in the MSSM Extended by Heavy Singlets	139
Acknowledgments		143
Bibliography		145

Introduction

The energy scale dependence of physical quantities, their so-called running, is a well-known effect in quantum field theory. Experimentally, it has been confirmed for the gauge coupling of the strong interaction [1]. Theoretically, it has manifold consequences. For instance, the potential meeting of the three gauge couplings in extensions of the Standard Model (SM) after their extrapolation to high energies opens up the possibility of a Grand Unified Theory (GUT) [2] of the known gauge interactions at energy scales some orders of magnitude below the Planck scale. Another example is the running of the parameters of the Higgs sector in the SM, which has led to upper and lower bounds for the Higgs mass from vacuum stability [3] and triviality [4]. It furthermore points towards the SM being an effective theory which has to be embedded into a more fundamental framework at high energies.

In recent years, experiments have discovered flavour conversions of neutrinos. Together with their explanation by neutrino oscillations, they have led to fascinating results for neutrino masses and lepton mixings. Unlike quarks, leptons have two large mixing angles and experiments with solar and atmospheric neutrinos found two small differences for their squared masses. From beta decay experiments and astrophysical observations, we have furthermore gained upper bounds for the neutrino mass scale. Neutrino masses are many orders of magnitude smaller than the masses of quarks and charged leptons. At present, our picture regarding neutrino masses is not complete yet. We do not know the neutrino mass scale, the values of possible physical CP violating phases and whether neutrinos are Dirac or Majorana particles. However, future experiments are expected to provide precision measurements of the neutrino mixings and mass squared differences and they may complete our knowledge of the parameters of the lepton sector.

From the theoretical point of view, these observations require an extension of the SM. Though there are many possibilities, it is attractive and rather model independent to introduce neutrino masses by an effective operator. Their smallness is then linked to the largeness of the energy scale where the operator is realized. Plausible scenarios beyond the effective approach use the so-called see-saw mechanism where the exchange of heavy particles leads to suppressed neutrino masses. Below the mass scales of these particles, which are typically some orders of magnitude below the gauge unification scale, the description by the effective operator can be applied. These scenarios nicely fit into left-right symmetric extensions of the SM, such as minimal left-right symmetric models [5–7], Pati-Salam models [8] or SO(10)-GUTs [9,10].

The goal of this thesis is to investigate the running of neutrino masses, lepton mixing angles and physical CP phases. It has to be taken into account, whenever these parameters at two different energy scales are compared. In particular, it is required for models aiming towards an explanation of the observed structure of fermion masses and mixings from physics at the GUT scale. In order to use the

experimental results in the lepton sector for probing such models, their predictions have to be evolved to low energy. Furthermore, it is possible that the running alters neutrino masses, lepton mixings and CP phases so much that interesting new possibilities for model-building arise. Another example where these parameters are required at very high energies is the mechanism of generating the observed baryon asymmetry of our universe via leptogenesis [11]. In this scenario, it is generated by the out-of-equilibrium decay of the same heavy singlet neutrinos which also lead to light neutrino masses via the see-saw mechanism. Typically, the masses of these singlets are assumed to be some orders of magnitude below the GUT scale. After extrapolating the neutrino mass matrix to this energy scale, it can be constrained from the requirement of a successful leptogenesis.

The outline of this thesis is as follows:

In chapter 1, we discuss some issues regarding the origin and description of neutrino masses. We briefly review the generation of fermion masses within the SM and summarize the present experimental data on fermion masses and mixings, including the results from the neutrino sector. We then review the possibilities to generate neutrino masses by minimal extensions of the SM particle content and their relation to the description of neutrino masses by the lowest dimensional effective operator allowed by gauge symmetry. They can be realized naturally within left-right symmetric models, for example. Finally, we demonstrate that instead of introducing a fundamental Higgs field, it is possible to break the electroweak symmetry by neutrino condensation. In this scenario, small neutrino masses emerge from a dynamical see-saw mechanism.

The running of physical quantities is determined by the Renormalization Group Equations (RGEs). In order to evaluate the energy scale dependence of neutrino masses, lepton mixings and CP phases, the RGE for the effective neutrino mass matrix is required. When this study started, the existing RGEs for the lowest dimensional effective neutrino mass operators in the SM and in Two-Higgs-Doublet Models (2HDMs) were not in agreement. In chapter 2, we will therefore calculate them in the SM, in 2HDMs and in the Minimal Supersymmetric Standard Model (MSSM). For comparing the predictions of GUT models with the experimental results, the effective approach is usually not sufficient, since the neutrino mass operator is realized at intermediate energy scales in many cases. We therefore discuss the matching conditions and calculate the RGEs which are required for a RG analysis of minimal see-saw models.

The RGEs of a theory provide a coupled system of differential equations for the energy scale dependence of all the physical quantities. To obtain the RG flow, they have to be solved simultaneously. In chapter 3, we will analyze the RG evolution of neutrino masses, lepton mixings and CP phases in the SM and the MSSM with the lowest dimensional neutrino mass operator as well as in the minimal see-saw extensions of these models. We will use analytical as well as numerical methods in order to understand its characteristic properties.

1 Origin and Description of Neutrino Masses

The SM has been very successful in describing particle physics at energies of the order of the electroweak (EW) scale. The particle masses in the SM are generated via spontaneous symmetry breaking (SSB) of the EW symmetry, where the scalar Higgs particle acquires a vacuum expectation value (vev). The strong evidence for neutrino masses on the other hand is the first clear signal for physics beyond the SM. There are of course several mechanisms to generate neutrino masses in many possible extensions of the SM. We restrict ourselves to the most minimalistic examples. A rather model-independent approach is to consider the SM as an effective theory. Without introducing additional particles, the neutrinos can obtain masses from the lowest dimensional effective operator allowed by gauge symmetry. The possible realizations of this operator at some high energy scale nicely fit into theories with left-right extended gauge symmetry and particle spectrum and left-right symmetric GUTs. An alternative to introducing a fundamental scalar Higgs field is the generation of a composite Higgs particle. In a minimal model we illustrate that by neutrino condensation, it is possible to break the EW symmetry and to generate small neutrino masses by a dynamical see-saw mechanism.

1.1 Fermion Masses in the Standard Model

The SM is a $SU(3)_C \times SU(2)_L \times U(1)_Y := G_{321}$ gauge theory which is spontaneously broken to $SU(3)_C \times U(1)_e$. In addition to the gauge fields, the SM contains fermionic fields and a complex scalar $SU(2)_L$ -doublet, the Higgs. The fermions can be separated into quarks q, d^C, u^C and leptons ℓ, e^C which all exist in three generations and transform under the SM gauge group as shown in table 1.1.

1.1.1 Electroweak Symmetry Breaking

The Higgs field Lagrangian is given by

$$\mathcal{L}_{\text{Higgs}}^{\text{SM}} = (D_\mu \phi)^\dagger (D^\mu \phi) - m^2 \phi^\dagger \phi - \frac{1}{4} \lambda (\phi^\dagger \phi)^2. \quad (1.1)$$

$D_\mu = \partial_\mu + ig_A T_A V^A$ is the gauge-covariant derivative, where T_A ($1 \leq A \leq \dim(G_{321})$) are the representations of the Lie algebra generators as defined in table 1.2.

Field	ϕ	q^f	d^{Cf}	u^{Cf}	ℓ^f	e^{Cf}
SU(3) _C	1	3	$\bar{\mathbf{3}}$	$\bar{\mathbf{3}}$	1	1
SU(2) _L	2	2	1	1	2	1
q_Y	$+\frac{1}{2}$	$+\frac{1}{6}$	$+\frac{1}{3}$	$-\frac{2}{3}$	$-\frac{1}{2}$	$+1$

Table 1.1: The Higgs and the fermions of the SM, written as left-handed Weyl spinors, and the corresponding representations of the SM gauge group. $f \in \{1, 2, 3\}$ is a flavour index and $q_Y^U := \sqrt{3/5} q_Y$ denotes the U(1)_Y charge in the so-called GUT normalization.

	gauge group	coupling g_A	T_A	gauge field V_μ^A
$A = 0$	U(1) _Y	g_1	q_Y	B_μ
$A = 1, 2, 3$	SU(2) _L	g_2	$\frac{\tau_i}{2}$ ($i = A$)	W_μ^i
$A = 4, \dots, 11$	SU(3) _C	g_3	$\frac{\lambda_l}{2}$ ($l = A - 3$)	G_μ^l

Table 1.2: Notation for the generators of the SM gauge group G_{321} , given here in the fundamental representation. τ_i are the Pauli matrices and λ_l the Gell-Mann matrices.

The minimization of the Higgs potential shows that the EW symmetry is spontaneously broken for $m^2 < 0$ and that the true ground state satisfies $\langle \phi^\dagger \phi \rangle = v_{\text{EW}}^2/2$ with $v_{\text{EW}} = (-4m^2/\lambda)^{1/2}$. We can now expand the SU(2)_L-doublet ϕ around a chosen specific vev,

$$\phi = \begin{pmatrix} \phi^+ \\ \phi^0 \end{pmatrix} = \begin{pmatrix} G_1^+ + iG_2^+ \\ \frac{1}{\sqrt{2}}(v_{\text{EW}} + h + iG^0) \end{pmatrix}, \quad (1.2)$$

defining the embedding of the unbroken U(1)_e into SU(2)_L × U(1)_Y. With t_3 defined by the eigenvalue of $\frac{\tau_3}{2}$, the U(1)_e-charge q_e of the fields is given by $q_e = t_3 + q_Y$. The superscripts in equation (1.2) indicate the charge q_e of the SU(2)_L-component fields. The Goldstone bosons G_1^+ , G_2^+ and G^0 are “eaten” by the linear combinations of gauge fields $W_\mu^\pm = (W_\mu^1 \mp W_\mu^2)/\sqrt{2}$ and $Z_\mu = -\sin(\theta_W)B_\mu + \cos(\theta_W)W_\mu^3$, which become massive. θ_W is the Weinberg angle, related to the gauge boson masses by $\cos^2(\theta_W) = m_{W^\pm}^2/m_Z^2$. h is the real SM Higgs-field with a mass given by $m_h^2 = -2m^2 = \frac{1}{2}\lambda v_{\text{EW}}^2$.

1.1.2 Fermion Masses

The masses for the fermions are generated by the Yukawa interactions

$$\mathcal{L}_{\text{Yuk}}^{\text{SM}} = -(Y_e)_{gf} \bar{e}_R^g \phi^\dagger \ell_L^f - (Y_u)_{gf} \bar{u}_R^g \tilde{\phi}^\dagger q_L^f - (Y_d)_{gf} \bar{d}_R^g \phi^\dagger q_L^f + \text{h.c.}, \quad (1.3)$$

where $\tilde{\phi} := i\tau^2\phi^* =: \varepsilon\phi^*$ is the charge conjugate of the Higgs. We have used the common notation of writing the Weyl spinors as chirality projected 4-component spinors and assigned the following components to the $SU(2)_L$ -doublets,

$$q_L^f = \begin{pmatrix} u_L^f \\ d_L^f \end{pmatrix}, \quad \ell_L^f = \begin{pmatrix} \nu_L^f \\ e_L^f \end{pmatrix}. \quad (1.4)$$

After SSB, we obtain the mass matrices

$$M_u = \frac{v_{EW}}{\sqrt{2}} Y_u, \quad M_d = \frac{v_{EW}}{\sqrt{2}} Y_d \quad \text{and} \quad M_e = \frac{v_{EW}}{\sqrt{2}} Y_e \quad (1.5)$$

for the up-type and down-type quarks and the charged leptons, respectively. The neutrinos remain massless within the SM.

1.1.3 Experimental Results for Fermion Masses and Mixings

We will now give a brief overview over the present status of our knowledge about fermion masses, mixings and CP phases. The results are summarized in table 1.3. The conventions for the definition of the mixing parameters for leptons will be given in appendix A.1.

Experiments on neutrino oscillations have found strong evidence that neutrinos are massive. For the solar angle θ_{12} and the solar mass squared difference, the so-called LMA solution has been confirmed by the KamLAND [12] experiment. It points towards a large, but not maximal mixing angle θ_{12} . The results for the solar and atmospheric mass squared differences of the neutrinos and for the lepton mixings shown in table 1.3 stem from the analysis [13] of the recent KamLAND [12] and the SNO data [14], the Super-Kamiokande atmospheric data [15] and the CHOOZ experiment [16]. We left aside the controversially discussed results of the LSND experiment [17], which requires a third mass squared difference. For a summary of present and planned experiments on neutrino oscillations, see e.g. [18].

The neutrino mass scale has not yet been determined by experiment. At present, the most stringent bounds are $m_i < 0.23$ eV from WMAP [19] and $\langle m_\nu \rangle \lesssim 0.35$ eV, with some uncertainty due to nuclear matrix elements, from neutrino-less double beta decay experiments [20,21]. Note that the latter search for an effective mass defined by $\langle m_\nu \rangle = |\sum_i (U_{MNS})_{1i}^2 m_i| = |m_1 c_{12}^2 c_{13}^2 e^{i\varphi_1} + m_2 s_{12}^2 c_{13}^2 e^{i\varphi_2} + m_3 s_{13}^2 e^{2i\delta}|$ and are only sensitive to Majorana masses. The sign of Δm_{atm}^2 is unknown at present and θ_{23} can be above or below 45° . The nature of neutrino masses, i.e. if they are of Majorana or Dirac type, as well as the phases in the lepton sector are unconstrained by experiments.

The masses of the quarks and leptons at M_Z are taken from [22]. For the quark mixings, the results stem from the Particle Data Book 2002 and for the value of the CKM phase we refer to [23].

1 Origin and Description of Neutrino Masses

	Best-fit value	Range	C.L.
$m_u(M_Z)$ [GeV]	$2.33 \cdot 10^{-3}$	$1.88 \cdot 10^{-3} - 2.75 \cdot 10^{-3}$	1σ
$m_c(M_Z)$ [GeV]	0.677	0.616 – 0.733	1σ
$m_t(M_Z)$ [GeV]	181	± 13	1σ
$m_d(M_Z)$ [GeV]	$4.69 \cdot 10^{-3}$	$4.03 \cdot 10^{-3} - 5.29 \cdot 10^{-3}$	1σ
$m_s(M_Z)$ [GeV]	0.0934	0.0804 – 0.1054	1σ
$m_b(M_Z)$ [GeV]	3.00	± 0.11	1σ
θ_{12}^q [°]	12.8794	12.7502 – 13.0088	2σ
θ_{13}^q [°]	0.206265	0.166158 – 0.246373	2σ
θ_{23}^q [°]	2.36125	2.24657 – 2.47595	2σ
δ_{CKM} [°]	63.5	56.5 – 70.5	1σ
$m_e(M_Z)$ [GeV]	$0.48684727 \cdot 10^{-3}$	$\pm 1.4 \cdot 10^{-10}$	1σ
$m_\mu(M_Z)$ [GeV]	0.10275138	$\pm 3.3 \cdot 10^{-7}$	1σ
$m_\tau(M_Z)$ [GeV]	1.74669	1.74642 – 1.74699	1σ
θ_{12}^ℓ [°]	32.6	25.6 – 42.0	3σ
θ_{13}^ℓ [°]	–	0.0 – 9.2	90%
θ_{23}^ℓ [°]	45.0	33.2 – 56.8	3σ
Δm_{sol}^2 [eV ²]	$7.3 \cdot 10^{-5}$	$4 \cdot 10^{-5} - 2.8 \cdot 10^{-4}$	3σ
$ \Delta m_{\text{atm}}^2 $ [eV ²]	$2.5 \cdot 10^{-3}$	$1.2 \cdot 10^{-3} - 5.0 \cdot 10^{-3}$	3σ

Table 1.3: Experimental data for the quark masses at M_Z , quark mixings θ_{ij}^q and the CKM-phase δ_{CKM} , charged lepton masses at M_Z , lepton mixing angles θ_{ij}^ℓ and neutrino mass squared differences.

1.2 Extensions of the Standard Model Particle Content

In the SM, a renormalizable neutrino mass term of the Dirac as well as of the Majorana type is not possible in the Lagrangian. The same holds in the MSSM or in 2HDMs, which we will discuss in the next chapter in more detail. If the particle spectrum of the SM is extended, the neutrino masses, i.e. mass terms that appear in the effective Lagrangian after SSB, can arise at tree-level or at a higher loop order. We restrict ourselves to the tree-level case in this section. The additional particles may carry baryon and lepton number. For the case of Majorana masses, it is necessary to introduce explicitly lepton number violating interactions or Higgs fields which carry lepton number and break it spontaneously.

The possible extensions which generate tree-level masses for the neutrinos either require an additional Higgs field or an additional fermion, which couple to two lepton doublets or a lepton doublet and the Higgs doublet, respectively (table 1.4). A comprehensive introduction to neutrino masses can e.g. be found in [24].

coupled fields	representations
ℓ_L^f, ℓ_L^g	$(\mathbf{1}, \mathbf{2}, -\frac{1}{2}) \times (\mathbf{1}, \mathbf{2}, -\frac{1}{2}) \rightarrow (\mathbf{1}, \mathbf{1}, -1) + (\mathbf{1}, \mathbf{3}, -1)$
ℓ_L^f, ϕ	$(\mathbf{1}, \mathbf{2}, -\frac{1}{2}) \times (\mathbf{1}, \mathbf{2}, +\frac{1}{2}) \rightarrow (\mathbf{1}, \mathbf{1}, 0) + (\mathbf{1}, \mathbf{3}, 0)$

Table 1.4: Irreducible representations of G_{321} , contained in the product representations of two lepton doublets and a lepton doublet and a Higgs doublet, which are relevant for the generation of neutrino masses.

1.2.1 Additional Higgs Triplet

As shown in table 1.4, there are two ways to couple scalar fields to the two lepton doublets. The scalars could either be $SU(2)_L$ -singlets with an electric charge +1 after EWSB or $SU(2)_L$ -triplets in the representation $(\mathbf{1}, \mathbf{3}, +1)$. Obviously, only the triplet can acquire an $U(1)_e$ invariant vev. The $SU(2)$ -invariant mass term with the $SU(2)_L$ -triplet Higgs Δ can be written as

$$\mathcal{L}_{\text{Yuk},\nu}^{\Delta} = -\frac{1}{2}(Y_{\nu}^{\Delta})_{gf} \overline{\ell_L^{\text{C}g}} (\vec{\tau} \cdot \vec{\Delta}) \ell_L^f, \quad (1.6)$$

where $(\vec{\tau} \cdot \vec{\Delta})^{ab}$ is defined as $((\tau^A)^a{}_c \varepsilon^{cb} \Delta_A)$ with $a, b, c, d \in \{1, 2\}$ being $SU(2)_L$ indices. The superscript C denotes charge conjugation of the 4-component spinor.

If the $U(1)_e$ -neutral component of Δ acquires a vev $v_\Delta := \langle \Delta^0 \rangle$, a Majorana mass matrix

$$m_\nu = Y_\nu^\Delta v_\Delta \quad (1.7)$$

for the SM neutrinos emerges (figure 1.1(a)). v_Δ is however severely constrained by the ρ -parameter, defined as

$$\rho := \left(\frac{m_{W^\pm}}{m_Z \cos(\theta_W)} \right). \quad (1.8)$$

It is equal to 1 in the SM at tree-level and modified in the presence of a $SU(2)_L$ -triplet Higgs to

$$\rho = \frac{v_{EW}^2 + 2v_\Delta^2}{v_{EW}^2 + 4v_\Delta^2}, \quad (1.9)$$

since the gauge boson masses are now $m_{W^\pm} = \frac{1}{4}g_2^2(v_{EW}^2 + 2v_\Delta^2)$ and $m_Z = \frac{1}{4}(g_1^2 + g_2^2)(v_{EW}^2 + 4v_\Delta^2)$. Experimentally, the ρ -parameter is given by $1.0012_{-0.0014}^{+0.0023}$ [25] and thus the vev of a triplet Higgs has to be much smaller than v_{EW} . It is however possible to explain such a small triplet-vev in left-right models where a bi-doublet and two triplet Higgs fields are present, since there is a vev see-saw relation which follows from the minimization condition of the Higgs potential (see section 1.4.1). A large vev v_R for the triplet Δ_R implies a small vev v_L for Δ_L . The small vev is induced, which means that it appears after the breaking of the EW symmetry.

1.2.2 Additional Fermion Singlets

Dirac masses for the neutrinos can be achieved by adding n_G fermionic $SU(2)_L$ -singlets N^{Ci} ($i \in \{1, \dots, n_G\}$) in the representation $(\mathbf{1}, \mathbf{1}, 0)$ or $SU(2)$ -triplets Σ in the representation $(\mathbf{1}, \mathbf{3}, 0)$ of G_{321} to the SM spectrum. We consider the first possibility in more detail. Neutrinos can then obtain a tree-level Dirac mass term via a Yukawa coupling (see figure 1.1(b)) in analogy to the other SM fermions,

$$\mathcal{L}_{\text{Yuk}, \nu}^{\text{SM}} = -(Y_\nu)_{if} \overline{N_R^i} \widetilde{\phi}_L^\dagger \ell_L^f + \text{h.c.}, \quad (1.10)$$

yielding a Dirac mass matrix

$$M_\nu^{(D)} = \frac{v_{EW}}{\sqrt{2}} Y_\nu. \quad (1.11)$$

Once the singlets are introduced, one should note that they can obtain a direct Majorana mass term (see figure 1.1(c))

$$\mathcal{L}_M^{\text{SM}} = -\frac{1}{2} \overline{N_R^i} M_{ij} N_R^{Cj} + \text{h.c.}. \quad (1.12)$$

The most general case after EWSB is a $(3 + n_G) \times (3 + n_G)$ Majorana mass matrix in the basis of fields $\{\nu_L^f, N_R^{Ci}\}$. A special case occurs if M vanishes exactly. The result would be pure Dirac masses from equation (1.11). The neutrino mass scale is however more than 6 orders of magnitude smaller than the mass scale of the lightest other fermion and thus very small neutrino Yukawa couplings are required.

One should also remark that there can be scalar SU(2)-singlet Higgs-fields χ in the representation $(\mathbf{1}, \mathbf{1}, 0)$, which can acquire vevs and would contribute to the Majorana mass matrix M (see figure 1.1(d)). This is used in the Froggatt-Nielsen mechanism, which will be discussed in section 1.3.

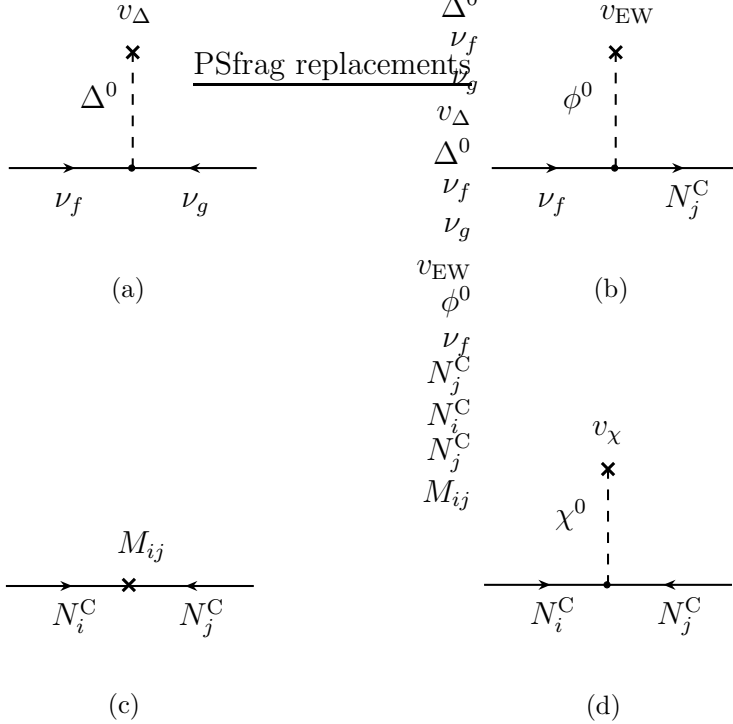


Figure 1.1: Diagrammatic illustration of the tree level mass terms which are possible, if a triplet Higgs and singlet fermions are added to the SM particle spectrum. Figure (a) gives a Majorana mass term after EWSB by the coupling to a Higgs triplet, (b) a Dirac mass term, (c) a direct mass term for the singlets and (d) a Majorana mass term for the singlets by a singlet Higgs χ .

1.2.3 The See-Saw Mechanism

If no symmetry protects against a Majorana mass term as in equation (1.12), we can in general assume that the mass eigenvalues M_i are large compared to the EW scale. Then, the $(3 + n_G) \times (3 + n_G)$ Majorana mass matrix can be approximately block-diagonalized,

$$\mathcal{L}_{\widetilde{M}}^{\text{SM}} = -\frac{1}{2} \begin{pmatrix} \overline{\nu_L^{Cf}} \\ \overline{N_R^j} \end{pmatrix}^T \begin{pmatrix} 0 & (Y_\nu^T)_{fi} \frac{v_{\text{EW}}}{\sqrt{2}} \\ (Y_\nu)_{jg} \frac{v_{\text{EW}}}{\sqrt{2}} & M_{ji} \end{pmatrix} \begin{pmatrix} \nu_L^g \\ N_R^{Ci} \end{pmatrix} + \text{h.c.} \quad (1.13a)$$

$$\approx -\frac{1}{2} \begin{pmatrix} \overline{\nu_L^{Cf}} \\ \overline{N_R^j} \end{pmatrix}^T \begin{pmatrix} (m_\nu)_{fg} & 0 \\ 0 & M_{ji} \end{pmatrix} \begin{pmatrix} \nu_L^g \\ N_R^{Ci} \end{pmatrix} + \text{h.c.} , \quad (1.13b)$$

where, neglecting $\mathcal{O}(M_i^{-1})$ -terms, $\nu_L^f \approx \nu_L^f$ and $N_R^{Ci} \approx N_R^{Ci}$ and where the Majorana mass matrix m_ν for the SM neutrinos is given by

$$m_\nu \approx -\frac{v_{\text{EW}}^2}{2} Y_\nu^T M^{-1} Y_\nu . \quad (1.14)$$

The suppression by M^{-1} provides a natural explanation for the smallness of neutrino masses and is referred to as the canonical (or type I) see-saw mechanism [26–29]. If a mass matrix from a Higgs triplet is allowed as well, equation (1.14) has to be modified to $m_\nu \approx Y_\nu^\Delta v_\Delta - \frac{1}{2} v_{\text{EW}}^2 Y_\nu^T M^{-1} Y_\nu$ and is now referred to as type II see-saw [30–32].

1.3 Neutrino Masses in an Effective Theory Approach

We now assume that there are no other light particles than the ones of the minimal SM and that the effects of possible extensions of the SM are decoupled at low energy. The SM is then an effective theory valid up to some energy scale Λ , where new physics has to be taken into account. The effects from unknown physics above Λ have to be taken into account by admitting higher dimensional and therefore non-renormalizable operators in the Lagrangian. They are in general suppressed by $1/\Lambda^n$ for an operator of mass dimension $4 + n$. This suppression arises since the effective operators enter the theory when particles with masses of the order Λ are integrated out. The heavy particles effectively do not propagate in the theory far below their mass scales. This approach allows to treat the neutrino masses in a quite model independent way. Above Λ , the enlargement of the particle spectrum in extensions of the SM opens up many possibilities for realizing the neutrino mass operators by integrating out the heavy degrees of freedom. In principle, this is done in the path integral formalism. In practice, at the scale Λ the full theory is matched with the effective theory containing in principle all higher-dimensional operators allowed by symmetry. An introduction to effective field theory and more details about the matching procedure can e.g. be found in [33].

1.3.1 The Lowest Dimensional Effective Neutrino Mass Operator

In the SM, the lowest dimensional operator, which gives Majorana masses for the neutrinos, has mass-dimension 5 and couples two Higgs and two lepton doublets. It is given by

$$\mathcal{L}_\kappa = \frac{1}{4} \kappa_{gf} \overline{\ell_{Lc}^g} \varepsilon^{cd} \phi_d \ell_{Lb}^f \varepsilon^{ba} \phi_a + \text{h.c.} . \quad (1.15)$$

κ_{gf} has mass dimension -1 and is symmetric under interchange of the generation indices f and g . If we decompose the operator of equation (1.15) into components, neutrino masses emerge after EWSB from the part

$$\mathcal{L}_{\kappa,\nu} = \frac{1}{4} \kappa_{gf} \overline{\nu_L^g} \nu_L^f \phi^0 \phi^0 + \text{h.c.} \xrightarrow{\text{EWSB}} \frac{\kappa_{gf} v_{\text{EW}}^2}{4} \frac{1}{2} \overline{\nu_L^g} \nu_L^f + \text{h.c.} . \quad (1.16)$$

A diagrammatic illustration is given in figure 1.2. The neutrino mass operator provides a good description of neutrino masses up to an energy scale where new physics has to be taken into account which generates the effective operator. Typically, this is the mass scale of a heavy particle. At this scale, the effective operator is realized by integrating the heavy particle out of the theory. We now study the possible minimalistic realizations of this operator at tree-level and at one-loop order. Clearly, this requires an extension of the SM with at least one lepton number violating interaction, since \mathcal{L}_κ violates lepton number by 2 units. For the diagrammatic illustration,

instead of the full $SU(2)_L \times U(1)_Y$ invariant operator, we will only study the part $\mathcal{L}_{\kappa,\nu}$ which contains the neutrinos.

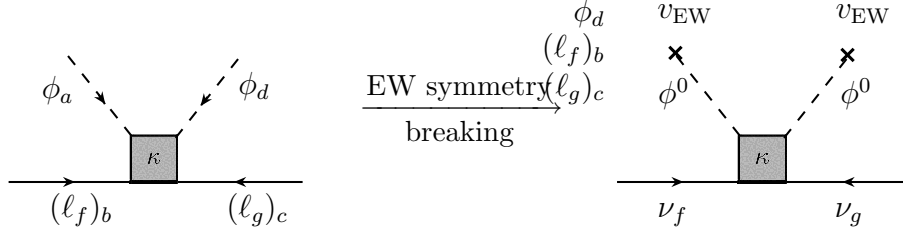


Figure 1.2: The lowest dimensional effective neutrino mass operator in the unbroken and in the broken phase after EWSB. It yields an effective Majorana mass matrix for the light neutrinos. $a, b, c, d \in \{1, 2\}$ are $SU(2)_L$ indices. All fermions are written as left-handed Weyl spinors.

1.3.2 Tree-Level Realizations of the Neutrino Mass Operator

The heavy particle, which is exchanged for the tree-level realization of the dimension 5 operator, has to have a $SU(2)_L \times U(1)_Y$ invariant coupling to either two lepton doublets (and two Higgs doublets), if it is a scalar, or to a Higgs-doublet and a lepton doublet, if it is a fermion. Furthermore, it has to have a component which is uncharged under $U(1)_e$, since it has to couple to the neutrinos and to the electrically neutral component of the Higgs doublet. The possible fields to be exchanged can again be extracted from table 1.4 and the corresponding diagrams are shown in figure 1.3. The exchanged fermion can either be a $SU(2)$ -singlet N^C or the electrically neutral component of a $SU(2)$ -triplet Σ . The heavy scalar field has to have an electrically neutral component and can thus only be the $SU(2)$ -triplet Δ .

1.3.3 Loop Realizations of the Neutrino Mass Operator

One generic possibility for a one-loop realization of the neutrino mass operator is shown in figure 1.4. It has the same topology as the well-known Zee-model [34]. We assume that at least one of the four particles ω, ρ, η and ξ , which appear in the loop, is heavy and will thus be integrated out.

From the couplings in the diagram of figure 1.4, we can infer the properties of the fields ω, ρ, η and ξ . From the coupling of ω and ρ to the Higgs doublet, we know that one of them has to be a $SU(2)$ -doublet. Without loss of generality, we therefore choose ω in the representation $(\mathbf{r}_\omega^{SU(3)}, \mathbf{2}, q_\omega)$. Consequently we obtain $\rho \sim (\bar{\mathbf{r}}_\omega^{SU(3)}, \mathbf{r}_\rho^{SU(2)}, -q_\omega + \frac{1}{2})$, where $\mathbf{r}_\rho^{SU(2)} \in \{\mathbf{1}, \mathbf{3}\}$ and further $\xi \sim (\mathbf{r}_\omega^{SU(3)}, \mathbf{2}, q_\omega)$, $\eta \sim (\bar{\mathbf{r}}_\omega^{SU(3)}, \mathbf{r}_\eta^{SU(2)}, -q_\omega + \frac{1}{2})$, where $\mathbf{r}_\eta^{SU(2)} \in \{\mathbf{1}, \mathbf{3}\}$. All the possibilities with this topology

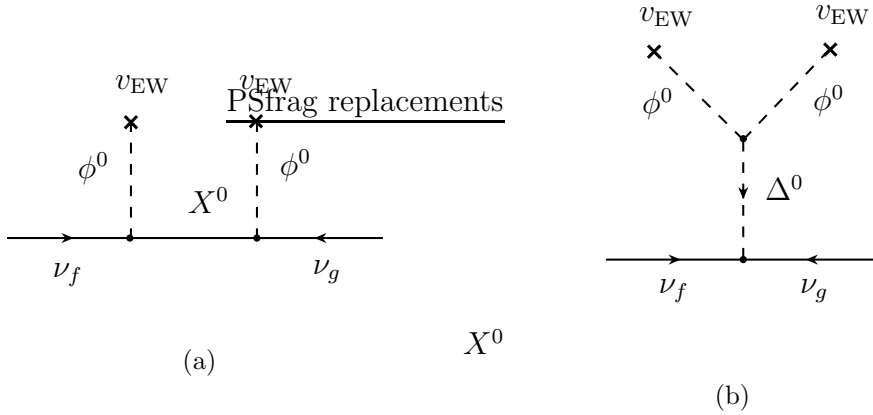


Figure 1.3: Realization of the neutrino mass operator by the exchange of a heavy fermion X^0 with a Majorana mass (a) and a heavy scalar Δ^0 (b). The superscripts indicate the electric charge q_e . X^0 can either be a $SU(2)_L$ -singlet N^C or the electrically neutral component of a $SU(2)_L$ -triplet Σ . Δ^0 is the electrically neutral component of a $SU(2)_L$ -triplet Δ , as explained in the text.

are thus classified by specifying e.g. the set of quantities $\{\bar{\mathbf{r}}_\omega^{\text{SU}(3)}, q_\omega, \mathbf{r}_\rho^{\text{SU}(2)}, \mathbf{r}_\eta^{\text{SU}(2)}\}$. There are of course other possible realizations of the neutrino mass operator at one-loop and also from higher orders in perturbation theory (see e.g. [35]).

1.3.4 Higher Dimensional Operators for Neutrino Masses

If the SM is e.g. extended by n_G heavy singlet fermions N_i^C and also by n_χ singlet Higgses χ_m , several higher-dimensional operators for neutrino masses can be constructed as illustrated in figure 1.5. There can be diverse suppression factors, according to the masses M_i of the heavy fermions N_i^C and the vevs v_{χ_m} of the singlet Higgses. Usually, due to some horizontal symmetry, for a given combination of neutrino flavours only specific operators of this kind are allowed. This mechanism is called universal see-saw or Froggatt-Nielsen mechanism [36]. It was originally invented in order to explain the hierarchy in the quark mass spectrum. If the singlet fermions and Higgses are heavy, integrating them out of the theory will give a contribution to the dimension 5 neutrino mass operator. A classification of several higher dimensional neutrino mass operators can be found in [37].

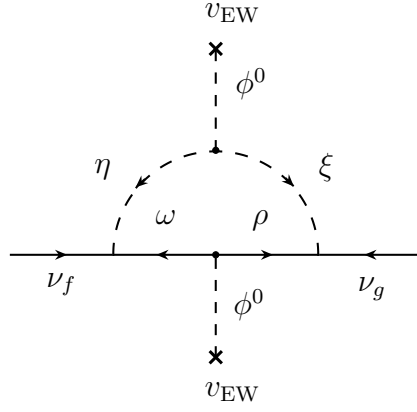


Figure 1.4: One generic possibility for a 1-loop realization of the effective neutrino mass operator.

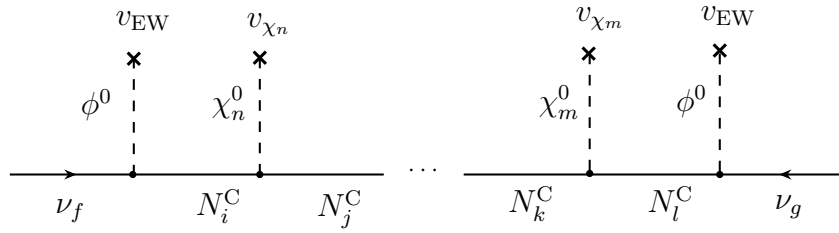


Figure 1.5: Froggatt-Nielsen-type diagram, which corresponds to the tree-level realization of a higher dimensional neutrino mass operator. The indices $n, m \in \{1, \dots, n_\chi\}$ run over the singlet scalar Higgs-fields and the indices $i, j, k, l \in \{1, \dots, n_G\}$ over the singlet fermions.

1.4 Neutrino Masses in Left-Right Symmetric Extensions of the Standard Model

In minimal left-right symmetric extensions of the SM, the fermion particle spectrum is extended by three generations of SM-singlets, which can be interpreted as right-handed neutrinos. Every left-handed fermion now has a right-handed counterpart, and by extending the gauge sector, a left-right symmetric structure can be achieved. We will now consider briefly the left-right symmetric scenarios with this fermion content and their consequences for neutrino masses.

1.4.1 Minimal Left-Right Symmetric Models

The minimal left-right symmetric extension of the SM gauge group is given by

$$G_{3221} = \text{SU}(3)_C \times \text{SU}(2)_L \times \text{SU}(2)_R \times \text{U}(1)_{B-L}. \quad (1.17)$$

The particle spectrum contains the fermions of the SM plus the additional singlets N^{Cf} , which can be written as doublets

$$q_L^f = \begin{pmatrix} u_L^f \\ d_L^f \end{pmatrix}, \quad \ell_L^f = \begin{pmatrix} \nu_L^f \\ e_L^f \end{pmatrix}, \quad q_R^f = \begin{pmatrix} u_R^f \\ d_R^f \end{pmatrix}, \quad \ell_R^f = \begin{pmatrix} N_R^f \\ e_R^f \end{pmatrix} \quad (1.18)$$

of $\text{SU}(2)_L$ or $\text{SU}(2)_R$, respectively. The fields have been written as chirality projected 4-component spinors. The transformation properties of the fermions and of some possible Higgs fields are summarized in table 1.5. The minimal left-right models can have an additional discrete left-right symmetry, which interchanges “left” and conjugate “right” fields of table 1.5. However, it has to be introduced by hand.

Field	q_L^f	q_R^{Cf}	ℓ_L^f	ℓ_R^{Cf}	Φ	χ_L	χ_R^*	Δ_L	Δ_R^*
$\text{SU}(3)_C$	3	$\bar{\mathbf{3}}$	1	1	1	1	1	1	1
$\text{SU}(2)_L$	2	1	2	1	2	2	1	3	1
$\text{SU}(2)_R$	1	2	1	2	2	1	2	1	3
q_{B-L}	$+\frac{1}{3}$	$-\frac{1}{3}$	-1	+1	0	+1	-1	+2	-2

Table 1.5: The fermions and some possible Higgs fields of the minimal left-right model, written as left-handed Weyl spinors, and the corresponding representations of G_{3221} . The indices L and R indicate the transformation properties under $\text{SU}(2)_L$ and $\text{SU}(2)_R$ in this notation.

After the breaking to $\text{SU}(3)_C \times \text{U}(1)_e$, we obtain a $\text{U}(1)_e$ -charge q_e given by $q_e = t_{3L} + t_{3R} + \frac{1}{2}q_{B-L}$, which defines the embedding of $\text{U}(1)_e$ in $\text{SU}(3)_C \times \text{SU}(2)_L \times \text{SU}(2)_R \times \text{U}(1)_{B-L}$.

Fermion Masses in Minimal Left-Right Models

There are two minimal ways to break the G_{3221} gauge symmetry spontaneously to $SU(3)_C \times U(1)_e$, using a bi-doublet and two doublets

$$\chi_L = \begin{pmatrix} \chi_L^+ \\ \chi_L^0 \end{pmatrix}, \quad \chi_R = \begin{pmatrix} \chi_R^+ \\ \chi_R^0 \end{pmatrix}, \quad (1.19)$$

or a bi-doublet and two triplets

$$\varepsilon \Delta_L = \vec{\tau} \cdot \vec{\Delta}_L = \varepsilon \begin{pmatrix} \Delta_L^+ & \Delta_L^{++} \\ \Delta_L^0 & -\Delta_L^+ \end{pmatrix}, \quad \varepsilon \Delta_R = \vec{\tau} \cdot \vec{\Delta}_R = \varepsilon \begin{pmatrix} \Delta_R^+ & \Delta_R^{++} \\ \Delta_R^0 & -\Delta_R^+ \end{pmatrix}. \quad (1.20)$$

The bi-doublet

$$\Phi = \begin{pmatrix} \phi^{(1)0} & \phi^{(2)+} \\ \phi^{(1)-} & \phi^{(2)0} \end{pmatrix} \quad (1.21)$$

transforms as $(\mathbf{1}, \mathbf{2}, \mathbf{2}, 0)$ under the LR gauge group (1.17). A vev $\langle \Phi \rangle = \text{diag}(v_\Phi, v'_\Phi)$ can give masses via Yukawa-like couplings to the fermions but does not break $U(1)_{B-L}$. We can break $U(1)_{B-L}$, while leaving the SM gauge group intact, by generating Majorana mass terms for the right-handed neutrinos, e.g. with the doublet χ_R or the triplet Δ_R . Schematically,

$$G_{3221} \xrightarrow{\langle \Delta_R \rangle \text{ or } \langle \chi_R \rangle} G_{321} \xrightarrow{\langle \Phi \rangle} SU(3)_C \times U(1)_e. \quad (1.22)$$

Using the doublet, Majorana masses for the singlets can be achieved via the effective operator

$$\mathcal{L}_{M_R} = -\frac{\rho_{fg}}{\Lambda_\rho} (\bar{\ell}_R^f \cdot \chi_R) (\ell_R^{Cg} \cdot \chi_R) \xrightarrow{\langle \chi_R \rangle} -\frac{1}{2} (M_R)_{fg} \bar{N}_R^f N_R^{Cg}. \quad (1.23)$$

E.g. with $\Lambda_\rho \approx M_{\text{Pl}} \approx 10^{19}$ GeV and $\langle \chi_R \rangle \approx M_{GUT} \approx 10^{16}$ GeV, this would give singlet masses in the right range for the see-saw mechanism. By effective operators, Majorana masses for the left-handed neutrinos as well as Dirac masses for the quarks and leptons can be generated. In principle, no bi-doublet is needed at all (see e.g. [38]).

With the triplets and the bi-doublet, lepton masses arise after SSB from the Yukawa-type interactions

$$\begin{aligned} \mathcal{L}_Y = & -\frac{1}{2} (Y_\ell^{\Delta_L})_{gf} \bar{\ell}_L^{Cg} (\varepsilon \Delta_L) \ell_L^f - \frac{1}{2} (Y_\ell^{\Delta_R})_{gf} \bar{\ell}_R^{Cg} (\varepsilon \Delta_R)^* \ell_R^{Cf} \\ & - (Y_\ell^\Phi)_{gf} \bar{\ell}_R^{Cg} \Phi \ell_L^f - (Y_\ell^{\tilde{\Phi}})_{gf} \bar{\ell}_R^{Cg} \tilde{\Phi} \ell_L^f + \text{h.c.}, \end{aligned} \quad (1.24)$$

with $\tilde{\Phi} := \tau_2 \Phi^* \tau_2$. Note that the Majorana mass for the right-handed neutrinos would be $M_R = Y_\ell^{\Delta_R} v_R$ in our notation, where $v_R := \langle \Delta_R^0 \rangle$ is the vev of Δ_R .

The minimization of the most general Higgs potential with a bi-doublet and the two triplets leads to the so-called vev see-saw relation (see e.g. [39])

$$v_L v_R = \lambda_\Delta v_\Phi^2, \quad (1.25)$$

in the approximation that v_Φ^2 is negligible. λ_Δ depends on the parameters of the Higgs potential and $v_R := \langle \Delta_R^0 \rangle$, $v_L := \langle \Delta_L^0 \rangle$. First, we make the assumption that v_R is much larger than the EW scale in order to accomplish a see-saw mechanism for the SM neutrinos. We then see that there are in principle two ways to proceed. We could either eliminate the vev see-saw by imposing a symmetry from beyond the left-right symmetric model, which enforces $\lambda_\Delta = 0$ and thus leads to a type I see-saw mechanism for the neutrino masses or we could not eliminate it. The latter leads to an induced small vev for Δ_L after the EW symmetry is broken and Φ obtains its vev. This yields a type II see-saw mechanism.

1.4.2 The Pati-Salam Model

The Pati-Salam model is a left-right symmetric extension of the SM gauge group which unifies quarks and leptons into $SU(4)_C$ -multiplets. The gauge symmetry is given by

$$G_{422} = SU(4)_C \times SU(2)_L \times SU(2)_R. \quad (1.26)$$

The fermion fields are contained in the quartets f_L^f and f_R^{Cf} of $SU(4)_C$ and doublets of $SU(2)_L$ and $SU(2)_R$, respectively,

$$f_L^f = \begin{pmatrix} u_{Lr}^f & u_{Ly}^f & u_{Lb}^f & \nu_L^f \\ d_{Lr}^f & d_{Ly}^f & d_{Lb}^f & e_L^f \end{pmatrix}, \quad f_R^f = \begin{pmatrix} u_{Rr}^f & u_{Ry}^f & u_{Rb}^f & N_R^f \\ d_{Rr}^f & d_{Ry}^f & d_{Rb}^f & e_R^f \end{pmatrix}. \quad (1.27)$$

The indices r, y, b correspond to $SU(3)_C$ -color and lepton number acts as the fourth color. The fermion representations and some possible Higgs fields are listed in table 1.6. As in the minimal left-right model, an additional discrete left-right symmetry can be introduced.

Fermion Masses in Pati-Salam Models

After the breaking of G_{422} to $SU(3)_C \times U(1)_e$, we obtain a $U(1)_e$ -charge q_e , given by $q_e = t_{3L} + t_{3R} + \frac{1}{2}q_{B-L}$ as in the minimal left-right model. The breaking of $B-L$, i.e. Majorana masses for the right-handed neutrinos, and the breaking of $SU(4)_C$ to $SU(3)_C$ can e.g. be achieved by a vev of the triplet Δ_R or by an effective operator

$$\mathcal{L}_M^{G_{422}} = -\frac{\rho fg}{\Lambda} (\overline{f_R^f} \chi_R) (f_R^{Cg} \chi_R) \xrightarrow{\langle \chi_R \rangle} -\frac{1}{2} M_{fg} \overline{N_R^f} N_R^{Cg}, \quad (1.28)$$

Field	f_L^f	f_R^{Cf}	Φ	Φ'	χ_L	χ_R^*	Δ_L	Δ_R^*
$SU(4)_C$	4	$\bar{\mathbf{4}}$	1	15	4	$\bar{\mathbf{4}}$	10	$\bar{\mathbf{10}}$
$SU(2)_L$	2	1	2	2	2	1	3	1
$SU(2)_R$	1	2	2	2	1	2	1	3

Table 1.6: The fermions and some possible Higgs fields of the Pati-Salam model and the corresponding representations of the gauge group G_{422} . The fermion fields are written as left-handed Weyl spinors.

where the Higgs χ_R has a vev in the N_R -component. Dirac masses for the fermions can e.g. emerge from the bi-doublets Φ or Φ' or from effective operators using the $SU(4)_C$ -doublet Higgses. Schematically, we have

$$G_{422} \xrightarrow{\langle \Delta_R \rangle \text{ or } \langle \chi_R \rangle} G_{321} \xrightarrow{\langle \Phi \rangle, \langle \Phi' \rangle} SU(3)_C \times U(1)_e . \quad (1.29)$$

Due to the quark-lepton unification, the Yukawa couplings which arise from one Higgs Φ in the representation $(\mathbf{1}, \mathbf{2}, \mathbf{2})_{G_{422}}$ have the property

$$Y_u = Y_\nu , \quad Y_d = Y_e . \quad (1.30)$$

A Higgs field Φ' in the representation $(\mathbf{15}, \mathbf{2}, \mathbf{2})_{G_{422}}$ leads to Yukawa couplings

$$Y_\nu = -3Y_u , \quad Y_e = -3Y_d , \quad (1.31)$$

since the elements of $\mathbf{15}$ of $SU(4)_C$ can be represented by traceless 4×4 matrices.

In Pati-Salam models as well as in the minimal left-right models, see-saw suppressed neutrino masses can arise naturally. Whether a type I or a type II see-saw occurs, depends on the specific model under consideration.

1.4.3 SO(10)-Unification

In SO(10) GUTs, all fermions of the minimal left-right models can be unified into one irreducible representation $\mathbf{16}_{SO(10)}$, for each generation. The Pati-Salam group G_{422} as well as G_{3221} are contained in SO(10) as subgroups. In addition, SO(10) contains a discrete left-right symmetry. The content of $\mathbf{16}_{SO(10)}^f$ in terms of G_{422} is given by

$$\mathbf{16}_{SO(10)}^f = (\mathbf{4}, \mathbf{2}, \mathbf{1})_{G_{422}}^f + (\bar{\mathbf{4}}, \mathbf{1}, \mathbf{2})_{G_{422}}^f = f_L^f + f_R^{Cf} . \quad (1.32)$$

For the breaking of SO(10) to G_{321} , there are many possibilities, which require diverse Higgs representations, as for example $\{\mathbf{16}\}_{SO(10)}$, $\{\mathbf{45}\}_{SO(10)}$, $\{\mathbf{54}\}_{SO(10)}$, $\{\mathbf{120}\}_{SO(10)}$ and $\{\mathbf{126}\}_{SO(10)}$. The brackets indicate the Higgs-fields in this section. We will not consider the breaking of SO(10) in detail here and restrict ourselves to the generation of fermion masses.

Fermion Masses in SO(10) GUT Models

In order to determine the Higgs-fields, which can couple to two fermions in the representation $\mathbf{16}_{\text{SO}(10)}^f$, we have to consider the irreducible representations contained in the product

$$\mathbf{16}_{\text{SO}(10)} \otimes \mathbf{16}_{\text{SO}(10)} = \mathbf{10}_{\text{SO}(10)} + \mathbf{120}_{\text{SO}(10)} + \mathbf{126}_{\text{SO}(10)}. \quad (1.33)$$

Consequently, the possible interactions which can generate mass terms in a renormalizable Lagrangian after symmetry breaking, have the form

$$\mathcal{L}_Y = - (Y^{(10)})_{gf} \mathbf{16}_{\text{SO}(10)}^{gT} \mathcal{C} \{ \mathbf{10} \}_{\text{SO}(10)}^i \Gamma_i \mathbf{16}_{\text{SO}(10)}^f + \text{h.c.} \quad (1.34a)$$

$$- (Y^{(120)})_{gf} \mathbf{16}_{\text{SO}(10)}^{gT} \mathcal{C} \{ \mathbf{120} \}_{\text{SO}(10)}^{ijk} \Gamma_{ijk} \mathbf{16}_{\text{SO}(10)}^f + \text{h.c.} \quad (1.34b)$$

$$- (Y^{(126)})_{gf} \mathbf{16}_{\text{SO}(10)}^{gT} \mathcal{C} \{ \overline{\mathbf{126}} \}_{\text{SO}(10)}^{ijklm} \Gamma_{ijklm} \mathbf{16}_{\text{SO}(10)}^f + \text{h.c.}, \quad (1.34c)$$

where \mathcal{C} is the charge conjugation matrix for the SO(10) spinor representation. Γ^i ($i \in \{1, \dots, 10\}$) are the generators of the Clifford algebra in 10 dimensions and Γ_{ijk} and Γ_{ijklm} denote the antisymmetrized products of three and five generators, respectively. The Yukawa matrices satisfy the relations

$$(Y^{(10)})_{gf} = (Y^{(10)})_{fg}, \quad (Y^{(120)})_{gf} = -(Y^{(120)})_{fg}, \quad (Y^{(126)})_{gf} = (Y^{(126)})_{fg}. \quad (1.35)$$

We consider the decomposition of the Higgs fields into representations of G_{422} , given by (see e.g. [40])

$$\{ \mathbf{10} \}_{\text{SO}(10)} = (\mathbf{1}, \mathbf{2}, \mathbf{2})_{G_{422}} + (\mathbf{6}, \mathbf{1}, \mathbf{1})_{G_{422}}, \quad (1.36a)$$

$$\begin{aligned} \{ \mathbf{120} \}_{\text{SO}(10)} &= (\mathbf{1}, \mathbf{2}, \mathbf{2})_{G_{422}} + (\mathbf{10}, \mathbf{1}, \mathbf{1})_{G_{422}} + (\overline{\mathbf{10}}, \mathbf{1}, \mathbf{1})_{G_{422}} \\ &\quad + (\mathbf{6}, \mathbf{3}, \mathbf{1})_{G_{422}} + (\mathbf{6}, \mathbf{1}, \mathbf{3})_{G_{422}} + (\mathbf{15}, \mathbf{2}, \mathbf{2})_{G_{422}}, \end{aligned} \quad (1.36b)$$

$$\begin{aligned} \{ \mathbf{126} \}_{\text{SO}(10)} &= (\mathbf{6}, \mathbf{1}, \mathbf{1})_{G_{422}} + (\mathbf{10}, \mathbf{3}, \mathbf{1})_{G_{422}} + (\overline{\mathbf{10}}, \mathbf{1}, \mathbf{3})_{G_{422}} \\ &\quad + (\mathbf{15}, \mathbf{2}, \mathbf{2})_{G_{422}}. \end{aligned} \quad (1.36c)$$

We see that the triplets and bi-doublets, which we have already encountered in the Pati-Salam models, are contained in the SO(10)-Higgses. Since all the fermions belong to one representation, we have additional predictions for the Yukawa couplings to the various Higgses.

If fermion masses are generated by one $\{ \mathbf{10} \}_{\text{SO}(10)}$, which contains the bi-doublet $(\mathbf{1}, \mathbf{2}, \mathbf{2})_{G_{422}}$, we obtain the prediction

$$Y_u = Y_\nu = Y_d = Y_e \quad (1.37)$$

at the GUT scale and the property that the Yukawa matrices are symmetric.

The Higgs $\{ \mathbf{126} \}_{\text{SO}(10)}$ contains the bi-doublet $(\mathbf{15}, \mathbf{2}, \mathbf{2})_{G_{422}}$, which is in a non-trivial representation of $\text{SU}(4)_C$ and leads to symmetric Yukawa matrices which satisfy

$$Y_\nu = -3Y_u, \quad Y_e = -3Y_d. \quad (1.38)$$

It also contains the representations $(\mathbf{10}, \mathbf{3}, \mathbf{1})_{G_{422}}$ and $(\overline{\mathbf{10}}, \mathbf{1}, \mathbf{3})_{G_{422}}$. The latter can yield a $B-L$ -breaking Majorana mass term for the right-handed neutrinos,

$$(Y^{(126)})^{gf} v_{126} \overline{N}_R^g N_R^{Cf} , \quad (1.39)$$

whereas the first can obtain an induced vev, required for a type II see-saw. The discussion, whether a type I or type II see-saw mechanism is realized, is quite similar to the case of the minimal left-right models.

From the Higgs $\{\mathbf{120}\}_{\text{SO}(10)}$, which contains $(\mathbf{15}, \mathbf{2}, \mathbf{2})_{G_{422}}$ as well as $(\mathbf{1}, \mathbf{2}, \mathbf{2})_{G_{422}}$, there can be antisymmetric contributions to the Yukawa matrices.

Note that it is also possible to introduce an effective operator containing two Higgses $\{\mathbf{16}\}_{\text{SO}(10)}$ and two fermion representations $\mathbf{16}_{\text{SO}(10)}^f$, which gives Majorana masses for the right-handed neutrinos after the Higgs acquires a vev.

In summary, we find that the description of neutrino masses by the lowest dimensional effective operator, realized within a see-saw scenario, is rather natural from the point of view of left-right symmetric extensions of the SM. As we have seen, quark-lepton unification in Pati-Salam models or grand unification within $\text{SO}(10)$ can lead to various constraints for generating neutrino masses. In many models based on these scenarios, further effective operators and/or horizontal symmetries are introduced in order to be predictive and realistic (see e.g. [41–47]). One main problem is to explain the large, but not maximal mixing angle θ_{12} in the lepton sector, which in many cases requires unwanted fine-tuning. However, the discussion of such models is beyond the scope of this thesis. Instead, we will focus of the RG evolution of neutrino masses, lepton mixings and CP phases, which is required in order to compare the predictions for them with the experimental results.

1.5 Dynamical Electroweak Symmetry Breaking by a Neutrino Condensate

In order to break the electroweak symmetry, in the SM the Higgs scalar field is introduced. However, as has been shown in the context of top condensation [48,49], the Higgs can be a composite particle formed dynamically by two fermions. While the minimal models of top condensation predict too large top quark and Higgs masses, we have shown that it is possible to realize this mechanism in a phenomenologically acceptable way with neutrinos alone [50]. The reason for the prediction of a large top quark mass is the compositeness-condition of a large, non-perturbative top-quark Yukawa coupling at the condensation scale. Neutrino condensation is a possible alternative, since neutrinos can have Yukawa couplings which are even larger than that of the top, if the smallness of neutrino masses is explained by the see-saw mechanism. Clearly, if the singlet neutrinos completely decoupled at low energy and could thus be integrated out of the theory, no condensation of neutrinos would be possible. From a detailed analysis of the coupled non-perturbative Dirac-Majorana gap equation, however, we will see that it is possible to obtain a dynamical realization of EW symmetry breaking by neutrino condensation.

We will now show the essential aspects of such a scenario. For simplification, we consider only one generation of condensing neutrinos. Instead of the SM Higgs field we assume an effective four-fermion coupling involving a lepton doublet and a singlet neutrino,

$$\mathcal{L}_{4\nu} = G^{(\nu)} (\bar{\ell}_L N_R)(\bar{N}_R \ell_L). \quad (1.40)$$

We further assume a large Majorana mass $\mathcal{L}_M = -\frac{1}{2}M \bar{N}_R N_R^C + \text{h.c.}$ for the singlet. In order to determine, whether the four-fermion interaction leads to the formation of a condensate, we solve the coupled Dirac-Majorana gap equations. If a non-trivial solution produces dynamically a large Dirac mass term, it breaks the EW symmetry and a neutrino condensate forms, which effectively acts as the SM Higgs particle (see figure 1.6). The presence of the huge singlet Majorana mass will then lead to a dynamical see-saw mechanism with small neutrino masses.

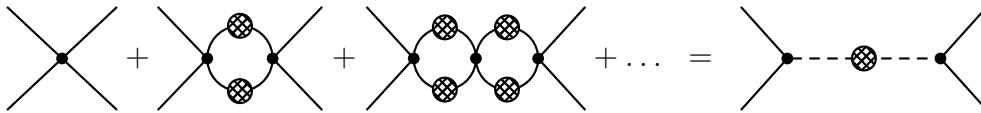


Figure 1.6: The exchange of a virtual composite Higgs scalar can be seen as a sum over all loop contributions involving the four-fermion vertex in the so-called bubble sum approximation. Hatched blobs denote full propagators.

1.5.1 Mass Eigenbasis for the Dynamical See-Saw Mechanism

We will now study in detail the dynamical generation of neutrino masses. A computation of the gap equation in the basis of mass eigenstates must therefore include in a self-consistent way the possibility of a dynamically generated Dirac mass term,

$$\mathcal{L}_D = -D \bar{\nu}_L N_R + \text{h.c.} . \quad (1.41)$$

For any value of D , the mass eigenstates are two Majorana fermions, given by

$$\begin{pmatrix} \lambda \\ \rho \end{pmatrix} = U \cdot \begin{pmatrix} \lambda' \\ \rho' \end{pmatrix}, \quad U = \begin{pmatrix} \cos \varphi & \sin \varphi \\ -\sin \varphi & \cos \varphi \end{pmatrix} =: \begin{pmatrix} c & s \\ -s & c \end{pmatrix}, \quad (1.42)$$

with $\lambda' := \nu_L + \nu_L^C$ and $\rho' := N_R + N_R^C$. The corresponding mass eigenvalues

$$m_\lambda = \frac{1}{2} \left(M - \sqrt{4D^2 + M^2} \right), \quad m_\rho = \frac{1}{2} \left(M + \sqrt{4D^2 + M^2} \right) \quad (1.43)$$

are related to φ by $\varphi = \arctan \sqrt{-m_\lambda/m_\rho}$. For convenience, we rewrite the singlet Majorana mass term as well as the neutrino part of the four-fermion interaction (1.40) in terms of Majorana fermions,

$$\begin{aligned} -\mathcal{L}_M &= \frac{1}{2} M \bar{N}_R N_R^C + \text{h.c.} = \frac{1}{2} M \bar{\rho}' P_R \rho'^C + \text{h.c.} = \frac{1}{2} M \bar{\rho}' \rho', \\ \mathcal{L}_{4\nu} &= G^{(\nu)} (\bar{\nu}_L N_R) (\bar{N}_R \nu_L) = G^{(\nu)} (\bar{\lambda}' P_R \rho') (\bar{\rho}' P_L \lambda'). \end{aligned} \quad (1.44)$$

Using equation (1.42), for the calculation of the gap equations it is useful to change basis to the Majorana fermions λ and ρ .

1.5.2 The Coupled Dirac-Majorana Gap Equations

The non-perturbative gap equations for the masses m_λ and m_ρ are given in diagrammatic form in figure 1.7. They correspond to the Bethe-Salpeter equation with a four-fermion interaction in the bubble sum approximation. The calculation yields

$$m_\lambda = 2G^{(\nu)} c^2 s^2 [m_\lambda I_{\text{gap}}(m_\lambda) - m_\rho I_{\text{gap}}(m_\rho)] + s^2 M, \quad (1.45a)$$

$$m_\rho = 2G^{(\nu)} c^2 s^2 [m_\rho I_{\text{gap}}(m_\rho) - m_\lambda I_{\text{gap}}(m_\lambda)] + c^2 M. \quad (1.45b)$$

We have introduced

$$-\frac{1}{2} I_{\text{gap}}(m) := \frac{\Lambda^2}{16\pi^2} \left[1 - \frac{m^2}{\Lambda^2} \ln \left(\frac{\Lambda^2}{m^2} + 1 \right) \right], \quad (1.46)$$

where Λ is the condensation scale, which acts as a cutoff. Since $m_\lambda + m_\rho = M$, as can be seen from equation (1.43), the gap equations are linearly dependent. It is

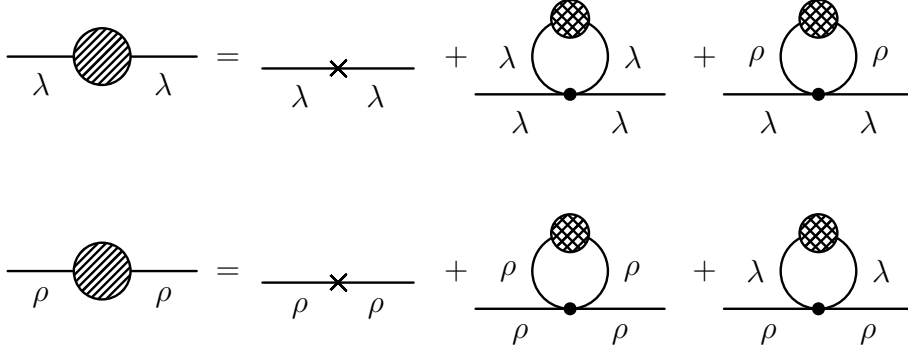


Figure 1.7: Gap equations for m_λ , the mass eigenvalue of the light neutrino, and m_ρ , the mass eigenvalue of the heavy neutrino. The direct Majorana mass, which is not of dynamical origin, is indicated by a cross. The shaded blobs on the left side are the OPI 2-point vertex functions, whereas the hatched blobs on the right side are full propagators.

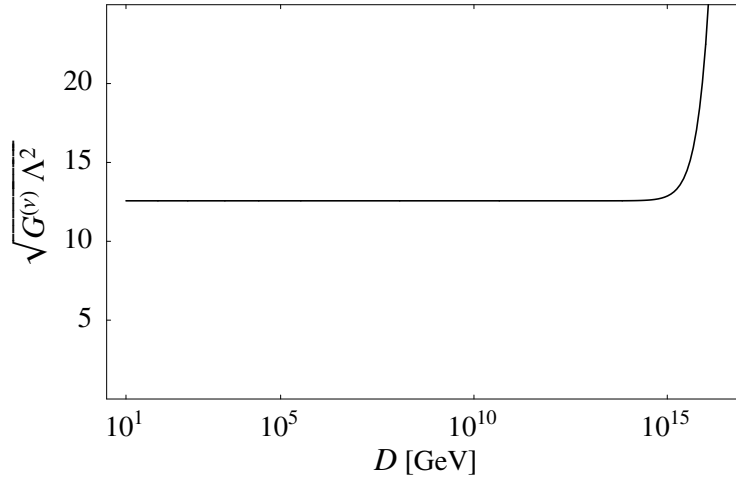


Figure 1.8: Characteristic numerical solution of the gap equation for the four-fermion coupling $G^{(\nu)}$ and the dynamically generated Dirac mass D with a Majorana mass $M = 10^{14}$ GeV and a condensation scale $\Lambda = 10^{16}$ GeV.

thus sufficient to solve one of them. Note that non-trivial solutions for m_λ and m_ρ also imply a dynamically generated Dirac mass D .

The gap equation (1.45a) for m_λ can be considered as an equation for $G^{(\nu)}$ and D , if fixed values are assigned to M and Λ . For $M = 10^{14}$ GeV and $\Lambda = 10^{16}$ GeV, the solution is shown in figure 1.8. Instead of $G^{(\nu)}$, we plot the dimensionless coupling constant $g = \sqrt{G^{(\nu)}}\Lambda^2$. We find non-trivial solutions for D , if the coupling g is larger than a critical value. This result is quite similar to top condensation [48], even though the right-handed neutrino has a large Majorana mass. We should note that such solutions do not appear, if M is larger than the condensation scale.

In order to obtain a Dirac mass of the order of the EW scale, in the used bubble sum approximation some fine-tuning is required, as can be seen from the extremely small slope of the graph in figure 1.8. Even if the same fine-tuning is present in the exact gap equation, loop corrections, which destabilize the hierarchy in the usual perturbative framework, do not pose an additional problem here. The destabilization of the hierarchy by radiative corrections is part of the so-called hierarchy problem. The other part is the missing explanation why the EW vev $v_{\text{EW}} \approx 246$ GeV and accordingly the Higgs mass is so much lower than the fundamental Planck scale, which is of the order of 10^{19} GeV. Given that viewpoint, the dynamical scenario under consideration solves the first part of the hierarchy problem.

1.5.3 Implications for Neutrino Masses

The neutrino condensation scenario can be extended to include masses for the other fermions of the SM as well. Following the method of [48], one can show that the effective theory below the condensation scale is just the SM extended by heavy singlets with additional boundary conditions. The latter imply that the neutrino Yukawa coupling is non-perturbatively large in the energy range where the condensate forms. In order to compare this prediction from the condensation scale with bounds on neutrino masses obtained at low-energy experiments, we have to calculate their energy scale dependence. Below the mass scales of the heavy singlets, the neutrino masses can be effectively described by the dimension 5 neutrino mass operator. It turns out that with $\Lambda \approx M_{\text{GUT}}$, due to the see-saw and a strong energy scale dependence of the neutrino Yukawa couplings, small neutrino masses far below the present bounds are possible in this scenario [50].

2 The β -Functions for the Effective Neutrino Mass Matrix

In the previous chapter, we have investigated possibilities for generating neutrino masses in extensions of the SM, restricting ourselves to rather minimal examples. We have found that they can be introduced in a minimal and quite model-independent way by the lowest dimensional effective operator allowed by gauge symmetry.

In order to determine the energy scale dependence of the neutrino mass matrix, we first calculate the RGEs for the effective neutrino mass operator. They govern its energy scale dependence in the energy range where the effective description discussed in section 1.3 can be applied. The calculations are performed at 1-loop in the SM and in a class of 2HDMS, where the previous results in the literature turn out to be not entirely correct. In the MSSM, we confirm the existing 1-loop result by a calculation in component fields and, using supergraph techniques, we extend it to the 2-loop level.

As we have seen, there are many possibilities for realizing the neutrino mass operator radiatively or at tree-level within a renormalizable theory. The tree-level realizations from integrating out heavy singlet fermions and/or Higgs triplets naturally appear for instance in left-right-symmetric extensions of the SM or MSSM and have been introduced in section 1.2.3 as type I and type II see-saw mechanisms.

We will study these types of scenarios in a minimal approach, where only singlets with large intermediate scale masses are explicitly added to the particle spectrum. Other particles, which correspond to the generation of a type II see-saw or to some GUT-model degrees of freedom, are assumed to be so heavy that they are already integrated out of the theory. We explicitly perform the tree-level matching for the singlets and the triplet and compute the RGEs of the effective neutrino mass matrix in the various effective theories between and above the mass thresholds of the singlets.

Before we turn to the calculations, we give a brief introduction to renormalization and introduce the RGEs. We further derive a general method for calculating RGEs from counterterms, which works for tensorial quantities.

2.1 Preliminaries on Renormalization

The naive calculation of loop diagrams, required in order to calculate quantum corrections to physical processes, yields divergent results in many cases. At the first glance, this seems to be a disaster. However, quantum field theories are most likely effective theories which are no longer valid at least at energy scales of the order of the Planck scale. If loop diagrams are calculated, integrations of the momenta of the particles running in the loop from zero to infinity are performed, which would be only entirely adequate if the theory provided a correct description at all energy scales. This is a possible origin of the appearing divergences. Nevertheless, in order to make sense out of quantum field theory, a method of dealing with these divergences has to be found.

The first step is to render the theory tentatively finite by introducing a regulator which isolates the divergencies. One typical example is a cutoff which introduces an upper limit for the integration over momentum. In this thesis we use dimensional regularization, which defines the theory formally in $d := 4 - \epsilon$ dimensions. The divergences are recovered as ϵ goes to zero. In d dimensions, the mass dimensions of fermion, scalar and gauge fields are given by $[\psi] = \frac{d-1}{2}$, $[\phi] = \frac{d-2}{2}$ and $[A] = \frac{d-2}{2}$. Since the mass dimension of the Lagrangian is d and we would like to maintain the mass dimensions of the couplings as they are in 4 dimensions, we have to introduce a mass dependent quantity, the so-called renormalization scale μ , in the interaction terms of the Lagrangian. E.g. for the neutrino mass operator, we have to replace $\kappa \rightarrow \mu^\epsilon \kappa$. The calculation of loop diagrams now leads to isolated infinities in terms of poles in ϵ .

However, even if the theory was completely finite, it should be kept in mind that the bare physical quantities, i.e. couplings, masses and fields which would appear in the Lagrangian of a free field theory, are generally shifted in the presence of interactions. The usual strategy is to reformulate the theory in terms of new, i.e. the shifted quantities. This is the method of renormalization and the introduced quantities are called renormalized. Of course, in particle physics the interactions cannot be turned off and consequently the bare quantities are not directly observable. However, they can in principle be extracted from the comparison of physical processes with calculations which include the quantum corrections. In practice, perturbation theory in the couplings is performed, which is truncated after a given order. The divergent loop diagrams then lead to divergent bare quantities, which absorb the infinities.

We now introduce renormalized quantities, which we define to be finite, and resolve the formal problem of the divergent bare quantities by regularization. We then reformulate the theory in terms of the renormalized quantities and the so-called renormalization constants Z_{ϕ_i} and $\delta Q^{(j)}$, which leads to a Lagrangian

$$\mathcal{L}_B = \mathcal{L}_R + \mathcal{C} \ , \tag{2.1}$$

where only renormalized quantities appear on the right side and \mathcal{L}_R and the coun-

terterm Lagrangian \mathcal{L} have the same form as \mathcal{L}_B . The relation between the bare and the renormalized quantities has the general form

$$\phi_B^{(i)} = Z_{\phi_i}^{1/2} \phi_R^{(i)} \quad \text{with} \quad Z_{\phi_i}^{1/2} = 1 + \delta Z_{\phi_i}^{1/2} \quad (2.2)$$

for fields and

$$Q_B^{(j)} = [Q_R^{(j)} + \delta Q^{(j)}] \prod_i Z_{\phi_i}^{n_i} \quad (2.3)$$

for scalar valued couplings, with all divergences absorbed in the renormalization constants. The index R to denote renormalized quantities will be omitted in the following. Theories which can be made finite by this method to any given loop-order in perturbation theory are called renormalizable. Obviously, the counterterms are not uniquely defined by this requirement. Finite terms can be added to them, which is the freedom to choose a specific renormalization scheme. In this work, we will make use of the mass independent Minimal Subtraction (MS) scheme [51], where just the poles in ϵ are absorbed by the counterterms. For a comprehensive treatment of renormalization theory, see e.g. [52].

It has been proven that gauge theories like the SM are renormalizable [53–55]. Generation of masses via SSB is compatible with renormalization, since the gauge symmetry is still present, it is just non-linearly realized. Explicitly, the counterterms calculated in the unbroken phase still renormalize the theory after SSB in the broken phase. We will make use of this property and calculate the counterterms, and thus as we will see also the RGEs, in the unbroken phase.

Finally, in this thesis we will deal with the effective neutrino mass operator, which has mass dimension 5 and is thus strictly speaking non-renormalizable by power-counting. However, as we have seen in section 1.3, in effective theories such operators are suppressed by the inverse of a large mass scale Λ , which is of the order of the scale where the operator is realized by a “full” theory. In this case it is possible to renormalize the theory by performing an expansion in $1/\Lambda$ to a given order.

2.1.1 Renormalization Group Equations

We will now introduce the RGEs and show their relation to the energy scale dependence of one particle irreducible (OPI) vertex functions, which appear as effective parameters in the effective action. For simplicity and since the generalization is straightforward, we consider just one field and one coupling, like e.g. in φ^4 theory. The bare n -point OPI vertex function $\Gamma_B^{(n)}$ and the renormalized n -point OPI vertex function $\Gamma^{(n)}$ are related by

$$\Gamma^{(n)}(\{p_i\}, \lambda, m, \mu_0, \epsilon) = Z_{\phi}^{\frac{n}{2}} \Gamma_B^{(n)}(\{p_i\}, \lambda_B, m_B, \epsilon), \quad i \in \{1, \dots, n\}. \quad (2.4)$$

$\Gamma_{\text{B}}^{(n)}$ is μ_0 -independent by definition, which yields

$$\begin{aligned} 0 &= \mu_0 \frac{d}{d\mu_0} Z_i^{-\frac{n}{2}} \Gamma^{(n)}(\{p_i\}, \lambda, m, \mu_0, \epsilon) \\ &= \left[\mu_0 \frac{\partial}{\partial \mu_0} + \beta_\lambda \frac{\partial}{\partial \lambda} + \gamma_m m \frac{\partial}{\partial m} - n\gamma_Z \right] \Gamma^{(n)}(\{p_i\}, \lambda, m, \mu_0, \epsilon), \end{aligned} \quad (2.5)$$

defining the functions β_λ, γ_m and γ_Z . μ_0 is an arbitrary but fixed scale introduced in dimensional regularization. λ and m are renormalized quantities, where the MS scheme with renormalization scale μ_0 has been used. Scaling of μ_0 by a factor e^t leads to

$$0 = \left[\frac{\partial}{\partial t} + \beta_\lambda \frac{\partial}{\partial \lambda} + \gamma_m m \frac{\partial}{\partial m} - n\gamma_Z \right] \Gamma^{(n)}(\{p_i\}, \lambda, m, \mu_0 e^t, \epsilon). \quad (2.6)$$

Its solution can be written in the form

$$\Gamma^{(n)}(\{p_i\}, \lambda, m, \mu_0 e^{-t}, \epsilon) = \Gamma^{(n)}(\{p_i\}, \lambda(t), m(t), \mu_0, \epsilon) e^{-n \int_0^t dt' \gamma_Z(t')}, \quad (2.7)$$

where $\lambda(t)$ and $m(t)$ are the so-called running quantities. They are defined as solutions to the RGEs

$$\frac{d\lambda(t)}{dt} = \mu \frac{d\lambda(\mu)}{d\mu} = \beta_\lambda, \quad \lambda(t=0) \stackrel{!}{=} \lambda, \quad (2.8)$$

$$\frac{dm(t)}{dt} = \mu \frac{dm(\mu)}{d\mu} = \gamma_m m \equiv \beta_m, \quad m(t=0) \stackrel{!}{=} m, \quad (2.9)$$

where we have defined $\mu = \mu_0 e^t$. The right-hand sides of the RGEs, β_λ and β_m , are referred to as β -functions. Equation (2.7) gives the dependence of $\Gamma^{(n)}$ on the change of the renormalization scale. The coupling λ is assumed to have mass dimension D_λ .

Equation (2.7) can be used to derive the dependence of $\Gamma^{(n)}$ on the scaling of the external momenta $\{p_i\}$ by a factor e^t , which corresponds e.g. to the scaling of the center of mass energy of some physical scattering process. Note that this is only possible for massless external particles. The masses of particles propagating in the theory are generally problematic in mass independent schemes, since they are insensitive to mass-thresholds. We thus remark that in practice we work in energy ranges where we either can assume the particles as massless or integrate them out of the theory. The latter is adequate far below the mass scales of the particles if they decouple [56]. If we use the naive scaling of an OPI vertex function $\Gamma^{(n)}$ with mass dimension D_Γ ,

$$\Gamma^{(n)}(\{e^t p_i\}, e^{D_\lambda t} \lambda, e^t m, \mu_0 e^t, \epsilon) = e^{D_\Gamma t} \Gamma^{(n)}(\{p_i\}, \lambda, m, \mu_0, \epsilon), \quad (2.10)$$

we obtain the formula

$$\begin{aligned}
 & \Gamma^{(n)}(\{e^t p_i\}, \lambda, m, \mu_0, \epsilon) \\
 & \stackrel{(2.7)}{=} \Gamma^{(n)}(\{e^t p_i\}, e^{D\lambda t} e^{-D\lambda t} \lambda(t), e^t e^{-t} m(t), \mu_0 e^t, \epsilon) e^{-n \int_0^t dt' \gamma_{Z_i}(t')} \\
 & \stackrel{(2.10)}{=} e^{D\Gamma t} \Gamma^{(n)}(\{p_i\}, e^{-D\lambda t} \lambda(t), e^{-t} m(t), \mu_0, \epsilon) e^{-n \int_0^t dt' \gamma_{Z_i}(t')} .
 \end{aligned} \tag{2.11}$$

Equation (2.11) shows that the energy scale dependence of the vertices is governed by the running of the physical quantities, which are the solutions of the RGEs. The OPI vertex functions give the coefficients of the terms in the effective action, e.g. the effective couplings or masses. Therefore, in order to find the energy scale dependence of neutrino masses, lepton mixings and CP phases, we have to calculate the RGE for the effective neutrino mass matrix.

2.1.2 Calculating RGEs from Tensor-Valued Counterterms

The counterterms for a given loop order are calculated from the requirement that all n -point vertex functions be finite. In mass-independent (MS-like) renormalization schemes, they only absorb constant finite terms in addition to the divergences. In order to calculate the counterterms, it is sufficient to consider the OPI diagrams. We now generalize the usual formalism for calculating β -functions in MS-like renormalization schemes to include tensorial quantities as well as non-multiplicative renormalization. The β -function for a quantity Q is defined as

$$\beta_Q := \mu \frac{dQ}{d\mu} . \tag{2.12}$$

For scalar valued couplings, the relations of the bare and renormalized quantities are given by the equations (2.2) and (2.3). For the tensor valued case, this has to be generalized to

$$\begin{aligned}
 Q_B &= Z_{\phi_1}^{n_1} \cdots Z_{\phi_M}^{n_M} [Q + \delta Q] \mu^{D_Q \epsilon} Z_{\phi_{M+1}}^{n_{M+1}} \cdots Z_{\phi_N}^{n_N} \\
 &= \left(\prod_{i \in I} Z_{\phi_i}^{n_i} \right) [Q + \delta Q] \mu^{D_Q \epsilon} \left(\prod_{j \in J} Z_{\phi_j}^{n_j} \right) ,
 \end{aligned} \tag{2.13}$$

where $I = \{1, \dots, M\}$, $J = \{M+1, \dots, N\}$ and D_Q is related to the mass dimension of Q . δQ and the wavefunction renormalization constants depend on Q and some additional variables $\{V_A\}$,

$$\delta Q = \delta Q(Q, \{V_A\}) , \tag{2.14a}$$

$$Z_{\phi_i} = Z_{\phi_i}(Q, \{V_A\}) , \quad (1 \leq i \leq N) . \tag{2.14b}$$

The renormalized quantities $Q = Q(\mu)$ and $V_A = V_A(\mu)$ are functions of the renormalization scale μ . We now use the fact that Q_B is independent of μ by definition

and that δQ and Z_{ϕ_i} do not depend explicitly on μ in an MS-like renormalization scheme. We thus obtain

$$\begin{aligned}
 0 \stackrel{!}{=} & \mu^{-D_Q \epsilon} \mu \frac{d}{d\mu} Q_B \stackrel{(2.13)}{=} \left(\prod_{i \in I} Z_{\phi_i}^{n_i} \right) \left[\beta_Q + \left\langle \frac{d\delta Q}{dQ} \middle| \beta_Q \right\rangle + \right. \\
 & \left. + \sum_A \left\langle \frac{d\delta Q}{dV_A} \middle| \beta_{V_A} \right\rangle + \epsilon D_Q (Q + \delta Q) \right] \left(\prod_{j \in J} Z_{\phi_j}^{n_j} \right) \\
 & + \left(\prod_{i \in I} Z_{\phi_i}^{n_i} \right) [Q + \delta Q] \left\{ \sum_{j \in J} \left(\prod_{j' < j} Z_{\phi_{j'}}^{n_{j'}} \right) \times \right. \\
 & \left. \times \left[\left\langle \frac{dZ_{\phi_j}^{n_j}}{dQ} \middle| \beta_Q \right\rangle + \sum_A \left\langle \frac{dZ_{\phi_j}^{n_j}}{dV_A} \middle| \beta_{V_A} \right\rangle \right] \left(\prod_{j'' > j} Z_{\phi_{j''}}^{n_{j''}} \right) \right\} \\
 & + \left\{ \sum_{i \in I} \left(\prod_{i' < i} Z_{\phi_{i'}}^{n_{i'}} \right) \left[\left\langle \frac{dZ_{\phi_i}^{n_i}}{dQ} \middle| \beta_Q \right\rangle + \sum_A \left\langle \frac{dZ_{\phi_i}^{n_i}}{dV_A} \middle| \beta_{V_A} \right\rangle \right] \times \right. \\
 & \left. \times \left(\prod_{i'' > i} Z_{\phi_{i''}}^{n_{i''}} \right) \right\} [Q + \delta Q] \left(\prod_{j \in J} Z_{\phi_j}^{n_j} \right), \tag{2.15}
 \end{aligned}$$

with $\langle \frac{dF}{dx} | y \rangle$ defined as $\frac{dF}{dx} y$ for scalars, $\sum_n \frac{dF}{dx_n} y_n$ for vectors, $\sum_{m,n} \frac{dF}{dx_{mn}} y_{mn}$ for matrices and analog for arbitrary tensors x, y . Equation (2.15) and the corresponding expression for V_A can be solved in an MS-like scheme by expanding all quantities in powers of $\epsilon := 4 - d$,

$$\delta Q = \sum_{k \geq 1} \frac{\delta Q_{,k}}{\epsilon^k}, \tag{2.16a}$$

$$Z_{\phi_i} = \mathbb{1} + \sum_{k \geq 1} \frac{\delta Z_{\phi_i, k}}{\epsilon^k} =: \mathbb{1} + \delta Z_{\phi_i}. \tag{2.16b}$$

The β -functions, on the other hand, are of course finite as $\epsilon \rightarrow 0$. We can therefore make the ansatz

$$\beta_Q = \beta_Q^{(0)} + \epsilon \beta_Q^{(1)} + \cdots + \epsilon^n \beta_Q^{(n)}, \tag{2.17a}$$

$$\beta_{V_A} = \beta_{V_A}^{(0)} + \epsilon \beta_{V_A}^{(1)} + \cdots + \epsilon^n \beta_{V_A}^{(n)}, \tag{2.17b}$$

where n is an arbitrary integer. From (2.16) and (2.17) we find that

$$\frac{dZ_{\phi_i}^{n_i}}{dQ} = n_i Z_{\phi_i}^{n_i-1} \frac{dZ_{\phi_i}}{dQ} = n_i \frac{d\delta Z_{\phi_i}}{dQ} + \mathcal{O}\left(\frac{1}{\epsilon^2}\right) = \mathcal{O}\left(\frac{1}{\epsilon}\right), \tag{2.18}$$

where the lowest possible power of $\frac{1}{\epsilon}$ appearing on the right side of (2.18) is 1. An analogous relation holds for $Q \leftrightarrow V_A$. We now use these observations to analyze

equation (2.15). Starting with the inspection of the ϵ^n term, we find that $\beta_Q^{(n)}$ vanishes. From the analog of equation (2.15) for β_{V_A} , we obtain that $\beta_{V_A}^{(n)}$ vanishes as well. This argument, repeated for successively smaller positive powers of ϵ , implies that

$$\beta_Q^{(k)} = \beta_{V_A}^{(k)} = 0 \quad \forall k \in \{2, \dots, n\}, \quad (2.19a)$$

$$\beta_Q^{(1)} = -\epsilon D_Q Q, \quad (2.19b)$$

$$\beta_{V_A}^{(1)} = -\epsilon D_{V_A} V_A. \quad (2.19c)$$

Obviously, these terms do not contribute to the β -function in 4 dimensions, i.e. for $\epsilon \rightarrow 0$, but they are necessary to read off $\beta_Q^{(0)}$ from equation (2.15). Using the relations of equation (2.19), from equation (2.15) we obtain [57]

$$\begin{aligned} \beta_Q^{(0)} = & \left[D_Q \left\langle \frac{d\delta Q_{,1}}{dQ} \middle| Q \right\rangle + \sum_A D_{V_A} \left\langle \frac{d\delta Q_{,1}}{dV_A} \middle| V_A \right\rangle - D_Q \delta Q_{,1} \right] \\ & + Q \cdot \sum_{j \in J} n_j \left[D_Q \left\langle \frac{dZ_{\phi_j,1}}{dQ} \middle| Q \right\rangle + \sum_A D_{V_A} \left\langle \frac{dZ_{\phi_j,1}}{dV_A} \middle| V_A \right\rangle \right] \\ & + \sum_{i \in I} n_i \left[D_Q \left\langle \frac{dZ_{\phi_i,1}}{dQ} \middle| Q \right\rangle + \sum_A D_{V_A} \left\langle \frac{dZ_{\phi_i,1}}{dV_A} \middle| V_A \right\rangle \right] \cdot Q. \end{aligned} \quad (2.20)$$

Note that for complex quantities Q and V_A we have to treat the complex conjugates Q^* and V_A^* as additional independent variables. Formula (2.20) allows to calculate the β -functions for tensor valued β -functions from the counterterms. We have chosen a general form for the counterterm, in order to make the formula applicable to multiplicative as well as additive renormalization.

2.2 The Neutrino Mass Operator in Non-Supersymmetric Theories

The method of section 2.1.2 will now be applied to calculate the RGEs for the lowest dimensional effective neutrino mass operator at one loop order. For the models under consideration, the SM and a class of 2HDMs, we will proceed as follows: First, we define the counterterms and determine the relation between the bare and the renormalized couplings. Then we calculate the relevant counterterms in the MS scheme by the requirement that they just absorb the divergences of the corresponding OPI vertex functions. Finally, we apply the formula (2.20) to compute the RGE for the dimension 5 neutrino mass operator.

2.2.1 Calculation of the RGE in the SM

Following the strategy described above, we will now perform the calculation in the SM. The relevant Feynman rules are given in appendix A.3.1. In order to obtain the RGEs for the neutrino mass operator, we have to define and calculate the counterterms which enter the relation between the bare and the renormalized quantities κ_B and κ . The Lagrangian consists of $\mathcal{L}_{\text{SM}} + \mathcal{L}_\kappa$ and proper counterterms \mathcal{C}_{SM} and \mathcal{C}_κ . We define the counterterm for κ by

$$\mathcal{C}_\kappa = \frac{1}{4} \delta \kappa_{gf} \overline{\ell_{Lc}^g} \varepsilon^{cd} \phi_d \ell_{Lb}^f \varepsilon^{ba} \phi_a + \text{h.c.} . \quad (2.21)$$

From the definition

$$\mathcal{L}_{B\kappa} = \mathcal{L}_\kappa + \mathcal{C}_\kappa = \frac{1}{4} (\kappa_{gf} + \delta \kappa_{gf}) \overline{\ell_{Lc}^g} \varepsilon^{cd} \phi_d \ell_{Lb}^f \varepsilon^{ba} \phi_a + \text{h.c.} \quad (2.22)$$

we obtain the relation between κ_B and κ ,

$$\kappa_B = Z_\phi^{-\frac{1}{2}} (Z_{\ell_L}^T)^{-\frac{1}{2}} [\kappa + \delta \kappa] \mu^\epsilon Z_{\ell_L}^{-\frac{1}{2}} Z_\phi^{-\frac{1}{2}} . \quad (2.23)$$

The counterterms for the kinetic and mass terms for the Higgs and the charged lepton are defined as

$$\mathcal{C}_{\text{kin}(\ell_L)} = \overline{\ell_L^g} (i\gamma^\mu \partial_\mu) (\delta Z_{\ell_L})_{gf} \ell_L^f , \quad (2.24a)$$

$$\mathcal{C}_{\text{Higgs}} = \delta Z_\phi (\partial_\mu \phi)^\dagger (\partial^\mu \phi) - \delta m^2 \phi^\dagger \phi - \frac{1}{4} \delta \lambda (\phi^\dagger \phi)^2 . \quad (2.24b)$$

The δZ_i ($i \in \{\ell_L, \phi\}$) determine the wavefunction renormalization constants $Z_i = \mathbb{1} + \delta Z_i$. Note that Z_{ℓ_L} is a matrix in flavour space.

The next step is to calculate the renormalization constants $\delta \kappa$, δZ_{ℓ_L} and δZ_ϕ from the vertex corrections and self-energy diagrams, respectively. The 1-loop vertex corrections which contribute to the renormalization of the neutrino mass operator in the SM are shown in figure 2.1.

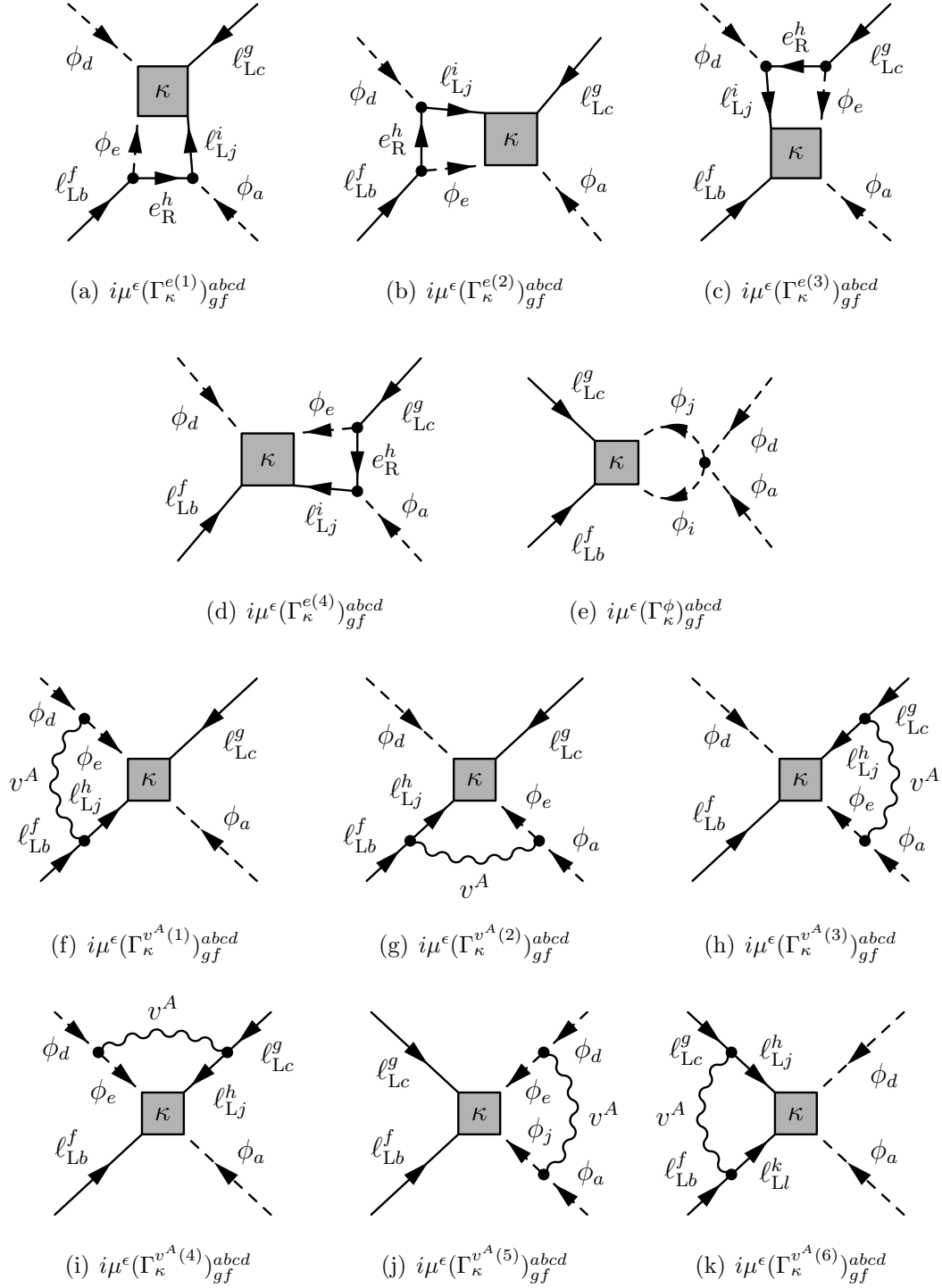


Figure 2.1: Contributions to the renormalization of the effective vertex. For the gauge bosons of $U(1)_Y$ and $SU(2)_L$, we use the condensed notation v^A with $(v^0, v^1, v^2, v^3) = (B, W^1, W^2, W^3)$.

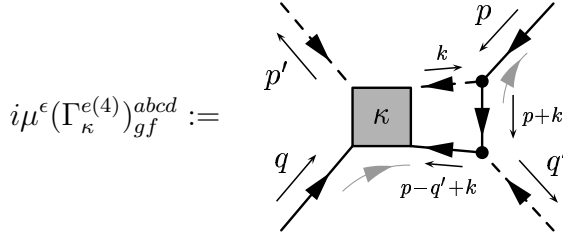
We will now calculate explicitly the diagrams (a) – (d) of figure 2.1. They contribute to the part of the β -function with a non-trivial flavour structure, where the existing RGEs [58,59] are not in agreement.

$$\begin{aligned}
 i\mu^\epsilon (\Gamma_\kappa^{e(1)})_{gf}^{abcd} &:= \text{Diagram (a)} \\
 &= [i\mu^\epsilon \kappa_{gi} \frac{1}{2} (\varepsilon_{cd} \varepsilon_{je} + \varepsilon_{ce} \varepsilon_{jd})] [-i\mu^{\frac{\epsilon}{2}} (Y_e^\dagger)_{ih} \delta_{aj}] [-i\mu^{\frac{\epsilon}{2}} (Y_e)_{hf} \delta_{eb}] \times \\
 &\quad \times \int \frac{d^d k}{(2\pi)^d} P_L \frac{i(q - q' + k)}{(q - q' + k)^2} P_R \frac{i(q + k)}{(q + k)^2} P_L \frac{i}{k^2 - m^2} \\
 &= \frac{i}{8\pi^2} \mu^\epsilon (\kappa Y_e^\dagger Y_e)_{gf} \frac{1}{2} (\varepsilon_{cd} \varepsilon_{ba} + \varepsilon_{cb} \varepsilon_{da}) P_L \frac{1}{\epsilon} + \text{UV finite} , \tag{2.25}
 \end{aligned}$$

$$\begin{aligned}
 i\mu^\epsilon (\Gamma_\kappa^{e(2)})_{gf}^{abcd} &:= \text{Diagram (b)} \\
 &= [i\mu^\epsilon \kappa_{gi} \frac{1}{2} (\varepsilon_{ca} \varepsilon_{je} + \varepsilon_{ce} \varepsilon_{ja})] [-i\mu^{\frac{\epsilon}{2}} (Y_e^\dagger)_{ih} \delta_{dj}] [-i\mu^{\frac{\epsilon}{2}} (Y_e)_{hf} \delta_{eb}] \times \\
 &\quad \times \int \frac{d^d k}{(2\pi)^d} P_L \frac{i(q - p' + k)}{(q - p' + k)^2} P_R \frac{i(q + k)}{(q + k)^2} P_L \frac{i}{k^2 - m^2} \\
 &= \frac{i}{8\pi^2} \mu^\epsilon (\kappa Y_e^\dagger Y_e)_{gf} \frac{1}{2} (\varepsilon_{ca} \varepsilon_{bd} - \varepsilon_{cb} \varepsilon_{da}) P_L \frac{1}{\epsilon} + \text{UV finite} , \tag{2.26}
 \end{aligned}$$

$$\begin{aligned}
 i\mu^\epsilon (\Gamma_\kappa^{e(3)})_{gf}^{abcd} &:= \text{Diagram (c)}
 \end{aligned}$$

$$\begin{aligned}
 &= [-i\mu^{\frac{\epsilon}{2}}(Y_e^T)_{gh}\delta_{ce}] [-i\mu^{\frac{\epsilon}{2}}(Y_e^*)_{hi}\delta_{dj}] [i\mu^\epsilon\kappa_{if}\frac{1}{2}(\varepsilon_{je}\varepsilon_{ba} + \varepsilon_{ja}\varepsilon_{be})] \times \\
 &\quad \times \int \frac{d^d k}{(2\pi)^d} P_L \frac{-i(\not{p} + \not{k})}{(p+k)^2} P_R \frac{-i(\not{p} - \not{p}' + \not{k})}{(p-p'+k)^2} P_L \frac{i}{k^2 - m^2} \\
 &= \frac{i}{8\pi^2} \mu^\epsilon (Y_e^T Y_e^* \kappa)_{gf} \frac{1}{2} (\varepsilon_{cd}\varepsilon_{ba} + \varepsilon_{cb}\varepsilon_{da}) P_L \frac{1}{\epsilon} + \text{UV finite} , \tag{2.27}
 \end{aligned}$$



$$\begin{aligned}
 i\mu^\epsilon (\Gamma_\kappa^{e(4)})_{gf}^{abcd} &:= \\
 &= [-i\mu^{\frac{\epsilon}{2}}(Y_e^T)_{gh}\delta_{ce}] [-i\mu^{\frac{\epsilon}{2}}(Y_e^*)_{hi}\delta_{aj}] [i\mu^\epsilon\kappa_{if}\frac{1}{2}(\varepsilon_{je}\varepsilon_{bd} + \varepsilon_{be}\varepsilon_{jd})] \times \\
 &\quad \times \int \frac{d^d k}{(2\pi)^d} P_L \frac{-i(\not{p} + \not{k})}{(p+k)^2} P_R \frac{-i(\not{p} - \not{q}' + \not{k})}{(p-q'+k)^2} P_L \frac{i}{k^2 - m^2} \\
 &= \frac{i}{8\pi^2} \mu^\epsilon (Y_e^T Y_e^* \kappa)_{gf} \frac{1}{2} (\varepsilon_{ca}\varepsilon_{bd} - \varepsilon_{cb}\varepsilon_{da}) P_L \frac{1}{\epsilon} + \text{UV finite} . \tag{2.28}
 \end{aligned}$$

In order to obtain the divergent parts, we substitute the integrals by Passarino-Veltman functions, defined in appendix A.2.3. The $\frac{1}{\epsilon}$ -poles of the Passarino-Veltman functions are known and summarized in table A.1. The reduction is also implemented in the package FeynCalc [60], which provides a useful way to check the results.

In addition to the counterterm for the vertex, the wavefunction renormalization constants are required. The Higgs self-energy diagrams are shown in figure 2.3, and the corresponding diagrams for the lepton doublet in figure 2.2. A detailed treatment of all relevant vertex corrections and self-energies can be found in [61]. The results for the $\frac{1}{\epsilon}$ -poles, required for the calculation of the renormalization constants, are listed in appendix A.4.1.

The wavefunction renormalization constants are calculated from the relations

$$0 = \sum_i \left(\Sigma_\phi^i \Big|_{\text{div}} \right) + (p^2 \delta Z_\phi - \delta m^2) , \tag{2.29a}$$

$$0 = \sum_i \left(\Sigma_{\ell_L}^i \Big|_{\text{div}} \right) + \not{p} \delta Z_{\ell_L} P_L = 0 , \tag{2.29b}$$

where the subscript “div” indicates the divergent part of the corresponding expression. The renormalization constant $\delta\kappa$ is determined by demanding that it exactly

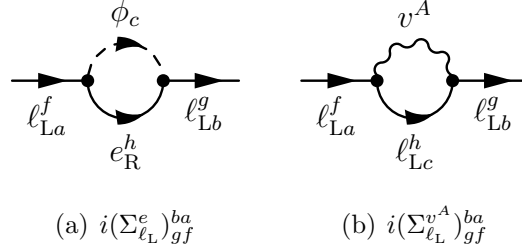


Figure 2.2: Self-energy diagrams for the leptonic doublets ℓ_L . We write v^A for the gauge bosons of $U(1)_Y$ and $SU(2)_L$.

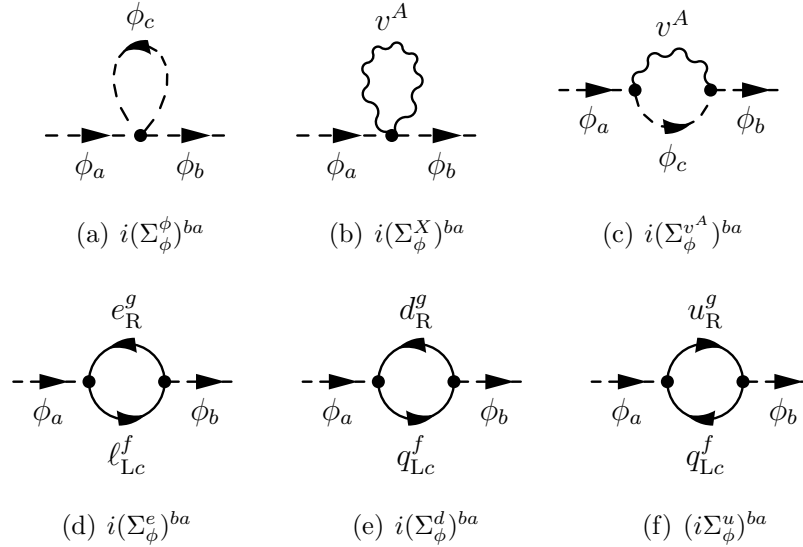


Figure 2.3: One-loop diagrams which potentially contribute to the computation of the self-energy of the Higgs field. For simplicity, the fermion flow is not shown explicitly here. For the gauge bosons of $U(1)_Y$ and $SU(2)_L$, we use the condensed notation v^A .

cancels the divergent part of sum of the the vertex corrections,

$$0 = \sum_i (\Gamma_\kappa^i)_{gf}^{abcd} \Big|_{\text{div}} + \delta\kappa_{gf} \frac{1}{2} (\varepsilon_{cd}\varepsilon_{ba} + \varepsilon_{ca}\varepsilon_{bd}) P_L. \quad (2.30)$$

From these requirements, we obtain for the counterterms

$$\delta Z_{\ell_L,1} = -\frac{1}{16\pi^2} (Y_e^\dagger Y_e + \frac{1}{2}\xi_B g_1^2 + \frac{3}{2}\xi_W g_2^2), \quad (2.31a)$$

$$\delta Z_{\phi,1} = -\frac{1}{16\pi^2} \left[2 \text{Tr} \left(Y_e^\dagger Y_e + 3Y_u^\dagger Y_u + 3Y_d^\dagger Y_d \right) - \frac{1}{2}(3 - \xi_B)g_B^2 - \frac{3}{2}(3 - \xi_W)g_2^2 \right], \quad (2.31b)$$

$$\delta\kappa_{,1} = -\frac{1}{16\pi^2} \left[2\kappa(Y_e^\dagger Y_e) + 2(Y_e^\dagger Y_e)^T \kappa - \lambda\kappa - \left(\frac{3}{2} - \xi_B\right)g_1^2\kappa - \left(\frac{3}{2} - 3\xi_W\right)g_2^2\kappa \right]. \quad (2.31c)$$

The β -function $\beta_\kappa := \mu \frac{d\kappa}{d\mu}$ for the dimension 5 neutrino mass operator can now be computed from formula (2.20). First, using equation (2.23), we find the relation

$$\beta_\kappa = \delta\kappa_{,1} - \frac{1}{2} (\delta Z_{\phi,1} + \delta Z_{\ell_L,1})^T \kappa - \frac{1}{2} \kappa (\delta Z_{\phi,1} + \delta Z_{\ell_L,1}). \quad (2.32)$$

Inserting the results from equation (2.31) for the counterterms finally results in [57]

$$16\pi^2 \beta_\kappa = -\frac{3}{2} \left[\kappa (Y_e^\dagger Y_e) + (Y_e^\dagger Y_e)^T \kappa \right] + \lambda\kappa - 3g_2^2\kappa + 2 \text{Tr} \left(3Y_u^\dagger Y_u + 3Y_d^\dagger Y_d + Y_e^\dagger Y_e \right) \kappa. \quad (2.33)$$

Compared to earlier results [59], we find a coefficient $-\frac{3}{2}$ instead of $-\frac{1}{2}$ in front of the term $\kappa(Y_e^\dagger Y_e) + (Y_e^\dagger Y_e)^T \kappa$ with a non-trivial flavour structure. Our result has been confirmed by an independent calculation [62]. We will apply it in chapter 3 in order to study the running of the neutrino mass matrix in the SM.

2.2.2 Calculation of the RGEs in 2HDMs

We now consider the renormalization of the effective neutrino mass matrix in extensions of the SM with a Higgs sector enlarged by an additional $SU(2)_L$ -doublet, $\phi^{(i)}$ ($1 \in \{1, 2\}$). As pointed out in [63–65], it is very hard to construct viable models in which one type of SM fermions e , d and u couples to two or more Higgs bosons, since this in general leads to tree-level flavor-changing neutral currents (FCNCs).

In order to avoid such FCNCs, we will therefore consider only schemes in which each of the right-handed SM fermions couples to exactly one Higgs boson. This can be achieved by imposing the \mathbb{Z}_2 symmetry $\phi^{(1)} \rightarrow \phi^{(1)}$, $\phi^{(2)} \rightarrow -\phi^{(2)}$ and corresponding transformations in the fermion sector. These only allow the schemes of table 2.1. For example, in scheme (ii) all fields transform trivially except for $\phi^{(2)} \rightarrow -\phi^{(2)}$ and $u \rightarrow -u$.

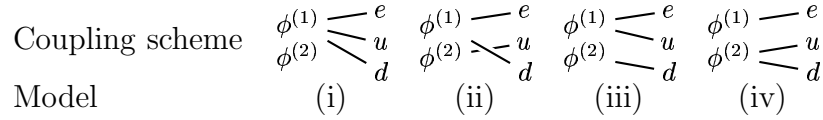


Table 2.1: Classification of the 2HDMs with natural suppression of FCNCs and tree-level mass terms for all SM fermions except neutrinos. Note that model (i) is usually referred to as “type I” and (ii) as “type II” in the literature.

By convention, the Higgs which couples to e is $\phi^{(1)}$. The Yukawa couplings of the Higgs doublets to the SM fermions are then given by

$$\begin{aligned}
 \mathcal{L}_{\text{Yukawa}}^{(i)} &= -(Y_e)_{gf} \overline{e}_R^g \phi_a^{(1)\dagger} \delta^{ab} \ell_L^f \\
 &\quad - \sum_{i=1}^2 z_d^{(i)} (Y_d)_{gf} \overline{d}_R^g \phi_a^{(i)\dagger} \delta^{ab} q_{Lb}^f - \sum_{i=1}^2 z_u^{(i)} (Y_u)_{gf} \overline{u}_R^g q_{Lb}^f \varepsilon^{ba} \phi_a^{(i)}, \quad (2.34)
 \end{aligned}$$

where the coefficients $z_d^{(i)}$ and $z_u^{(i)}$ for the models classified in table 2.1 are given in table 2.2. In the chosen notation, the $\phi^{(i)}$ transform as $(\mathbf{1}, \mathbf{2}, \frac{1}{2})$ under G_{321} .

	(i)	(ii)	(iii)	(iv)
$z_u^{(1)}$	1	0	1	0
$z_u^{(2)}$	0	1	0	1
$z_d^{(1)}$	1	1	0	0
$z_d^{(2)}$	0	0	1	1

Table 2.2: The coefficients $z_d^{(i)}$ and $z_u^{(i)}$ for the Two-Higgs-Doublet Models classified in table 2.1.

In the considered 2HDMs, there are two dimension 5 effective neutrino mass operators,

$$\begin{aligned} \mathcal{L}_\kappa = & \frac{1}{4} \kappa_{gf}^{(11)} \overline{\ell}_{Lc}^g \varepsilon^{cd} \phi_d^{(1)} \ell_{Lb}^f \varepsilon^{ba} \phi_a^{(1)} \\ & + \frac{1}{4} \kappa_{gf}^{(22)} \overline{\ell}_{Lc}^g \varepsilon^{cd} \phi_d^{(2)} \ell_{Lb}^f \varepsilon^{ba} \phi_a^{(2)} + \text{h.c.} . \end{aligned} \quad (2.35)$$

It is possible that only one of these operators arises from integrating out heavy degrees of freedom in a specific model. However, as we shall see, both mix due to the renormalization group evolution and therefore have to be taken into account simultaneously. As long as the discrete symmetry is valid, $\mathcal{L}_\kappa^{(11)}$ and $\mathcal{L}_\kappa^{(22)}$ represent the only possible dimension 5 operators containing two ℓ_L fields. The most general Higgs self-interaction Lagrangian compatible with the \mathbb{Z}_2 symmetry is

$$\begin{aligned} \mathcal{L}_{2\text{Higgs}} = & -\frac{\lambda_1}{4} (\phi^{(1)\dagger} \phi^{(1)})^2 - \frac{\lambda_2}{4} (\phi^{(2)\dagger} \phi^{(2)})^2 \\ & - \lambda_3 (\phi^{(1)\dagger} \phi^{(1)}) (\phi^{(2)\dagger} \phi^{(2)}) - \lambda_4 (\phi^{(1)\dagger} \phi^{(2)}) (\phi^{(2)\dagger} \phi^{(1)}) \\ & - \left[\frac{\lambda_5}{4} (\phi^{(1)\dagger} \phi^{(2)})^2 + \text{h.c.} \right] . \end{aligned} \quad (2.36)$$

We define the wavefunction renormalization constants analogous to the SM case. For the vertices, we need two counterterms for the two neutrino mass operators allowed by symmetry,

$$\begin{aligned} \mathcal{C}_\kappa = & \frac{1}{4} \delta \kappa_{gf}^{(11)} \overline{\ell}_{Lc}^g \varepsilon^{cd} \phi_d^{(1)} \ell_{Lb}^f \varepsilon^{ba} \phi_a^{(1)} \\ & + \frac{1}{4} \delta \kappa_{gf}^{(22)} \overline{\ell}_{Lc}^g \varepsilon^{cd} \phi_d^{(2)} \ell_{Lb}^f \varepsilon^{ba} \phi_a^{(2)} + \text{h.c.} . \end{aligned} \quad (2.37)$$

For the bare and the renormalized quantities we obtain the relations

$$\kappa_B^{(11)} = Z_{\phi^{(1)}}^{-\frac{1}{2}} (Z_{\ell_L}^T)^{-\frac{1}{2}} [\kappa^{(11)} + \delta \kappa^{(11)}] \mu^\epsilon Z_{\ell_L}^{-\frac{1}{2}} Z_{\phi^{(1)}}^{-\frac{1}{2}} , \quad (2.38a)$$

$$\kappa_B^{(22)} = Z_{\phi^{(2)}}^{-\frac{1}{2}} (Z_{\ell_L}^T)^{-\frac{1}{2}} [\kappa^{(22)} + \delta \kappa^{(22)}] \mu^\epsilon Z_{\ell_L}^{-\frac{1}{2}} Z_{\phi^{(2)}}^{-\frac{1}{2}} . \quad (2.38b)$$

The vertex corrections for the calculation of the counterterms $\delta \kappa^{(ii)}$ ($i = 1, 2$) are partly similar to the ones in the SM. For instance, the corrections for the flavour non-trivial part have the same structure as the diagrams (a) – (d) of figure 2.1 and the same holds for the gauge boson contributions, diagram (f) – (k) of figure 2.1. Note that for each diagram there are two potential counterparts with the exchange of a virtual $\phi^{(1)}$ and $\phi^{(2)}$. However, the contributions from the the diagrams with Higgs self-interactions are different and lead to a mixing of the two neutrino mass operators. They are shown in figure 2.4.

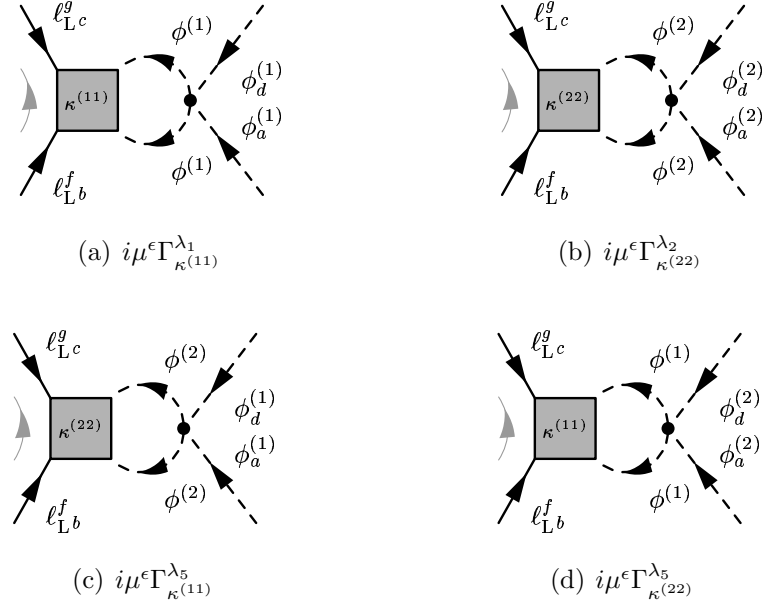


Figure 2.4: Vertex corrections containing Higgs self-interactions. The diagrams (c) and (d) lead to a mixing between the operators $\mathcal{L}_\kappa^{(11)}$ and $\mathcal{L}_\kappa^{(22)}$.

Let us consider diagram (c) as an example. The other diagrams can be calculated analogously.

$$\begin{aligned}
 i\mu^\epsilon (\Gamma_{\kappa^{(22)}}^{\lambda_5})_{gf}^{abcd} &:= \text{Diagram (c)} \\
 &= \frac{1}{2} \left[i\mu^\epsilon \kappa_{gf}^{(22)} \frac{1}{2} (\varepsilon_{bi} \varepsilon_{cj} + \varepsilon_{ci} \varepsilon_{bj}) \right] \left[-i\mu^\epsilon \lambda_5^* \frac{1}{2} (\delta_{ai} \delta_{dj} + \delta_{aj} \delta_{di}) \right] \times \\
 &\quad \times \int \frac{d^d k}{(2\pi)^d} P_L \frac{i}{(p+q+k)^2 - m_2^2} \frac{i}{k^2 - m_2^2} \\
 &= -\frac{i}{16\pi^2} \mu^\epsilon \lambda_5^* \kappa_{gf}^{(22)} \frac{1}{2} (\varepsilon_{ba} \varepsilon_{cd} + \varepsilon_{ca} \varepsilon_{bd}) P_L \frac{1}{\epsilon} + \text{UV finite} . \tag{2.39}
 \end{aligned}$$

The factor $\frac{1}{2}$ in the second line is a symmetry factor. The calculation of the wave-function renormalization constants in the 2HDMs is analogous to the SM case. The types of diagrams for the self-energies are similar to the ones shown in the figures 2.3 and 2.2. Differences occur for the self-energy diagrams of the Higgs fields, since

in a specific 2HDM, each of the Higgses couples only to some of the fermions, as defined in table 2.1. More details can be found in [66]. The $\frac{1}{\epsilon}$ -poles of the relevant vertex corrections and self-energies, which are required for the calculation of the renormalization constants, are listed in appendix A.4.2.

From the requirements

$$0 = \sum_i \left(\Sigma_{\phi^{(j)}}^i \Big|_{\text{div}} \right) + (p^2 \delta Z_\phi - \delta m_j^2), \quad (2.40a)$$

$$0 = \sum_i \left(\Sigma_{\ell_L}^i \Big|_{\text{div}} \right) + \not{p} \delta Z_{\ell_L} P_L = 0, \quad (2.40b)$$

$$0 = \sum_i \left(\Gamma_\kappa^i \Big|_{\text{div}} \right)^{abcd} + \delta \kappa_{gf} \frac{1}{2} (\varepsilon_{cd} \varepsilon_{ba} + \varepsilon_{ca} \varepsilon_{bd}) P_L, \quad (2.40c)$$

we determine the renormalization constants in the 2HDMs. This yields

$$\delta Z_{\phi^{(i)},1} = -\frac{1}{16\pi^2} \left[\delta_{i1} 2 \text{Tr}(Y_e^\dagger Y_e) + z_u^{(i)} 6 \text{Tr}(Y_u^\dagger Y_u) + z_d^{(i)} 6 \text{Tr}(Y_d^\dagger Y_d) \right. \\ \left. + \frac{1}{2} (\xi_B - 3) g_1^2 + \frac{3}{2} (\xi_W - 3) g_2^2 \right], \quad (2.41a)$$

$$\delta Z_{\ell_L,1} = -\frac{1}{16\pi^2} \left[Y_e^\dagger Y_e + \frac{1}{2} \xi_B g_1^2 + \frac{3}{2} \xi_W g_2^2 \right], \quad (2.41b)$$

$$\delta \kappa_{,1}^{(ii)} = -\frac{1}{16\pi^2} \left[\delta_{i1} 2 \kappa^{(ii)} (Y_e^\dagger Y_e) + \delta_{i1} 2 (Y_e^\dagger Y_e)^T \kappa^{(ii)} \right. \\ \left. - \lambda_i \kappa^{(ii)} - \delta_{i1} \lambda_5^* \kappa^{(22)} - \delta_{i2} \lambda_5 \kappa^{(11)} \right. \\ \left. + \left(\xi_B - \frac{3}{2} \right) g_1^2 \kappa^{(ii)} + \left(3\xi_W - \frac{3}{2} \right) g_2^2 \kappa^{(ii)} \right]. \quad (2.41c)$$

Using formula (2.20) and equation (2.38a), we obtain the relation

$$\beta_{\kappa^{(ii)}} = \delta \kappa_{,1}^{(ii)} - \frac{1}{2} (\delta Z_{\phi^{(i)},1} + \delta Z_{\ell_L,1})^T \kappa^{(ii)} - \frac{1}{2} \kappa^{(ii)} (\delta Z_{\phi^{(i)},1} + \delta Z_{\ell_L,1}), \quad (2.42)$$

which, by inserting (2.41), directly leads to the results [67]

$$16\pi^2 \beta_{\kappa^{(ii)}} = \left(\frac{1}{2} - 2\delta_{i1} \right) \left[\kappa^{(ii)} (Y_e^\dagger Y_e) + (Y_e^\dagger Y_e)^T \kappa^{(ii)} \right] \\ + \left[\delta_{i1} 2 \text{Tr}(Y_e^\dagger Y_e) + z_u^{(i)} 6 \text{Tr}(Y_u^\dagger Y_u) + z_d^{(i)} 6 \text{Tr}(Y_d^\dagger Y_d) \right] \kappa^{(ii)} \\ + \lambda_i \kappa^{(ii)} + \delta_{i1} \lambda_5^* \kappa^{(22)} + \delta_{i2} \lambda_5 \kappa^{(11)} - 3g_2^2 \kappa^{(ii)}. \quad (2.43)$$

The terms proportional to λ_5 are responsible for the mixing of the two effective neutrino mass operators. As in the SM, our result for $\beta_{\kappa^{(11)}}$ corrects the previous one [59] by a factor of 3 in the part with a non-trivial flavour structure.

2.3 The Neutrino Mass Operator in the MSSM

The β -function for the lowest dimensional effective operator for neutrino masses will now be calculated in the MSSM. For the calculations, we use two independent techniques: the component field formalism and the supergraph method. Before that, we give a brief introduction to $N=1$ supersymmetric extensions of the SM.

2.3.1 Preliminaries on $N=1$ Supersymmetric Theories

Supersymmetry is an extension of the external Poincaré symmetry group. According to the no-go theorem of Coleman and Mandula [68], there is no such extension by bosonic operators. Haag, Lopuszański and Sohnius [69] introduced fermionic operators Q_α^i and $\bar{Q}_{\dot{\alpha}}^i$ ($i = 1, \dots, N$), which generate supersymmetry (SUSY) transformations and satisfy the so-called super-Poincaré algebra. Since the MSSM is of the $N=1$ type, we will restrict ourselves to this case in the following. Acting on component fields, the SUSY-generators change the spin by half a unit, thus transforming fermions into bosons. Since supersymmetry is an extension of space-time symmetry, it is natural to extend space-time to a supermanifold with additional fermionic coordinates θ_α and $\bar{\theta}_{\dot{\alpha}}$. Fields defined on superspace contain bosons as well as fermions and auxiliary fields. The SUSY generators now generate the translations in the directions of the superspace coordinates. Comprehensive introductions to supersymmetric theories can e.g. be found in [70,71].

Supersymmetric extensions of the SM have some attractive properties. One of the most important is that they solve a part of the gauge hierarchy problem. Above the scale where SUSY is broken, the hierarchy between the EW scale and the Planck scale is stable against large radiative corrections due to cancellations of contributions from bosonic and fermionic loop diagrams. However, since no superpartner of a SM particle has been observed so far, SUSY has to be broken by some mechanism. In order to maintain the stabilization of the hierarchy of scales, the SUSY-breaking scales, i.e. the mass scales of the superpartners, should not be too far above the EW scale. It is remarkable that under this restriction, the MSSM has the property that the gauge couplings meet at $\approx 2 \cdot 10^{16}$ GeV. Though SUSY is a rather economical principle, which reduces the freedom for constructing Lagrangians, the fact that it has to be broken leads to a large number of additional parameters. Furthermore, usually the so-called R -parity is required in order to avoid unobserved large baryon number violation.¹ If R -parity is conserved, the lightest supersymmetric particle (LSP) is stable and provides an attractive candidate for cold dark matter.

¹It is possible to generate neutrino masses from small R -parity violating interactions (see e.g. [72]). In this thesis, however, we will restrict ourselves to the R -parity conserving case.

The General Lagrangian of $N=1$ Supersymmetric Theories

The Lagrangian of a general $N=1$ supersymmetric theory can be written as

$$\begin{aligned} \mathcal{L} = & \int d^2\theta d^2\bar{\theta} \sum_{i,j=1}^{N_\Phi} \bar{\Phi}^{(i)} [\exp(2g \cdot \mathbb{V})]_{ij} \Phi^{(j)} + \left[\frac{1}{4} \int d^2\theta \sum_{n=1}^S \mathbb{W}_\alpha^n \mathbb{W}^{n\alpha} + \text{h.c.} \right] \\ & + \left[\int d^2\theta \mathcal{W} + \text{h.c.} \right] + \mathcal{L}_{\text{Ghost}} + \mathcal{L}_{\text{Gauge Fixing}} , \end{aligned} \quad (2.44)$$

where we have defined

$$\mathbb{W}_\alpha^n := \frac{1}{8g_n} \bar{\mathbf{D}}^2 [\exp(2g_n \mathbb{V}^n) \mathbf{D}_\alpha \exp(-2g_n \mathbb{V}^n)] , \quad (2.45a)$$

$$g \cdot \mathbb{V} := \sum_{n=1}^S g_n \mathbb{V}^n \quad \text{and} \quad \mathbb{V}^n = \sum_{A_n=1}^{\dim G_n} \mathbb{V}_n^{A_n} \mathbb{T}_n^{A_n} , \quad (2.45b)$$

and where \mathcal{W} is the superpotential. $\Phi^{(i)}$ ($i \in \{1, \dots, N_\Phi\}$) are chiral superfields which contain the usual matter fields and \mathbb{V}^n are the vector superfields, corresponding to the internal gauge symmetry group G_n . As usual, $\mathbb{T}_n^{A_n}$ ($A_n = 1, \dots, \dim G_n$) denote the generators of G_n . $\mathbf{D}_\alpha := \partial_\alpha + i\sigma_{\alpha\beta}^\mu \bar{\theta}^\beta \partial_\mu$ and $\bar{\mathbf{D}}_{\dot{\alpha}} := -\bar{\partial}_{\dot{\alpha}} - i\theta^\alpha \sigma_{\alpha\dot{\alpha}}^\mu \partial_\mu$ are the SUSY-covariant derivatives. For the integration over superspace, our convention is chosen such that $\int d^2\theta \theta^2 = 1$ and $\int d^2\bar{\theta} \bar{\theta}^2 = 1$ holds. The theory is completely defined by specifying the gauge symmetry $G_1 \times \dots \times G_S$, the corresponding couplings g_n ($n \in \{1, \dots, S\}$) and the superpotential \mathcal{W} .

Particle Content and Interactions of the MSSM

Before we turn to the calculation of the RGE for the lowest dimensional neutrino mass operator, we briefly summarize some properties of the MSSM, relevant for our calculations. Since we want to calculate the RGE for the running at energy scales far above the SUSY-breaking scale, we can neglect the soft-breaking terms. As in the non-SUSY case, it is useful to perform the calculation in the $SU(2)_L \times U(1)_Y$ -unbroken phase. The MSSM without soft supersymmetry breaking terms is a G_{321} gauge theory with a R -parity conserving superpotential given by

$$\begin{aligned} \mathcal{W}_{\text{MSSM}} = & m h_a^{(1)} \varepsilon^{ab} h_b^{(2)} + (Y_e)_{gf} e^{Cg} h_a^{(1)} \varepsilon^{ab} \mathbb{q}_b^f \\ & + (Y_u)_{gf} u^{Cg} h_a^{(2)} (\varepsilon^T)^{ab} \mathbb{q}_b^f + (Y_d)_{gf} d^{Cg} h_a^{(1)} \varepsilon^{ab} \mathbb{q}_b^f . \end{aligned} \quad (2.46)$$

In addition, we consider the lowest dimensional effective operator which gives Majorana masses to the light neutrinos. $\mathcal{L}_\kappa^{\text{MSSM}}$ is given by the F -term

$$\mathcal{L}_\kappa^{\text{MSSM}} = \mathcal{W}_\kappa|_{\theta\theta} + \text{h.c.} = -\frac{1}{4} \kappa_{gf} \mathbb{f}_c^g \varepsilon^{cd} h_d^{(2)} \mathbb{f}_b^f \varepsilon^{ba} h_a^{(2)}|_{\theta\theta} + \text{h.c.} . \quad (2.47)$$

Note that contrary to non-supersymmetric 2HDMs, in the MSSM only one such operator is possible in the superpotential due to holomorphicity. The superfields e^C , d^C and u^C contain the $SU(2)_L$ -singlet charged leptons, down-type quarks and up-type quarks, respectively. q contains the $SU(2)_L$ quark doublets and ℓ the $SU(2)_L$ lepton doublets. $h^{(1)}$ and $h^{(2)}$ are the superfields which contain the Higgses. Note that two Higgs superfields with opposite $U(1)_Y$ -charges are required in order to cancel gauge anomalies. The quantum numbers of the superfields are specified in table 2.3. R -parity is defined by $R = (-1)^{3(B-L)+2S}$, where B is the baryon number, L the lepton number and S the spin of the particle. This gives even R -parity to the known particles of the SM and odd R -parity to their superpartners. Note that GUT theories can have automatic R -parity conservation, as e.g. $SO(10)$ GUTs if $B-L$ is broken by two units via a Higgs $\{\mathbf{126}\}_{SO(10)}$.

Field	$h^{(1)}$	$h^{(2)}$	q^f	d^{Cf}	u^{Cf}	ℓ^f	e^{Cf}
$SU(3)_C$	1	1	3	$\bar{\mathbf{3}}$	$\bar{\mathbf{3}}$	1	1
$SU(2)_L$	2	2	2	1	1	2	1
q_Y	$-\frac{1}{2}$	$+\frac{1}{2}$	$+\frac{1}{6}$	$+\frac{1}{3}$	$-\frac{2}{3}$	$-\frac{1}{2}$	$+1$

Table 2.3: Quantum numbers of the superfields. $q_Y^U = \sqrt{3/5}q_Y$ is the $U(1)_Y$ -charge in GUT normalization. The corresponding gauge coupling constant is redefined as $g_1^U = \sqrt{5/3}g_1$ in this case.

2.3.2 Component-Field Calculation of the RGE

For the calculations using component fields, we have to compute the interaction Lagrangian explicitly. The straightforward way would be to insert the usual expansion of the chiral superfields $\Phi^{(i)}$ in fermionic coordinates,

$$\Phi^{(i)} = A_i + \sqrt{2}\theta\psi_i + \theta\theta F_i, \quad (2.48)$$

to perform the integration over them and to eliminate the auxiliary fields by their algebraic equations of motion. A_i is a complex scalar, ψ_i is a Weyl spinor in the fundamental representation of $SL(2, \mathbb{C})$ and F_i is an auxiliary field. The expansion of the MSSM-superfields in component fields is given by

$$\ell^f = \tilde{\ell}^f + \sqrt{2}\theta\ell^f + \theta\theta F_\ell^f, \quad (2.49a)$$

$$e^{Cg} = \tilde{e}^{Cg} + \sqrt{2}\theta e^{Cg} + \theta\theta F_e^g, \quad (2.49b)$$

$$q^f = \tilde{q}^f + \sqrt{2}\theta q^f + \theta\theta F_q^f, \quad (2.49c)$$

$$u^{Cg} = \tilde{u}^{Cg} + \sqrt{2}\theta u^{Cg} + \theta\theta F_u^g, \quad (2.49d)$$

$$d^{Cg} = \tilde{d}^{Cg} + \sqrt{2}\theta d^{Cg} + \theta\theta F_d^g, \quad (2.49e)$$

$$\mathfrak{h}^{(1)} = \phi^{(1)} + \sqrt{2}\theta\tilde{\phi}^{(1)} + \theta\theta F_{h^{(1)}} , \quad (2.49f)$$

$$\mathfrak{h}^{(2)} = \phi^{(2)} + \sqrt{2}\theta\tilde{\phi}^{(2)} + \theta\theta F_{h^{(2)}} . \quad (2.49g)$$

However, to extract specific vertices, it is useful to expand $\mathcal{W}(\{\Phi^{(i)}\})$ itself in the fermionic coordinates,

$$\begin{aligned} \mathcal{W}(\{\Phi^{(i)}\}) &= \mathcal{W}(\{\Phi^{(i)}\})|_{\theta=0} + \partial_i \mathcal{W}(\{\Phi^{(i)}\})|_{\theta=0} (\sqrt{2}\theta\psi_i + \theta\theta F_i) \\ &\quad + \frac{1}{2} \partial_i \partial_j \mathcal{W}(\{\Phi^{(i)}\})|_{\theta=0} (\sqrt{2}\theta\psi_i + \theta\theta F_i) (\sqrt{2}\theta\psi_j + \theta\theta F_j) , \end{aligned} \quad (2.50)$$

where $\partial_i \mathcal{W} := \partial \mathcal{W} / \partial \Phi^{(i)}$. The F -term of \mathcal{W} is then given by

$$\mathcal{W}(\{\Phi^{(i)}\})|_{\theta\theta} = \partial_i \mathcal{W}(\{\Phi^{(i)}\})|_{\theta=0} F_i - \frac{1}{2} \partial_i \partial_j \mathcal{W}(\{\Phi^{(i)}\})|_{\theta=0} \psi_i \psi_j . \quad (2.51)$$

Inserting the algebraic equations of motion for the auxiliary fields F_i , which are given by $F_i = -(\partial_i \mathcal{W})^*|_{\theta=0}$, yields the useful result

$$\begin{aligned} \mathcal{W}(\{\Phi^{(i)}\})|_{\theta\theta} &= -\partial_i \mathcal{W}(\{\Phi^{(i)}\}) (\partial_i \mathcal{W}(\{\Phi^{(i)}\}))^*|_{\theta=0} \\ &\quad - \frac{1}{2} \partial_i \partial_j \mathcal{W}(\{\Phi^{(i)}\})|_{\theta=0} \psi_i \psi_j . \end{aligned} \quad (2.52)$$

In the above equations the sum over the indices i and j , which denote the superfields of the superpotential, is implicit. We will apply equation (2.52) in appendix A.3.3 where the Feynman rules relevant for the calculations of this section are given.

The kinetic terms, gauge-matter interactions and D -term contributions are contained in the first term of equation (2.44), which in the MSSM is given by

$$\mathcal{L}_{\text{kin}} = \int d^2\theta d^2\bar{\theta} \bar{\Phi}^{(i)} \exp \{ 2g_3 \mathbb{V}_3 + 2g_2 \mathbb{V}_2 + 2g_1 \mathbb{V}_1 \} \Phi^{(i)} , \quad (2.53)$$

with $\mathbb{V}_3 := \mathbb{V}_3^A \mathbb{T}_A$ ($A \in \{4, \dots, 11\}$), $\mathbb{V}_2 := \mathbb{V}_2^A \mathbb{T}_A$ ($A \in \{1, 2, 3\}$), and $\mathbb{V}_1 := \mathbb{V}_1^0 \mathbb{T}_0 = g_1 \mathbb{V}_1^0 y_i \mathbb{1}$. y_i is the $U(1)_Y$ -charge of the matter superfield $\Phi^{(i)}$. We now write the gauge-matter interactions in component fields by inserting the vector superfields in Wess-Zumino (WZ) gauge,

$$\mathbb{V}^A = -\theta\sigma^\mu\bar{\theta} v_\mu^A + i(\theta\theta)(\bar{\theta}\bar{\lambda}^A) - i(\bar{\theta}\bar{\theta})(\theta\lambda^A) + \frac{1}{2}(\bar{\theta}\bar{\theta})(\theta\theta) D^A , \quad (2.54)$$

making use of the identities $(\theta\phi)(\theta\psi) = -\frac{1}{2}(\phi\psi)(\theta\theta)$ and $(\bar{\theta}\bar{\phi})(\bar{\theta}\bar{\psi}) = -\frac{1}{2}(\bar{\phi}\bar{\psi})(\bar{\theta}\bar{\theta})$. The interaction terms involving one of the superfields $\Phi^{(i)}$ are

$$\begin{aligned} \mathcal{L}_{\text{g-m}}^{\Phi^{(i)}} &= (\partial_\mu A_i - ig v_\mu^A \mathbb{T}_A A_i)^\dagger (\partial^\mu A_i - ig v^{\mu A} \mathbb{T}_A A_i) \\ &\quad - g \bar{\psi}_{iL} (\gamma^\mu v_\mu^A \mathbb{T}_A) \psi_{iL} + g^2 A_{ia}^* v^{A\mu} (\mathbb{T}_A \mathbb{T}_B)^{ab} v_\mu^B A_{ib} \\ &\quad - i\sqrt{2}g (\bar{\psi}_{iLb} P_R \lambda^A \mathbb{T}_A^{ba} A_{ia} - A_{ia}^* \bar{\lambda}^A \mathbb{T}_A^{ab} P_L \psi_{iLb}) . \end{aligned} \quad (2.55)$$

v_μ^A are the gauge fields, λ^A the gauginos, which are Majorana fermions, and D is an auxiliary field. The condensed notation with the index A running from 0 to 11 is defined in table 1.2 on page 2 .

\mathcal{L}_{kin} also contains the part

$$\mathcal{L}_D = -\frac{1}{2}D_A D_A = -\frac{1}{2} \left(\sum_{i,A} g_i^2 A_{ia}^* \Gamma_A^{ab} A_{ib} \right)^2 \quad (2.56)$$

of the scalar potential. In particular, there are Higgs self-interactions

$$\begin{aligned} \mathcal{L}_D^{4\text{Higgs},g_1^2} &= -\frac{1}{2}g_1^2 \left(\phi_a^{(1)*} y_{\phi^{(1)}} \delta^{ab} \phi_b^{(1)} - \phi_a^{(2)*} \delta^{ab} \phi_b^{(2)} \right)^2 \\ &= -\frac{1}{2}g_1^2 y_{\phi^{(1)}}^2 (\phi^{(1)\dagger} \phi^{(1)}) (\phi^{(1)\dagger} \phi^{(1)}) - \frac{1}{2}g_1^2 y_{\phi^{(2)}}^2 (\phi^{(2)\dagger} \phi^{(2)}) (\phi^{(2)\dagger} \phi^{(2)}) \\ &\quad - g_1^2 y_{\phi^{(1)}} y_{\phi^{(2)}} (\phi^{(1)\dagger} \phi^{(1)}) (\phi^{(2)\dagger} \phi^{(2)}) \end{aligned} \quad (2.57)$$

proportional to g_1^2 and

$$\begin{aligned} \mathcal{L}_D^{4\text{Higgs},g_2^2} &= -\frac{1}{2}g_2^2 \left(\phi_a^{(1)*} \frac{\tau_A^{ab}}{2} \delta^{ab} \phi_b^{(1)} - \phi_a^{(2)*} \frac{\tau_A^{ab}}{2} \phi_b^{(2)} \right)^2 \\ &= -\frac{1}{4} \left(\frac{1}{2}g_2^2 \right) ((\phi^{(1)\dagger} \phi^{(1)})^2 - \frac{1}{4} \left(\frac{1}{2}g_2^2 \right) ((\phi^{(2)\dagger} \phi^{(2)})^2 \\ &\quad + \text{mixed terms with } \phi^{(1)} \text{ and } \phi^{(2)}) \end{aligned} \quad (2.58)$$

proportional to g_2^2 , which will be relevant for the calculation of the vertex corrections in the MSSM.

Calculation of the RGE for the Neutrino Mass Operator

The counterterm for the usual effective neutrino mass operator of equation (1.15), which is contained in $\mathcal{L}_\kappa^{\text{MSSM}}$ of equation (2.47), can be defined as in the non-supersymmetric theories,

$$\mathcal{C}_\kappa = \frac{1}{4} \delta \kappa_{gf} \overline{\ell_{Lc}^C} \varepsilon^{cd} \phi_d^{(2)} \ell_{Lb}^f \varepsilon^{ba} \phi_a^{(2)} + \text{h.c.} . \quad (2.59)$$

This leads to the relation

$$\kappa_B = Z_{\phi^{(2)}}^{-\frac{1}{2}} (Z_{\ell_L}^T)^{-\frac{1}{2}} [\kappa + \delta \kappa] \mu^\epsilon Z_{\ell_L}^{-\frac{1}{2}} Z_{\phi^{(2)}}^{-\frac{1}{2}} \quad (2.60)$$

between the renormalized and the bare quantities κ and κ_B . The wavefunction renormalization constants in component field notation are defined as usual.

We now turn to the calculation of the vertex corrections relevant for the computation of $\delta \kappa$ in the MSSM. One might think that in supersymmetric theories, for couplings of the superpotential the sum over all vertex corrections should be finite due to the non-renormalization theorem. However, in the component field formalism SUSY is not manifest, since for the calculation a super-gauge like Wess-Zumino gauge has to be fixed. Thus, the non-renormalization theorem cannot be applied naively. As expected, we find that only the sum over the corrections proportional to

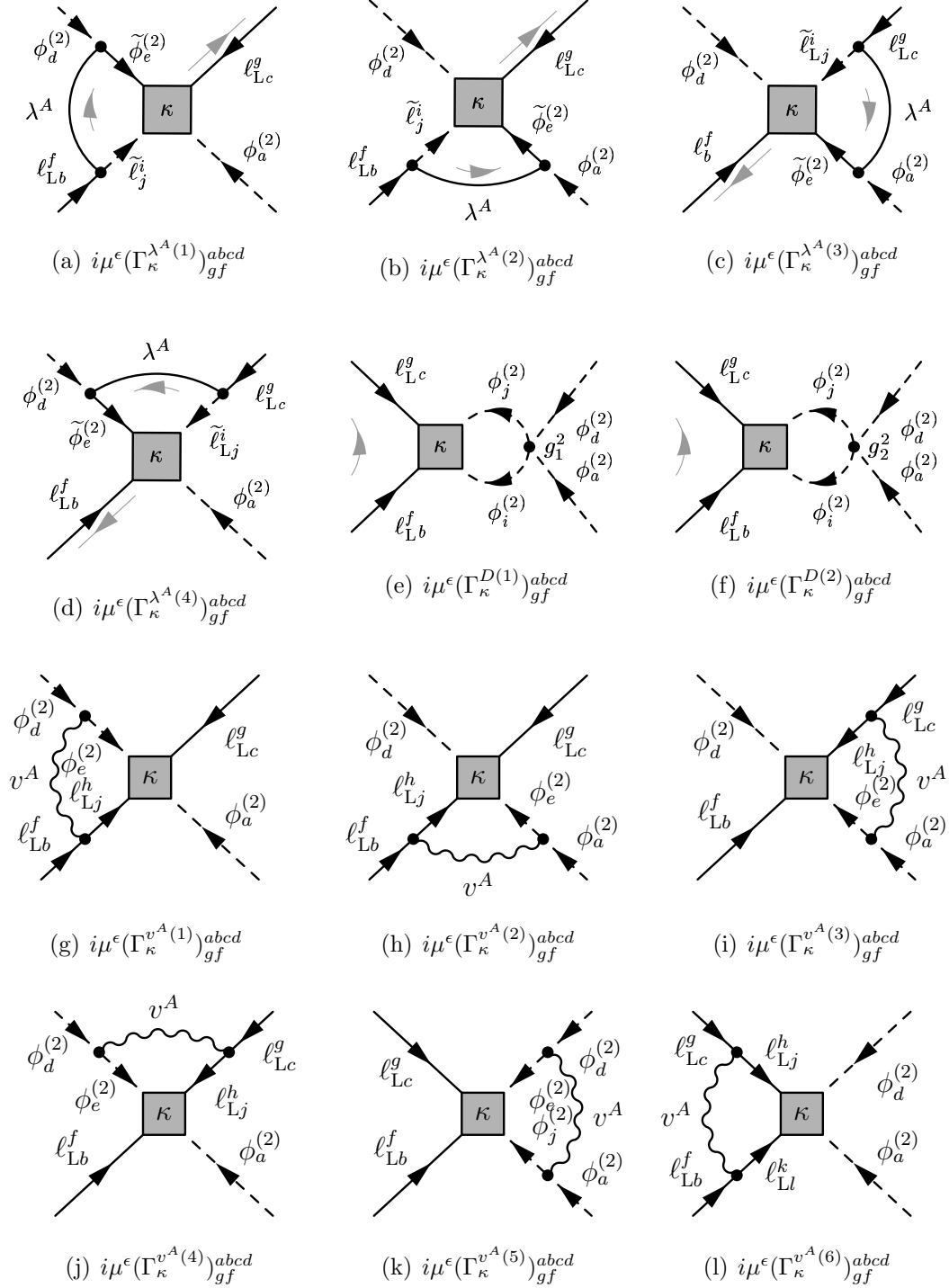


Figure 2.5: Figures (a)–(d) are the contributions from the gauginos λ^A to the renormalization of the dimension 5 operator in the MSSM. Figures (e) and (f) show the D -term contributions. Figures (g)–(l) are the gauge contributions as in the 2HDM of type (ii). The gray arrow indicates the fermion flow as defined in [73].

the gauge couplings has a pole in ϵ and thus contributes to $\delta\kappa$ in the MS scheme. We will now calculate these contributions in R_ξ gauge. They stem from the exchange of virtual gauge bosons, gauginos and Higgs doublets and are shown in figure 2.5.

As an example for the contributions proportional to the gauge couplings (diagrams (g) – (l) of figure 2.5), we calculate diagram (g),

$$\begin{aligned}
 i\mu^\epsilon (\Gamma_\kappa^{v^A(1)})_{gf}^{abcd} &:= \text{Diagram (g)} \\
 &= [i\mu^\epsilon \kappa_{gh} \frac{1}{2} (\epsilon_{ce} \epsilon_{ja} + \epsilon_{ca} \epsilon_{je})] [i\mu^{\frac{\epsilon}{2}} g_v \delta_{hf} \mathbb{T}_{jb}] [i\mu^{\frac{\epsilon}{2}} g_v \mathbb{T}_{ed}] \times \\
 &\quad \times \int \frac{d^d k}{(2\pi)^d} \left[P_L \frac{i(q+k)}{(q+k)^2} \gamma_\mu P_L i \frac{-\eta^{\mu\nu} + (1-\xi_v) \frac{k^\mu k^\nu}{k^2}}{k^2} \times \right. \\
 &\quad \left. \times (2p'_\nu + k_\nu) \frac{i}{(p'+k)^2 - m^2} \right] \\
 &= \frac{-2i}{16\pi^2} \xi_v \mu^\epsilon g_v^2 \kappa_{gf} \frac{1}{2} (\epsilon_{ce} \epsilon_{ja} + \epsilon_{ca} \epsilon_{je}) \mathbb{T}_{jb}^i \mathbb{T}_{ed}^i P_L \frac{1}{\epsilon} + \text{UV finite} \\
 &= \frac{-2i}{16\pi^2 \epsilon} \mu^\epsilon \kappa_{gf} P_L \left\{ \begin{array}{ll} -\frac{1}{4} g_1^2 \xi_B \frac{1}{2} (\epsilon_{cd} \epsilon_{ba} + \epsilon_{ca} \epsilon_{bd}) & \text{for } A = 0 \\ \frac{1}{4} g_2^2 \xi_W \frac{1}{2} (2\epsilon_{cb} \epsilon_{da} - 3\epsilon_{ca} \epsilon_{db} - \epsilon_{cd} \epsilon_{ba}) & \text{for } A \in \{1, 2, 3\} \end{array} \right. \\
 &\quad + \text{UV finite} . \tag{2.61}
 \end{aligned}$$

We have used the relations $\sum_A \mathbb{T}_{jb}^A \mathbb{T}_{ed}^A = \frac{1}{4} (2\delta_{jd} \delta_{be} - \delta_{jb} \delta_{ed})$ for the $SU(2)_L$ and $\sum_A \mathbb{T}_{jb}^A \mathbb{T}_{ed}^A = y_{\phi^{(2)}} y_{\ell_L} \delta_{jb} \delta_{ed} = -\frac{1}{4} \delta_{jb} \delta_{ed}$ for the $U(1)_Y$ case. The general relation for the generators \mathbb{T}^A of $SU(N)$ ($N \geq 2$) is given by

$$\sum_A (\mathbb{T}^A)_{ij} (\mathbb{T}^A)_{kl} = \frac{1}{2} (\delta_{il} \delta_{jk} - \frac{1}{N} \delta_{ij} \delta_{kl}) , \tag{2.62}$$

in the usual normalization $\text{Tr}(\mathbb{T}^A \mathbb{T}^B) = \frac{1}{2} \delta^{AB}$. As an example for the gaugino contributions (diagrams (a) – (d) of figure 2.5), we explicitly calculate diagram (a),

$$\begin{aligned}
 i\mu^\epsilon (\Gamma_\kappa^{\lambda^A(1)})_{gf}^{abcd} &:= \text{Diagram (a)} \\
 &= \text{Diagram (a)}
 \end{aligned}$$

$$\begin{aligned}
 &= \sum_A \int \frac{d^d k}{(2\pi)^d} \left[-\sqrt{2} g \mu^{\epsilon/2} (\Gamma^T)_{bj}^A \delta_{if} P_L \right] \frac{i}{(p+k)^2} \times \\
 &\quad \times \left[i \mu^\epsilon \kappa_{gi} \frac{1}{2} (\varepsilon_{ce} \varepsilon_{ja} + \varepsilon_{ca} \varepsilon_{je}) P_L \right] \frac{i(q-k)}{(q-k)^2} \left[\sqrt{2} g \mu^{\epsilon/2} \Gamma_{ed}^A P_R \right] \frac{i(-k)}{k^2} \\
 &= \frac{-4i}{16\pi^2 \epsilon} \mu^\epsilon \kappa_{gf} P_L \left\{ \begin{array}{ll} -\frac{1}{4} g_1^2 \frac{1}{2} (\varepsilon_{cd} \varepsilon_{ba} + \varepsilon_{ca} \varepsilon_{bd}) & \text{for } A = 0 \\ \frac{1}{4} g_2^2 \frac{1}{2} (2\varepsilon_{cb} \varepsilon_{da} - 3\varepsilon_{ca} \varepsilon_{db} - \varepsilon_{cd} \varepsilon_{ba}) & \text{for } A \in \{1, 2, 3\} \end{array} \right. \\
 &\quad + \text{UV finite} .
 \end{aligned}$$

Additionally we have to compute the wavefunction renormalization constants for the lepton doublet ℓ_L and the Higgs $\phi^{(2)}$. Compared to the 2HDM type (ii), there are additional diagrams with superpartners running in the loops. The diagrams for the wavefunction renormalization of the lepton doublets are shown in figure 2.6.

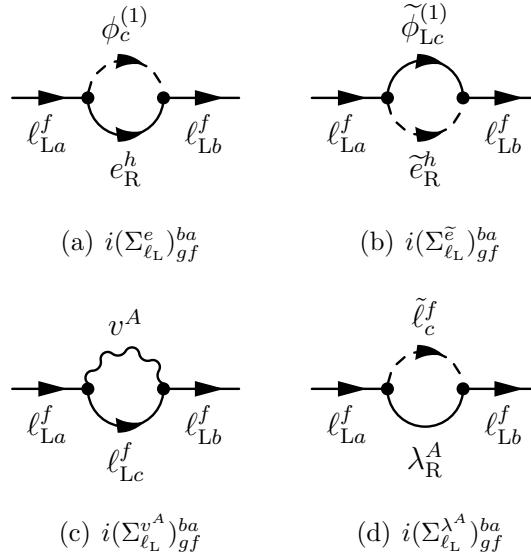


Figure 2.6: Contributions to the wavefunction renormalization of the lepton doublets in the MSSM. For the gauge bosons and gauginos of $U(1)_Y$ and $SU(2)_L$ we use the condensed notations v^A and λ^A .

We see that there is one additional contribution proportional to the Yukawa couplings (diagram (b)), where the Higgsino runs in the loop. Its calculation yields the same ϵ -pole as for diagram (a). The situation is similar for the contributions

proportional to the gauge couplings. Calculating diagram (d) gives

$$\begin{aligned}
 i\Sigma_{\ell_L}^{\lambda^A} &:= \text{Diagram (d)} \\
 &= \mu^\epsilon \sqrt{2} g_A \mathbb{T}_A^{ac} (-\sqrt{2}) g \mathbb{T}_A^{cb} \int \frac{d^d k}{(2\pi)^d} P_R \frac{i(\not{p} + \not{k})}{(p+k)^2} P_L \frac{i}{k^2} \\
 &= \frac{i}{8\pi^2} g_A^2 (\mathbb{T}_A^{ac} \mathbb{T}_A^{cb}) \not{p} P_L \frac{1}{\epsilon} + \text{UV finite} .
 \end{aligned} \tag{2.63}$$

This can be further evaluated using equation (2.62) for the generators of $SU(2)_L$ or the corresponding relation for $U(1)_Y$. We now turn to the wavefunction renormalization of $\phi^{(2)}$. The diagrams which contribute are shown in figure 2.7.

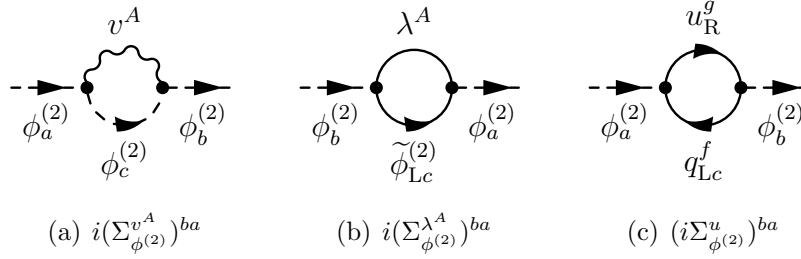


Figure 2.7: One-loop diagrams which contribute to the wavefunction renormalization of the Higgs field $\phi^{(2)}$ in the MSSM. For the gauge bosons and gauginos of $U(1)_Y$ and $SU(2)_L$ we use the condensed notation v^A and λ^A .

As an example, we calculate diagram (b) with the virtual gaugino running in the loop,

$$\begin{aligned}
 i\Sigma_{\phi^{(2)}}^{\lambda^A} &:= \text{Diagram (b)} \\
 &= \mu^\epsilon (-\sqrt{2}) g_A \mathbb{T}_A^{ac} \sqrt{2} g \mathbb{T}_A^{cb} (-1) \text{Tr} \left\{ \int \frac{d^d k}{(2\pi)^d} P_L \frac{i(\not{p} + \not{k})}{(p+k)^2} P_R \frac{i\not{k}}{k^2} \right\} \\
 &= \frac{4i}{16\pi^2} g_A^2 (\mathbb{T}_A^{ac} \mathbb{T}_A^{cb}) p^2 P_L \frac{1}{\epsilon} + \text{UV finite} .
 \end{aligned} \tag{2.64}$$

The results for the divergent parts of the relevant vertex corrections and self-energies are listed in appendix A.4.3.

The renormalization constants are determined from the requirements

$$0 = \sum_{i,j} \left(\Sigma_{\phi^{(j)}}^i \Big|_{\text{div}} \right) + (p^2 \delta Z_{\phi^{(j)}} - \delta m^2), \quad (2.65a)$$

$$0 = \sum_i \left(\Sigma_{\ell_L}^i \Big|_{\text{div}} \right) + \not{p} \delta Z_{\ell_L} P_L = 0, \quad (2.65b)$$

$$0 = \sum_i \left(\Gamma_{\kappa}^i \Big|_{\text{div}} \right) + \delta \kappa_{gf} \frac{1}{2} (\varepsilon_{cd} \varepsilon_{ba} + \varepsilon_{ca} \varepsilon_{bd}) P_L, \quad (2.65c)$$

which yield

$$\delta Z_{\ell_L,1} = -\frac{1}{16\pi^2} \left[2 Y_e^\dagger Y_e + \frac{1}{2} (\xi_B - 1) g_1^2 + \frac{3}{2} (\xi_W - 1) g_2^2 \right], \quad (2.66a)$$

$$\delta Z_{\phi^{(2)},1} = -\frac{1}{16\pi^2} \left[6 \text{Tr}(Y_u^\dagger Y_u) + \frac{1}{2} (\xi_B + 1) g_1^2 + \frac{3}{2} (\xi_W + 1) g_2^2 \right], \quad (2.66b)$$

$$\delta \kappa_{,1} = -\frac{1}{16\pi^2} \left[(\xi_B + 2) g_1^2 \kappa + 3 (\xi_W + 2) g_2^2 \kappa \right]. \quad (2.66c)$$

From the relation

$$\beta_\kappa = \delta \kappa_{,1} - \frac{1}{2} (\delta Z_{\phi,1} + \delta Z_{\ell_L,1})^T \kappa - \frac{1}{2} \kappa (\delta Z_{\phi,1} + \delta Z_{\ell_L,1}), \quad (2.67)$$

and the insertion of the results from equation (2.66) for the counterterms, we obtain the result for the 1-loop RGE in the MSSM [67],

$$16\pi^2 \beta_\kappa^{\text{MSSM}} = (Y_e^\dagger Y_e)^T \kappa + \kappa (Y_e^\dagger Y_e) + 6 \text{Tr}(Y_u^\dagger Y_u) \kappa - 2g_1^2 \kappa - 6g_2^2 \kappa. \quad (2.68)$$

We thus confirm the existing result of [58,59] by a component field calculation. In section 2.3.3, where we will calculate the 2-loop β -function using a different method, we will perform another independent check of the correctness of the 1-loop part.

2.3.3 Calculation of the 2-Loop RGE using Supergraphs

In order to calculate the 2-loop β -function for the lowest dimensional effective neutrino mass operator, we use supergraph techniques [74–77]. The calculation of β -functions is then simplified considerably, since due to the non-renormalization theorem [78,79] only wavefunction renormalization has to be considered for operators of the superpotential. As we have seen in section 2.3.2, in a component field description no naive use can be made of the theorem with respect to loop corrections proportional to the gauge couplings, since SUSY is no longer manifest when a supergauge, as for example Wess-Zumino-gauge, is fixed. The supergraph technique, on the other hand, allows to apply the non-renormalization theorem directly, since SUSY is kept manifest. The β -functions for operators of the superpotential can then be calculated from the wavefunction renormalization constants alone.

These operators can be renormalizable or non-renormalizable, since for the latter the non-renormalization theorem holds as well [80] and since they do not affect the wavefunction renormalization constants in leading order in an effective field theory expansion. For the wavefunction renormalization constants, general formulae exist in the literature. Thus, it is possible to formulate a construction kit for 2-loop beta functions in $N=1$ supersymmetric theories, which can be applied to renormalizable and non-renormalizable operators of the superpotential [81,66].

Formulae for the Wavefunction Renormalization Constants

We will now summarize the results for the 1- and 2-loop wavefunction renormalization constants in a general $N=1$ supersymmetric gauge theory. The general Lagrangian under consideration is given in equation (2.44). Apart from possible mass terms, which are omitted for the moment as they do not affect the β -functions, the renormalizable part of the superpotential can be written as

$$\mathcal{W}_{\text{ren}} = \frac{1}{6} \sum_{i,j,k=1}^{N_\Phi} \lambda_{(ijk)} \Phi^{(i)} \Phi^{(j)} \Phi^{(k)} . \quad (2.69)$$

The brackets indicate symmetrization of the indices of λ and the indices i, j and k run over all irreps, families and the representation space. The N_Φ superfields $\Phi^{(i)}$ transform under the irreducible representations (irreps) $R_1^{(i)} \times \dots \times R_S^{(i)}$ of the gauge group $G_1 \otimes \dots \otimes G_S$. In the following, we will make use of the group-theoretical constants

$$c_1(G) \delta^{AB} := \sum_{C,D} f^{ACD} f^B{}_{CD} , \quad (2.70a)$$

$$c_2(R) \delta_{ab} := \sum_A (\mathbb{T}^A \mathbb{T}^A)_{ab} , \quad (2.70b)$$

$$\ell(R) \delta^{AB} := \text{Tr}(\mathbb{T}^A \mathbb{T}^B) , \quad (2.70c)$$

with \mathbb{T}^A being the matrix representations of the generators of a simple group G corresponding to the irrep R and with the structure constants $f^A{}_{BC}$ defined by $[\mathbb{T}^A, \mathbb{T}^B] = i f^A{}_{BC} \mathbb{T}^C$. $\ell(R)$ is known as Dynkin index of the irrep R and $c_2(R)$ as the quadratic Casimir. They are related by

$$c_2(R) = \frac{\dim G}{\dim R} \ell(R) , \quad (2.71)$$

with $\dim G$ and $\dim R$ being the dimension of the group G and the irrep R , respectively. Usually, the generators of the irrep \mathbf{N} of $\text{SU}(N)$ are normalized such that $\ell(\mathbf{N}) = \frac{1}{2}$ holds. c_2 can then be obtained via $c_2(\mathbf{N}) = \frac{N^2-1}{2N}$ while for a $\text{U}(1)$ theory both $\ell(R)$ and $c_2(R)$ are replaced by q^2 where q is the $\text{U}(1)$ charge of Φ . For any

non-trivial irrep of $SU(N)$ the invariant $c_1(\mathbf{N})$ is given by N . The quadratic Casimir of the adjoint representation is also given by $c_2(G) = c_1(G) = N$ for $SU(N)$.

Due to the non-renormalization theorem, the RGEs for operators of the superpotential are governed by the wavefunction renormalization constants for the superfields $Z_{ij} = \mathbb{1}_{ij} + \delta Z_{ij}$, which relate the bare $\Phi_B^{(i)}$ and the renormalized superfields,

$$\Phi_B^{(i)} = \sum_{j=1}^{N_\Phi} Z_{ij}^{\frac{1}{2}} \Phi^{(j)}. \quad (2.72)$$

δZ_{ij} is given at 1-loop by

$$-\delta Z_{ij}^{(1)} = \frac{1}{(4\pi)^2} \frac{1}{\epsilon} \left[\sum_{k,\ell=1}^{N_\Phi} \lambda_{ik\ell}^* \lambda_{jkl} - 4 \sum_{n=1}^S g_n^2 c_2(R_n^{(i)}) \delta_{ij} \right] \quad (2.73)$$

and at 2-loop by [82]

$$\begin{aligned} -\delta Z_{ij}^{(2)} = & \frac{-2 + \epsilon}{(4\pi)^4 \epsilon^2} \left[4 \sum_{n,m=1}^S g_n^2 c_2(R_n^{(i)}) g_m^2 c_2(R_m^{(j)}) \delta_{ij} \right. \\ & + 2 \sum_{n=1}^S g_n^4 c_2(R_n^{(i)}) (\bar{\ell}_n - 3 c_1(G_n)) \delta_{ij} \\ & + \sum_{n=1}^S \sum_{k,\ell=1}^{N_\Phi} g_n^2 (-c_2(R_n^{(i)}) + 2 c_2(R_n^{(\ell)})) \lambda_{ik\ell}^* \lambda_{jkl} \\ & \left. - \frac{1}{2} \sum_{k,\ell,r,s,t=1}^{N_\Phi} \lambda_{ik\ell}^* \lambda_{lst} \lambda_{rst}^* \lambda_{jkr} \right]. \quad (2.74) \end{aligned}$$

We have introduced $\bar{\ell}_n$, which is defined by

$$\bar{\ell}_n := \sum_{i=1}^{N_\Phi} \frac{\ell(R_n^{(i)})}{\dim(R_n^{(i)})}. \quad (2.75)$$

The results have been obtained with regularization via dimensional reduction [83], modified minimal subtraction [84] and supersymmetric Fermi-Feynman gauge. The diagrams relevant for the calculation of the wavefunction renormalization constants for the matter superfield, equation (2.73) and (2.74), are shown in figure 2.8 and 2.9, respectively. We represent chiral superfields as straight double lines while vector superfields are indicated by wiggly double lines.

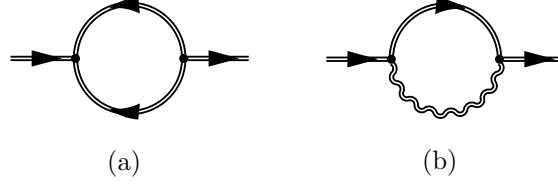


Figure 2.8: One-loop supergraphs which contribute to the $\bar{\Phi}\Phi$ propagator.

The Wavefunction Renormalization Constants in the MSSM

To calculate β -functions from the wavefunction renormalization constants, it is convenient to subdivide the general indices $\{i, j, \dots\}$ into indices $\{r, s, \dots\}$ for the irreducible representations, $\{f, g, \dots\}$ for the particle families and $\{a, b, \dots\}$ for the representation space, i.e. $i = (r, f, a)$. The wavefunction renormalization constants Z_{ij} are diagonal with respect to the representation and the representation space indices and are matrices in flavour-space. We will write $Z_{ij} = Z_r$ and suppress flavour and representation space indices.

From equation (2.73), we obtain the $1/\epsilon$ -coefficients of the relevant wavefunction renormalization constants at 1-loop,

$$-(4\pi)^2 Z_{\mathfrak{h}^{(2)},1}^{(1)} = 6 \operatorname{Tr}(Y_u^\dagger Y_u) - \frac{3}{5} (g_1^U)^2 - 3 g_2^2, \quad (2.76a)$$

$$-(4\pi)^2 Z_{\mathfrak{l},1}^{(1)} = 2 Y_e^\dagger Y_e - \frac{3}{5} (g_1^U)^2 - 3 g_2^2, \quad (2.76b)$$

where the Yukawa matrices as well as $Z_{\mathfrak{l}}$ are of course matrices in flavour space. g_1^U is the $U(1)_Y$ gauge coupling constant in GUT charge normalization. The 2-loop contributions can be calculated from equation (2.74) and are given by

$$\begin{aligned} -\frac{(4\pi)^4}{2} Z_{\mathfrak{h}^{(2)},1}^{(2)} &= -3 \operatorname{Tr}(Y_u^\dagger Y_d Y_d^\dagger Y_u) - 9 \operatorname{Tr}(Y_u^\dagger Y_u Y_u^\dagger Y_u) + \frac{4}{5} (g_1^U)^2 \operatorname{Tr}(Y_u^\dagger Y_u) \\ &+ 16 g_3^2 \operatorname{Tr}(Y_u^\dagger Y_u) + \frac{207}{100} (g_1^U)^4 + \frac{9}{10} (g_1^U)^2 g_2^2 + \frac{15}{4} g_2^4, \end{aligned} \quad (2.77a)$$

$$\begin{aligned} -\frac{(4\pi)^4}{2} Z_{\mathfrak{l},1}^{(2)} &= -2 Y_e^\dagger Y_e Y_e^\dagger Y_e - 3 Y_e^\dagger Y_e \operatorname{Tr}(Y_d Y_d^\dagger) - Y_e^\dagger Y_e \operatorname{Tr}(Y_e Y_e^\dagger) \\ &+ \frac{6}{5} (g_1^U)^2 Y_e^\dagger Y_e + \frac{207}{100} (g_1^U)^4 + \frac{9}{10} (g_1^U)^2 g_2^2 + \frac{15}{4} g_2^4. \end{aligned} \quad (2.77b)$$

The 2-Loop RGE for the Neutrino Mass Operator in the MSSM

From the wavefunction renormalization constants of equations (2.105) and (2.106), we can compute the β -functions for the lowest dimensional effective neutrino mass

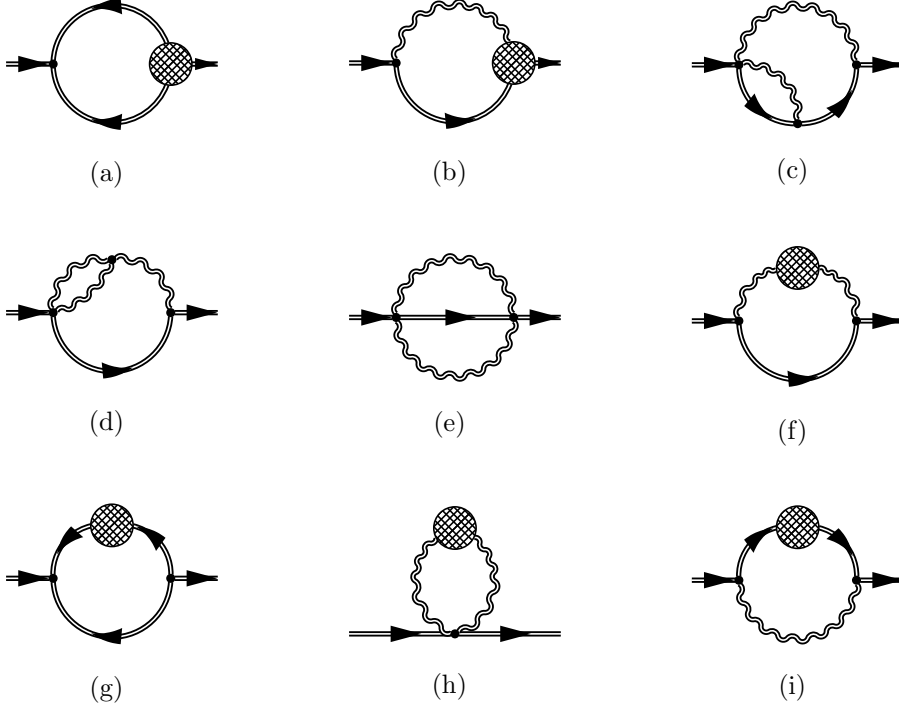


Figure 2.9: 2-loop supergraphs, which contribute to the $\bar{\Phi}\Phi$ propagator. Chiral superfields are represented as straight double lines while vector-superfields are indicated by wiggly double lines. A blob denotes the relevant one-particle irreducible graph including any 1-loop counterterm that may be required [82].

operator up to the 2-loop order using the formula of equation (2.20). We obtain [81]

$$\begin{aligned}
 (4\pi)^4 \beta_\kappa^{\text{MSSM}} = & (4\pi)^2 \left\{ (Y_e^\dagger Y_e)^T \kappa + \kappa Y_e^\dagger Y_e + \left[6 \text{Tr}(Y_u^\dagger Y_u) - \frac{6}{5} (g_1^U)^2 - 6g_2^2 \right] \kappa \right\} \\
 & + \left[-6 \text{Tr}(Y_u^\dagger Y_d Y_d^\dagger Y_u) - 18 \text{Tr}(Y_u^\dagger Y_u Y_u^\dagger Y_u) + \frac{8}{5} (g_1^U)^2 \text{Tr}(Y_u^\dagger Y_u) \right. \\
 & + 32 g_3^2 \text{Tr}(Y_u^\dagger Y_u) + \frac{207}{25} (g_1^U)^4 + \frac{18}{5} (g_1^U)^2 g_2^2 + 15 g_2^4 \left. \right] \kappa \\
 & - \left[2 (Y_e^\dagger Y_e Y_e^\dagger Y_e)^T + \left(-\frac{6}{5} (g_1^U)^2 + \text{Tr}(Y_e Y_e^\dagger) + 3 \text{Tr}(Y_d Y_d^\dagger) \right) (Y_e^\dagger Y_e)^T \right] \kappa \\
 & - \kappa \left[2 Y_e^\dagger Y_e Y_e^\dagger Y_e + \left(-\frac{6}{5} (g_1^U)^2 + \text{Tr}(Y_e Y_e^\dagger) + 3 \text{Tr}(Y_d Y_d^\dagger) \right) Y_e^\dagger Y_e \right]. \quad (2.78)
 \end{aligned}$$

The 1-loop part provides a second, independent confirmation of the existing MSSM result. The 2-loop accuracy may be required for the neutrino sector since due to the absence of hadronic uncertainties, high precision measurements of the neutrino parameters may be achieved in future experiments.

2.4 The Effective Theories of Minimal See-Saw Scenarios

We now calculate the RGEs for the running of the effective neutrino mass matrix in minimal see-saw scenarios, where the SM, 2HDM or MSSM is extended only by heavy singlet neutrinos with in general non-degenerate masses. All other particles, which correspond e.g. to the generation of a type II see-saw or to some GUT-model degrees of freedom, are assumed to be already integrated out of the theory in the considered energy range. We will refer to the scale where additional new physics has to be taken into account as M_U . In the MSSM, M_U might be the GUT scale M_{GUT} .

The minimal see-saw scenarios lead to various effective theories, where only the light particles propagate while the heavy degrees of freedom are integrated out. Below the mass scales of the singlets, to which we will refer as see-saw scales, we obtain the dimension 5 neutrino mass operator. Above the largest see-saw scale, the neutrino mass operator is realized at tree-level by the diagrams (a) and (b) of figure 2.10. If these are the only contributions to the effective neutrino mass operator, this corresponds to the type I see-saw scenario. In addition, there can be further contributions which, in the minimal scenario under consideration, stem from integrating out additional heavy particles with masses larger than M_U . In left-right symmetric extensions after $B-L$ breaking, there can be contributions from Higgs triplets as shown in diagram (c), yielding a type II see-saw scenario.

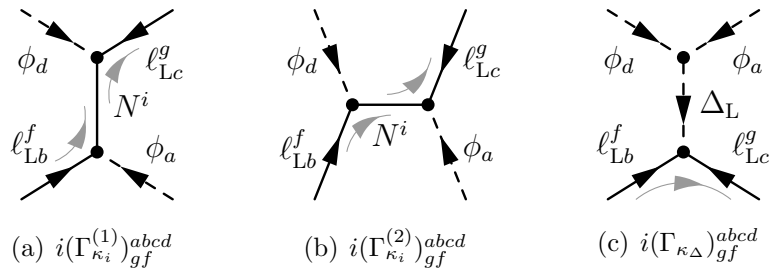


Figure 2.10: Tree-level realizations of the effective neutrino mass operator in type I (diagram (a) and (b)) or Type II (diagram (a),(b) and (c)) see-saw scenarios. ϕ and ℓ_L^f are SU(2)_L-doublets, N^i are singlets and Δ_L is a SU(2)_L-triplet.

2.4.1 Tree-Level Matching in Type I See-Saw Scenarios

Let us specify the modifications of the Lagrangians due to the appearance of the heavy neutrinos. In the SM above the highest mass threshold, the singlets N_R^i ($i \in \{1, \dots, n_G\}$) are added to the Lagrangian. In the MSSM we add the singlet

superfields ν^{Ci} , which contain the Weyl spinors N^{Ci} and their superpartners \tilde{N}^{Cj} . In addition to the kinetic terms, a Majorana mass term as well as the neutrino Yukawa interaction appear in the Lagrangians

$$\mathcal{L}_{\text{N,SM}} = -\frac{1}{2}\overline{N_{\text{R}}^i}M_{ij}N_{\text{R}}^{Cj} - (Y_{\nu})_{if}\overline{N_{\text{R}}^i}\tilde{\phi}_{\text{L}}^f\ell_{\text{L}}^f + \text{h.c.} , \quad (2.79\text{a})$$

$$\mathcal{L}_{\text{N,2HDM}} = -\frac{1}{2}\overline{N_{\text{R}}^i}M_{ij}N_{\text{R}}^{Cj} - \sum_{k=1}^2 z_{\nu}^{(k)}(Y_{\nu})_{if}\overline{N_{\text{R}}^i}\ell_{\text{Lb}}^f\varepsilon^{ba}\phi_a^{(k)} + \text{h.c.} , \quad (2.79\text{b})$$

$$\mathcal{L}_{\text{N,MSSM}} = \frac{1}{2}\nu^{Ci}M_{ij}\nu^{Cj}|_{\theta\theta} + (Y_{\nu})_{if}\nu^{Ci}h_a^{(2)}(\varepsilon^T)^{ab}\ell_b^f|_{\theta\theta} + \text{h.c.} , \quad (2.79\text{c})$$

where in the considered 2HDMs the variable $z_{\nu}^{(k)} \in \{0, 1\}$ specifies whether the singlet couples to $\phi^{(1)}$ or $\phi^{(2)}$. The expansion of the superfield ν^{Cj} is given by

$$\nu^{Cj} = \tilde{N}^{Cj} + \sqrt{2}\theta N^{Cj} + \theta\theta F_{\nu}^j . \quad (2.80)$$

We now consider the matching at one of the see-saw scales M_i with the neutrino mass operators, which are given by

$$\mathcal{L}_{\kappa}^{\text{SM}} = \frac{1}{4}\kappa_{gf}\overline{\ell_{\text{Lc}}^g}\varepsilon^{cd}\phi_d\ell_{\text{Lb}}^f\varepsilon^{ba}\phi_a + \text{h.c.} , \quad (2.81\text{a})$$

$$\mathcal{L}_{\kappa^{(ii)}}^{\text{2HDM}} = \frac{1}{4}\kappa_{gf}^{(ii)}\overline{\ell_{\text{Lc}}^g}\varepsilon^{cd}\phi_d^{(i)}\ell_{\text{Lb}}^f\varepsilon^{ba}\phi_a^{(i)} + \text{h.c.} , \quad (2.81\text{b})$$

$$\mathcal{L}_{\kappa}^{\text{MSSM}} = -\frac{1}{4}\kappa_{gf}\ell_{\text{Lc}}^g\varepsilon^{cd}h_d^{(2)}\ell_b^f\varepsilon^{ba}h_a^{(2)}|_{\theta\theta} + \text{h.c.} . \quad (2.81\text{c})$$

In the following, we will consider the extended SM explicitly as an example and will come back to the other models for the results. The diagrammatic form of the matching condition is

$$p^2 \ll M_i^2 \quad (2.82)$$

which is equivalent to

$$i(\Gamma_{\kappa_i}^{(1)})_{gf}^{abcd} + i(\Gamma_{\kappa_i}^{(2)})_{gf}^{abcd} \stackrel{p^2 \ll M_i^2}{=} i\kappa_{gf}\frac{1}{2}(\varepsilon_{cd}\varepsilon_{ba} + \varepsilon_{ca}\varepsilon_{bd}) . \quad (2.83)$$

We have used the notation introduced in figure 2.10. The calculation of the tree-level 4-point vertex functions yields (no summation over i)

$$i(\Gamma_{\kappa_i}^{(1)})_{gf}^{abcd} = [-i(Y_{\nu}^T)_{gi}\varepsilon_{cd}P_{\text{L}}] \frac{i(\not{p} + M_i)}{p^2 - M_i^2} [-i(Y_{\nu})_{if}(\varepsilon^T)_{ab}P_{\text{L}}] , \quad (2.84\text{a})$$

$$i(\Gamma_{\kappa_i}^{(2)})_{gf}^{abcd} = [-i(Y_{\nu}^T)_{gi}\varepsilon_{ca}P_{\text{L}}] \frac{i(\not{p} + M_i)}{p^2 - M_i^2} [-i(Y_{\nu})_{if}(\varepsilon^T)_{db}P_{\text{L}}] , \quad (2.84\text{b})$$

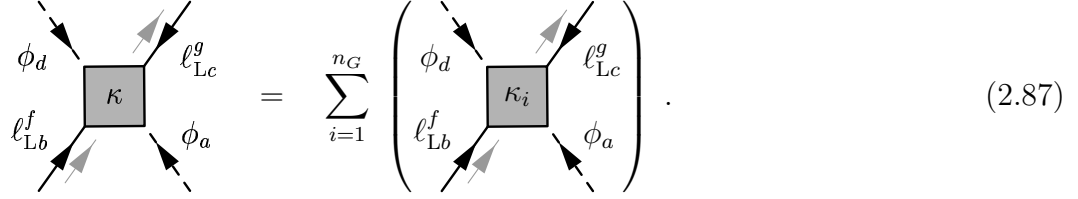
where p is the momentum of N^i . In the approximation $p^2 \ll M_i^2$, we thus obtain

$$i(\Gamma_{\kappa_i}^{(1)})_{gf}^{abcd} + i(\Gamma_{\kappa_i}^{(2)})_{gf}^{abcd} \stackrel{p^2 \ll M_i^2}{=} i 2(Y_\nu^T M_i^{-1} Y_\nu)_{gf} \frac{1}{2} (\varepsilon_{cd} \varepsilon_{ba} + \varepsilon_{ca} \varepsilon_{bd}) P_L, \quad (2.85)$$

which, from the matching requirement of equation (2.92a), implies the see-saw formula for one singlet,

$$\kappa_i = 2(Y_\nu^T)_{gi} M_i^{-1} (Y_\nu)_{if} \quad (\text{no sum over } i). \quad (2.86)$$

Note that the Yukawa matrices $(Y_\nu)_{if}$ for fixed i are just rows. After integrating out at each threshold, we obtain the complete neutrino mass operator by



$$\text{Diagram with } \kappa \text{ and external lines } \phi_d, \phi_a, \ell_{Lb}^f, \ell_{Lc}^g = \sum_{i=1}^{n_G} \left(\text{Diagram with } \kappa_i \text{ and external lines } \phi_d, \phi_a, \ell_{Lb}^f, \ell_{Lc}^g \right). \quad (2.87)$$

The neutrino mass matrix below the lowest realization scale M_1 is now given by the full type I see-saw formula. In a general basis, it is determined by the matrix $\kappa^{(1)}$ of the effective neutrino mass operator,

$$\kappa^{(1)} = \sum_i \kappa_i = 2(Y_\nu^T)_{gi} (M^{-1})_{ij} (Y_\nu)_{jf}. \quad (2.88)$$

2.4.2 Tree-Level Matching in Type II See-Saw Scenarios

In addition to the contributions from integrating out the heavy singlets, there can be a contribution to the effective neutrino mass operator from a $SU(2)_L$ -triplet Higgs. As we have discussed in chapter 1, in left-right symmetric models the triplet can obtain a small induced vev after EW symmetry breaking. In the $SU(2)_L$ -unbroken phase, integrating out the triplet generates the dimension 5 neutrino mass operator. The mass of the triplet, which arises after $B-L$ breaking, depends on the Higgs potential of the specific model under consideration. We will not go into the details here and assume that it is heavier than M_U . By considering the interaction terms which are typical for minimal left-right symmetric models, we will demonstrate the tree-level matching with the neutrino mass operator, which is rather generic and can be generalized to the desired specific model.

In minimal left-right symmetric models, the coupling of the lepton doublets ℓ_L^f to a triplet Δ_L of equation (1.24) as well as a coupling of two bi-doublets and the triplets Δ_L and Δ_R are present. As usual, L and R denote representations of $SU(2)_L$ and $SU(2)_R$, respectively. After $B-L$ breaking by a vev $v_R = \langle \Delta_R^0 \rangle$, the Higgs Lagrangian contains a coupling of two Higgs doublets to Δ_L ,

$$-\frac{1}{2} f_{ij}^\Delta \sum_{i,j=1}^2 \text{Tr}(\Delta_L^\dagger \Phi_i \Delta_R \Phi_j^\dagger) \xrightarrow[B-L \text{ breaking}]{\text{contains after}} -\frac{1}{2} f_{12}^\Delta v_R \phi_a^{(2)} (\tau^i \varepsilon \Delta_L^i)^{ab} \phi_b^{(2)}, \quad (2.89)$$

where we have defined $\Phi_1 := \Phi$ and $\Phi_2 := \tilde{\Phi} = \tau^2 \Phi \tau^2$ and the doublet $\phi^{(2)}$ is contained in Φ . The diagrammatic form of the matching condition is given by

$$(2.90)$$

which is equivalent to

$$i(\Gamma_{\kappa_{\Delta}})_{gf}^{abcd} \stackrel{p^2 \ll M_i^2}{=} i\kappa_{gf} \frac{1}{2} (\varepsilon_{cd} \varepsilon_{ba} + \varepsilon_{ca} \varepsilon_{bd}) , \quad (2.91)$$

using the notation of figure 2.10. We thus obtain

$$\begin{aligned} i(\Gamma_{\kappa_{\Delta}})_{gf}^{abcd} &= [-i(Y^{\Delta})_{gf} \{(\tau^i \varepsilon)_{cb} + (\tau^i \varepsilon)_{bc}\} P_L] \frac{i}{p^2 - M_{\Delta}^2} \times \\ &\quad \times [-if_{12}^{\Delta} v_R \frac{1}{2} \{(\tau^i \varepsilon)_{da} + (\tau^i \varepsilon)_{ad}\}] \\ &\stackrel{p^2 \ll M_i^2}{=} -2i(Y^{\Delta})_{gf} M_{\Delta}^{-2} (f^{\Delta} v_R) \frac{1}{2} (\varepsilon_{cd} \varepsilon_{ba} + \varepsilon_{ca} \varepsilon_{bd}) P_L , \end{aligned} \quad (2.92a)$$

where p is the momentum of Δ_L and M_{Δ} is its mass, which is generated after $B-L$ breaking. In the last step, we have used the relation $\tau_{ab}^i \tau_{cd}^i = 2\delta_{ad} \delta_{bc} - \delta_{ab} \delta_{cd}$, which follows from equation (2.62). We finally obtain the contribution κ_{Δ} of the triplet,

$$\kappa_{\Delta} = -2(Y^{\Delta})_{gf} M_{\Delta}^{-2} f^{\Delta} v_R , \quad (2.93)$$

and together with the type I part, the neutrino mass in the type II see-saw scenario below all mass thresholds is determined by

$$\kappa^{(1)} = \kappa_{\Delta} + \sum_i \kappa_i = -2(Y^{\Delta})_{gf} M_{\Delta}^{-2} (f_{12}^{\Delta} v_R) + 2(Y_{\nu}^T)_{gi} (M^{-1})_{ij} (Y_{\nu})_{jf} . \quad (2.94)$$

2.4.3 The Effective Theories

As we have described above, in the intermediate region between the $(n-1)$ th and the n th threshold, the singlets $\{N_R^n, \dots, N_R^{n_G}\}$ or singlet superfields $\{\nu^{Cn}, \dots, \nu^{Cn_G}\}$ are integrated out, leading to effective operators of the type (2.81a) with coupling constant $\kappa_{gf}^{(n)}$. In this region, the Yukawa matrix for the remaining singlet neutrinos

is a $(n-1) \times n_F$ matrix and will be referred to as $Y_\nu^{(n)}$,

$$Y_\nu \rightarrow \left. \begin{array}{c} \left(\begin{array}{ccc} (Y_\nu)_{1,1} & \cdots & (Y_\nu)_{1,n_F} \\ \vdots & & \vdots \\ (Y_\nu)_{n-1,1} & \cdots & (Y_\nu)_{n-1,n_F} \\ \hline 0 & \cdots & 0 \\ \vdots & & \vdots \\ 0 & \cdots & 0 \end{array} \right) \end{array} \right\} \begin{array}{l} =: Y_\nu^{(n)}, \\ \\ n_G - n + 1 \text{ heavy, sterile} \\ \text{neutrinos integrated out.} \end{array} \quad (2.95)$$

The tree-level matching condition for the effective coupling constant at the threshold corresponding to the largest eigenvalue M_n of $M^{(n+1)}$ is then given by

$$\kappa_{gf}^{(n)}|_{M_n} := \kappa_{gf}^{(n+1)}|_{M_n} + 2 \left(Y_\nu^{(n+1)T} \right)_{gn} M_n^{-1} \left(Y_\nu^{(n+1)} \right)_{nf} |_{M_n} \quad (\text{no sum over } n). \quad (2.96)$$

$\kappa_{gf}^{(1)}$ is the neutrino mass operator below the thresholds, which has been called κ_{gf} in the previous chapter.

In the context of the minimal see-saw scenarios, κ_{gf} denotes the effective neutrino mass operator above the mass thresholds of the singlets, which stems from realization mechanisms at energy scales above M_U . For example, in the case of a type II see-saw mechanism, $\kappa_{gf}|_{M_U}$ can be the contribution from the Higgs triplet

$$\kappa_{gf}|_{M_U} = (\kappa_\Delta)_{gf}|_{M_U}. \quad (2.97)$$

The various effective theories and the nomenclature for the couplings are illustrated in figure 2.11. We now calculate the RGEs for the neutrino Yukawa coupling matrix, the mass matrix of the singlets and for the neutrino mass operator in the various effective theories.

2.4.4 Component-Field Calculation of the RGEs

The definition and calculation of the counterterms is analogous to the previous sections, except for the effects of the additional singlets. The counterterms for the mass matrix and the Yukawa coupling matrix of the sterile neutrinos as well as for the effective vertex in the extended SM are

$$\mathcal{E}_{\text{mass(N)}}^{(n)} = -\frac{1}{2} \overline{N_R^i} \delta M_{ij} N_R^{Cj} + \text{h.c.}, \quad (2.98a)$$

$$\mathcal{E}_{Y_\nu}^{(n)} = -(\delta Y_\nu)_{if} \overline{N_R^i} \tilde{\phi}^\dagger \ell_L^f + \text{h.c.}, \quad (2.98b)$$

$$\mathcal{E}_\kappa^{(n)} = \frac{1}{4} \delta \kappa_{gf}^{(n)} \overline{\ell_{Lc}^g} \varepsilon^{cd} \phi_d \ell_{Lb}^f \varepsilon^{ba} \phi_a + \text{h.c.}, \quad (2.98c)$$

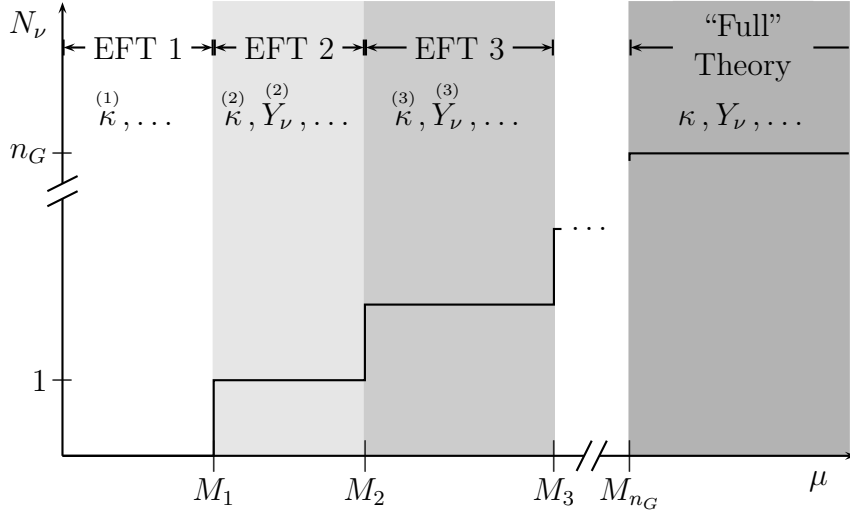


Figure 2.11: Illustration of the ranges of the different effective theories in minimal see-saw scenarios, where besides the n_G gauge singlets all additional particles have masses above the considered energy range. The effective field theories (EFTs) emerge from successively integrating out the heavy fields. “EFT 1” corresponds to the SM, 2HDM or MSSM with an additional dimension 5 operator for neutrino masses.

where the sums over i and j run from 1 to $n-1$. The wavefunction renormalization constants below the n th threshold are denoted by $Z^{(n)}$. In the MSSM and the 2HDMs, we use analogous definitions.

Calculation of the Counterterms

At 1-loop order, the singlets do not contribute to $\delta\kappa$. They enter the RGEs only via the wavefunction renormalization constants. The additional diagrams, which contribute to the self-energies of the Higgs and the lepton doublets, are shown in figure 2.12 in diagram (a) and (b). The diagrams relevant for the wavefunction renormalization of the singlets themselves are given in diagram (c) and (d) of figure 2.12. Finally, we obtain the following renormalization constants in the extended SM,

$$\delta Z_{\ell_L}^{(n)\text{SM}} = -\frac{1}{16\pi^2} \left[Y_\nu^\dagger Y_\nu + Y_e^\dagger Y_e + \frac{1}{2}\xi_B g_1^2 + \frac{3}{2}\xi_W g_2^2 \right] \frac{1}{\epsilon}, \quad (2.99a)$$

$$\begin{aligned} \delta Z_\phi^{(n)\text{SM}} = & -\frac{1}{16\pi^2} \left[2 \text{Tr}(Y_\nu^\dagger Y_\nu) + 2 \text{Tr}(Y_e^\dagger Y_e) + 6 \text{Tr}(Y_u^\dagger Y_u) + 6 \text{Tr}(Y_d^\dagger Y_d) \right. \\ & \left. + \frac{1}{2}(\xi_B - 3)g_1^2 + \frac{3}{2}(\xi_W - 3)g_2^2 \right] \frac{1}{\epsilon}, \quad (2.99b) \end{aligned}$$

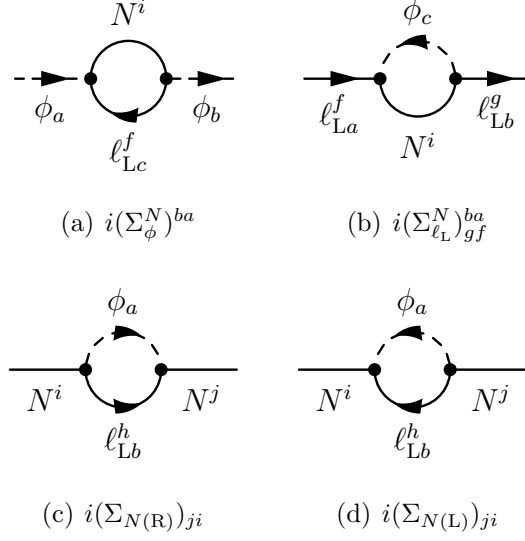


Figure 2.12: Additional 1-loop diagrams which contribute to the self-energies of the Higgs (diagram (a)) and the lepton doublets (diagram (b)) in the SM extended by heavy singlets and the diagrams for the wavefunction renormalization of the singlets (diagrams (c) and (d)).

$$\delta Z_N^{(n)\text{SM}} = -\frac{1}{16\pi^2} \left[2 Y_\nu^{(n)} Y_\nu^{\dagger(n)} \right] \frac{1}{\epsilon}. \quad (2.99c)$$

$$\delta Y_\nu^{(n)\text{SM}} = -\frac{1}{16\pi^2} \left[2 Y_\nu^{(n)} (Y_e^\dagger Y_e) + \frac{1}{2} \xi_B g_1^2 Y_\nu^{(n)} + \frac{3}{2} \xi_W g_2^2 Y_\nu^{(n)} \right] \frac{1}{\epsilon}, \quad (2.99d)$$

$$\delta M^{(n)\text{SM}} = 0, \quad (2.99e)$$

$$\delta \kappa^{(n)\text{SM}} = -\frac{1}{16\pi^2} \left[2 (Y_e^\dagger Y_e)^T \kappa^{(n)} + 2 \kappa^{(n)} (Y_e^\dagger Y_e) - \lambda \kappa^{(n)} + \frac{1}{2} (2\xi_B - 3) g_1^2 \kappa^{(n)} + \frac{3}{2} (2\xi_W - 1) g_2^2 \kappa^{(n)} \right] \frac{1}{\epsilon}. \quad (2.99f)$$

In the extended 2HDMs, we find at one loop

$$\delta Z_{\ell_L}^{(n)\text{2HDM}} = -\frac{1}{16\pi^2} \left[Y_\nu^{\dagger(n)} Y_\nu^{(n)} + Y_e^\dagger Y_e + \frac{1}{2} \xi_B g_1^2 + \frac{3}{2} \xi_W g_2^2 \right] \frac{1}{\epsilon}, \quad (2.100a)$$

$$\begin{aligned} \delta Z_{\phi^{(i)}}^{(n)\text{2HDM}} = & -\frac{1}{16\pi^2} \left[2 z_\nu^{(i)} \text{Tr}(Y_\nu^{\dagger(n)} Y_\nu^{(n)}) + 2 \delta_{1i} \text{Tr}(Y_e^\dagger Y_e) \right. \\ & + 6 z_u^{(i)} \text{Tr}(Y_u^\dagger Y_u) + 6 z_d^{(i)} \text{Tr}(Y_d^\dagger Y_d) \\ & \left. + \frac{1}{2} (\xi_B - 3) g_1^2 + \frac{3}{2} (\xi_W - 3) g_2^2 \right] \frac{1}{\epsilon}, \end{aligned} \quad (2.100b)$$

$$\delta Z_N^{(n)2\text{HDM}} = -\frac{1}{16\pi^2} \left[2 Y_\nu^{(n)} Y_\nu^{(n)\dagger} \right] \frac{1}{\epsilon}, \quad (2.100c)$$

$$\delta Y_\nu^{(n)2\text{HDM}} = -\frac{1}{16\pi^2} \left[2 Y_\nu^{(n)} (Y_e^\dagger Y_e) + \frac{1}{2} \xi_B g_1^2 Y_\nu^{(n)} + \frac{3}{2} \xi_W g_2^2 Y_\nu^{(n)} \right] \frac{1}{\epsilon}, \quad (2.100d)$$

$$\delta M^{(n)2\text{HDM}} = 0, \quad (2.100e)$$

$$\begin{aligned} \delta \kappa^{(n)2\text{HDM}} &= -\frac{1}{16\pi^2} \left[\delta_{i1} 2\kappa^{(ii)} (Y_e^\dagger Y_e) + \delta_{i1} 2(Y_e^\dagger Y_e)^T \kappa^{(ii)} \right. \\ &\quad \left. - \lambda_i \kappa^{(ii)} - \delta_{i1} \lambda_5^* \kappa^{(22)} - \delta_{i2} \lambda_5 \kappa^{(11)} \right. \\ &\quad \left. + \left(\xi_B - \frac{3}{2} \right) g_1^2 \kappa^{(ii)} + \left(3\xi_W - \frac{3}{2} \right) g_2^2 \kappa^{(ii)} \right] \frac{1}{\epsilon}. \end{aligned} \quad (2.100f)$$

The renormalization constants in the MSSM extended by heavy singlets are

$$\begin{aligned} \delta Z_{\ell_L}^{(n)\text{MSSM}} &= -\frac{1}{16\pi^2} \left[2 Y_\nu^{(n)\dagger} Y_\nu^{(n)} + 2 Y_e^\dagger Y_e + \frac{1}{2} (\xi_B - 1) g_1^2 \right. \\ &\quad \left. + \frac{3}{2} (\xi_W - 1) g_2^2 \right] \frac{1}{\epsilon}, \end{aligned} \quad (2.101a)$$

$$\begin{aligned} \delta Z_{\phi^{(2)}}^{(n)\text{MSSM}} &= -\frac{1}{16\pi^2} \left[2 \text{Tr} (Y_\nu^{(n)\dagger} Y_\nu^{(n)}) + 6 \text{Tr} (Y_u^\dagger Y_u) \right. \\ &\quad \left. + \frac{1}{2} (\xi_B + 1) g_1^2 + \frac{3}{2} (\xi_W + 1) g_2^2 \right] \frac{1}{\epsilon}, \end{aligned} \quad (2.101b)$$

$$\delta Z_N^{(n)\text{MSSM}} = -\frac{1}{16\pi^2} \left[4 Y_\nu^{(n)} Y_\nu^{(n)\dagger} \right] \frac{1}{\epsilon}, \quad (2.101c)$$

$$\delta Y_\nu^{(n)\text{MSSM}} = -\frac{1}{16\pi^2} \left[\frac{1}{2} (\xi_B + 2) g_1^2 Y_\nu^{(n)} + \frac{3}{2} (\xi_W + 2) g_2^2 Y_\nu^{(n)} \right] \frac{1}{\epsilon}, \quad (2.101d)$$

$$\delta M^{(n)\text{MSSM}} = 0, \quad (2.101e)$$

$$\delta \kappa^{(n)\text{MSSM}} = -\frac{1}{16\pi^2} \left[(\xi_B + 2) g_1^2 \kappa^{(n)} + 3(\xi_W + 2) g_2^2 \kappa^{(n)} \right] \frac{1}{\epsilon}. \quad (2.101f)$$

Computation of the RGEs in Minimal See-Saw Scenarios

Using the counterterms calculated above, we can now compute the RGEs. Note that above the largest see-saw scale, the superscript (n) is omitted. Below the lowest see-saw scale, the neutrino Yukawa couplings and the mass matrix of the singlets are set to zero. In the extended SM, we thus obtain [85]

$$\begin{aligned} 16\pi^2 \beta_\kappa^{\text{SM}} &= -\frac{3}{2} (Y_e^\dagger Y_e)^T \kappa^{(n)} - \frac{3}{2} \kappa^{(n)} (Y_e^\dagger Y_e) + \frac{1}{2} (Y_\nu^\dagger Y_\nu)^T \kappa^{(n)} + \frac{1}{2} \kappa^{(n)} (Y_\nu^\dagger Y_\nu) \\ &\quad + 2 \text{Tr} (Y_e^\dagger Y_e) \kappa^{(n)} + 2 \text{Tr} (Y_\nu^\dagger Y_\nu) \kappa^{(n)} + 6 \text{Tr} (Y_u^\dagger Y_u) \kappa^{(n)} \\ &\quad + 6 \text{Tr} (Y_d^\dagger Y_d) \kappa^{(n)} - 3g_2^2 \kappa^{(n)} + \lambda \kappa^{(n)}, \end{aligned} \quad (2.102a)$$

$$16\pi^2 \beta_{Y_\nu}^{(n)\text{SM}} = Y_\nu \left[\frac{3}{2} (Y_\nu^\dagger Y_\nu)^{(n)} - \frac{3}{2} (Y_e^\dagger Y_e) + \text{Tr} (Y_\nu^\dagger Y_\nu)^{(n)} + \text{Tr} (Y_e^\dagger Y_e) \right. \\ \left. + 3 \text{Tr} (Y_u^\dagger Y_u) + 3 \text{Tr} (Y_d^\dagger Y_d) - \frac{3}{4} g_1^2 - \frac{9}{4} g_2^2 \right], \quad (2.102b)$$

$$16\pi^2 \beta_M^{(n)\text{SM}} = (Y_\nu Y_\nu^\dagger)^{(n)} M + M (Y_\nu Y_\nu^\dagger)^{(n)T}. \quad (2.102c)$$

The RGEs in the 2HDMs are given by

$$16\pi^2 \beta_{\kappa^{(ii)}}^{(n)\text{2HDM}} = \left(\frac{1}{2} - 2\delta_{i1} \right) \left[\kappa^{(ii)} (Y_e^\dagger Y_e) + (Y_e^\dagger Y_e)^T \kappa^{(ii)} \right] \\ + z_\nu^{(i)} 2 \text{Tr} (Y_\nu^\dagger Y_\nu)^{(n)} + \left[\delta_{i1} 2 \text{Tr} (Y_e^\dagger Y_e) \right. \\ \left. + z_u^{(i)} 6 \text{Tr} (Y_u^\dagger Y_u) + z_d^{(i)} 6 \text{Tr} (Y_d^\dagger Y_d) \right] \kappa^{(ii)} \\ + \lambda_i \kappa^{(ii)} + \delta_{i1} \lambda_5^* \kappa^{(22)} + \delta_{i2} \lambda_5 \kappa^{(11)} - 3g_2^2 \kappa^{(ii)}, \quad (2.103a)$$

$$16\pi^2 \beta_{Y_\nu}^{(n)\text{2HDM}} = Y_\nu \left\{ \frac{3}{2} Y_\nu^\dagger Y_\nu + \left(\frac{1}{2} - 2z_\nu^{(1)} \right) \frac{3}{2} Y_e^\dagger Y_e - \frac{3}{4} g_1^2 - \frac{9}{4} g_2^2 \right. \\ \left. + \sum_{i=1}^2 z_\nu^{(i)} \text{Tr} \left[\delta_{i1} Y_e^\dagger Y_e + Y_\nu^\dagger Y_\nu \right. \right. \\ \left. \left. + 3z_d^{(i)} Y_d^\dagger Y_d + 3z_u^{(i)} Y_u^\dagger Y_u \right] \right\}, \quad (2.103b)$$

$$16\pi^2 \beta_M^{(n)\text{2HDM}} = (Y_\nu Y_\nu^\dagger)^{(n)} M + M (Y_\nu Y_\nu^\dagger)^{(n)T}. \quad (2.103c)$$

In the minimal see-saw extension of the MSSM, we find [85]

$$16\pi^2 \beta_\kappa^{(n)\text{MSSM}} = (Y_e^\dagger Y_e)^T \kappa^{(n)} + \kappa^{(n)} (Y_e^\dagger Y_e) + (Y_\nu^\dagger Y_\nu)^{(n)T} \kappa^{(n)} + \kappa^{(n)} (Y_\nu^\dagger Y_\nu)^{(n)} \\ + 2 \text{Tr} (Y_\nu^\dagger Y_\nu)^{(n)} \kappa^{(n)} + 6 \text{Tr} (Y_u^\dagger Y_u)^{(n)} \kappa^{(n)} - 2g_1^2 \kappa^{(n)} - 6g_2^2 \kappa^{(n)}, \quad (2.104a)$$

$$16\pi^2 \beta_{Y_\nu}^{(n)\text{MSSM}} = Y_\nu \left[3 Y_\nu^\dagger Y_\nu + Y_e^\dagger Y_e + \text{Tr} (Y_\nu^\dagger Y_\nu)^{(n)} + 3 \text{Tr} (Y_u^\dagger Y_u) \right. \\ \left. - g_1^2 - 3g_2^2 \right], \quad (2.104b)$$

$$16\pi^2 \beta_M^{(n)\text{MSSM}} = 2 (Y_\nu Y_\nu^\dagger)^{(n)} M + 2 M (Y_\nu Y_\nu^\dagger)^{(n)T}. \quad (2.104c)$$

The RG evolution of the effective neutrino mass matrix in such scenarios will be investigated in section 3.3. The RGEs for the remaining parameters are listed in appendix A.5.

2.4.5 Calculation of the RGEs at 2-Loop using Supergraphs

We now apply the supergraph method of section 2.3.3 to calculate the 2-loop β -functions for the effective neutrino mass operator, the neutrino Yukawa coupling matrix and the mass matrix of the heavy singlet superfields in the minimal see-saw scenarios.

The Wavefunction Renormalization Constants

We obtain the following $1/\epsilon$ -coefficients of the relevant wavefunction renormalization constants at one loop:

$$-(4\pi)^2 Z_{\mathfrak{h}^{(2)},1}^{(n)(1)} = 6 \operatorname{Tr}(Y_u^\dagger Y_u) + 2 \operatorname{Tr}(Y_\nu^\dagger Y_\nu) - \frac{3}{5} (g_1^U)^2 - 3 g_2^2, \quad (2.105a)$$

$$-(4\pi)^2 Z_{\mathfrak{l},1}^{(n)(1)} = 2 Y_e^\dagger Y_e + 2 Y_\nu^\dagger Y_\nu - \frac{3}{5} (g_1^U)^2 - 3 g_2^2, \quad (2.105b)$$

$$-(4\pi)^2 Z_{\mathfrak{v}^c,1}^{(n)(1)} = 4 Y_\nu^{*T} Y_\nu^T. \quad (2.105c)$$

Note that GUT charge normalization has been used for $U(1)_Y$. The 2-loop contributions can be calculated from equation (2.74) and are given by

$$\begin{aligned} -\frac{(4\pi)^4}{2} Z_{\mathfrak{h}^{(2)},1}^{(n)(2)} &= -3 \operatorname{Tr}(Y_u^\dagger Y_d Y_d^\dagger Y_u) - 9 \operatorname{Tr}(Y_u^\dagger Y_u Y_u^\dagger Y_u) - \operatorname{Tr}(Y_\nu^\dagger Y_e Y_e^\dagger Y_\nu) \\ &\quad - 3 \operatorname{Tr}(Y_\nu^\dagger Y_\nu Y_\nu^\dagger Y_\nu) + \frac{4}{5} (g_1^U)^2 \operatorname{Tr}(Y_u^\dagger Y_u) + 16 g_3^2 \operatorname{Tr}(Y_u^\dagger Y_u) \\ &\quad + \frac{207}{100} (g_1^U)^4 + \frac{9}{10} (g_1^U)^2 g_2^2 + \frac{15}{4} g_2^4, \end{aligned} \quad (2.106a)$$

$$\begin{aligned} -\frac{(4\pi)^4}{2} Z_{\mathfrak{l},1}^{(n)(2)} &= -2 Y_e^\dagger Y_e Y_e^\dagger Y_e - 2 Y_\nu^\dagger Y_\nu Y_\nu^\dagger Y_\nu - 3 Y_e^\dagger Y_e \operatorname{Tr}(Y_d Y_d^\dagger) \\ &\quad - Y_e^\dagger Y_e \operatorname{Tr}(Y_e Y_e^\dagger) - 3 Y_\nu^\dagger Y_\nu \operatorname{Tr}(Y_u Y_u^\dagger) - Y_\nu^\dagger Y_\nu \operatorname{Tr}(Y_\nu Y_\nu^\dagger) \\ &\quad + \frac{6}{5} (g_1^U)^2 Y_e^\dagger Y_e + \frac{207}{100} (g_1^U)^4 + \frac{9}{10} (g_1^U)^2 g_2^2 + \frac{15}{4} g_2^4, \end{aligned} \quad (2.106b)$$

$$\begin{aligned} -\frac{(4\pi)^4}{2} Z_{\mathfrak{v}^c,1}^{(n)(2)} &= -2 Y_\nu^{*T} Y_e^T Y_e^* Y_\nu^T - 2 Y_\nu^{*T} Y_\nu^T Y_\nu^* Y_\nu^T - 6 Y_\nu^{*T} Y_\nu^T \operatorname{Tr}(Y_u Y_u^\dagger) \\ &\quad - 2 Y_\nu^{*T} Y_\nu^T \operatorname{Tr}(Y_\nu Y_\nu^\dagger) + \frac{6}{5} (g_1^U)^2 Y_\nu^{*T} Y_\nu^T + 6 g_2^2 Y_\nu^{*T} Y_\nu^T. \end{aligned} \quad (2.106c)$$

Computation of the 2-Loop RGEs

We now evaluate the 2-loop β -functions, which govern the energy scale dependence of the effective neutrino mass matrix in the minimal see-saw scenarios. This can easily be done using the wavefunction renormalization constants and equation (2.20). The β -function for a physical quantity Q at two loop can be written as

$$\mu \frac{d}{d\mu} \overset{(n)}{Q} = \overset{(n)}{\beta}_Q = \overset{(n)}{\beta}_Q^{(1)} + \overset{(n)}{\beta}_Q^{(2)}, \quad (2.107)$$

where $\overset{(n)}{\beta}_Q^{(1)}$ is the 1-loop part and $\overset{(n)}{\beta}_Q^{(2)}$ the 2-loop part. The calculation of the 1-loop part confirms the component-field results of equation (2.104). In addition, for the 2-loop part of the β -functions we obtain

$$\begin{aligned} (4\pi)^4 \overset{(n)}{\beta}_\kappa^{(2)} = & \left[-6 \text{Tr} (Y_u^\dagger Y_d Y_d^\dagger Y_u) - 18 \text{Tr} (Y_u^\dagger Y_u Y_u^\dagger Y_u) - 2 \text{Tr} (\overset{(n)}{Y}_\nu^\dagger Y_e Y_e^\dagger \overset{(n)}{Y}_\nu) \right. \\ & - 6 \text{Tr} (\overset{(n)}{Y}_\nu^\dagger \overset{(n)}{Y}_\nu \overset{(n)}{Y}_\nu^\dagger \overset{(n)}{Y}_\nu) + \frac{8}{5} (g_1^U)^2 \text{Tr} (Y_u^\dagger Y_u) + 32 g_3^2 \text{Tr} (Y_u^\dagger Y_u) + \frac{207}{25} (g_1^U)^4 \\ & \left. + \frac{18}{5} (g_1^U)^2 g_2^2 + 15 g_2^4 \right] \overset{(n)}{\kappa} \\ & - \left[2 (Y_e^\dagger Y_e Y_e^\dagger Y_e)^T + 2 (\overset{(n)}{Y}_\nu^\dagger \overset{(n)}{Y}_\nu \overset{(n)}{Y}_\nu^\dagger \overset{(n)}{Y}_\nu)^T + \left(\text{Tr} (\overset{(n)}{Y}_\nu \overset{(n)}{Y}_\nu^\dagger) + 3 \text{Tr} (Y_u Y_u^\dagger) \right) (\overset{(n)}{Y}_\nu^\dagger \overset{(n)}{Y}_\nu)^T \right. \\ & \left. + \left(-\frac{6}{5} (g_1^U)^2 + \text{Tr} (Y_e Y_e^\dagger) + 3 \text{Tr} (Y_d Y_d^\dagger) \right) (Y_e^\dagger Y_e)^T \right] \overset{(n)}{\kappa} \\ & - \overset{(n)}{\kappa} \left[2 Y_e^\dagger Y_e Y_e^\dagger Y_e + 2 \overset{(n)}{Y}_\nu^\dagger \overset{(n)}{Y}_\nu \overset{(n)}{Y}_\nu^\dagger \overset{(n)}{Y}_\nu + \left(\text{Tr} (\overset{(n)}{Y}_\nu \overset{(n)}{Y}_\nu^\dagger) + 3 \text{Tr} (Y_u Y_u^\dagger) \right) \overset{(n)}{Y}_\nu^\dagger \overset{(n)}{Y}_\nu \right. \\ & \left. + \left(-\frac{6}{5} (g_1^U)^2 + \text{Tr} (Y_e Y_e^\dagger) + 3 \text{Tr} (Y_d Y_d^\dagger) \right) Y_e^\dagger Y_e \right], \quad (2.108a) \end{aligned}$$

$$\begin{aligned} (4\pi)^4 \overset{(n)}{\beta}_{Y_\nu}^{(2)} = & \overset{(n)}{Y}_\nu \left\{ -2 Y_e^\dagger Y_e Y_e^\dagger Y_e - 2 Y_e^\dagger Y_e \overset{(n)}{Y}_\nu^\dagger \overset{(n)}{Y}_\nu - 4 \overset{(n)}{Y}_\nu^\dagger \overset{(n)}{Y}_\nu \overset{(n)}{Y}_\nu^\dagger \overset{(n)}{Y}_\nu \right. \\ & - 3 Y_e^\dagger Y_e \text{Tr} (Y_d Y_d^\dagger) - Y_e^\dagger Y_e \text{Tr} (Y_e Y_e^\dagger) - 3 \overset{(n)}{Y}_\nu^\dagger \overset{(n)}{Y}_\nu \text{Tr} (\overset{(n)}{Y}_\nu \overset{(n)}{Y}_\nu^\dagger) - 9 \overset{(n)}{Y}_\nu^\dagger \overset{(n)}{Y}_\nu \text{Tr} (Y_u Y_u^\dagger) \\ & - \text{Tr} (\overset{(n)}{Y}_\nu^\dagger Y_e Y_e^\dagger \overset{(n)}{Y}_\nu) - 3 \text{Tr} (\overset{(n)}{Y}_\nu^\dagger \overset{(n)}{Y}_\nu \overset{(n)}{Y}_\nu^\dagger \overset{(n)}{Y}_\nu) - 3 \text{Tr} (Y_u^\dagger Y_d Y_d^\dagger Y_u) - 9 \text{Tr} (Y_u^\dagger Y_u Y_u^\dagger Y_u) \\ & + \frac{6}{5} (g_1^U)^2 Y_e^\dagger Y_e + \frac{6}{5} (g_1^U)^2 \overset{(n)}{Y}_\nu^\dagger \overset{(n)}{Y}_\nu + 6 g_2^2 \overset{(n)}{Y}_\nu^\dagger \overset{(n)}{Y}_\nu + \frac{4}{5} (g_1^U)^2 \text{Tr} (Y_u^\dagger Y_u) \\ & \left. + 16 g_3^2 \text{Tr} (Y_u^\dagger Y_u) + \frac{207}{50} (g_1^U)^4 + \frac{9}{5} (g_1^U)^2 g_2^2 + \frac{15}{2} g_2^4 \right\}, \quad (2.108b) \end{aligned}$$

$$\begin{aligned}
 (4\pi)^4 \beta_M^{(2)} &= M \left[-2 Y_\nu^* Y_e^T Y_e^* Y_\nu^T - 2 Y_\nu^* Y_\nu^T Y_\nu^* Y_\nu^T - 6 Y_\nu^* Y_\nu^T \text{Tr}(Y_u Y_u^\dagger) \right. \\
 &\quad \left. - 2 Y_\nu^* Y_\nu^T \text{Tr}(Y_\nu Y_\nu^\dagger) + \frac{6}{5} (g_1^U)^2 Y_\nu^* Y_\nu^T + 6 g_2^2 Y_\nu^* Y_\nu^T \right] \\
 &+ \left[-2 Y_\nu Y_e^\dagger Y_e Y_\nu^\dagger - 2 Y_\nu Y_\nu^\dagger Y_\nu Y_\nu^\dagger - 6 Y_\nu Y_\nu^\dagger \text{Tr}(Y_u Y_u^\dagger) - 2 Y_\nu Y_\nu^\dagger \text{Tr}(Y_\nu Y_\nu^\dagger) \right. \\
 &\quad \left. + \frac{6}{5} (g_1^U)^2 Y_\nu Y_\nu^\dagger + 6 g_2^2 Y_\nu Y_\nu^\dagger \right] M. \tag{2.108c}
 \end{aligned}$$

The 2-loop RGEs for the remaining Yukawa couplings, which contain additional terms proportional to the neutrino Yukawa couplings in the minimal see-saw extension of the MSSM, are calculated in [81] and summarized in appendix A.5.3.

3 Analysis of Running Neutrino Masses, Mixings and CP Phases

In the previous chapter, we have calculated the β -functions which are required to study the RG running of the effective neutrino mass matrix. It has to be taken into account whenever neutrino masses, mixings and CP phases at different energy scales are compared. In order to obtain the running of the physical parameters, there are two possibilities. One is to calculate the running of the neutrino mass matrix and of all the other quantities of the theory and to extract the neutrino parameters afterwards. We will use this “run and diagonalize” procedure for the numerical studies in this work. The other possibility is to “diagonalize and run”, which means to extract the parameters first and to derive differential equations for their RG evolutions. We will use this technique to derive analytical formulae for the running parameters.

For the analysis, we will first consider the description of neutrino masses by the lowest dimensional effective neutrino mass operator. There exists a large number of studies which have investigated the running parameters numerically (e.g. [86–105]). Exact analytical formulae are given in [90], where CP conservation is assumed, and in [91] for the general case. However, most of the expressions in [91] become rather long if one tries to write them explicitly in terms of the mixing parameters, in particular for non-vanishing CP phases. In order to understand the RG effects in the presence of CP phases, we derive compact analytical approximations in an expansion in the small mixing angle θ_{13} . To check and to illustrate the results, we compare them to numerical solutions of the RGEs. We furthermore investigate whether the RG corrections can be accessible to future precision experiments.

As we have seen in section 1.4, neutrino masses naturally appear in left-right symmetric extensions of the SM. Predictions for them might arise for example from models defined at the GUT scale. Particularly interesting in this context is the type I see-saw scenario with three generations of singlets. In this case we have to use the RGEs for the effective theories with the heavy singlets partly integrated out, which are derived in section 2.4. We investigate the possibility of generating the experimentally observed large but non-maximal solar mixing of the LMA solution by RG running in this scenario from vanishing as well as from maximal mixing at high energy.

3.1 Analytical Results in the Neutrino Mass Operator Approach

We will now derive analytical approximations for the running of neutrino masses, mixing angles and CP phases in an expansion in θ_{13} , where the formulae are pretty compact even in the presence of CP phases. We compare them to the numerical solutions of the coupled system of RGEs in the MSSM. For the numerical examples, we assume that below the SUSY breaking scale, the theory is effectively the SM.

3.1.1 Derivation of Analytical Formulae for the Running Parameters

The energy dependence of the effective neutrino mass matrix below the scale where the operator is generated (which we will call M_1 in the following) is described by its RGE. We will restrict ourselves to the SM and the MSSM in this section, where at the one-loop level the RGEs have the form

$$16\pi^2 \frac{d\kappa}{dt} = C (Y_e^\dagger Y_e)^T \kappa + C \kappa (Y_e^\dagger Y_e) + \alpha \kappa, \quad (3.1)$$

with $t := \ln(\mu/\mu_0)$. The coefficient C is defined by

$$C_{\text{SM}} = -\frac{3}{2}, \quad C_{\text{MSSM}} = 1, \quad (3.2)$$

and α is given by

$$\alpha_{\text{SM}} = 2(y_\tau^2 + y_\mu^2 + y_e^2) + 6(y_t^2 + y_b^2 + y_c^2 + y_s^2 + y_d^2 + y_u^2) - 3g_2^2 + \lambda, \quad (3.3a)$$

$$\alpha_{\text{MSSM}} = 6(y_t^2 + y_c^2 + y_u^2) - \frac{6}{5}(g_1^{\text{U}})^2 - 6g_2^2. \quad (3.3b)$$

We are interested in the running of the masses, which are proportional to the eigenvalues of κ , and of the mixing angles and physical phases of the MNS matrix U_{MNS} [106]. The parametrization we use is explained in appendix A.1.

In order to derive the analytical formulae for the running parameters, we follow the method of [107], which leads to a differential equation for the energy scale dependence of the MNS matrix. For the RGEs, we use the notation of equation (3.1) and introduce the abbreviation $C(Y_e^\dagger Y_e) =: P$. We further choose the basis where the charged lepton Yukawa matrix is diagonal. Since it remains diagonal during its RG evolution, the running of the MNS matrix is given by the running of the diagonalization matrix of κ , and the relation

$$U_{\text{MNS}}(t)^T \kappa(t) U_{\text{MNS}}(t) = D(t) = \frac{4}{v_{\text{EW}}^2} \text{diag}(m_1(t), m_2(t), m_3(t)) \quad (3.4)$$

holds at any energy scale. To describe the evolution of U_{MNS} , we introduce a matrix T which satisfies

$$\frac{d}{dt}U_{\text{MNS}} = U_{\text{MNS}} T . \quad (3.5)$$

Clearly, T has to be anti-Hermitian, as can easily be seen by calculating $\frac{d}{dt}(U_{\text{MNS}}^\dagger U_{\text{MNS}})$. From equation (3.4), we obtain

$$\begin{aligned} \frac{d}{dt} \left(U_{\text{MNS}}^* D U_{\text{MNS}}^\dagger \right) &= \dot{U}_{\text{MNS}}^* D U_{\text{MNS}}^\dagger + U_{\text{MNS}}^* D \dot{U}_{\text{MNS}}^\dagger + U_{\text{MNS}}^* \dot{D} U_{\text{MNS}}^\dagger \\ &\stackrel{(3.1)}{=} \frac{1}{16\pi^2} \left(\alpha U_{\text{MNS}}^* D U_{\text{MNS}}^\dagger + P^T U_{\text{MNS}}^* D U_{\text{MNS}}^\dagger + U_{\text{MNS}}^* D U_{\text{MNS}}^\dagger P \right), \end{aligned} \quad (3.6)$$

where a dot over a quantity denotes differentiation with respect to t . Multiplying with U_{MNS}^T from the left and with U_{MNS} from the right yields

$$U_{\text{MNS}}^T \dot{U}_{\text{MNS}}^* D + D \dot{U}_{\text{MNS}}^\dagger U_{\text{MNS}} + \dot{D} = \frac{1}{16\pi^2} [\alpha D + P'^T D + D P'] , \quad (3.7)$$

where we have introduced

$$P' = U_{\text{MNS}}^\dagger P U_{\text{MNS}} . \quad (3.8)$$

Inserting equation (3.5), we find

$$\dot{D} = \frac{1}{16\pi^2} (\alpha D + P'^T D + D P') - T^* D + D T , \quad (3.9)$$

where the anti-Hermiticity of T was used. Since the left-hand side of this equation is diagonal and real per definition, the right-hand side has to possess these properties as well,

$$\dot{m}_i = \frac{1}{16\pi^2} (\alpha m_i + 2 P'_{ii} m_i) + (T_{ii} - T_{ii}^*) m_i , \quad (3.10)$$

where we do not sum over the index i . The second bracket is purely imaginary, hence it has to cancel with the imaginary part of the first one,

$$2 \text{Im} T_{ii} = \frac{-1}{16\pi^2} (\text{Im} \alpha + 2 \text{Im} P'_{ii}) , \quad (3.11)$$

and we further confirm eq. (15) of [91], which translates with our conventions to

$$16\pi^2 \dot{m}_i = (\text{Re} \alpha + 2 \text{Re} P'_{ii}) m_i . \quad (3.12)$$

By comparing the off-diagonal parts of (3.9) we find

$$m_i T_{ij} - T_{ij}^* m_j = -\frac{1}{16\pi^2} (P'_{ij}{}^T m_j + m_i P'_{ij}) . \quad (3.13)$$

Adding and subtracting this equation and its complex conjugate, we obtain for $i \neq j$

$$16\pi^2 \operatorname{Re} T_{ij} = -\frac{m_j \operatorname{Re} P'_{ji} + m_i \operatorname{Re} P'_{ij}}{m_i - m_j}, \quad (3.14a)$$

$$16\pi^2 \operatorname{Im} T_{ij} = -\frac{m_j \operatorname{Im} P'_{ji} + m_i \operatorname{Im} P'_{ij}}{m_i + m_j}. \quad (3.14b)$$

Since P is Hermitian and α is real, the anti-Hermitian matrix T , which governs the energy scale dependence of the MNS matrix, is given by

$$T_{ij} = \begin{cases} -\frac{1}{16\pi^2} \operatorname{Im} P'_{ij} & \text{for } i = j, \\ -\frac{1}{16\pi^2} \left[\frac{m_i + m_j}{m_i - m_j} \operatorname{Re} P'_{ij} + i \cdot \frac{m_i - m_j}{m_i + m_j} \operatorname{Im} P'_{ij} \right] & \text{for } i \neq j, \end{cases} \quad (3.15)$$

where P' defined in equation (3.8) is Hermitian as well and where we have used $\operatorname{Re} P'_{ji} = \operatorname{Re} P'_{ij}^* = \operatorname{Re} P'_{ij}$ and an analogous relation for $\operatorname{Im} P'_{ij}$.

In order to obtain the RGEs for the mixing angles and phases, we use equation (3.5) in the form

$$U_{\text{MNS}}^\dagger \dot{U}_{\text{MNS}} = T. \quad (3.16)$$

Inserting the standard parametrization (A.23), we can express the left-hand side of (3.16) in terms of the mixing parameters and their derivatives. Now we can solve for the derivatives of the mixing parameters. Due to the separation of the evolution of the mass eigenvalues in equation (3.12), we have reduced the amount of parameters from 12 to 9. The discussion so far is very similar to the one of [91]. There, the RG evolutions of the mixing parameters are expressed in terms of the mixing matrix elements and P' . In order to obtain rather short explicit analytic formulae, which are useful for deriving analytic approximations, we first label the mixing parameters as

$$\{\xi_k\} = \{\theta_{12}, \theta_{13}, \theta_{23}, \delta, \delta_e, \delta_\mu, \delta_\tau, \varphi_1, \varphi_2\} \quad (3.17)$$

and observe that the left-hand side of (3.16) is linear in $\dot{\xi}_k$. Then, by solving the corresponding system of linear equations, we express the derivatives of the mixing parameters by the mixing parameters, the mass eigenvalues and the Yukawa couplings.

The resulting formulae are still too long to be presented here. We therefore perform an expansion in θ_{13} , which yields compact expressions [108]. They will be presented in the following sections. In addition, in the analytical expressions for the slope of the mixing angles, we will neglect y_e and y_μ against y_τ and further introduce the abbreviation

$$\zeta := \frac{\Delta m_{\text{sol}}^2}{\Delta m_{\text{atm}}^2}, \quad (3.18)$$

whose LMA best-fit value is about 0.03. In many cases, the length of the formulae can be further reduced by neglecting ζ against 1 without losing much accuracy. We furthermore define $m_i(t) := v_{\text{EW}}^2 \kappa_i(t)/4$ with $v_{\text{EW}} = 246$ GeV in the SM or $m_i(t) := v_u^2 \kappa_i(t)/4$ with $v_u = 246$ GeV $\cdot \sin \beta$ in the MSSM and, as usual, $\Delta m_{\text{sol}}^2 := m_2^2 - m_1^2$ and $\Delta m_{\text{atm}}^2 := m_3^2 - m_2^2$. Note that our formulae cannot be applied if one of the mass squared differences vanishes.

3.1.2 The Running of the Lepton Mixing Angles

With the conventions described above, we obtain the following analytical expressions for the mixing angles:

$$\dot{\theta}_{12} = -\frac{C y_\tau^2}{32\pi^2} \sin 2\theta_{12} s_{23}^2 \frac{|m_1 e^{i\varphi_1} + m_2 e^{i\varphi_2}|^2}{\Delta m_{\text{sol}}^2} + \mathcal{O}(\theta_{13}), \quad (3.19)$$

$$\begin{aligned} \dot{\theta}_{13} &= \frac{C y_\tau^2}{32\pi^2} \sin 2\theta_{12} \sin 2\theta_{23} \frac{m_3}{\Delta m_{\text{atm}}^2 (1 + \zeta)} \times \\ &\quad \times [m_1 \cos(\varphi_1 - \delta) - (1 + \zeta) m_2 \cos(\varphi_2 - \delta) - \zeta m_3 \cos \delta] \\ &\quad + \mathcal{O}(\theta_{13}), \end{aligned} \quad (3.20)$$

$$\begin{aligned} \dot{\theta}_{23} &= -\frac{C y_\tau^2}{32\pi^2} \sin 2\theta_{23} \frac{1}{\Delta m_{\text{atm}}^2} \left[c_{12}^2 |m_2 e^{i\varphi_2} + m_3|^2 + s_{12}^2 \frac{|m_1 e^{i\varphi_1} + m_3|^2}{1 + \zeta} \right] \\ &\quad + \mathcal{O}(\theta_{13}). \end{aligned} \quad (3.21)$$

Note that in order to apply equation (3.20) to the case $\theta_{13} = 0$, where δ is undefined, the analytic continuation of the latter, which will be given in equation (3.32), has to be inserted.

Discussion for θ_{12}

We will now compare the analytical results to the ones obtained by the numerical evolution of the mixing angles, starting with the best-fit values at low energy. For the case of θ_{12} , it is shown in figure 3.1. We see that the RG effects are rather strong in the case of quasi-degenerate neutrinos and vanishing CP phases, since the factor $(m_1 + m_2)/\Delta m_{\text{sol}}^2$ is very large. From the analytical formulae, we expect that a non-vanishing $\varphi_1 - \varphi_2$ leads to a suppression of the running. It should be maximal for $|\varphi_1 - \varphi_2| = 180^\circ$, which has also been observed in earlier studies, e.g. [93,94,98]. The dependence of the RG evolution on $|\varphi_1 - \varphi_2|$ obtained numerically is in agreement with this expectation. The $\mathcal{O}(\theta_{13})$ -terms can also have interesting effects on the

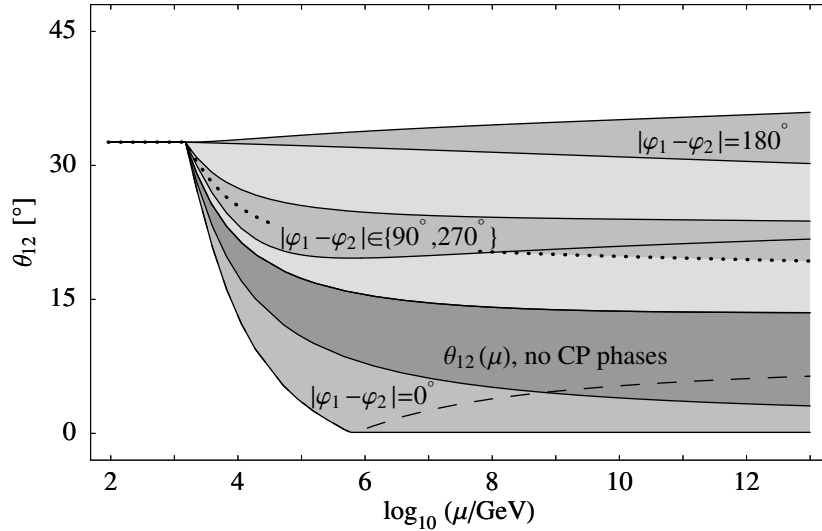


Figure 3.1: RG evolution of θ_{12} in the MSSM with $\tan\beta = 50$, a normal mass hierarchy and $m_1 = 0.1\text{eV}$. The dark-gray region shows the evolution with best-fit values for the neutrino parameters, $\theta_{13} \in [0^\circ, 9^\circ]$ and all CP phases equal to zero. The medium-gray regions show the evolution for $|\varphi_1 - \varphi_2| = 0^\circ$, $|\varphi_1 - \varphi_2| \in \{90^\circ, 270^\circ\}$ and $|\varphi_1 - \varphi_2| = 180^\circ$. They emerge from varying $\theta_{13} \in [0^\circ, 9^\circ]$ and $\delta \in \{0^\circ, 90^\circ, 180^\circ, 270^\circ\}$. The light-gray regions can be reached by choosing specific values for the CP phases different from the ones listed above. The dashed line shows the RG evolution with $|\varphi_1 - \varphi_2| = 0$, $\theta_{13} = 9^\circ$ and $\delta = 180^\circ$. Note that for the numerics we use the convention where θ_{12} is restricted to the interval $[0^\circ, 45^\circ]$, so that the angle increases again after reaching 0. The dotted line shows the evolution with $|\varphi_1 - \varphi_2| = 90^\circ$ and $\theta_{13} = 0^\circ$.

running of θ_{12} . The dominant contribution to the next-to-leading term is given by

$$\Upsilon_{\theta_{12}} = \frac{C y_\tau^2 m_2 + m_1}{32\pi^2 m_2 - m_1} \sin 2\theta_{23} \cos\left(\frac{\varphi_1 - \varphi_2}{2}\right) \times \\ \times \left[\cos(2\theta_{12}) \cos \delta \cos\left(\frac{\varphi_1 - \varphi_2}{2}\right) + \sin \delta \sin\left(\frac{\varphi_1 - \varphi_2}{2}\right) \right] \cdot \theta_{13}. \quad (3.22)$$

The largest running, where θ_{12} can even become zero, occurs for θ_{13} as large as experimentally allowed ($\approx 9^\circ$), $\delta = \pi$ and $\varphi_1 - \varphi_2 = 0$. In this case the leading and the next-to-leading term add up constructively. It is also interesting to observe that, due to $\mathcal{O}(\theta_{13})$ -effects, θ_{12} can run to slightly larger values. The damping due to the Majorana phases is maximal in this case, which almost eliminates the leading term. Then, the running comes mainly from the next-to-leading term (3.22).

Discussion for θ_{13} and θ_{23}

An example for the running of the mixing angles θ_{13} and θ_{23} is shown in figure 3.2. As already pointed out, in order to apply the formula for θ_{13} to the case $\theta_{13} = 0$, where δ is undefined, the analytic continuation of the latter has to be inserted. It will

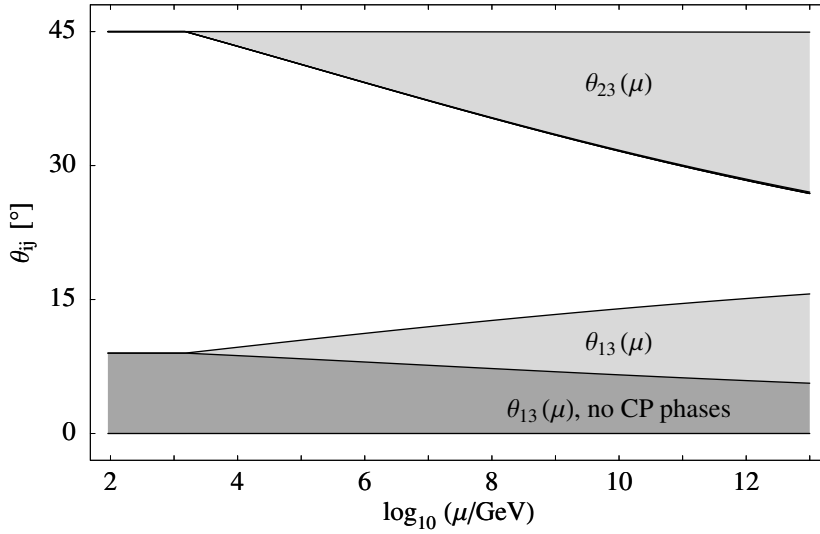


Figure 3.2: RG evolution of θ_{13} and θ_{23} in the MSSM with $\tan\beta = 50$, a normal mass hierarchy and $m_1 = 0.1$ eV. The dark-gray region shows the evolution with best-fit values for the neutrino parameters, $\theta_{13} \in [0^\circ, 9^\circ]$ and all CP phases equal to zero. For the θ_{23} case, we just obtain a thick gray line at the bottom of the gray region. The light-gray regions show the evolution which is possible if arbitrary CP phases are allowed.

be given in equation (3.32) in section 3.1.4, where the phases are treated in detail. The comparison with the numerical results in figure 3.2 shows that above M_{SUSY} the mixing angles run linearly on a logarithmic scale to a good approximation. Thus, using equation (3.20) with a constant right-hand side yields pretty accurate results. Interestingly, for the running of θ_{13} , cancellations between the first two terms in the second line of equation (3.20) appear for $\varphi_1 = \varphi_2$, in agreement with earlier studies, for instance [93,102], where it was discussed for the CP-conserving case $\varphi_1 = \varphi_2 = \pi$. With $\varphi_1 \neq \varphi_2$, significant RG effects can be expected for nearly degenerate masses. This is confirmed by the light-gray region in figure 3.2. We will discuss the RG changes of θ_{13} and θ_{23} in more detail in section 3.2, where we investigate their implications for future precision measurements.

3.1.3 The Running of the Neutrino Masses

The result for the neutrino masses are short enough to present them in the approximation $y_e = y_\mu = 0$ but for arbitrary θ_{13} . They are given by

$$16\pi^2 \dot{m}_1 = [\alpha + Cy_\tau^2 (2s_{12}^2 s_{23}^2 + X_1)] m_1, \quad (3.23a)$$

$$16\pi^2 \dot{m}_2 = [\alpha + Cy_\tau^2 (2c_{12}^2 s_{23}^2 + X_2)] m_2, \quad (3.23b)$$

$$16\pi^2 \dot{m}_3 = [\alpha + 2Cy_\tau^2 c_{13}^2 c_{23}^2] m_3, \quad (3.23c)$$

where X_1 and X_2 contain terms proportional to $\sin \theta_{13}$,

$$X_1 = -s_{13} \sin 2\theta_{12} \sin 2\theta_{23} \cos \delta + 2s_{13}^2 c_{12}^2 c_{23}^2, \quad (3.24a)$$

$$X_2 = s_{13} \sin 2\theta_{12} \sin 2\theta_{23} \cos \delta + 2s_{13}^2 s_{12}^2 c_{23}^2. \quad (3.24b)$$

Since only the mass squared differences have been measured so far, we also explicitly give the RGEs for the mass squared differences,

$$8\pi^2 \frac{d}{dt} \Delta m_{\text{sol}}^2 = \alpha \Delta m_{\text{sol}}^2 + C y_\tau^2 [2s_{23}^2 (m_2^2 c_{12}^2 - m_1^2 s_{12}^2) + X_{\text{sol}}], \quad (3.25a)$$

$$8\pi^2 \frac{d}{dt} \Delta m_{\text{atm}}^2 = \alpha \Delta m_{\text{atm}}^2 + C y_\tau^2 [2m_3^2 c_{13}^2 c_{23}^2 - 2m_2^2 c_{12}^2 s_{23}^2 + X_{\text{atm}}], \quad (3.25b)$$

where

$$X_{\text{sol}} = (m_1^2 + m_2^2) s_{13} \sin 2\theta_{12} \sin 2\theta_{23} \cos \delta + 2s_{13}^2 c_{23}^2 (m_2^2 s_{12}^2 - m_1^2 c_{12}^2), \quad (3.26a)$$

$$X_{\text{atm}} = -m_2^2 s_{13} \sin 2\theta_{12} \sin 2\theta_{23} \cos \delta - 2m_2^2 s_{13}^2 s_{12}^2 c_{23}^2. \quad (3.26b)$$

Discussion of the Running Neutrino Mass Scale

For the neutrino mass scale, at present there exist only upper bounds as discussed in section 1.1.3. In order to use them for constraining models of neutrino masses defined at high energies, the RG evolution of these bounds has to be computed. From the formulae we see that the running of the mass eigenvalues is significant even in the SM or for strongly hierarchical neutrino masses due to the factor α in the RGEs (3.23). Furthermore, the evolution is not directly dependent on the Majorana phases. This can be understood from equation (3.12) and

$$P'_{ii} = \sum_{jk} (U^\dagger)_{ij} P_{jk} U_{ki} = \sum_{jk} U_{ji}^* P_j \delta_{jk} U_{ki} = \sum_j |U_{ji}|^2 P_j, \quad (3.27)$$

which shows that only the moduli of the elements of the MNS matrix enter into \dot{m}_i . Note that we have chosen a basis where $P = C (Y_e^\dagger Y_e)$ is diagonal. Besides, \dot{m}_3 does not depend on δ , since only the moduli of the elements of the third column of the MNS matrix are relevant in this case. There is of course an indirect dependence on the phases, as these influence the running of the mixing angles.

Since the part which depends on the mixing parameters is proportional to y_τ^2 , apart from the MSSM with large $\tan \beta$ the running of the mass eigenvalues is approximately independent of the mixings and phases. In the SM, the Higgs mass m_H influences the running via the self-coupling λ – the heavier the Higgs, the larger the RG effects. Thus, in many cases the running is approximately given by a common scaling of the mass eigenvalues [98], which is obtained by neglecting y_τ and integrating equation (3.23),

$$m_i(t) \approx \exp \left[\frac{1}{16\pi^2} \int_{t_0}^t d\tau \alpha(\tau) \right] m_i(t_0) =: s(t, t_0) m_i(t_0). \quad (3.28)$$

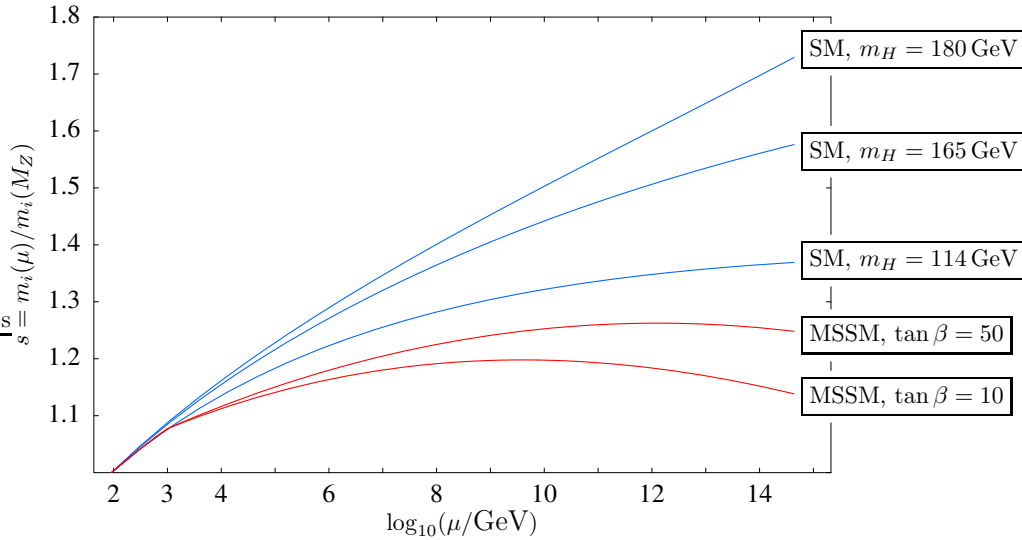


Figure 3.3: Scaling of the masses under the renormalization group in the SM and MSSM. The mixing parameters are chosen to be the LMA best-fit values (cf. Tab. 1.3), but they influence the running only marginally. We further used a SUSY-breaking scale $M_{\text{SUSY}} = 1 \text{ TeV}$. The upper curves show the evolution in the SM for $m_H = 114 \text{ GeV}$, $m_H = 165 \text{ GeV}$ and $m_H = 180 \text{ GeV}$, the lower ones correspond to the MSSM for $\tan \beta = 10$ and $\tan \beta = 50$ with $m_H = 120 \text{ GeV}$. These plots apply for all mass eigenvalues, except for large $\tan \beta$ in the MSSM where the scaling of m_3 is shown (using zero phases). Note also that a different SUSY-breaking scale changes the scaling factor in the MSSM.

The numerical evaluation of s in the SM and the MSSM is shown in figure 3.3 for some values of m_H and $\tan \beta$, respectively. The three SM curves correspond to different Higgs masses in the current experimentally allowed region at 95% confidence level, $114 \text{ GeV} \lesssim m_H \lesssim 200 \text{ GeV}$ [109]. $m_H = 180 \text{ GeV}$ is the value for which the self-coupling λ stays perturbative up to 10^{16} GeV , and $m_H = 165 \text{ GeV}$ is the minimal mass for which λ is positive up to 10^{16} GeV , so that the vacuum is stable in this region.¹ In the MSSM, we choose $m_H = 120 \text{ GeV}$ for the light Higgs mass, since the allowed range is further restricted by the upper limit at about 130 GeV here, and since it influences the RG scaling only marginally as long as M_{SUSY} and M_Z differ only by a few orders of magnitude. Moreover, further uncertainties due to threshold corrections and the unknown value of the SUSY-breaking scale can be equally important as the one due to the unknown Higgs mass. It turns out that the RG enhancement of the masses is smallest if $\tan \beta \approx 10$.

¹In some models (see, e.g. [50] for a viable model) λ can be larger, in particular if $M_1 \ll 10^{16} \text{ GeV}$. A negative value of λ at high energy implies a metastable vacuum.

It is interesting to note that the running of the bound on the effective mass $\langle m_\nu \rangle = (m_\nu)_{11} = |\sum_i (U_{\text{MNS}})_{1i}^2 m_i|$ from neutrinoless double beta decay experiments (see section 1.1.3) is determined by

$$16\pi^2 \frac{d}{dt} \langle m_\nu \rangle = (2C y_e^2 + \alpha) \langle m_\nu \rangle, \quad (3.29)$$

as can be seen directly from equation (3.1). Compared to α , the electron Yukawa coupling y_e is tiny and can be neglected. Thus, to a good approximation, $\langle m_\nu \rangle$ scales like one of the mass eigenvalues in (3.28) under the RG evolution.

Discussion for Δm_{sol}^2

We now consider the RGE for the solar mass squared difference, given in equation (3.25a). As described above, in the SM and the MSSM with small $\tan\beta$, the running is due to the common scaling of the masses described in the previous section and thus approximately independent of the mixing parameters. For large $\tan\beta$ and nearly degenerate masses, the influence of CP phases, in particular the Dirac phase, is crucial. The numerical example in figure 3.4 confirms this expectation and furthermore shows that Δm_{sol}^2 runs dramatically. On the one hand, it can grow by more than an order of magnitude. On the other hand, it can run to 0 at energy scales slightly beyond the maximum of 10^{13} GeV shown in the figure. For large $\tan\beta$, $\Delta m_{\text{sol}}^2 \ll m_1^2$ and not too small θ_{13} , the first term in X_{sol} is essential for understanding these effects, since it is proportional to the sum of the masses squared rather than the difference. For $\delta = \pi$ and θ_{13} near the CHOOZ bound, its sign is negative and its absolute value maximal, which causes the evolution of Δm_{sol}^2 towards zero. For $\delta = 0$, the sign becomes positive, so that the running towards larger values is enhanced, which explains the upper boundary of the light-gray region in figure 3.4.

Discussion for Δm_{atm}^2

The RGE for the running of Δm_{atm}^2 is given in equation (3.25b). From the numerical example in figure 3.5, we see that the evolution of Δm_{atm}^2 can be damped by the phases, but not significantly enhanced. Analogously to the case of the solar mass squared difference, the maximal damping is mainly due to the first term in X_{atm} , so that it occurs for large θ_{13} and $\delta = 0$. Compared to the case of the solar mass squared difference, the influence of δ is generically smaller here, because $\Delta m_{\text{atm}}^2/m_i^2$ is larger and because the phase-independent terms in the RGE do not nearly cancel. Depending on the CP phases, Δm_{atm}^2 grows by about 50% – 95%. Note that though the mass squared differences do not explicitly depend on the Majorana phases, their influence on the running of the other parameters can have significant effects here.

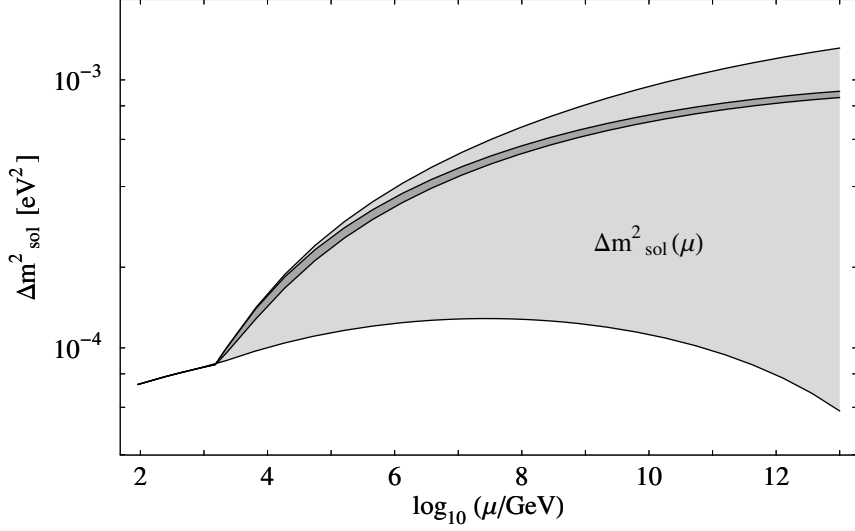


Figure 3.4: RG evolution of Δm_{sol}^2 in the MSSM with $\tan\beta = 50$, a normal mass hierarchy and $m_1 = 0.1 \text{ eV}$. The dark-gray region shows the evolution with LMA best-fit values for the neutrino parameters, $\theta_{13} \in [0^\circ, 9^\circ]$ and all CP phases equal to zero. The light-gray regions show the evolution which is possible if arbitrary CP phases are allowed.

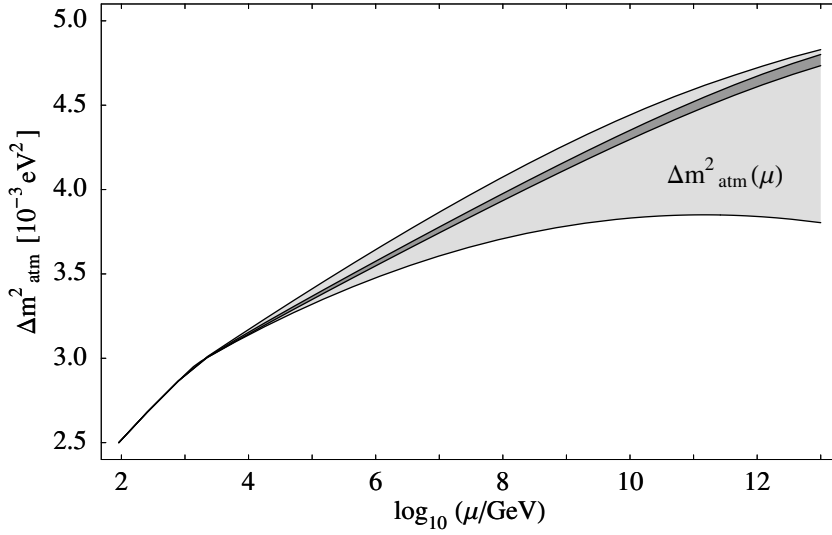


Figure 3.5: RG evolution of Δm_{atm}^2 in the MSSM with the same input parameters as in figure 3.4.

3.1.4 The Running of the Dirac CP Phase

Like the masses and mixing angles, the CP phases depend on the energy scale as well. For the RGE of the Dirac CP phase, we obtain in an expansion in θ_{13} ,

$$\dot{\delta} = \frac{C y_\tau^2}{32\pi^2} \frac{\delta^{(-1)}}{\theta_{13}} + \frac{C y_\tau^2}{8\pi^2} \delta^{(0)} + \mathcal{O}(\theta_{13}), \quad (3.30)$$

where $\delta^{(-1)}$ and $\delta^{(0)}$ are given by

$$\begin{aligned} \delta^{(-1)} = & \sin 2\theta_{12} \sin 2\theta_{23} \frac{m_3}{\Delta m_{\text{atm}}^2 (1 + \zeta)} \times \\ & \times [m_1 \sin(\varphi_1 - \delta) - (1 + \zeta) m_2 \sin(\varphi_2 - \delta) + \zeta m_3 \sin \delta], \end{aligned} \quad (3.31a)$$

$$\begin{aligned} \delta^{(0)} = & \frac{m_1 m_2 s_{23}^2 \sin(\varphi_1 - \varphi_2)}{\Delta m_{\text{sol}}^2} \\ & + m_3 s_{12}^2 \left[\frac{m_1 \cos 2\theta_{23} \sin \varphi_1}{\Delta m_{\text{atm}}^2 (1 + \zeta)} + \frac{m_2 c_{23}^2 \sin(2\delta - \varphi_2)}{\Delta m_{\text{atm}}^2} \right] \\ & + m_3 c_{12}^2 \left[\frac{m_1 c_{23}^2 \sin(2\delta - \varphi_1)}{\Delta m_{\text{atm}}^2 (1 + \zeta)} + \frac{m_2 \cos 2\theta_{23} \sin \varphi_2}{\Delta m_{\text{atm}}^2} \right]. \end{aligned} \quad (3.31b)$$

We see that the limit $\theta_{13} \rightarrow 0$ is dangerous, because in this case the RGE (3.30) diverges. However, we can show that $\dot{\delta}$ remains well-defined: The derivative of the MNS matrix U_{MNS} is given by (3.5), where U_{MNS} and T are continuous functions of $t = \ln(\mu/\mu_0)$. This implies that the matrix element $(U_{\text{MNS}})_{13}(t)$ describes a continuously differentiable curve in the complex plane. Consequently, θ_{13} and δ are continuously differentiable even for $\theta_{13} = 0$, if δ is extended continuously at this point. Note that restricting the parameters to certain ranges can nevertheless result in discontinuities. For example, if the RG evolution causes θ_{13} to change its sign and if we demand $0 \leq \theta_{13} < \frac{\pi}{2}$, then there will be a kink in the evolution of θ_{13} and δ will jump by π . However, even in the presence of such artificial discontinuities there must still be finite one-sided limits for δ and $\dot{\delta}$ as θ_{13} approaches 0. The limit for δ is determined by the requirement that $\dot{\delta}$ remains finite. Then the divergence of θ_{13}^{-1} has to be canceled by $\delta^{(-1)}$. For $\varphi_1 = \varphi_2 = 0$, this obviously implies $\delta = 0$ or $\delta = \pi$. In the general case, a short calculation yields

$$\cot \delta = \frac{m_1 \cos \varphi_1 - (1 + \zeta) m_2 \cos \varphi_2 - \zeta m_3}{m_1 \sin \varphi_1 - (1 + \zeta) m_2 \sin \varphi_2}. \quad (3.32)$$

Due to the periodicity of \cot , there are two solutions differing by π , corresponding to the different limits on the two sides of a node of θ_{13} . We will use this formula in section 3.2.1, where we study the corrections to $\theta_{13} = 0^\circ$ by RG running.

The running of the Dirac phase δ can have interesting effects. Consider for example the case where δ vanishes at some energy scale. Then a non-zero δ is produced by RG effects, since some of the terms in the RGE (3.30) do not vanish for $\delta \rightarrow 0$.

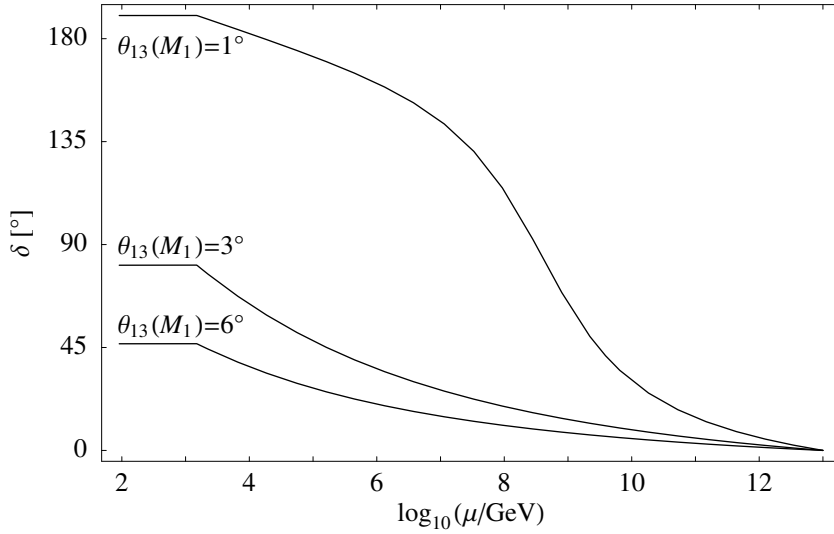


Figure 3.6: Radiative generation of a Dirac phase in the MSSM with $\tan\beta = 30$ and a normal hierarchy. Here the running is from high to low energy, i.e. the boundary conditions are given at the see-saw scale. δ is zero there but large at M_Z . The other starting values are $\theta_{12} = 18^\circ$, $\theta_{13} \in \{1^\circ, 3^\circ, 6^\circ\}$, $\theta_{23} = 34^\circ$, $m_1 = 0.17 \text{ eV}$, $\Delta m_{\text{atm}}^2 = 3.8 \cdot 10^{-3} \text{ eV}^2$, $\Delta m_{\text{sol}}^2 = 5.7 \cdot 10^{-4} \text{ eV}^2$, $\varphi_1 = 16^\circ$, $\varphi_2 = 140^\circ$.

This radiative generation of a Dirac phase by Majorana phases has previously been observed in [91]. An example is shown in figure 3.6. Obviously, the effect is enhanced for small θ_{13} because of the factor θ_{13}^{-1} in the first term of equation (3.30). If $\varphi_1 = \varphi_2$, this contribution is suppressed since the parts proportional to m_1 and m_2 nearly cancel. Note that in this case the first term of $\delta^{(0)}$ leads to a suppression of the next-to-leading order contribution as well.

3.1.5 The Running of the Majorana Phases

The RGEs for the evolution of the physical Majorana phases are given by

$$\dot{\varphi}_1 = \frac{Cy_\tau^2}{4\pi^2} \left\{ m_3 \cos 2\theta_{23} \frac{m_1 s_{12}^2 \sin \varphi_1 + (1 + \zeta) m_2 c_{12}^2 \sin \varphi_2}{\Delta m_{\text{atm}}^2 (1 + \zeta)} + \frac{m_1 m_2 c_{12}^2 s_{23}^2 \sin(\varphi_1 - \varphi_2)}{\Delta m_{\text{sol}}^2} \right\} + \mathcal{O}(\theta_{13}), \quad (3.33)$$

$$\dot{\varphi}_2 = \frac{Cy_\tau^2}{4\pi^2} \left\{ m_3 \cos 2\theta_{23} \frac{m_1 s_{12}^2 \sin \varphi_1 + (1 + \zeta) m_2 c_{12}^2 \sin \varphi_2}{\Delta m_{\text{atm}}^2 (1 + \zeta)} + \frac{m_1 m_2 s_{12}^2 s_{23}^2 \sin(\varphi_1 - \varphi_2)}{\Delta m_{\text{sol}}^2} \right\} + \mathcal{O}(\theta_{13}). \quad (3.34)$$

Note that singularities can appear in the $\mathcal{O}(\theta_{13})$ -terms at points in parameter space where the phases are not well-defined.

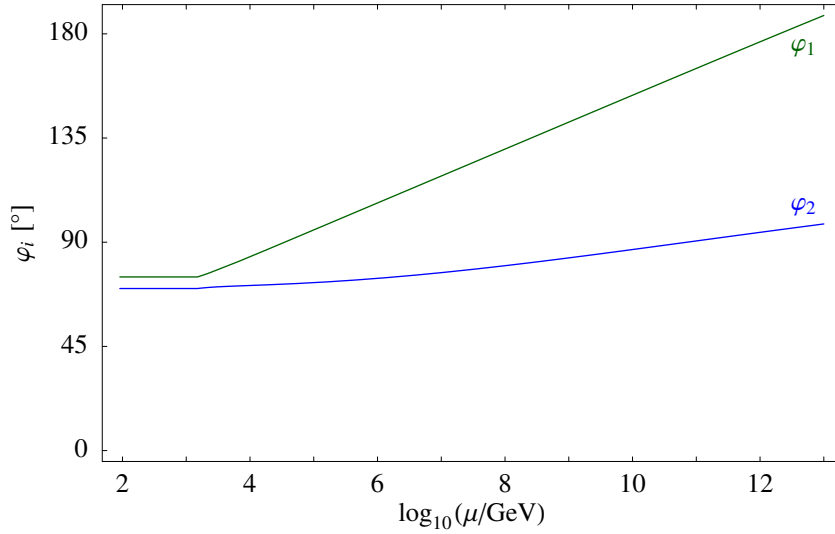


Figure 3.7: Running of the Majorana phases in the MSSM with a normal hierarchy, $\tan\beta = 50$, $\varphi_1 = 75^\circ$, $\varphi_2 = 70^\circ$, $\theta_{13} = 0$, $m_1 = 0.15\text{ eV}$, and best-fit values for the mass squared differences, θ_{12} and θ_{23} at M_Z . RG effects are substantial, and the difference $\varphi_1 - \varphi_2$ increases with increasing energy.

As we have seen, the Majorana phases can have a strong influence on the running of the other parameters. While the RGEs for the Majorana phases are somewhat lengthy, there is a simple expression for the running of their difference for small θ_{13} ,

$$\dot{\varphi}_1 - \dot{\varphi}_2 = \frac{C y_\tau^2}{4\pi^2} \frac{m_1 m_2}{\Delta m_{\text{sol}}^2} \cos 2\theta_{12} \sin^2 \theta_{23} \sin(\varphi_1 - \varphi_2) + \mathcal{O}(\theta_{13}). \quad (3.35)$$

It shows that for $\theta_{13} = 0$, the phases remain equal, if they are equal at some scale. Obviously, $\dot{\varphi}_1 - \dot{\varphi}_2 > 0$ for $\varphi_1 > \varphi_2$ and vice versa, which means that the difference between the phases tends to increase with increasing energy. In other words, a large difference at the see-saw scale becomes smaller at low energy. An example is shown in figure 3.7.

3.1.6 Estimating the Generic Size of the RG Effects

From the analytical formulae for the running of the neutrino masses, mixings and phases, we can extract generic enhancement and suppression factors for the RG evolution. They depend on whether the mass scheme is hierarchical, partially degenerate or nearly degenerate. We have listed these factors in the approximation of small θ_{13} in table 3.1. Note that as we have seen, they can be compensated by cancellations due to a special alignment of the phases.

Table 3.1 is very useful for estimating the generic size of RG effects. The Yukawa coupling of the τ lepton is given by $y_\tau^{\text{SM}} = \frac{\sqrt{2}}{v_{\text{EW}}} m_\tau \approx 0.01$ in the SM and $y_\tau^{\text{MSSM}} =$

3.1 Analytical Results in the Neutrino Mass Operator Approach

	$\dot{\theta}_{12}$	$\dot{\theta}_{13}$	$\dot{\theta}_{23}$	$\dot{\delta}$	$\dot{\varphi}_i$
n.h.	1	$\sqrt{\zeta}$	1	$\sqrt{\zeta} \theta_{13}^{-1}$	$\sqrt{\zeta}$
p.d.(n.)	$\frac{m_1^2}{\Delta m_{\text{sol}}^2}$	$\frac{m_1}{\sqrt{\Delta m_{\text{atm}}^2}}$	1	$\frac{m_1}{\sqrt{\Delta m_{\text{atm}}^2}} \theta_{13}^{-1} + \frac{m_1^2}{\Delta m_{\text{sol}}^2}$	$\frac{m_1^2}{\Delta m_{\text{sol}}^2}$
i.h.	ζ^{-1}	$\mathcal{O}(\theta_{13})$	1	ζ^{-1}	ζ^{-1}
p.d.(i.)	ζ^{-1}	$\frac{m_3}{\sqrt{\Delta m_{\text{atm}}^2}}$	1	$\frac{m_3}{\sqrt{\Delta m_{\text{atm}}^2}} \theta_{13}^{-1} + \zeta^{-1}$	ζ^{-1}
d.	$\frac{m^2}{\Delta m_{\text{sol}}^2}$	$\frac{m^2}{\Delta m_{\text{atm}}^2}$	$\frac{m^2}{\Delta m_{\text{atm}}^2}$	$\frac{m^2}{\Delta m_{\text{atm}}^2} \theta_{13}^{-1} + \frac{m^2}{\Delta m_{\text{sol}}^2}$	$\frac{m^2}{\Delta m_{\text{sol}}^2}$

Table 3.1: Generic enhancement and suppression factors for the RG evolution of the mixing parameters. A ‘1’ indicates that there is no generic enhancement or suppression. ‘n.h.’ and ‘p.d.(n.)’ denote the hierarchical and partially degenerate mass spectrum in the case of a normal hierarchy, i.e. $m_1^2 \ll \Delta m_{\text{sol}}^2$ or $\Delta m_{\text{sol}}^2 \ll m_1^2 \lesssim \Delta m_{\text{atm}}^2$. ‘i.h.’ and ‘p.d.(i.)’ denote the analogous spectra in the inverted case, i.e. $m_3^2 \ll \Delta m_{\text{sol}}^2$ or $\Delta m_{\text{sol}}^2 \ll m_3^2 \lesssim \Delta m_{\text{atm}}^2$. Finally, ‘d.’ means nearly degenerate masses, $\Delta m_{\text{atm}}^2 \ll m_1^2 \sim m_2^2 \sim m_3^2 \sim m^2$.

$y_\tau^{\text{SM}} (1 + \tan^2 \beta)$ in the MSSM. Thus the typical factor in the RGEs for the mixing angles and phases in the case of the MSSM amounts to

$$\frac{(y_\tau^{\text{MSSM}})^2}{32\pi^2} \approx 0.3 \cdot 10^{-6} (1 + \tan^2 \beta). \quad (3.36)$$

If the running was purely logarithmic, the evolution in the range between the EW scale and for example $M_1 = 10^{13}$ GeV would yield a factor of

$$\ln \frac{M_1}{M_Z} \approx \ln \frac{10^{13}}{10^2} \approx 25. \quad (3.37)$$

If we assume that the solar and atmospheric angle are large and that the phases do not cause excessive cancellations, then multiplying the above two contributions with the enhancement factor Γ_{enh} from table 3.1 yields a rough estimate for the change of the angles and phases due to the RG evolution,

$$\Delta_{\text{RG}} \sim 10^{-5} (1 + \tan^2 \beta) \Gamma_{\text{enh}}. \quad (3.38)$$

Obviously, for quasi-degenerate neutrinos large enhancement factors are possible if the small mass squared differences appear in the denominators of the enhancement factors. Note that also quite small RG changes might be interesting in combination with precision measurements of neutrino parameters, as we will see in section 3.2.

3.2 RG Corrections Compared to Sensitivities of Future Experiments

At present, the values $\theta_{13} = 0^\circ$ and $\theta_{23} = 45^\circ$ are experimentally allowed and might be given by some model at a high energy scale from a specific set of textures. Future experiments on neutrino oscillations are expected to have high sensitivities to these mixing angles. Therefore, we calculate in a model-independent way the size of RG corrections to θ_{13} and θ_{23} from the running of the effective neutrino mass operator between the see-saw scale and the electroweak scale. We find that in large regions of the currently allowed parameter space, the RG corrections exceed the expected sensitivities of future precision experiments.

3.2.1 Radiative Corrections for the Mixing Angle θ_{13}

For the analysis of the RG effects, we will apply the analytical formula of equation (3.20). As pointed out in section 3.1.2, it is a rather good approximation to assume $\theta_{13} \simeq \text{const.}$, which leads to an RG evolution with a constant slope depending on the Dirac CP phase δ and the Majorana phases φ_1 and φ_2 . In order to calculate the RG correction for the initial value $\theta_{13} = 0$ between some high energy scale M_1 , where neutrino masses are generated, and low energy, i.e. 10^2 GeV , we have to use the analytic continuation for the CP phase δ of equation (3.32). For the examples, we take $M_1 = 10^{12} \text{ GeV}$. The approximate size of the RG corrections to $\sin^2 2\theta_{13}$ in the MSSM is shown in figure 3.8. In the upper diagram it is plotted as a function of $\tan \beta$ and the lightest neutrino mass m_1 for constant Majorana phases $\varphi_1 = 0$ and $\varphi_2 = \pi$. The lower diagram shows the dependence of the corrections on φ_1 and φ_2 for $\tan \beta = 50$ and $m_1 = 0.08 \text{ eV}$ in the case of a normal mass hierarchy. The diagrams look rather similar for an inverted hierarchy.

Planned reactor experiments [110] and next generation superbeam experiments [111,112] are expected to have an approximate sensitivity to $\sin^2 2\theta_{13}$ of 10^{-2} . From figure 3.8 we find that the radiative corrections exceed this value for large regions of the currently allowed parameter space, unless there are cancellations due to Majorana phases, i.e. $\varphi_1 = \varphi_2$. If so, the effects are generically smaller than 10^{-2} as can be seen from the lower diagram. Future upgraded superbeam experiments like JHF-HyperKamiokande have the potential to further push the sensitivity to about 10^{-3} and with a neutrino factory even about 10^{-4} might be reached.

From the theoretical point of view, one would expect that even if some model predicted $\theta_{13} = 0$ at the energy scale of neutrino mass generation, RG effects would at least produce a non-zero value of the order shown in figure 3.8. Consequently, experiments with such a sensitivity have a large discovery potential for θ_{13} . We should point out that this is a conservative estimate, since if neutrino masses are e.g. determined by GUT scale physics, model-dependent radiative corrections in the

region between M_1 and M_{GUT} contribute as well. On the other hand, if experiments do not measure θ_{13} , parameter space regions where the corrections are larger than this bound will then appear unnatural from the theoretical point of view.

3.2.2 Radiative Corrections for the Mixing Angle θ_{23}

RG corrections also induce a deviation of θ_{23} from 45° , even if some model predicted this specific value at high energy. From the analytical formula (3.21) with a constant right-hand side, we now calculate the running in the MSSM between M_Z and the see-saw scale, which we take as $M_1 = 10^{12}$ GeV for our examples. As initial conditions we assume small θ_{13} at M_1 and low-energy best-fit values for the remaining lepton mixings and the neutrino mass squared differences. In leading order in θ_{13} , the evolution is of course independent of the Dirac phase δ .

Figure 3.9 shows the size of the RG corrections in the MSSM. From the upper diagram it can be read off for desired values of $\tan \beta$ and the lightest mass eigenvalue m_1 in an example with vanishing Majorana phases. The lower diagram shows its dependence on the Majorana phases φ_1 and φ_2 for $\tan \beta = 50$, $m_1 = 0.1$ eV and a normal mass hierarchy. The diagrams look rather similar in the case of an inverted hierarchy. The effects of the Majorana phases, shown in the lower diagram, can easily be understood from equation (3.21). In the region with $\varphi_1 \approx \varphi_2 \approx \pi$, both $|m_2 e^{i\varphi_2} + m_3|^2$ and $|m_1 e^{i\varphi_1} + m_3|^2$ are small for quasi-degenerate neutrinos, which gives the ellipse with small radiative corrections in the center of the lower diagram. Even if a model predicted $\theta_{23} = 45^\circ$ at some high energy scale, we would thus expect radiative corrections to produce at least a deviation from this value of the size shown in figure 3.9, so that experiments with such a sensitivity are expected to measure a deviation of θ_{23} from 45° .

The expected sensitivity on $\sin^2 2\theta_{23}$ of future superbeam experiments like JHF-SuperKamiokande is approximately 1% (see e.g. [113]). This can now be compared with figure 3.9. We find that the radiative corrections exceed this value for large regions of the currently allowed parameter space, where no significant cancellations due to Majorana phases occur. This means that φ_1 and φ_2 must not be too close to π . Otherwise, the effects are generically smaller as can be seen from the lower diagram. Upgraded superbeam experiments or a neutrino factory might even reach a sensitivity of about 0.5%. As argued for the case of θ_{13} , if experiments measure θ_{23} rather close to 45° , parameter combinations implying larger radiative corrections than the measured deviation will appear unnatural from the theoretical side.

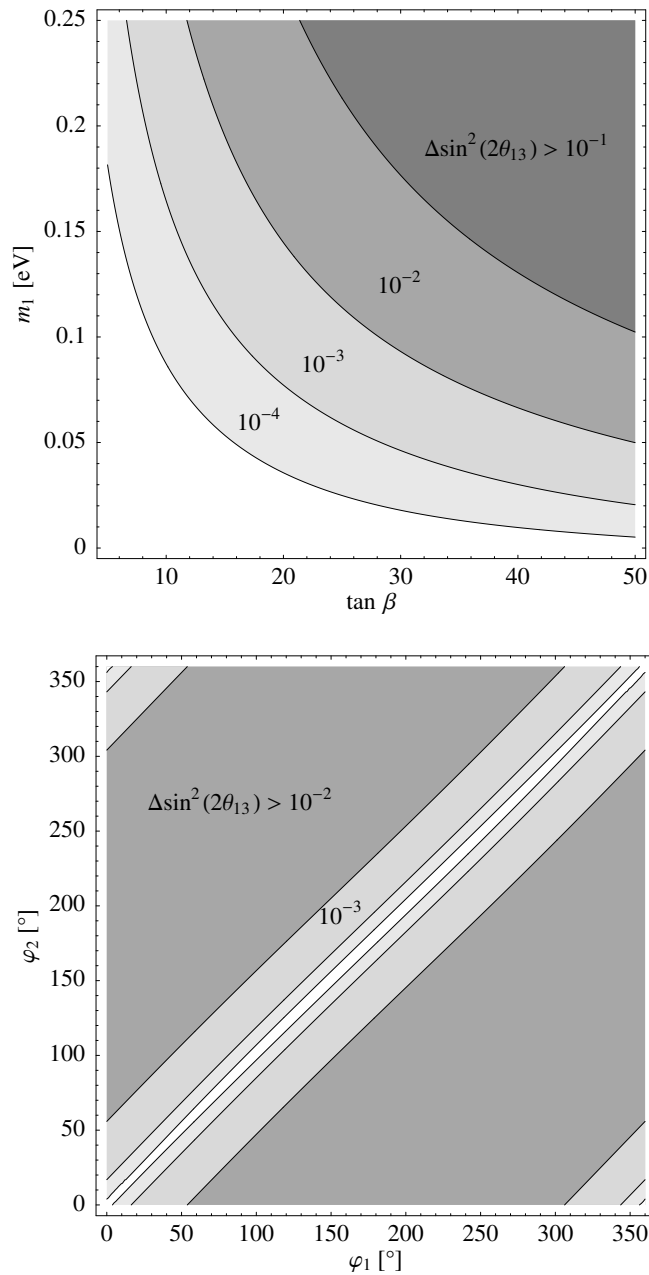


Figure 3.8: Corrections to θ_{13} from the RG evolution between 10^2 and 10^{12} GeV in the MSSM, calculated using the analytical approximations with initial conditions $\theta_{13} = 0$ and LMA best-fit values for the remaining parameters. The upper diagram shows the dependence on $\tan \beta$ and on the mass of the lightest neutrino for the case of a normal mass hierarchy and phases $\varphi_1 = 0$ and $\varphi_2 = \pi$. In the lower diagram the dependence on the Majorana phases φ_1 and φ_2 is shown for $\tan \beta = 50$ and $m_1 = 0.08$ eV. The contour lines are defined as in the upper diagram. In order to apply equation (3.20) to the case $\theta_{13} = 0$, where δ is undefined, the analytic continuation of equation (3.32) has been used.

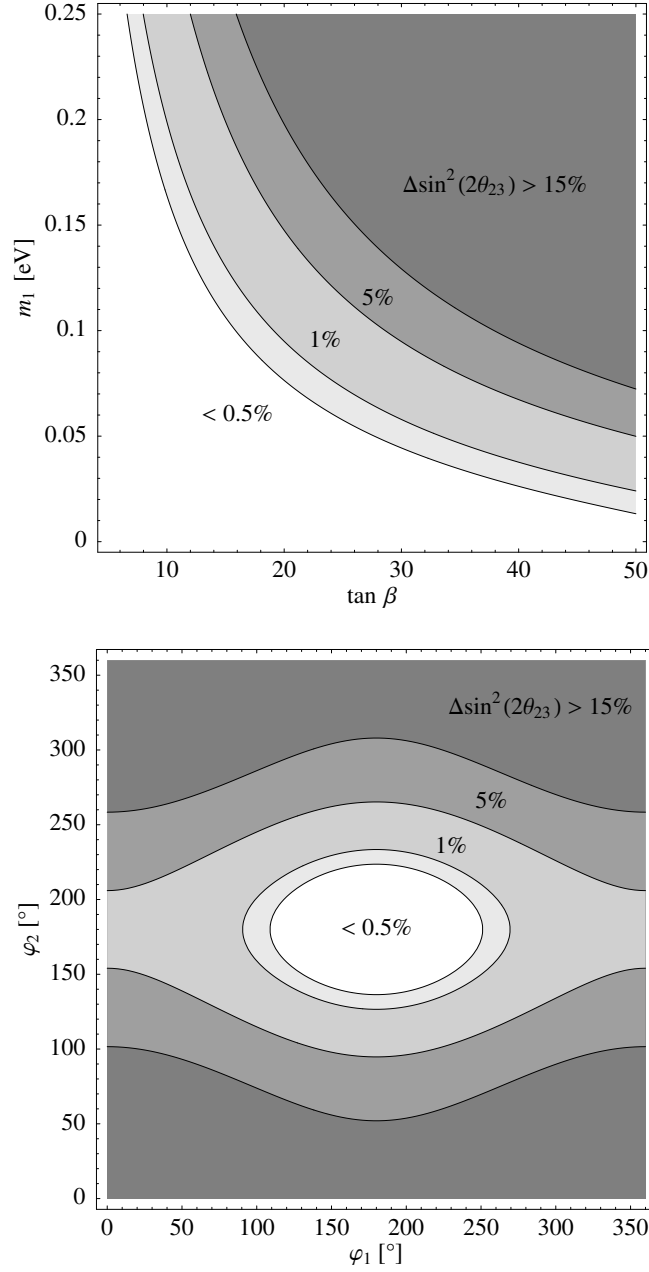


Figure 3.9: Corrections to θ_{23} from the RG evolution between 10^2 GeV and 10^{12} GeV in the MSSM, calculated from the analytical approximation equation (3.21) with initial conditions $\theta_{23} = 45^\circ$, small θ_{13} and LMA best-fit values for the remaining parameters. The upper diagram shows the dependence on $\tan \beta$ and on the mass m_1 of the lightest neutrino for the case of a normal mass hierarchy and phases $\varphi_1 = \varphi_2 = 0$. In the lower diagram the dependence on the Majorana phases φ_1 and φ_2 is shown for the example $\tan \beta = 50$ and $m_1 = 0.1$. Note that for small θ_{13} the results are independent of the Dirac phase to a good approximation.

3.3 The Running in Type I See-Saw Models

The RGEs required for the RG study of the neutrino mass matrix in minimal see-saw scenarios have been calculated in section 2.4. We now apply them to investigate the running of the lepton mixing angles in such minimal type I models with three generations of singlets. We describe the procedure of solving the coupled systems of RGEs for the various effective theories which arise from successively integrating out the heavy fields and discuss the running in the energy ranges above and between the mass thresholds of the singlets.

3.3.1 Solving the RGEs for Non-Degenerate See-Saw Scales

The notation for the parameters of the effective theories is explained in section 2.4 and illustrated in figure 2.11 on page 59 for the general case of n_G singlets. In such scenarios, the low-energy effective neutrino mass matrix can be calculated as follows:

1. At M_U , we start with the Yukawa matrices Y_ν and the Majorana mass matrix M for the sterile neutrinos. We calculate the RG running of Y_ν , M and the remaining parameters of the theory until we reach the first threshold corresponding to the largest mass eigenvalue M_{n_G} of the mass matrix M of the singlets using the RGEs for this energy range. A summary of the required RGEs in the minimal see-saw extensions of the SM, 2HDMs and MSSM can be found in appendix A.5.
2. At the mass threshold, we integrate out the corresponding sterile neutrino and perform tree-level matching according to equation (2.96). Note that this procedure is only possible in the mass eigenbasis at the threshold, which is different from the original one at M_U , since the RG evolution in general produces non-zero off-diagonal entries in M . Therefore, the mass matrix has to be diagonalized by a unitary transformation, $M \rightarrow U^T M U$, which leads to the redefinitions $N_R \rightarrow U^T N_R$, $\nu^C \rightarrow U^T \nu^C$ and $Y_\nu \rightarrow U^T Y_\nu$ of the singlet neutrino fields and their Yukawa matrix.
3. Below the mass threshold, the superscript (n) of κ , $Y_\nu^{(n)}$ and $M^{(n)}$ denotes the effective theory below the n th threshold. The parameters are now evolved down to the next threshold, which is the largest eigenvalue of the remaining mass matrix of the singlets. Next, we continue with step 2. This procedure finally yields the low-energy effective neutrino mass matrix.

Model	Quantity	C_e	C_ν	α_e	α_ν	α_d	α_u	α_{g_1}	α_{g_2}	α_λ
SM	${}^{(n)}\kappa$	$-\frac{3}{2}$	$\frac{1}{2}$	2	2	6	6	0	-3	1
SM	$2 Y_\nu^T M^{-1} Y_\nu^{(n)}$	$-\frac{3}{2}$	$\frac{1}{2}$	2	2	6	6	$-\frac{3}{2}$	$-\frac{9}{2}$	0
MSSM	${}^{(n)}\kappa$	1	1	0	2	0	6	-2	-6	0
MSSM	$2 Y_\nu^T M^{-1} Y_\nu^{(n)}$	1	1	0	2	0	6	-2	-6	0

Table 3.2: Coefficients of the β -functions of equation (3.40), which govern the running of the effective neutrino mass matrix in minimal see-saw models.

3.3.2 The Running of the Effective Neutrino Mass Matrix

As effective neutrino mass matrix in the various theories, we define the quantity

$$m_\nu = \frac{v_{\text{EW}}^2}{4} \left({}^{(n)}\kappa + 2 Y_\nu^T M^{-1} Y_\nu^{(n)} \right). \quad (3.39)$$

Above the largest see-saw scale, the superscripts (n) are omitted. In type I scenarios, κ is set to zero there. The running of m_ν is given by the running of the two parts, where the β -function for the second part has to be composed from the RGEs of the neutrino Yukawa matrix and the mass matrix of the singlets. In the SM and the MSSM, the β -functions have the general form

$$\begin{aligned} 16\pi^2 \beta_X^{(n)} &= C_e (Y_e^\dagger Y_e)^T \kappa^{(n)} + C_e \kappa^{(n)} (Y_e^\dagger Y_e) + C_\nu (Y_\nu^\dagger Y_\nu)^T \kappa^{(n)} + C_\nu \kappa^{(n)} (Y_\nu^\dagger Y_\nu) \\ &+ \alpha_e \text{Tr}(Y_e^\dagger Y_e) \kappa^{(n)} + \alpha_\nu \text{Tr}(Y_\nu^\dagger Y_\nu) \kappa^{(n)} + \alpha_d \text{Tr}(Y_d^\dagger Y_d) \kappa^{(n)} \\ &+ \alpha_u \text{Tr}(Y_u^\dagger Y_u) \kappa^{(n)} + \alpha_{g_1} g_1^2 \kappa^{(n)} + \alpha_{g_2} g_2^2 \kappa^{(n)} + \alpha_\lambda \lambda \kappa^{(n)}, \end{aligned} \quad (3.40)$$

where X stands for ${}^{(n)}\kappa$ or $2 Y_\nu^T M^{-1} Y_\nu^{(n)}$, respectively. The coefficients C_i and α_i are given in table 3.2.

Let us now specify, which parameters influence the running of the effective neutrino mass matrix in type I models, if we start running at M_U . We therefore choose a basis where Y_e is diagonal at M_U , $Y_e|_{M_U} = \text{diag}(y_e|_{M_U}, y_\mu|_{M_U}, y_\tau|_{M_U})$, and fix the initial condition for the effective neutrino mass matrix by

$$m_\nu|_{M_U} = V_{\text{MNS}}|_{M_U} \cdot m_{\text{diag}}|_{M_U} \cdot V_{\text{MNS}}^T|_{M_U}, \quad (3.41)$$

with

$$m_{\text{diag}}|_{M_U} := \text{diag}(m_1|_{M_U}, m_2|_{M_U}, m_3|_{M_U}) \quad (3.42a)$$

$$V_{\text{MNS}}|_{M_U} := V_{\text{MNS}}(\theta_{12}|_{M_U}, \theta_{13}|_{M_U}, \theta_{23}|_{M_U}, \delta|_{M_U}, \varphi_1|_{M_U}, \varphi_2|_{M_U}). \quad (3.42b)$$

In addition, the running depends on $Y_\nu^{\dagger(n)} Y_\nu^{(n)}$, which can be decomposed at M_U into

$$(Y_\nu^\dagger Y_\nu)|_{M_U} = U|_{M_U} \cdot \text{diag}(y_1^2|_{M_U}, y_2^2|_{M_U}, y_3^2|_{M_U}) \cdot U^\dagger|_{M_U}, \quad (3.43)$$

where the $y_i|_{M_U}$ can be chosen real and $U|_{M_U}$ is an arbitrary unitary matrix. m_ν as well as the β -functions are of course invariant under a change of basis for the singlets.

3.3.3 Analytical Results for the Running of the Mixing Angles

In type I see-saw scenarios, where κ vanishes above the mass thresholds of the singlets, the running of the mixing angles and CP phases is determined by the part of the RGEs which has a non-trivial flavour-structure. These are the terms proportional to C_e and C_ν in the β -functions of equation (3.40).

As we have seen, compared to the energy range below the thresholds, the running of the mixing angles is now additionally influenced by the neutrino Yukawa matrix. Analytical formulae for the running of the neutrino masses, mixings and CP phases with all the parameters would be very lengthy. We therefore restrict ourselves to the case of a real neutrino Yukawa matrix and vanishing CP phases of the MNS matrix. In this case, we obtain the simpler parametrization

$$(Y_\nu^\dagger Y_\nu)|_{M_U} = O|_{M_U} \cdot \text{diag}(y_1|_{M_U}, y_2|_{M_U}, y_3|_{M_U}) \cdot O^T|_{M_U} \quad (3.44)$$

with an orthogonal matrix $O|_{M_U} = O(\phi_1|_{M_U}, \phi_2|_{M_U}, \phi_3|_{M_U})$ in standard parametrization, which is defined analogous to the one for a unitary matrix (see appendix A.1). m_ν at M_U can then be parametrized as

$$m_\nu|_{M_U} = V(\theta_{12}, \theta_{13}, \theta_{23})|_{M_U} \cdot m_{\text{diag}}|_{M_U} \cdot V^T(\theta_{12}, \theta_{13}, \theta_{23})|_{M_U}. \quad (3.45)$$

By differentiating equation (3.45) with respect to t and inserting the RGE (3.39) for the energy range above the thresholds, we obtain analytical expressions for $\dot{\theta}_{ij}$ and \dot{m}_i at M_U , which are, however, still too long to be presented here.

We now focus on the running of the mixing angles and assume $\theta_{13}|_{M_U} = 0^\circ$, $\theta_{23}|_{M_U} = 45^\circ$ and specific initial values for $\theta_{12}|_{M_U}$ in order to simplify the expressions. We further assume that the running from the charged lepton Yukawa matrix can be neglected against the one from the neutrino Yukawa matrix. The ratios $\dot{\theta}_{12}/\dot{\theta}_{13}$ and $\dot{\theta}_{12}/\dot{\theta}_{23}$ at M_U are then given as functions of the remaining initial conditions. Note that these functions are the same for the SM and the MSSM. We find that generically the RG evolution of θ_{12} is much larger than the change of the other

angles, unless m_1 is very small. For the special case $\theta_{12}|_{M_U} = 0$, we obtain

$$\begin{aligned} \left. \frac{\dot{\theta}_{12}}{\dot{\theta}_{13}} \right|_{M_U}^{\theta_{12}=0^\circ} &= \frac{(m_2 + m_1) (m_3 - m_1) G_1}{(m_2 - m_1) (m_3 + m_1) G_2} \\ &\approx \begin{cases} \pm \frac{m_2 + m_1}{m_2 - m_1} \frac{G_1}{G_2} & \text{for hierarchical neutrino masses} \\ \frac{\Delta m_{\text{atm}}^2}{\Delta m_{\text{sol}}^2} \frac{G_1}{G_2} & \text{for degenerate neutrino masses} \end{cases} \end{aligned} \quad (3.46a)$$

$$\begin{aligned} \left. \frac{\dot{\theta}_{12}}{\dot{\theta}_{23}} \right|_{M_U}^{\theta_{12}=0^\circ} &= \frac{(m_2 + m_1) (m_3 - m_2) G_1}{(m_2 - m_1) (m_3 + m_2) G_3} \\ &\approx \begin{cases} \pm \frac{m_2 + m_1}{m_2 - m_1} \frac{G_1}{G_3} & \text{for hierarchical neutrino masses} \\ \frac{\Delta m_{\text{atm}}^2}{\Delta m_{\text{sol}}^2} \frac{G_1}{G_3} & \text{for degenerate neutrino masses} \end{cases} \end{aligned} \quad (3.46b)$$

where G_1 , G_2 and G_3 depend on $\{y_1, y_2, y_3, \phi_{12}, \phi_{13}, \phi_{32}\}$ and are given by

$$\begin{aligned} G_1 &= 8 \cos(\phi_{12}) \left\{ (2y_1^2 - y_2^2 - y_3^2) \cos(\phi_{13}) [\sin(\phi_{13}) - \cos(\phi_{13}) \sin(\phi_{12})] \right\} \\ &\quad + 4 \cos(\phi_{12}) \left\{ (y_2^2 - y_3^2) \cos(2\phi_{23}) [(3 - \cos(2\phi_{13})) \sin(\phi_{12}) + \sin(2\phi_{13})] \right\} \\ &\quad + 8 (y_2^2 - y_3^2) (\cos(2\phi_{12}) \sin(\phi_{13}) - \cos(\phi_{13}) \sin(\phi_{12})) \sin(2\phi_{23}), \end{aligned} \quad (3.47a)$$

$$\begin{aligned} G_2 &= -8 (2y_1^2 - y_2^2 - y_3^2) \cos(\phi_{12}) \cos(\phi_{13}) (\cos(\phi_{13}) \sin(\phi_{12}) + \sin(\phi_{13})) \\ &\quad - 4 (y_2^2 - y_3^2) \cos(\phi_{12}) \cos(2\phi_{23}) [(\cos(2\phi_{13}) - 3) \sin(\phi_{12}) + \sin(2\phi_{13})] \\ &\quad + 8 (y_2^2 - y_3^2) (\cos(\phi_{13}) \sin(\phi_{12}) + \cos(2\phi_{12}) \sin(\phi_{13})) \sin(2\phi_{23}), \end{aligned} \quad (3.47b)$$

$$\begin{aligned} G_3 &= \sqrt{2} (2y_1^2 - y_2^2 - y_3^2) [\cos^2(\phi_{12}) + (\cos(2\phi_{12}) - 3) \cos(2\phi_{13})] \\ &\quad + \sqrt{2} (y_2^2 - y_3^2) [(\cos(2\phi_{12}) - 3) \cos(2\phi_{13}) - 6 \cos^2(\phi_{12})] \cos(2\phi_{23}) \\ &\quad + 4\sqrt{2} (y_2^2 - y_3^2) \sin(2\phi_{12}) \sin(\phi_{13}) \sin(2\phi_{23}). \end{aligned} \quad (3.47c)$$

For the case $\theta_{12} = 45^\circ$ at M_U , the result is

$$\begin{aligned} \left. \frac{\dot{\theta}_{12}}{\dot{\theta}_{13}} \right|_{M_U}^{\text{bimax}} &= \frac{2\sqrt{2} (m_1 + m_2) (m_3 - m_1) (m_3 - m_2) F_1}{(m_2 - m_1) [8 (m_3^2 - m_1 m_2) F_2 + 4\sqrt{2} (m_2 - m_1) m_3 F_3]} \\ &\approx \begin{cases} \pm \frac{1}{2\sqrt{2}} \frac{m_2 + m_1}{m_2 - m_1} \frac{F_1}{F_2} & \text{for hierarchical neutrino masses} \\ \frac{1}{2\sqrt{2}} \frac{\Delta m_{\text{atm}}^2}{\Delta m_{\text{sol}}^2} \frac{F_1}{F_2} & \text{for degenerate neutrino masses} \end{cases} \end{aligned} \quad (3.48a)$$

$$\begin{aligned}
 \left. \frac{\dot{\theta}_{12}}{\dot{\theta}_{23}} \right|_{M_U}^{\text{bimax}} &= \frac{2\sqrt{2} (m_1 + m_2) (m_3 - m_1) (m_3 - m_2) F_1}{(m_2 - m_1) [8 (m_2 - m_1) m_3 F_2 + 4\sqrt{2} (m_3^2 - m_1 m_2) F_3]} \\
 &\approx \begin{cases} \pm \frac{1}{2} \frac{m_2 + m_1}{m_2 - m_1} \frac{F_1}{F_3} & \text{for hierarchical neutrino masses} \\ \frac{1}{2} \frac{\Delta m_{\text{atm}}^2}{\Delta m_{\text{sol}}^2} \frac{F_1}{F_3} & \text{for degenerate neutrino masses} \end{cases} \quad (3.48b)
 \end{aligned}$$

where F_1, F_2, F_3 depend on $\{y_1, y_2, y_3, \phi_{12}, \phi_{13}, \phi_{32}\}$,

$$\begin{aligned}
 F_1 &= (y_1^2 - y_2^2) \{ \cos(2\phi_{12}) [(\cos(2\phi_{13}) - 3) \sin(2\phi_{23}) - 6 \cos^2(\phi_{13})] \\
 &\quad - 4 \cos(2\phi_{23}) \sin(2\phi_{12}) \sin(\phi_{13}) \} \\
 &\quad + (y_1^2 + y_2^2 - 2y_3^2) [\cos(2\phi_{13}) (\sin(2\phi_{23}) - 3) + (1 + \sin(2\phi_{23}))] , \quad (3.49a)
 \end{aligned}$$

$$\begin{aligned}
 F_2 &= 2 (y_1^2 - y_2^2) \cos(\phi_{13}) \sin(2\phi_{12}) (\sin(\phi_{23}) - \cos(\phi_{23})) \\
 &\quad - (y_1^2 + y_2^2 - 2y_3^2 + (y_1^2 - y_2^2) \cos(2\phi_{12})) \sin(2\phi_{13}) (\cos(\phi_{23}) + \sin(\phi_{23})) , \quad (3.49b)
 \end{aligned}$$

$$\begin{aligned}
 F_3 &= (y_1^2 - y_2^2) [\cos(2\phi_{12}) (\cos(2\phi_{13}) - 3) \cos(2\phi_{23}) \\
 &\quad + 4 \sin(2\phi_{12}) \sin(\phi_{13}) \sin(2\phi_{23})] + 2 (y_1^2 + y_2^2 - 2y_3^2) \cos^2(\phi_{13}) \cos(2\phi_{23}) . \quad (3.49c)
 \end{aligned}$$

Note that the approximations made above for hierarchical neutrino masses are also valid for relatively weak hierarchies, where m_3 is a few times larger or smaller than m_1 or m_2 . The constants F_i and G_i depend on the choice of $Y_\nu|_{M_U}$. However, unless the parameters $\{y_1, y_2, y_3, \phi_{12}, \phi_{13}, \phi_{32}\}$ are fine-tuned, we expect the ratios of these quantities to be of the order one.

Consequently, the RG change of θ_{12} is generically larger than that of the other angles if the mass-dependent factors in the equations (3.46) and (3.48) are large. This is always the case for quasi-degenerate neutrino masses, since $\Delta m_{\text{atm}}^2 \gg \Delta m_{\text{sol}}^2$. As $(m_1 - m_2)$ is related to the small solar mass squared difference, it is also true for non-degenerate mass schemes, unless m_1 is very small.

It is therefore interesting to study, whether it is possible to reach the experimentally confirmed LMA solution for the mixing angle θ_{12} from these special initial conditions with $\theta_{12} = 45^\circ$ or $\theta_{12} = 0^\circ$ at M_U .

3.3.4 The Running Between the Thresholds

In the energy ranges between the mass thresholds of the singlets, the running of the effective neutrino mass matrix of equation (3.39) is given by the RGEs of equation (3.40).

Running Caused by the Neutrino Yukawa Matrix

Between the see-saw scales, the singlets are partly integrated out, which implies that only a $(n-1) \times 3$ -submatrix of the neutrino Yukawa matrix remains. Therefore,

we expect that the running between the thresholds caused by the neutrino Yukawa matrix can differ significantly from the running above or below them.

Running Caused by Interactions with Trivial Flavour Structure

We now investigate the running due to the terms in the β -functions with a flavour structure proportional to the unit matrix. Below the see-saw scales and above them in type I scenarios, they only cause a common scaling of the elements of the neutrino mass matrix and thus leave the mixing angles and phases unchanged. Between the thresholds, where the effective neutrino mass matrix consists of two parts, this is only the case if both parts are scaled equally.

From table 3.2, we see that $\beta_{\kappa}^{(n)}$ and $\beta_{2Y_{\nu}^T M^{-1} Y_{\nu}}^{(n)}$, which govern the RG scaling of the two parts, have different coefficients in the terms proportional to the gauge couplings and to the Higgs self-coupling in the SM. This difference can be understood by looking at the corresponding diagrams of the “full” and the effective theory. For instance, the diagram for the correction to the effective vertex proportional to λ and its counterpart with the heavy singlet running in the loop are shown in figure 3.10. Diagram (a), which is similar to diagrams calculated in section 2.2.2, is UV divergent, whereas diagram (b) is UV finite. We thus get no contribution proportional to λ for the β -function of the composite object. The situation is similar for some of the diagrams corresponding to the vertex corrections proportional to the gauge couplings. Due to the non-renormalization theorem in supersymmetric theories, we immediately conclude that this does not happen in the MSSM.

Thus, in the SM, the RG scaling of the two parts $\kappa^{(n)}$ and $2Y_{\nu}^{(n)T} M^{-1} Y_{\nu}^{(n)}$ of the effective mass matrix between the thresholds, caused by the interactions with trivial flavour structure, is different. This implies a running of the mixing angles and CP phases in addition to the running of the mass eigenvalues. Numerical examples, where this effect gives the dominant contribution to the running of the mixing angles, will be shown in section 3.4 in figure 3.14.

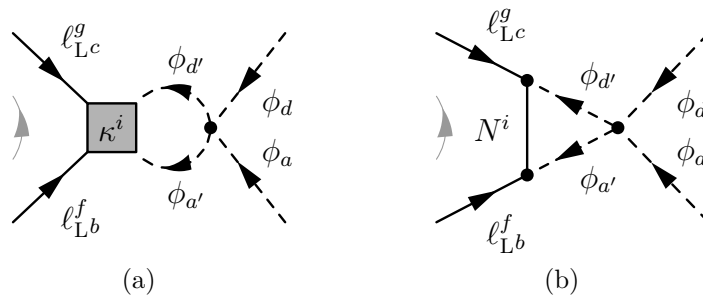


Figure 3.10: Figure (a) shows the diagram which gives the contribution proportional to the Higgs self-coupling in the β -function of the neutrino mass operator. Figure (b) shows its finite counterpart with the heavy singlet running in the loop.

3.4 Radiative Generation of the LMA Solution in Type I See-Saw Models

As found in section 3.3.3, the running of the angle θ_{12} is generically enhanced compared to the RG evolution of the other mixing angles. Exceptions are possible, if the neutrino mass scheme is strongly hierarchical or if the parameters of the neutrino Yukawa coupling matrix conspire to suppress the running of the solar angle. In addition, we expect that CP phases can have a damping effect on the running, as in the energy range below the mass thresholds of the singlets.

Therefore, we now investigate if the large, but not maximal mixing of the LMA solution can be reached by RG running from the special case of bimaximal mixing ($\theta_{12} = \theta_{23} = 45^\circ$, $\theta_{13} = 0^\circ$) [114] or from $\theta_{12} = \theta_{13} = 0^\circ$, $\theta_{23} = 45^\circ$ [115] at the high energy scale M_U .

3.4.1 The LMA solution from Bimaximal Lepton Mixing

For the special case of bimaximal mixing, $\theta_{12} = 45^\circ$, $\theta_{13} = 0^\circ$ and $\theta_{23} = 45^\circ$, we obtain the so-called bimaximal mixture form

$$m_\nu^{\text{bimax}}|_{M_U} = \begin{pmatrix} a-b & c & -c \\ c & a & b \\ -c & b & a \end{pmatrix} \quad (3.50)$$

as initial condition at M_U . The parameters a, b and c are related to the mass eigenvalues of m_ν by

$$a = \frac{1}{4}(m_1 + m_2 + 2m_3), \quad b = \frac{1}{4}(-m_1 - m_2 + 2m_3), \quad c = \frac{m_2 - m_1}{2\sqrt{2}}. \quad (3.51)$$

Inverting equations (3.51) yields

$$m_1 = a - b - \sqrt{2}c, \quad m_2 = a - b + \sqrt{2}c, \quad m_3 = a + b. \quad (3.52)$$

From equation (3.51) we see that $a > 0$. Equations (3.52) imply that the solar mass squared difference $\Delta m_{\text{sol}}^2 = m_2^2 - m_1^2$ is related to c , while the atmospheric one, $\Delta m_{\text{atm}}^2 = m_3^2 - m_2^2$, is controlled by b . Thus, $a > |b| > |c|$. For $b > 0$ we obtain a normal mass hierarchy, while for $b < 0$ the mass hierarchy is inverted. The different mass schemes are illustrated in figure A.1 on page 108. For positive c , $m_1 < m_2$, otherwise $m_1 > m_2$. Hence, Δm_{sol}^2 is positive only if c is. If $a \gg |b|, |c|$, the spectrum is quasi-degenerate. As explained in appendix A.1, we use the convention that the mass label 2 is attached in such a way that $0 \leq \theta_{12} \leq 45^\circ$. This can always be accomplished by the replacement $c \leftrightarrow -c$.

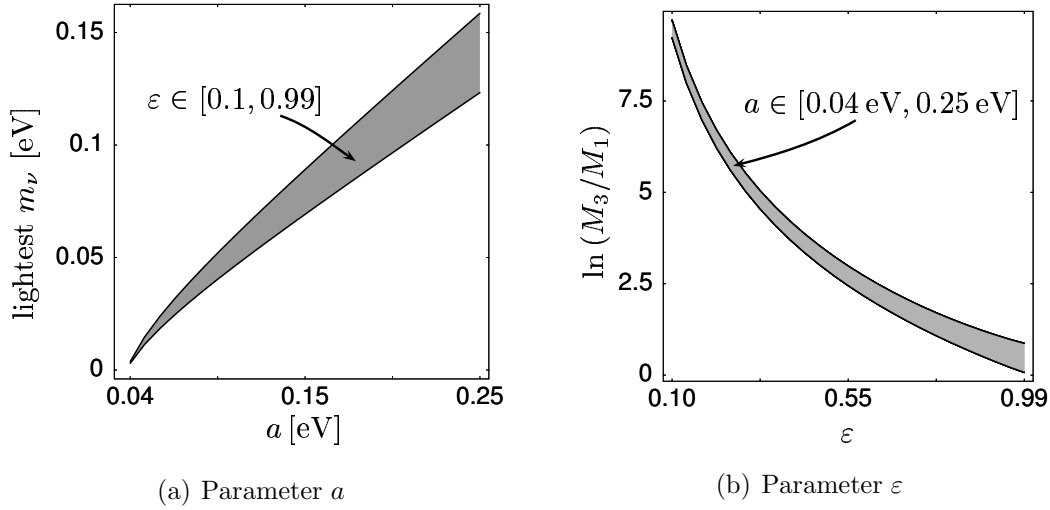


Figure 3.11: Plot 3.15(a) shows the mass of the lightest neutrino (at low energy) as a function of parameter a for the SM and the MSSM with normal mass hierarchy, $X = 1$ and $\epsilon \in [0.1, 0.99]$ (grey region). Plot 3.15(b) shows the degeneracy of the see-saw scales, parametrized by $\ln(M_3/M_1)$ (at M_U), as a function of ϵ for the same cases with $a \in [0.04 \text{ eV}, 0.25 \text{ eV}]$ (grey region).

Reduced Parameter Space at M_U

To reduce the parameter space for the numerical analysis, we choose a specific neutrino Yukawa coupling Y_ν at M_U . We assume, as an example, that it is diagonal and of the form

$$Y_\nu = X \text{diag}(1, \epsilon, \epsilon^2). \quad (3.53)$$

Y_ν and M are now determined by the parameters $\{\epsilon, X, a, b, c\}$. Moreover, we fix the values of b and c at M_U by the requirement that the solar and atmospheric mass squared differences obtained at the EW scale after the RG evolution be compatible with the allowed experimental regions. Thus, we are left with the free parameters X , ϵ and a . Of course, all the other parameters like e.g. quark masses and gauge couplings are chosen at M_U such that they are compatible with experiments at low energy (see table 1.3 on page 4). The parameter ϵ controls the hierarchy of the entries in Y_ν and thus the degeneracy of the see-saw scales, while a determines the mass of the lightest neutrino. The dependence of physical quantities on ϵ and a is shown in figure 3.11.

Numerical Results for the Allowed Parameter Space Regions

We can now scan over the two relevant parameters at M_U and perform the running down to the EW or SUSY breaking scale. The parameter space regions in which

the RG evolution produces low-energy values compatible with the LMA solution are shown in figure 3.12 for the SM and the MSSM ($\tan\beta = 5$) with a normal mass hierarchy. We find that for the form of Y_ν under consideration, hierarchical and degenerate neutrino mass schemes as well as degenerate and non-degenerate see-saw scales are possible. For inverted neutrino mass spectra, allowed parameter space regions exist as well. We would like to stress that the shapes of the allowed parameter space regions strongly depend on the choice of the initial value of Y_ν at M_U . One also has to ensure that the sign of Δm_{sol}^2 is positive, as the LMA solution requires this if the convention is used that the solar mixing angle is smaller than 45° . With bimaximal mixing at M_U , the sign of Δm_{sol}^2 is not defined by the initial conditions. Using the analytic approximation of section 3.3.3, the sign just below M_U can be calculated. We find $\Delta m_{\text{sol}}^2 > 0$ for $F_1 < 0$ and vice versa. However, in order to predict the sign of Δm_{sol}^2 at low energy, the numerical RG evolution has to be used. This excludes some of the possible choices for the neutrino Yukawa coupling Y_ν at M_U . For example, among the possibilities with diagonal Y_ν it excludes $Y_\nu = \text{diag}(\varepsilon^2, \varepsilon, 1)$. From figure 3.12, we see that obtaining the LMA solution from RG running does not require any fine-tuning. The allowed regions in the parameter space cover a quite large range of degeneracies of the see-saw scales and lightest neutrino masses.

Examples for the Running of the Lepton Mixing Angles

We now turn to some examples out of the allowed parameter space regions. Figures 3.13(a) and 3.13(b) show typical numerical examples for the running of the mixing angles from M_U to the EW or SUSY-breaking scale. The kinks in the plots correspond to the mass thresholds at the see-saw scales and the grey-shaded regions mark the various effective theories. As expected from the analytical formulae of section 3.3.3, the solar angle θ_{12} changes drastically, while the changes of θ_{13} and θ_{23} are comparatively small. The mixing angles θ_{13} and θ_{23} are of course affected by the RG evolution as well, i.e. they do not stay at their initial values $\theta_{13} = 0^\circ$ and $\theta_{23} = 45^\circ$. Their low energy values are compatible with experiments.

As discussed in section 3.3.4, in the SM there can be contributions to the running of the mixing angles from interactions with a trivial flavour structure. Therefore, it is possible to obtain the LMA solution by RG running even if the neutrino Yukawa couplings are small and do not have a sizable effect (figure 3.14(a)). It is thus also possible to obtain the LMA solution from RG running with a negative CP parity for the state with mass m_2 (i.e. $\varphi_1 = 0^\circ$ and $\varphi_2 = 180^\circ$), as shown in figure 3.14(b). For this example we have chosen a different diagonal structure for Y_ν , $Y_\nu = X \text{diag}(\varepsilon^2, \varepsilon, 1)$, at M_U .

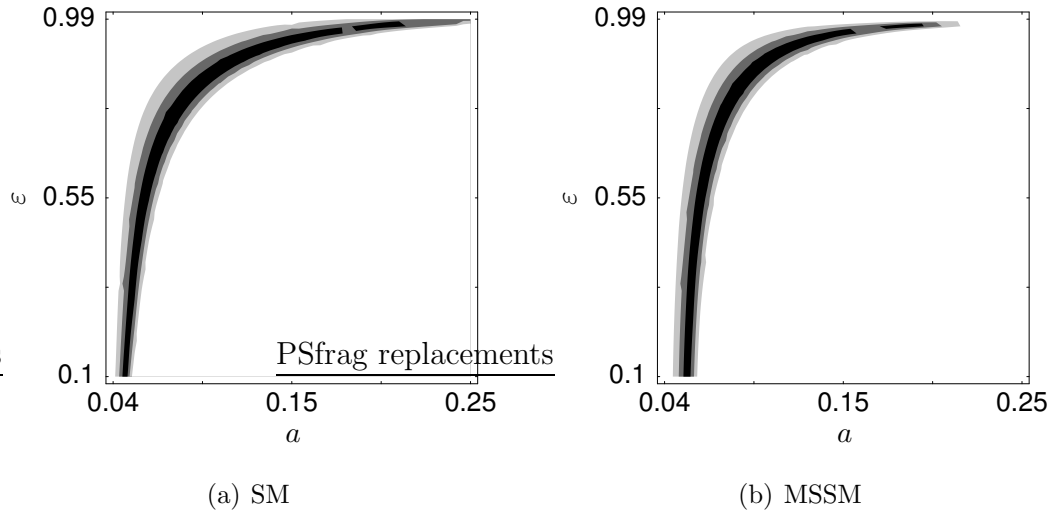
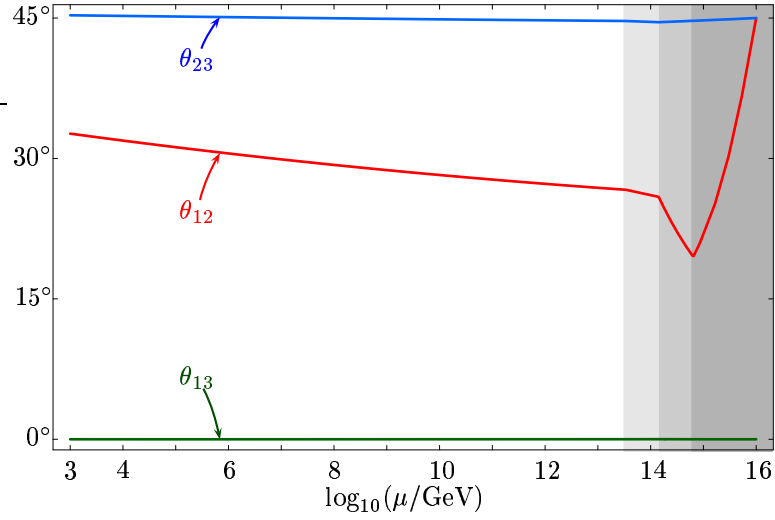
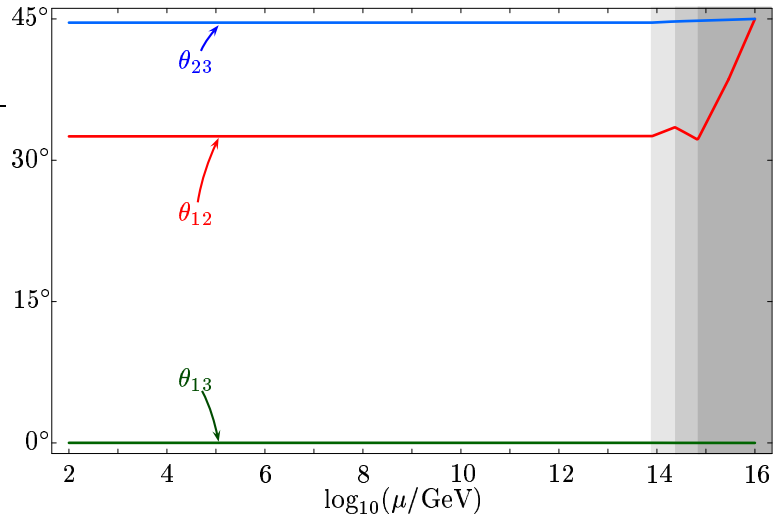


Figure 3.12: Parameter space regions compatible with the LMA solution of the solar neutrino problem for the example $Y_\nu|_{M_U} = \text{diag}(1, \varepsilon, \varepsilon^2)$. The initial condition at $M_U = 10^{16}$ GeV is bimaximal mixing, and the comparison with the experimental data is performed at the EW scale or at 1 TeV for the SM and the MSSM, respectively. The white regions of the plots are excluded by the data at 3σ . The black (dark grey) regions have a deviation of the best-fit value smaller than $\frac{1}{3}$ ($\frac{2}{3}$) of the 3σ -uncertainty. For this example, we consider the case of a normal neutrino mass hierarchy and $X = 1$ for the scale factor of the neutrino Yukawa couplings.

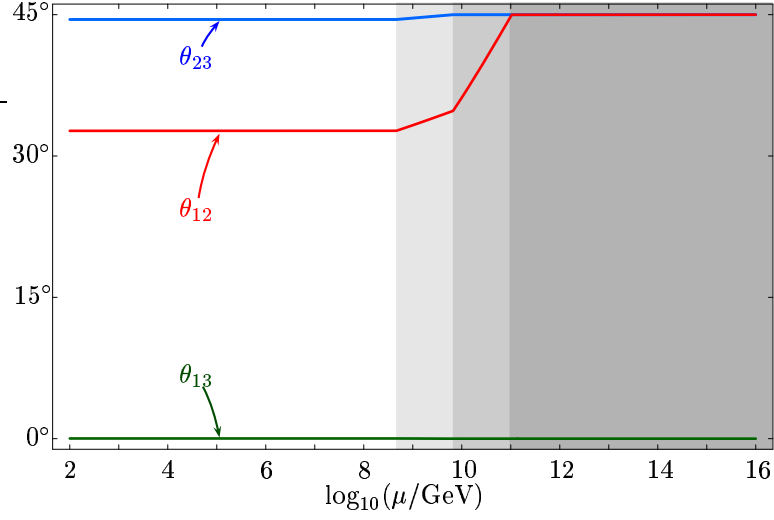
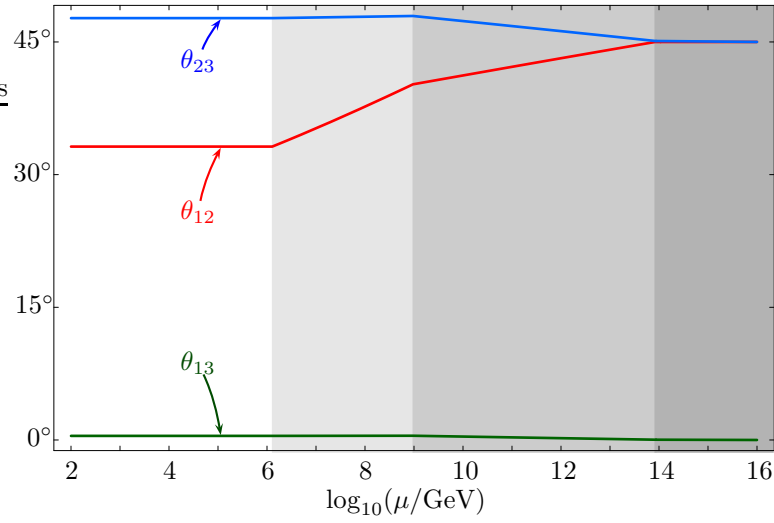


(a) MSSM



(b) SM

Figure 3.13: RG evolution of the mixing angles in the canonical see-saw model from M_U to the EW or SUSY-breaking scale (taken to be ≈ 1 TeV), respectively. In these examples we have chosen a normal mass hierarchy and $Y_\nu = X \text{diag}(1, \varepsilon, \varepsilon^2)$ with $X = 1$. In the MSSM example we have in addition $\tan \beta = 5$, $\varepsilon = 0.525$, $a = 0.0675$ eV while in the SM example $\varepsilon = 0.65$ and $a = 0.0655$ eV. The parameter a , related to the mass of the lightest neutrino, is explained in the text and the meaning of ε and a are illustrated in figure 3.11. The kinks in the plots correspond to the mass thresholds at the see-saw scales. The grey-shaded regions mark the various effective theories.


 (a) Small Y_ν


(b) Majorana Parity

Figure 3.14: Examples for the RG evolution in the canonical see-saw scenario in the SM, where the running from bimaximal mixing to the LMA solution takes place between the see-saw scales. In figure (a), we have chosen $X = 0.01$, $\varepsilon = 0.3$, $a = 0.0535$ eV and a normal mass hierarchy. In figure (b), we have considered the case of a negative CP parity for m_2 , $X = 0.5$, $\varepsilon = 3.5 \cdot 10^{-3}$ and a normal mass hierarchy. The lightest neutrino has a mass of 0.004 eV (at low energy) in this example.

3.4.2 The LMA Solution from Vanishing Solar Neutrino Mixing

We now illustrate that the LMA solution can be reached in a rather natural way by RG running from vanishing solar mixing ($\theta_{12} = 0^\circ$) and $\theta_{13} = 0^\circ$, $\theta_{23} = 45^\circ$ at M_U .

Reduced Parameter Space at M_U

For our examples, we choose the specific form

$$Y_\nu|_{M_U} = X \cdot \begin{pmatrix} \varepsilon^2 & \varepsilon^3 & 0 \\ \varepsilon^3 & \varepsilon & 0 \\ 0 & 0 & 1 \end{pmatrix} \quad (3.54)$$

for the neutrino Yukawa coupling at M_U . With a given $Y_\nu|_{M_U}$, $M|_{M_U}$ can be calculated from $m_\nu|_{M_U}$ by the see-saw formula (3.39). The parameter ε introduced in equation (3.54) controls the hierarchy of the entries in Y_ν and thus the degeneracy of the see-saw scales. Moreover, we choose the lightest neutrino mass at M_U , $m_1|_{M_U}$ for a normal and $m_3|_{M_U}$ for an inverted spectrum as a further initial condition. We fix the values of the two remaining masses at M_U by the requirement that the solar and atmospheric mass squared differences obtained at the EW scale after the RG evolution be compatible with the allowed experimental regions. Figure 3.15 shows the dependence of the physical parameters on ε and $m_1|_{M_U}$.

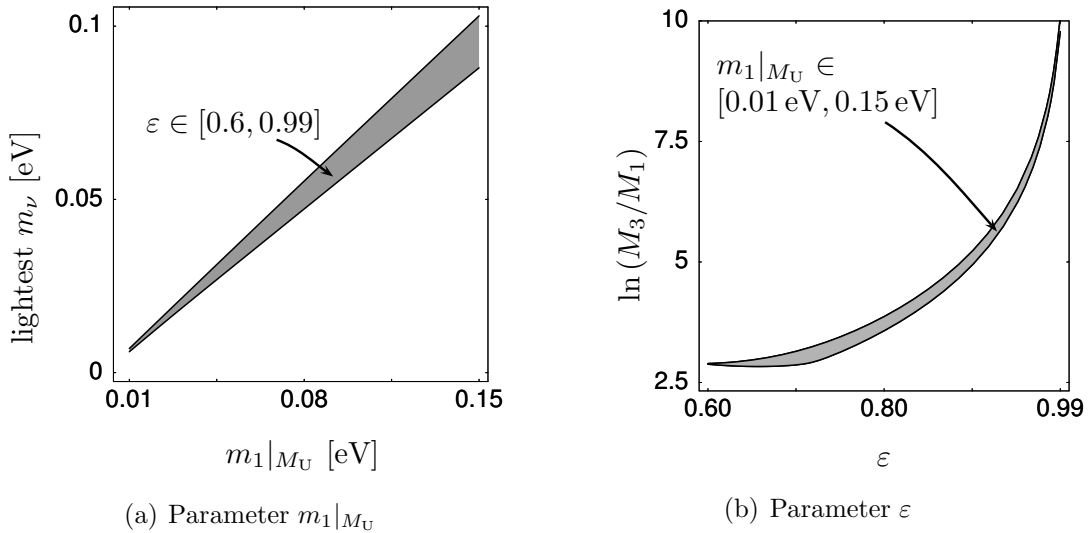


Figure 3.15: Plot 3.15(a) shows the mass of the lightest neutrino (at low energy) as a function of $m_1|_{M_U}$ for the SM and the MSSM with normal mass hierarchy, $X = 0.5$ and $\varepsilon \in [0.6, 0.99]$ (grey region). Plot 3.15(b) shows the degeneracy of the see-saw scales, parametrized by $\ln(M_3/M_1)$ (at M_U), as a function of ε for the same cases with $m_1|_{M_U} \in [0.01 \text{ eV}, 0.15 \text{ eV}]$ (grey region).

Numerical Results for the Allowed Parameter Space Regions

Thus, we are left with the free parameters X , ε and $m_1|_{M_U}$ or $m_3|_{M_U}$. The parameter space regions in which the RG evolution produces low-energy values compatible with the LMA solution are shown in figure 3.16 for the SM and the MSSM ($\tan\beta = 5$) with a normal mass hierarchy and Y_ν given in equation (3.54).

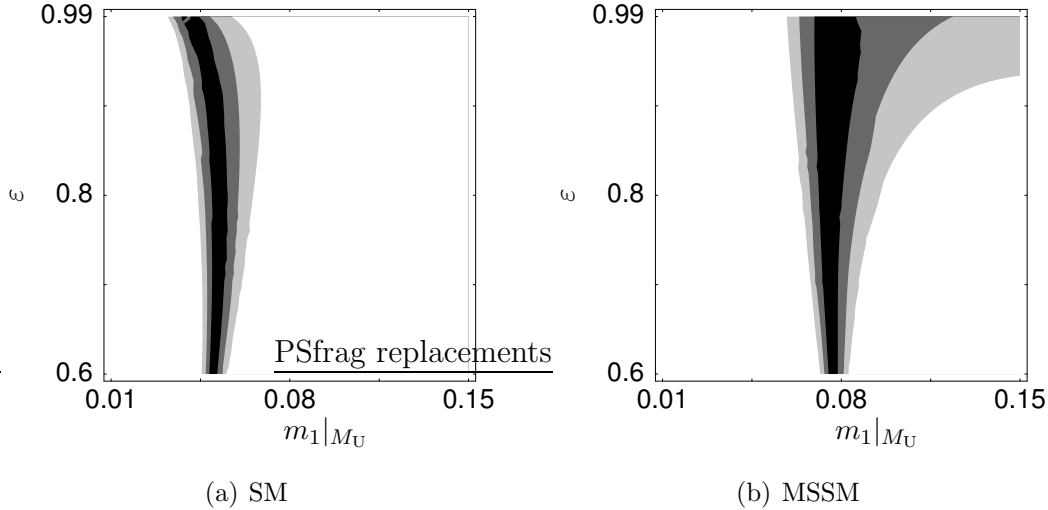
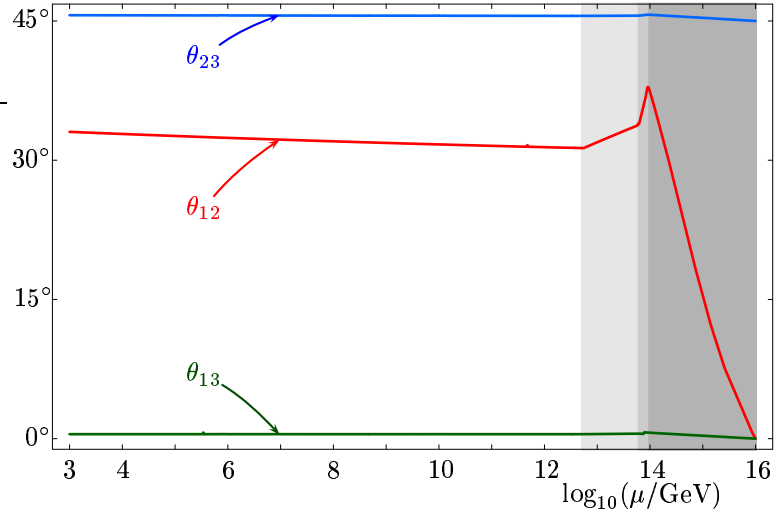


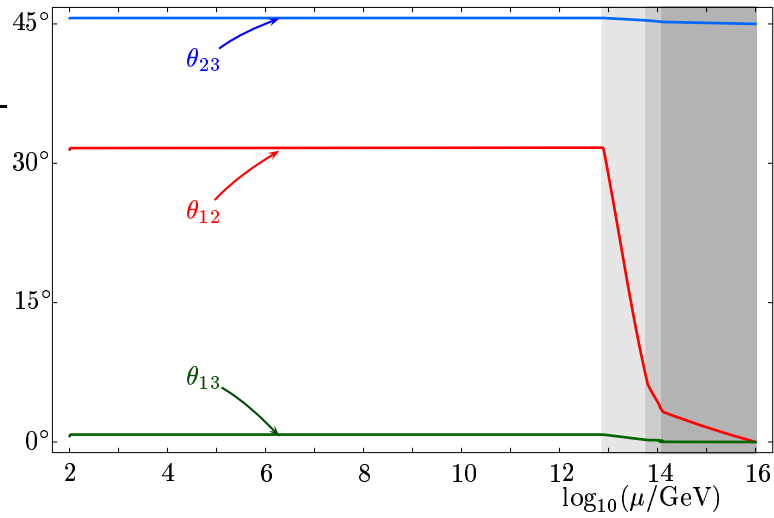
Figure 3.16: Parameter space regions compatible with the LMA solution of the solar neutrino problem for the example with $Y_\nu|_{M_U}$ given by equation (3.54). The initial condition at $M_U = 10^{16}$ GeV is vanishing mixing for θ_{12} and θ_{13} and maximal mixing for θ_{23} . The comparison with the experimental data is performed at the EW scale or at 1 TeV for the SM and the MSSM, respectively. The shaded regions are defined as in figure 3.12. For this example, we consider the case of a normal neutrino mass hierarchy and $X = 0.5$ for the scale factor of the neutrino Yukawa couplings.

Examples for the Running of the Lepton Mixing Angles

Figures 3.17(a) and 3.17(b) show numerical examples for the running of the lepton mixing angles from M_U to the EW or SUSY-breaking scale, which produce the mixing angles of the LMA solution. Again we find that the solar mixing angle runs sizably, whereas the evolution of the other angles is comparatively small. Furthermore, we find examples where most of the running takes place between the see-saw scales (e.g. figure 3.17(b)). Thus, if the see-saw scales are non-degenerate, it is crucial to take the running in these energy ranges into account.



(a) MSSM



(b) SM

Figure 3.17: RG evolution of the mixing angles in the canonical see-saw scenario from M_U to the EW or SUSY-breaking scale (taken to be ≈ 1 TeV), respectively. For both examples we have considered a normal mass hierarchy and $X = 0.5$. The additional parameters for the example in the MSSM are $\tan\beta = 5$, $\varepsilon = 0.65$ and $m_1|_{M_U} = 0.076$ eV. In the SM, we have shown an example with $\varepsilon = 0.6$ and $m_1|_{M_U} = 0.049$ eV. In the SM example, most of the running takes place between the see-saw scales.

Conclusions

In this thesis, we have studied the energy scale dependence of neutrino masses, lepton mixings and CP phases. Parts of the results have been published in collaborations with M. Drees, J. Kersten, M. Lindner and M. Ratz in diverse combinations.

We have considered the effective description of neutrino masses by the lowest dimensional effective operator and discussed its possible origin. From the point of view of left-right symmetric extensions of the SM, its realization by type I or II see-saw scenarios, where heavy singlets and/or $SU(2)_L$ -triplets are integrated out of the theory, appears particularly natural. In addition, neutrinos may also trigger a dynamical generation of fermion masses. In spite of large Majorana masses of the singlet neutrinos, the formation of a composite Higgs particle by neutrino condensation is possible in a phenomenologically acceptable way in see-saw scenarios [50].

We have calculated the RGEs for the lowest dimensional neutrino mass operator in various theories. In the SM, where results in the literature were not in agreement, we have derived the correct RGE, which differs from the previous ones in the part with a non-trivial flavour structure [57]. Similar corrections have been made in 2HDMs [67]. In the MSSM, we have confirmed the existing 1-loop RGE [58,59] and extended it to the 2-loop level [81]. The RGEs govern the energy scale dependence of the neutrino masses, lepton mixings and CP phases. The correct results are thus required, whenever these parameters at different energies below the realization scale of the operator are compared.

We have further calculated the RGEs and the tree-level matching conditions for minimal see-saw extensions of the SM, 2HDMs and the MSSM, where singlet neutrinos with intermediate scale masses are added to the particle spectrum [85]. Integrating them out successively leads to various effective theories. We have performed the tree-level matching with the neutrino mass operator, which is required at each mass threshold of the singlets. Additional contributions to the mass operator can stem from integrating out a heavy triplet of $SU(2)_L$ in the context of a type II see-saw mechanism or from additional higher dimensional operators, for example. The RGEs can also be applied to these scenarios below the corresponding realization scales, e.g. below the masses of the triplet-components. They are relevant for the RG study of many models for fermion masses, which are defined at energies of the order of the GUT scale.

Using the calculated RGEs, we have analyzed the running of neutrino masses, lepton mixing angles and CP phases in the SM and the MSSM. In the case of the description of neutrino masses by the effective neutrino mass operator, we have derived analytical approximations for the running of neutrino masses, lepton mixings and Dirac and Majorana CP phases in an expansion in the small mixing angle θ_{13} .

We have compared them with numerical results obtained using the “run and diagonalize” procedure and have found that they allow to understand the RG change qualitatively and to a quite good approximation also quantitatively [108]. For example, it can easily be seen from our formulae that Dirac and Majorana CP phases can have a drastic influence on the RG evolution of the mixing angles. Furthermore, interesting effects arise for the running of the CP phases themselves. Our formulae are useful for simplifying the inclusion of the RG effects. As an application, we have calculated the size of RG corrections to θ_{13} and θ_{23} produced by the running between the lowest see-saw scale and the electroweak scale. We have found that in large regions of the currently allowed parameter space, future experiments would measure a deviation from $\theta_{13} = 0^\circ$ and $\theta_{23} = 45^\circ$, even if some model predicted these values at high energy.

In the minimal see-saw extensions, we have considered the running of the effective neutrino mass matrix in the various effective theories, whose energy ranges are given by the masses of the heavy singlet neutrinos. The structure of the RGEs shows that the running above and between the thresholds differs substantially from that below the lowest see-saw scale. First, it depends on additional parameters from the neutrino Yukawa coupling matrix, which is a $(n-1) \times 3$ -matrix below the n th threshold. Next, in non-supersymmetric theories between the thresholds, the part of the β -functions proportional to the unit matrix in flavour space can contribute to the running of the lepton mixing angles. This is in contrast to the energy range below the lowest see-saw scale, where they only run due to the terms with a non-trivial flavour structure. This effect can lead to a large running of the mixings, even if the neutrino and charged lepton Yukawa couplings are very small or if the running from the Yukawa couplings is suppressed by CP phases. If the neutrino Yukawa couplings are large at high energy, which would for instance be the case in scenarios with Yukawa unification or in non-perturbative models like [50], the RG corrections from above and between the thresholds can be considerably larger than those from the running of the effective neutrino mass operator below the see-saw scales. In the restricted parameter space with zero CP phases, real neutrino Yukawa matrices, $\theta_{13} = 0^\circ$ and $\theta_{23} = 45^\circ$, we have found by an analytical calculation that the running of θ_{12} above the thresholds is generically stronger than that of θ_{13} and θ_{23} , unless the neutrino masses have a strong normal hierarchy. By a numerical analysis of the running of the mixing angles we have therefore investigated if the LMA solution with $\theta_{12} \approx 33^\circ$ at low energy can be generated by RG running from the specific values $\theta_{12} = 0^\circ$ or $\theta_{12} = 45^\circ$ at high energy. We have found that in both cases, this is possible for a quite large range of neutrino masses and degeneracies of the see-saw scales [114,115]. The running thus opens up new possibilities for building models towards an explanation of the origin of neutrino masses, lepton mixings and CP phases.

A Appendix

A.1 The Mixing Parameters of Quarks and Leptons

A.1.1 Definition of the Mixing Parameters

Mass matrices of Dirac type have complex entries in general. They can be diagonalized by bi-unitary transformations,

$$U_R^{(u)\dagger} M_u U_L^{(u)} = D_u , \quad (\text{A.1})$$

$$U_R^{(d)\dagger} M_d U_L^{(d)} = D_d , \quad (\text{A.2})$$

$$U_R^{(e)\dagger} M_e U_L^{(e)} = D_e . \quad (\text{A.3})$$

The masses, i.e. the diagonal elements of D_u, D_d and D_e , can be chosen real and positive. In the quark sector and for the charged leptons, they are arranged by increasing magnitude. In the neutrino sector, the arrangement is more subtle. We will discuss it in detail below. Mass matrices of Majorana type are symmetric and in general complex. They can therefore be diagonalized by one unitary matrix,

$$U^{(\nu)T} m_\nu U^{(\nu)} = D_\nu . \quad (\text{A.4})$$

Marking the flavour basis with a prime, under the change to the mass eigenbasis, the fields transform as

$$u_L^{\prime f} = (U_L^{(u)})_{fg} u_L^g , \quad u_R^{\prime f} = (U_R^{(u)})_{fg} u_R^g , \quad (\text{A.5})$$

$$d_L^{\prime f} = (U_L^{(d)})_{fg} d_L^g , \quad d_R^{\prime f} = (U_R^{(d)})_{fg} d_R^g , \quad (\text{A.6})$$

$$e_L^{\prime f} = (U_L^{(e)})_{fg} e_L^g , \quad e_R^{\prime f} = (U_R^{(e)})_{fg} e_R^g , \quad (\text{A.7})$$

$$\nu_L^{\prime f} = (U^{(\nu)})_{fg} \nu_L^g . \quad (\text{A.8})$$

Definition of the CKM and MNS Matrix

The Maki-Nakagawa-Sakata (MNS) mixing matrix in the lepton sector is the analogue of the Cabibbo-Kobayashi-Maskawa (CKM) matrix in the quark sector. The mixing of flavour and mass eigenstates is defined by the charged electroweak currents,

$$\overline{e_L^{\prime f}} \gamma^\mu \nu_L^{\prime f} = \overline{e_L^f} \gamma^\mu \tilde{V}_{MNS} \nu_L^f \quad \text{for the leptons and} \quad (\text{A.9})$$

$$\overline{u_L^{\prime f}} \gamma^\mu d_L^{\prime f} = \overline{u_L^f} \gamma^\mu \tilde{V}_{CKM} d_L^f \quad \text{for the quarks.} \quad (\text{A.10})$$

The relation of the mixing matrices to the diagonalization matrices is thus given by

$$\tilde{V}_{MNS} = U_L^{(e)\dagger} U^{(\nu)} , \quad (\text{A.11})$$

$$\tilde{V}_{CKM} = U_L^{(u)\dagger} U_L^{(d)} . \quad (\text{A.12})$$

\tilde{V}_{MNS} and \tilde{V}_{CKM} contain unphysical degrees of freedom. They can be eliminated by unobservable global phase transformations of the fields, as will be discussed

below. Considering only physical degrees of freedom, the mixing matrices are called CKM matrix V_{MNS} and MNS matrix V_{CKM} and can be parametrized by

$$V_{MNS} = \begin{cases} R_{23}R_{13}R_{12} & \text{for Dirac neutrinos,} \\ R_{23}R_{13}R_{12}P_{\text{Maj}} & \text{for Majorana neutrinos,} \end{cases} \quad (\text{A.13})$$

$$V_{CKM} = R_{23}R_{13}R_{12}, \quad (\text{A.14})$$

where R_{12} , R_{13} , R_{23} and P_{Maj} are given by

$$\begin{aligned} R_{12} &= \begin{pmatrix} c_{12} & s_{12} & 0 \\ -s_{12} & c_{12} & 0 \\ 0 & 0 & 1 \end{pmatrix}, & R_{13} &= \begin{pmatrix} c_{13} & 0 & s_{13}e^{-i\delta} \\ 0 & c_{13} & 0 \\ -s_{13}e^{i\delta} & 0 & c_{13} \end{pmatrix}, \\ R_{23} &= \begin{pmatrix} 1 & 0 & 0 \\ 0 & c_{23} & s_{23} \\ 0 & -s_{23} & c_{23} \end{pmatrix}, & P_{\text{Maj}} &= \begin{pmatrix} e^{-i\frac{\varphi_1}{2}} & 0 & 0 \\ 0 & e^{-i\frac{\varphi_2}{2}} & 0 \\ 0 & 0 & 1 \end{pmatrix}. \end{aligned} \quad (\text{A.15})$$

P_{Maj} contains the phases φ_1 and φ_2 , which are physical degrees of freedom if neutrinos are of Majorana type, and we have defined $c_{ij} := \cos \theta_{ij}$ and $s_{ij} := \sin \theta_{ij}$. θ_{ij} are the mixing angles and δ is called the Dirac CP phase for the quarks or neutrinos, respectively. The Majorana phases φ_1 and φ_2 are unobservable in neutrino oscillations, but they enter the effective mass relevant for neutrinoless double beta decay experiments.

Unphysical Degrees of Freedom

Changing the mass eigenbasis in a way that the diagonalization matrices are transformed as

$$\begin{aligned} U_{\text{L}}^{(u)} &\longrightarrow U_{\text{L}}^{(u)} P^{(u)}, & U_{\text{R}}^{(u)} &\longrightarrow U_{\text{R}}^{(u)} P^{(u)}, \\ U_{\text{L}}^{(d)} &\longrightarrow U_{\text{L}}^{(d)} P^{(d)}, & U_{\text{R}}^{(d)} &\longrightarrow U_{\text{R}}^{(d)} P^{(d)}, \\ U_{\text{L}}^{(e)} &\longrightarrow U_{\text{L}}^{(e)} P^{(e)}, & U_{\text{R}}^{(e)} &\longrightarrow U_{\text{R}}^{(e)} P^{(e)}, \\ U^{(\nu)} &\longrightarrow U^{(\nu)} S^{(\nu)}, \end{aligned} \quad (\text{A.16})$$

with

$$\begin{aligned} P^{(j)} &= \begin{pmatrix} e^{-i\delta_1^{(j)}} & 0 & 0 \\ 0 & e^{-i\delta_2^{(j)}} & 0 \\ 0 & 0 & e^{-i\delta_3^{(j)}} \end{pmatrix}, & P^{(d)} &= \begin{pmatrix} e^{-i\delta_4^{(d)}} & 0 & 0 \\ 0 & e^{-i\delta_5^{(d)}} & 0 \\ 0 & 0 & 1 \end{pmatrix}, \\ S^{(\nu)} &= \begin{pmatrix} \pm 1 & 0 & 0 \\ 0 & \pm 1 & 0 \\ 0 & 0 & \pm 1 \end{pmatrix}, \end{aligned} \quad (\text{A.17})$$

$j \in \{u, e\}$, does not alter the mass matrices and is physically unobservable. Note that only phase differences are considered here because transforming all mass eigenstates by a global phase has no effect at all. The third phase in $P^{(d)}$ is chosen to be the overall global phase and therefore set equal to 1 without loss of generality. \tilde{V}_{MNS} and V_{MNS} or \tilde{V}_{CKM} and V_{CKM} are related by

$$\tilde{V}_{MNS} = P^{(e)}V_{MNS}S^{(\nu)}, \quad (\text{A.18})$$

$$\tilde{V}_{CKM} = P^{(u)}V_{MNS}P^{(d)}. \quad (\text{A.19})$$

The transformations $\{P^{(e)}, S^{(\nu)}\}$ or $\{P^{(u)}, P^{(d)}\}$ can absorb 3 or 5 of the 9 parameters and they are furthermore used to restrict the parameter space of φ_1, φ_2 and θ_{ij} .

The Lepton Mixing Parameters

We will now specify the convention for the lepton mixing parameters which is used in this work. Without loss of generality, we change to the flavour basis where the mass matrix of the charged leptons, or equivalently the Yukawa matrix Y_e , is diagonal. This can be done by the simultaneous transformations

$$\begin{aligned} e'_L{}^f &\longrightarrow (U_L^{(e)\dagger})_{fg}e'^g{}_L, \\ e'_R{}^f &\longrightarrow (U_R^{(e)\dagger})_{fg}e'^g{}_R, \\ \nu'^f{}_L &\longrightarrow (U_L^{(e)\dagger})_{fg}\nu'^g{}_L, \\ m_\nu &\longrightarrow U_L^{(e)T}m_\nu U_L^{(e)}, \end{aligned} \quad (\text{A.20})$$

where $U_L^{(e)}$ and $U_R^{(e)}$ are defined by

$$\begin{aligned} U_L^{(e)\dagger}Y_e^\dagger Y_e U_L^{(e)} &= \text{diag.}, \\ U_R^{(e)\dagger}Y_e Y_e^\dagger U_R^{(e)} &= \text{diag.}. \end{aligned} \quad (\text{A.21})$$

In this basis, $\tilde{V}_{MNS} = U^{(\nu)}$ transforms the neutrino mass eigenstates into flavour eigenstates,

$$\begin{pmatrix} \nu_{eL} \\ \nu_{\mu L} \\ \nu_{\tau L} \end{pmatrix} = \tilde{V}_{MNS} \begin{pmatrix} \nu_{1L} \\ \nu_{2L} \\ \nu_{3L} \end{pmatrix} = \begin{pmatrix} \tilde{V}_{e1} & \tilde{V}_{e2} & \tilde{V}_{e3} \\ \tilde{V}_{\mu 1} & \tilde{V}_{\mu 2} & \tilde{V}_{\mu 3} \\ \tilde{V}_{\tau 1} & \tilde{V}_{\tau 2} & \tilde{V}_{\tau 3} \end{pmatrix} \begin{pmatrix} \nu_{1L} \\ \nu_{2L} \\ \nu_{3L} \end{pmatrix}.$$

To define the diagonalization matrix for the neutrino Majorana mass m_ν , we have to determine how the positive mass eigenvalues are arranged. Let the diagonalized neutrino mass matrix be

$$D_\nu = \begin{pmatrix} m_1 & 0 & \\ 0 & m_2 & 0 \\ 0 & 0 & m_3 \end{pmatrix}. \quad (\text{A.22})$$

From the experiments, we know that there is a small mass squared difference corresponding to oscillations of solar neutrinos, called $\Delta m_{\text{sol}}^2 = m_i^2 - m_j^2$, and a larger one corresponding to oscillations of atmospheric neutrinos, referred to as $\Delta m_{\text{atm}}^2 = m_k^2 - m_\ell^2$. We now choose the convention that the masses are labeled such that $i, j \neq 3$ while either k or ℓ equals 3. This fixes the assignment of the mass m_3 . The two possible schemes are illustrated in Figure A.1.

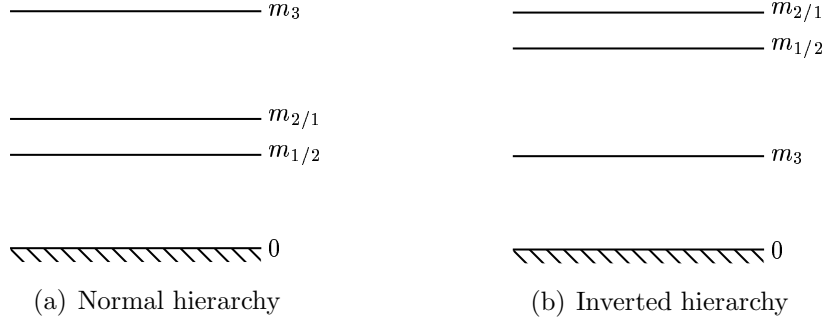


Figure A.1: Possible mass hierarchies for the light neutrinos. We use the convention that m_1 and m_2 are chosen in such a way that $0 \leq \theta_{12} \leq 45^\circ$. The LMA solution then requires $m_2 > m_1$ at low energy. If the mass-differences are small compared to the mass of the lightest neutrino, the spectrum is called quasi-degenerate, otherwise hierarchical.

To diagonalize m_ν , we calculate the eigenvalues and corresponding eigenvectors of $m_\nu^\dagger m_\nu$, where we assume non-degenerate mass eigenvalues. A diagonalization matrix U with the property $U^\dagger m_\nu^\dagger m_\nu U = \text{diag}(m_i^2, m_j^2, m_k^2) := D_\nu^2$, $m_i \in \{m_1, m_2, m_3\}$, has the eigenvectors corresponding to the eigenvalues m_i^2 as columns. The assignment of m_3 therefore fixes the third column of \tilde{V}_{MNS} . The remaining two mass eigenvalues and columns are assigned such that $|V_{e2}| \leq |V_{e1}|$. This will allow to restrict the solar mixing angle θ_{12} to the interval $[0, \pi/4]$. It turns out that θ_{23} and θ_{13} can be chosen in the range $[0, \pi/2]$. For the phases, the range $[0, 2\pi]$ is required.

A.1.2 Extraction of Mixing Angles and CP Phases

For the RG analysis, we have to extract the mixing angles and physical phases from \tilde{V}_{MNS} for the leptons and from \tilde{V}_{CKM} for the quarks. We will now treat the case of the MNS-matrix in detail and briefly comment on the differences for the quarks. For each unitary matrix, we use the standard parametrization in the form $\tilde{V} = \text{diag}(e^{i\delta_1}, e^{i\delta_2}, e^{i\delta_3}) \cdot V \cdot \text{diag}(e^{-i\varphi_1/2}, e^{-i\varphi_2/2}, 1)$, which gives

$$\begin{pmatrix} e^{i\delta_1 - i\frac{\varphi_1}{2}} c_{12} c_{13} & e^{i\delta_1 - i\frac{\varphi_2}{2}} s_{12} c_{13} & s_{13} e^{i\delta_1 - i\delta} \\ e^{i\delta_2 - i\frac{\varphi_1}{2}} (-c_{23} s_{12} - s_{23} s_{13} c_{12} e^{i\delta}) & e^{i\delta_2 - i\frac{\varphi_2}{2}} (c_{23} c_{12} - s_{23} s_{13} s_{12} e^{i\delta}) & e^{i\delta_2} s_{23} c_{13} \\ e^{i\delta_3 - i\frac{\varphi_1}{2}} (s_{23} s_{12} - c_{23} s_{13} c_{12} e^{i\delta}) & e^{i\delta_3 - i\frac{\varphi_2}{2}} (-s_{23} c_{12} - c_{23} s_{13} s_{12} e^{i\delta}) & e^{i\delta_3} c_{23} c_{13} \end{pmatrix}.$$

As we have seen in the previous section, not all of these 9 parameters are physical. In the lepton sector, we can eliminate δ_1, δ_2 and δ_3 by physically unobservable phase re-definitions. In the quark sector the phases φ_1 and φ_2 can be eliminated as well while they are physical in the lepton sector, if neutrinos are of Majorana type. The parameters can be read off by the following procedure:

1. $\theta_{13} = \arcsin(|U_{13}|)$
2. $\theta_{12} = \begin{cases} \arctan\left(\frac{|U_{12}|}{|U_{11}|}\right) & \text{if } U_{11} \neq 0 \\ \frac{\pi}{2} & \text{else} \end{cases}$
3. $\theta_{23} = \begin{cases} \arctan\left(\frac{|U_{23}|}{|U_{33}|}\right) & \text{if } U_{33} \neq 0 \\ \frac{\pi}{2} & \text{else} \end{cases}$
4. $\delta_2 = \arg(U_{23})$
5. $\delta_3 = \arg(U_{33})$
6. $\delta = -\arg\left(\frac{\frac{U_{ii}^* U_{ij} U_{ji} U_{jj}^*}{c_{12} c_{13}^2 c_{23} s_{13}} + c_{12} c_{23} s_{13}}{s_{12} s_{23}}\right)$
 where $i, j \in \{1, 2, 3\}$ and $i \neq j$
7. $\delta_1 = \arg(e^{i\delta} U_{13})$
8. $\varphi_1 = 2 \arg(e^{i\delta_1} U_{11}^*)$
9. $\varphi_2 = 2 \arg(e^{i\delta_1} U_{12}^*)$

For the extraction of δ , we use the relation

$$U_{ii}^* U_{ij} U_{ji} U_{jj}^* = c_{12} c_{13}^2 c_{23} s_{13} (e^{-i\delta} s_{12} s_{23} - c_{12} c_{23} s_{13}),$$

which holds for $i, j \in \{1, 2, 3\}$ and $i \neq j$. It is often used in order to introduce the Jarlskog invariant [116]

$$\begin{aligned} J_{\text{CP}} &= \frac{1}{2} |\text{Im}(U_{11}^* U_{12} U_{21} U_{22}^*)| = \frac{1}{2} |\text{Im}(U_{11}^* U_{13} U_{31} U_{33}^*)| \\ &= \frac{1}{2} |\text{Im}(U_{22}^* U_{23} U_{32} U_{33}^*)| = \frac{1}{2} |c_{12} c_{13}^2 c_{23} \sin \delta s_{12} s_{13} s_{23}|. \end{aligned} \quad (\text{A.23})$$

In order to increase the numerical stability, one can choose any of the three combinations. In particular, if the modulus of one of the U_{ij} is very small, it turns out to be more accurate to choose a combination in which this specific U_{ij} does not appear. We use this procedure for studying the running parameters numerically in the “run and diagonalize” approach.

A.2 Useful Formulae and Notations

A.2.1 Weyl, Dirac and Majorana Spinors

The universal covering group of the Lorentz group in four dimensions is $\text{Spin}(3,1) \cong \text{SL}(2, \mathbb{C})$. The left-handed Weyl spinor representation is the fundamental representation $D^{(\frac{1}{2}, 0)}$. $D^{(0, \frac{1}{2})}$ is the non-equivalent complex conjugate representation called the right-handed Weyl spinor representation. As usual, we denote $D^{(\frac{1}{2}, 0)}$ spinor indices by Greek letters (e.g. ψ_α), whereas $D^{(0, \frac{1}{2})}$ spinor indices are denoted by dotted Greek letters. In addition, we denote spinors of the $D^{(0, \frac{1}{2})}$ representation by a bar over the field symbol, e.g. $\bar{\xi}_{\dot{\alpha}}$. Spinor indices can be raised and lowered by

$$\psi^\alpha = \varepsilon^{\alpha\beta} \psi_\beta, \quad \bar{\xi}^{\dot{\alpha}} = \varepsilon^{\dot{\alpha}\dot{\beta}} \bar{\xi}_{\dot{\beta}}, \quad (\text{A.24})$$

where the ε symbol is defined as

$$\varepsilon = (\varepsilon^{\alpha\beta}) = (\varepsilon^{\dot{\alpha}\dot{\beta}}) = \begin{pmatrix} 0 & 1 \\ -1 & 0 \end{pmatrix}, \quad \varepsilon^T = (\varepsilon_{\alpha\beta}) = (\varepsilon_{\dot{\alpha}\dot{\beta}}) = \begin{pmatrix} 0 & -1 \\ 1 & 0 \end{pmatrix}. \quad (\text{A.25})$$

If a Dirac mass term but no Majorana mass term is present, it is useful to work with Dirac spinors. In the Weyl basis, where γ_5 is diagonal, the generators of the Clifford algebra are given by

$$\gamma_5 = \begin{pmatrix} \mathbb{1}_2 & 0 \\ 0 & -\mathbb{1}_2 \end{pmatrix}, \quad \gamma^\mu = \begin{pmatrix} 0 & \sigma^\mu \\ \bar{\sigma}^\mu & 0 \end{pmatrix}, \quad (\text{A.26})$$

with the σ -matrices defined by $\sigma_{\alpha\dot{\alpha}}^0 := \mathbb{1}_2$,

$$\sigma_{\alpha\dot{\alpha}}^1 := \begin{pmatrix} 0 & 1 \\ 1 & 0 \end{pmatrix}, \quad \sigma_{\alpha\dot{\alpha}}^2 := \begin{pmatrix} 0 & -i \\ i & 0 \end{pmatrix}, \quad \sigma_{\alpha\dot{\alpha}}^3 := \begin{pmatrix} 1 & 0 \\ 0 & -1 \end{pmatrix} \quad (\text{A.27})$$

and $\bar{\sigma}^0 = \sigma^0$, $\bar{\sigma}^\mu = -\sigma^\mu$ ($\mu = 1, 2, 3$). Two Weyl spinors ξ and η can be combined to a Dirac spinor

$$\Psi := \begin{pmatrix} \xi_\alpha \\ \bar{\eta}^{\dot{\alpha}} \end{pmatrix}. \quad (\text{A.28})$$

We can recover the degrees of freedom of the Weyl spinors with the projectors $P_{L/R} = (\mathbb{1} \pm \gamma_5)/2$. We use them to define left- and right-handed 4-component spinors,

$$\Psi_L := P_L \Psi \quad \text{and} \quad \Psi_R := P_R \Psi. \quad (\text{A.29})$$

The charge conjugate of a Dirac spinor is defined by

$$\Psi^C = \begin{pmatrix} \xi_\alpha \\ \bar{\eta}^{\dot{\alpha}} \end{pmatrix}^C = \begin{pmatrix} \eta_\alpha \\ \bar{\xi}^{\dot{\alpha}} \end{pmatrix} = C \bar{\Psi}^T \quad \text{with} \quad C := \begin{pmatrix} \varepsilon_{\alpha\beta} & 0 \\ 0 & \varepsilon^{\dot{\alpha}\dot{\beta}} \end{pmatrix} \quad (\text{A.30})$$

in the Weyl basis. The charge conjugation matrix C satisfies $C^\dagger = C^{-1}$, $C^T = -C$ and $C\gamma_\mu^T C^{-1} = -\gamma_\mu$. Spinors which fulfill the condition $\Psi^C = \Psi$ are called Majorana spinors. We have introduced the Dirac adjoint $\bar{\Psi} = \Psi^\dagger \gamma_0$, which is given by

$$\bar{\Psi} = \overline{\begin{pmatrix} \xi_\alpha \\ \bar{\eta}^{\dot{\alpha}} \end{pmatrix}} = \begin{pmatrix} \eta^\alpha \\ \bar{\xi}_{\dot{\alpha}} \end{pmatrix}^T. \quad (\text{A.31})$$

For the Dirac adjoint, the relations $\bar{\psi}_L = \bar{\psi} P_R$ and $\bar{\psi}_R = \bar{\psi} P_L$ hold. In the following, we will furthermore use the abbreviations $\psi_L^C := (\psi_L)^C$ and $\psi_R^C := (\psi_R)^C$.

A.2.2 Clifford Algebra in d Dimensions

For the calculations using dimensional regularization, we have to deal with the Clifford algebra in d dimensions. Since for the 1-loop calculations in this work it is sufficient to use naive dimensional regularization, we will not go into detail about the subtleties concerning γ_5 in d dimensions. The Clifford algebra is defined as

$$\{\gamma^\mu, \gamma^\nu\} = 2\eta^{\mu\nu}, \quad (\text{A.32})$$

where $\eta^{\mu\nu}$ is the Minkowski metric tensor in d dimensions. For products of γ -matrices, we have the rules

$$\gamma_\mu \gamma^\mu = d, \quad (\text{A.33a})$$

$$\gamma_\nu \gamma^\mu \gamma^\nu = (2-d)\gamma^\mu, \quad (\text{A.33b})$$

$$\gamma_\lambda \gamma^\mu \gamma^\nu \gamma^\lambda = 4\eta^{\mu\nu} - (4-d)\gamma^\mu \gamma^\nu, \quad (\text{A.33c})$$

$$\gamma_\rho \gamma^\mu \gamma^\nu \gamma^\lambda \gamma^\rho = -2\gamma^\lambda \gamma^\nu \gamma^\mu + (4-d)\gamma^\mu \gamma^\nu \gamma^\lambda. \quad (\text{A.33d})$$

For evaluating traces of γ matrices which do not contain γ_5 , we use the relations

$$\text{Tr}(\mathbb{1}) = 4, \quad (\text{A.34a})$$

$$\text{Tr}(\text{odd number of } \gamma\text{'s}) = 0, \quad (\text{A.34b})$$

$$\text{Tr}(\gamma^\mu \gamma^\nu) = 4\eta^{\mu\nu}, \quad (\text{A.34c})$$

$$\text{Tr}(\gamma^\mu \gamma^\nu \gamma^\rho \gamma^\sigma) = 4(\eta^{\mu\nu} \eta^{\rho\sigma} - \eta^{\mu\rho} \eta^{\nu\sigma} + \eta^{\mu\sigma} \eta^{\nu\rho}). \quad (\text{A.34d})$$

For dealing with γ_5 , we will use the rule that it anti-commutes with all Dirac matrices as usual, $\{\gamma_5, \gamma^\mu\} = 0$ and satisfies the relations $\text{Tr}(\gamma_5) = 0$ and $\text{Tr}(\gamma_5 \gamma^\mu \gamma^\nu) = 0$.

A.2.3 Passarino Veltman Functions

For calculating the RGEs in mass independent renormalization schemes and dimensional regularization, we are interested in the $\frac{1}{\epsilon}$ -poles of the diagrams under consideration. In order to obtain them, we first calculate the diagrams in a Minkowski space with $d = 4 - \epsilon$ spacetime dimensions. We then express the integrals in terms

of Passarino-Veltman functions [117], which have a known pole structure (see table A.1 on page 114). In this context, the package FeynCalc [60] is very useful, since it allows to perform the reduction to Passarino-Veltman functions by the computer.

Explicit results for the Passarino-Veltman functions can e.g. be found in reference [118]. The integral for the one-point function is given by

$$A_0(m^2) := \frac{\mu^\epsilon}{i\pi^2} \int d^d k \frac{1}{k^2 - m^2}. \quad (\text{A.35})$$

For calculating 2-point functions, we use the integrals

$$B_0(p^2, m_1^2, m_2^2) := \frac{\mu^\epsilon}{i\pi^2} \int d^d k \frac{1}{(k^2 - m_1^2) [(k+p)^2 - m_2^2]}, \quad (\text{A.36a})$$

$$B_\mu(p^2, m_1^2, m_2^2) := \frac{\mu^\epsilon}{i\pi^2} \int d^d k \frac{k_\mu}{(k^2 - m_1^2) [(k+p)^2 - m_2^2]}, \quad (\text{A.36b})$$

$$B_{\mu\nu}(p^2, m_1^2, m_2^2) := \frac{\mu^\epsilon}{i\pi^2} \int d^d k \frac{k_\mu k_\nu}{(k^2 - m_1^2) [(k+p)^2 - m_2^2]}. \quad (\text{A.36c})$$

B_μ and $B_{\mu\nu}$ can be expressed in terms of the external momentum p and further scalar functions,

$$B_\mu = p_\mu B_1, \quad (\text{A.37a})$$

$$B_{\mu\nu} = \eta_{\mu\nu} B_{00} + p_\mu p_\nu B_{11}, \quad (\text{A.37b})$$

where the arguments, which are the same as in equations (A.36), have been omitted. The integrals for the 3-point functions read

$$C_0 := \frac{\mu^\epsilon}{i\pi^2} \int d^d k \frac{1}{(k^2 - m_1^2) [(k+p)^2 - m_2^2] [(k+q)^2 - m_3^2]}, \quad (\text{A.38a})$$

$$C_\mu := \frac{\mu^\epsilon}{i\pi^2} \int d^d k \frac{k_\mu}{(k^2 - m_1^2) [(k+p)^2 - m_2^2] [(k+q)^2 - m_3^2]}, \quad (\text{A.38b})$$

$$C_{\mu\nu} := \frac{\mu^\epsilon}{i\pi^2} \int d^d k \frac{k_\mu k_\nu}{(k^2 - m_1^2) [(k+p)^2 - m_2^2] [(k+q)^2 - m_3^2]}, \quad (\text{A.38c})$$

$$C_{\mu\nu\rho} := \frac{\mu^\epsilon}{i\pi^2} \int d^d k \frac{k_\mu k_\nu k_\rho}{(k^2 - m_1^2) [(k+p)^2 - m_2^2] [(k+q)^2 - m_3^2]}, \quad (\text{A.38d})$$

where the arguments, which again have been omitted, are as in

$$C_0 = C_0(p^2, (p-q)^2, q^2, m_1^2, m_2^2, m_3^2). \quad (\text{A.39})$$

Again, the integrals with a tensor structure can be reduced to expressions containing

coefficient functions with a known pole structure,

$$C_\mu = p_\mu C_1 + q_\mu C_2, \quad (\text{A.40a})$$

$$C_{\mu\nu} = \eta_{\mu\nu} C_{00} + p_\mu p_\nu C_{11} + q_\mu q_\nu C_{22} + (p_\mu q_\nu + q_\mu p_\nu) C_{12}, \quad (\text{A.40b})$$

$$\begin{aligned} C_{\mu\nu\rho} = & (\eta_{\mu\nu} p_\rho + \eta_{\nu\rho} p_\mu + \eta_{\mu\rho} p_\nu) C_{001} + (\eta_{\mu\nu} q_\rho + \eta_{\nu\rho} q_\mu + \eta_{\mu\rho} q_\nu) C_{002} + \\ & + p_\mu p_\nu p_\rho C_{111} + q_\mu q_\nu q_\rho C_{222} + (p_\mu p_\nu q_\rho + p_\mu q_\nu p_\rho + q_\mu p_\nu p_\rho) C_{112} \\ & + (q_\mu q_\nu p_\rho + q_\mu p_\nu q_\rho + p_\mu q_\nu q_\rho) C_{122}. \end{aligned} \quad (\text{A.40c})$$

Note that C_0 and C_μ are finite, while some of the $C_{\mu\nu}$ and $C_{\mu\nu\rho}$ contain poles in ϵ . Finally, we list the integrals for the 4-point functions,

$$D_0 := \int \frac{d^d k (\mu^\epsilon / i\pi^2)}{(k^2 - m_1^2) [(k + p_1)^2 - m_2^2] [(k + p_2)^2 - m_3^2] [(k + p_3)^2 - m_4^2]}, \quad (\text{A.41a})$$

$$D_\mu := \int \frac{d^d k (\mu^\epsilon / i\pi^2) k_\mu}{(k^2 - m_1^2) [(k + p_1)^2 - m_2^2] [(k + p_2)^2 - m_3^2] [(k + p_3)^2 - m_4^2]}, \quad (\text{A.41b})$$

$$D_{\mu\nu} := \int \frac{d^d k (\mu^\epsilon / i\pi^2) k_\mu k_\nu}{(k^2 - m_1^2) [(k + p_1)^2 - m_2^2] [(k + p_2)^2 - m_3^2] [(k + p_3)^2 - m_4^2]}, \quad (\text{A.41c})$$

$$D_{\mu\nu\rho} := \int \frac{d^d k (\mu^\epsilon / i\pi^2) k_\mu k_\nu k_\rho}{(k^2 - m_1^2) [(k + p_1)^2 - m_2^2] [(k + p_2)^2 - m_3^2] [(k + p_3)^2 - m_4^2]}, \quad (\text{A.41d})$$

$$D_{\mu\nu\rho\sigma} := \int \frac{d^d k (\mu^\epsilon / i\pi^2) k_\mu k_\nu k_\rho k_\sigma}{(k^2 - m_1^2) [(k + p_1)^2 - m_2^2] [(k + p_2)^2 - m_3^2] [(k + p_3)^2 - m_4^2]}. \quad (\text{A.41e})$$

They have arguments as in

$$D_0 = D_0(p_1^2, (p_1 - p_2)^2, (p_2 - p_3)^2, p_3^2, p_2^2, (p_1 - p_3)^2, m_1^2, m_2^2, m_3^2, m_4^2). \quad (\text{A.42})$$

Only the four-point function D_{0000} has a pole. $D_{\mu\nu\rho\sigma}$ can be decomposed as

$$D_{\mu\nu\rho\sigma} = (\eta_{\mu\nu}\eta_{\rho\sigma} + \eta_{\mu\rho}\eta_{\nu\sigma} + \eta_{\mu\sigma}\eta_{\nu\rho}) D_{0000} + \text{UV finite}, \quad (\text{A.43})$$

where only the part containing a pole in ϵ has been written explicitly. The poles of all divergent Passarino-Veltman functions are listed in table A.1.

Integral	Divergent part
$A_0(m^2)$	$\frac{2}{\epsilon}m^2$
$B_0(p^2, m_1^2, m_2^2)$	$\frac{2}{\epsilon}$
$B_1(p^2, m_1^2, m_2^2)$	$-\frac{1}{\epsilon}$
$B_{00}(p^2, m_1^2, m_2^2)$	$-\frac{1}{6\epsilon}(p^2 - 3m_1^2 - 3m_2^2)$
$B_{11}(p^2, m_1^2, m_2^2)$	$\frac{2}{3\epsilon}$
C_{00}	$\frac{1}{2\epsilon}$
$C_{00i} (i \in \{1, 2\})$	$-\frac{1}{6\epsilon}$
D_{0000}	$\frac{1}{12\epsilon}$

Table A.1: The divergent parts of the Passarino-Veltman functions [118].

A.3 Summary of Feynman Rules

We use the notation defined in section 2.4, with the superscript (n) denoting the effective theories which arise when the SM, 2HDM or the MSSM are extended by heavy singlets. This allows to present the Feynman rules in the most general form used for the calculations in this work. The Feynman rules for the SM, 2HDM or MSSM can be recovered by setting the neutrino Yukawa coupling to zero. For all calculations, we choose a basis where the mass matrix of the heavy singlets is diagonal with eigenvalues denoted by M_i . We will perform our calculations in the $SU(2)_L$ -unbroken phase, since the counterterms calculated there also renormalize the theory in the spontaneously broken phase. In the MSSM, we will consider energy scales above the SUSY breaking scale, where we can omit the soft breaking terms.

The Feynman rules of the theories under consideration involve Majorana fermions. We treat them, following the prescription given in [73]. For the calculation of a diagram which contains Majorana fermions, we introduce a fermion flow for the leptons, indicated by a gray arrow. It coincides with the lepton number flow, if lepton number is conserved. However, if this is not the case as in the models we are considering, the fermion flow may be parallel or antiparallel to the lepton number flow. We will therefore give the rules for both directions of the fermion flow. One has to read Feynman diagrams reverse to the direction of the fermion flow and write down the corresponding analytic expressions from left to right. We further present the Feynman rules in $d = 4 - \epsilon$ dimensions, so that they can directly be used for the calculations with dimensional regularization.

A.3.1 Feynman Rules in the Extended SM

The most relevant parts of the Lagrangian of the extended SM have been specified in sections 1.1.1 and 2.4. The complete Lagrangian is given by

$$\mathcal{L}'_{\text{SM}} = \mathcal{L}_{\text{kin(F)}} + \mathcal{L}_{\text{Mass}} + \mathcal{L}_{\text{Higgs}} + \mathcal{L}_{\text{Yuk}} + \mathcal{L}_{\text{kin(G)}} + \mathcal{L}_{\text{FP}} + \mathcal{L}_{\text{GF}} + \mathcal{L}_{\kappa} \quad (\text{A.44})$$

where \mathcal{L}_{kin} contains the kinetic terms for the fermions and the gauge bosons, \mathcal{L}_{GF} is the gauge fixing part and \mathcal{L}_{FP} contains the Faddeev-Popov ghosts. $\mathcal{L}_{\text{Mass}}$ contains the direct Majorana mass term of the singlet fermions. In this section, we will use 4-component Majorana spinors $N^i := N_{\text{R}}^i + (N_{\text{R}}^i)^{\text{C}}$, where the mass term has the form

$$\mathcal{L}_{\text{Mass}} = -\frac{1}{2} \overline{N}^j M_{ji}^{(n)} N^i . \quad (\text{A.45})$$

Rules for the Propagators

$$\begin{array}{c} \text{---} \blacktriangleright \text{---} \\ \hline N^i \qquad N^j \end{array} : iS_N(p) = \frac{i(\not{p} + M_i)}{p^2 - M_i^2 + i\varepsilon} \delta_{ji} \quad (\text{A.46a})$$

$$\begin{array}{c} \text{---} \blacktriangleright \text{---} \\ \hline \ell_{La}^f \qquad \ell_{Lb}^g \end{array} : iS_{\ell_L}(p) = \frac{i\not{p}}{p^2 + i\varepsilon} \delta_{gf} \delta_{ba} \quad (\text{A.46b})$$

$$\begin{array}{c} \text{---} \blacktriangleright \text{---} \\ \hline e_R^f \qquad e_R^g \end{array} : iS_{e_R}(p) = \frac{i\not{p}}{p^2 + i\varepsilon} \delta_{gf} \quad (\text{A.46c})$$

$$\begin{array}{c} \text{---} \blacktriangleleft \text{---} \\ \hline \ell_{La}^f \qquad \ell_{Lb}^g \end{array} : iS_{\ell_L}(-p) = \frac{-i\not{p}}{p^2 + i\varepsilon} \delta_{gf} \delta_{ba} \quad (\text{A.46d})$$

$$\begin{array}{c} \text{---} \blacktriangleleft \text{---} \\ \hline e_R^f \qquad e_R^g \end{array} : iS_{e_R}(-p) = \frac{-i\not{p}}{p^2 + i\varepsilon} \delta_{gf} \quad (\text{A.46e})$$

$$\begin{array}{c} \text{---} \blacktriangleright \text{---} \\ \hline q_{La}^f \qquad q_{Lb}^g \end{array} : iS_{q_L}(p) = \frac{i\not{p}}{p^2 + i\varepsilon} \delta_{gf} \delta_{ba} \quad (\text{A.46f})$$

$$\begin{array}{c} \text{---} \blacktriangleright \text{---} \\ \hline u_R^f \qquad u_R^g \end{array} : iS_{u_R}(p) = \frac{i\not{p}}{p^2 + i\varepsilon} \delta_{gf} \quad (\text{A.46g})$$

$$\begin{array}{c} \text{---} \blacktriangleright \text{---} \\ \hline d_R^f \qquad d_R^g \end{array} : iS_{d_R}(p) = \frac{i\not{p}}{p^2 + i\varepsilon} \delta_{gf} \quad (\text{A.46h})$$

$$\begin{array}{c} \text{---} \blacktriangleright \text{---} \\ \hline \phi_a \qquad \phi_b \end{array} : iS_\phi(p) = \frac{i}{p^2 - m^2 + i\varepsilon} \delta_{ba} \quad (\text{A.46i})$$

$$\begin{array}{c} \text{~~~~~} \\ \hline B^\mu \qquad B^\nu \end{array} : iD_B^{\mu\nu}(p) = i \frac{-\eta^{\mu\nu} + (1 - \xi_B) \frac{p^\mu p^\nu}{p^2}}{p^2 + i\varepsilon} \quad (\text{A.46j})$$

$$\begin{array}{c} \text{~~~~~} \\ \hline W^{A\mu} \qquad W^{B\nu} \end{array} : iD_{W^A}^{\mu\nu}(p) = i \frac{-\eta^{\mu\nu} + (1 - \xi_W) \frac{p^\mu p^\nu}{p^2}}{p^2 + i\varepsilon} \delta_{AB} \quad (\text{A.46k})$$

The momentum p in the above diagrams flows from left to right. The $i\varepsilon$ -term in the denominators, which defines the integration contour for the Fourier transformation of the propagators to position space, is not written explicitly in the calculations of the main part.

Rules for the Yukawa Interactions

$$\begin{array}{c}
 \begin{array}{c} N^j \\ \swarrow \\ \bullet \\ \nearrow \\ \ell_{Lb}^f \end{array} \begin{array}{c} \phi_a \\ \dashrightarrow \end{array} : -i\mu^{\frac{\epsilon}{2}} (Y_\nu^{(n)})_{gf} (\varepsilon^T)_{ab} P_L \\
 \end{array}
 \qquad
 \begin{array}{c}
 \begin{array}{c} N^j \\ \swarrow \\ \bullet \\ \nearrow \\ \ell_{Lb}^f \end{array} \begin{array}{c} \phi_a \\ \dashrightarrow \end{array} : -i\mu^{\frac{\epsilon}{2}} (Y_\nu^{(n)T})_{fg} \varepsilon_{ba} P_L \\
 \end{array}
 \tag{A.47a}$$

$$\begin{array}{c}
 \begin{array}{c} \ell_{Lb}^f \\ \swarrow \\ \bullet \\ \nearrow \\ N^j \end{array} \begin{array}{c} \phi_a \\ \dashrightarrow \end{array} : -i\mu^{\frac{\epsilon}{2}} (Y_\nu^\dagger)_{fg} \varepsilon_{ba} P_R \\
 \end{array}
 \qquad
 \begin{array}{c}
 \begin{array}{c} \ell_{Lb}^f \\ \swarrow \\ \bullet \\ \nearrow \\ N^j \end{array} \begin{array}{c} \phi_a \\ \dashrightarrow \end{array} : -i\mu^{\frac{\epsilon}{2}} (Y_\nu^*)_{gf} (\varepsilon^T)_{ab} P_R \\
 \end{array}
 \tag{A.47b}$$

$$\begin{array}{c}
 \begin{array}{c} e_R^g \\ \swarrow \\ \bullet \\ \nearrow \\ \ell_{Lb}^f \end{array} \begin{array}{c} \phi_a \\ \dashrightarrow \end{array} : -i\mu^{\frac{\epsilon}{2}} (Y_e)_{gf} \delta_{ab} P_L \\
 \end{array}
 \qquad
 \begin{array}{c}
 \begin{array}{c} e_R^g \\ \swarrow \\ \bullet \\ \nearrow \\ \ell_{Lb}^f \end{array} \begin{array}{c} \phi_a \\ \dashrightarrow \end{array} : -i\mu^{\frac{\epsilon}{2}} (Y_e^T)_{fg} \delta_{ab} P_L \\
 \end{array}
 \tag{A.47c}$$

$$\begin{array}{c}
 \begin{array}{c} \ell_{Lb}^f \\ \swarrow \\ \bullet \\ \nearrow \\ e_R^g \end{array} \begin{array}{c} \phi_a \\ \dashrightarrow \end{array} : -i\mu^{\frac{\epsilon}{2}} (Y_e^\dagger)_{fg} \delta_{ab} P_R \\
 \end{array}
 \qquad
 \begin{array}{c}
 \begin{array}{c} \ell_{Lb}^f \\ \swarrow \\ \bullet \\ \nearrow \\ e_R^g \end{array} \begin{array}{c} \phi_a \\ \dashrightarrow \end{array} : -i\mu^{\frac{\epsilon}{2}} (Y_e^*)_{gf} \delta_{ab} P_R \\
 \end{array}
 \tag{A.47d}$$

$$\begin{array}{c}
 \begin{array}{c} u_R^g \\ \swarrow \\ \bullet \\ \nearrow \\ q_{Lb}^f \end{array} \begin{array}{c} \phi_a \\ \dashrightarrow \end{array} : -i\mu^{\frac{\epsilon}{2}} (Y_u)_{gf} (\varepsilon^T)_{ab} P_L \\
 \end{array}
 \qquad
 \begin{array}{c}
 \begin{array}{c} q_{Lb}^f \\ \swarrow \\ \bullet \\ \nearrow \\ u_R^g \end{array} \begin{array}{c} \phi_a \\ \dashrightarrow \end{array} : -i\mu^{\frac{\epsilon}{2}} (Y_u^\dagger)_{fg} \varepsilon_{ba} P_R \\
 \end{array}
 \tag{A.47e}$$

$$\begin{array}{c}
 \begin{array}{c} d_R^g \\ \swarrow \\ \bullet \\ \nearrow \\ q_{Lb}^f \end{array} \begin{array}{c} \phi_a \\ \dashrightarrow \end{array} : -i\mu^{\frac{\epsilon}{2}} (Y_d)_{gf} \delta_{ab} P_L \\
 \end{array}
 \qquad
 \begin{array}{c}
 \begin{array}{c} q_{Lb}^f \\ \swarrow \\ \bullet \\ \nearrow \\ d_R^g \end{array} \begin{array}{c} \phi_a \\ \dashrightarrow \end{array} : -i\mu^{\frac{\epsilon}{2}} (Y_d^\dagger)_{fg} \delta_{ab} P_R \\
 \end{array}
 \tag{A.47f}$$

Some Rules for Gauge Boson and Higgs Interactions

$$\begin{array}{cc}
 \begin{array}{c} \ell_{Lb}^g \\ \nearrow \\ \bullet \\ \nwarrow \\ \ell_{La}^f \end{array} B_\mu & : \frac{i}{2} \mu^{\frac{\epsilon}{2}} g_1 \delta_{gf} \delta_{ba} \gamma_\mu P_L & \begin{array}{c} \ell_{Lb}^g \\ \nearrow \\ \bullet \\ \nwarrow \\ \ell_{La}^f \end{array} B_\mu & : -\frac{i}{2} \mu^{\frac{\epsilon}{2}} g_1 \delta_{fg} \delta_{ab} \gamma_\mu P_R \\
 \end{array} \tag{A.48a}$$

$$\begin{array}{cc}
 \begin{array}{c} \ell_{Lb}^g \\ \nearrow \\ \bullet \\ \nwarrow \\ \ell_{La}^f \end{array} W_\mu^i & : -\frac{i}{2} \mu^{\frac{\epsilon}{2}} g_2 \delta_{gf} \tau_{ba}^i \gamma_\mu P_L & \begin{array}{c} \ell_{Lb}^g \\ \nearrow \\ \bullet \\ \nwarrow \\ \ell_{La}^f \end{array} W_\mu^i & : \frac{i}{2} \mu^{\frac{\epsilon}{2}} g_2 \delta_{fg} (\tau^{iT})_{ab} \gamma_\mu P_R \\
 \end{array} \tag{A.48b}$$

$$\begin{array}{cc}
 \begin{array}{c} e_R^g \\ \nearrow \\ \bullet \\ \nwarrow \\ e_R^f \end{array} B_\mu & : i \mu^{\frac{\epsilon}{2}} g_1 \delta_{gf} \gamma_\mu P_R & \begin{array}{c} e_R^g \\ \nearrow \\ \bullet \\ \nwarrow \\ e_R^f \end{array} B_\mu & : -i \mu^{\frac{\epsilon}{2}} g_1 \delta_{fg} \gamma_\mu P_L \\
 \end{array} \tag{A.48c}$$

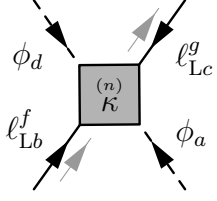
$$\begin{array}{cc}
 \begin{array}{c} \phi_b \\ \nearrow \\ \bullet \\ \nwarrow \\ \phi_a \end{array} B_\mu & : -\frac{i}{2} \mu^{\frac{\epsilon}{2}} g_1 (p_\mu + q_\mu) \delta_{ba} & \begin{array}{c} \phi_b \\ \nearrow \\ \bullet \\ \nwarrow \\ \phi_a \end{array} W_\mu^i & : -\frac{i}{2} \mu^{\frac{\epsilon}{2}} g_2 (p_\mu + q_\mu) \tau_{ba}^i \\
 \end{array} \tag{A.48d}$$

$$\begin{array}{cc}
 \begin{array}{c} \phi_b \\ \nearrow \\ \bullet \\ \nwarrow \\ \phi_a \end{array} \begin{array}{c} B_\mu \\ B_\nu \end{array} & : \frac{i}{2} \mu^\epsilon g_1^2 \eta_{\mu\nu} \delta_{ba} & \begin{array}{c} \phi_b \\ \nearrow \\ \bullet \\ \nwarrow \\ \phi_a \end{array} \begin{array}{c} W_\mu^i \\ W_\nu^j \end{array} & : \frac{i}{2} \mu^\epsilon g_2^2 \eta_{\mu\nu} \delta_{ij} \delta_{ba} \\
 \end{array} \tag{A.48e}$$

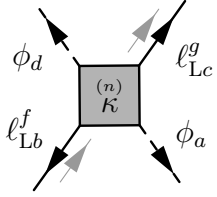
$$\begin{array}{cc}
 \begin{array}{c} \phi_b \\ \nearrow \\ \bullet \\ \nwarrow \\ \phi_a \end{array} \begin{array}{c} B_\mu \\ W_\nu^i \end{array} & : \frac{i}{2} \mu^\epsilon g_1 g_2 \eta_{\mu\nu} \tau_{ba}^i & \begin{array}{c} \phi_a \\ \nearrow \\ \bullet \\ \nwarrow \\ \phi_b \end{array} \begin{array}{c} \phi_c \\ \nearrow \\ \bullet \\ \nwarrow \\ \phi_d \end{array} & : -i \mu^\epsilon \frac{\lambda}{2} (\delta_{ca} \delta_{db} + \delta_{cb} \delta_{da}) \\
 \end{array} \tag{A.48f}$$

In the derivation of the rules with derivatives we have used the rule that $\partial_\mu \phi$ in the Lagrangian yields a factor of $-ip_\mu$ in the Feynman rule.

Rules for the Effective Dimension 5 Neutrino Mass Operator



$$: i\mu^\epsilon \kappa_{gf}^{(n)} \frac{1}{2} (\varepsilon_{cd}\varepsilon_{ba} + \varepsilon_{ca}\varepsilon_{bd}) P_L \quad (\text{A.49a})$$



$$: i\mu^\epsilon (\kappa^{(n)\dagger})_{gf} \frac{1}{2} (\varepsilon_{cd}\varepsilon_{ba} + \varepsilon_{ca}\varepsilon_{bd}) P_R . \quad (\text{A.49b})$$

Definition of the Counterterms

We first give the definition of the counterterms in the SM, which can easily be generalized to the 2HDMs or to the MSSM component fields. First, the wavefunction renormalization constants are defined by the following relations of the bare and renormalized fields

$$\psi_B^f = \left(Z_\psi^{\frac{1}{2}}\right)_{fg} \psi^g , \quad (\text{A.50a})$$

$$\phi_B = Z_\phi^{\frac{1}{2}} \phi , \quad (\text{A.50b})$$

$$V_B = Z_V^{\frac{1}{2}} V \quad (\text{A.50c})$$

for the fermions ψ^f , the Higgs field ϕ and gauge bosons V . For the Majorana singlets, the wavefunction renormalization constant has a left-handed and a right-handed part,

$$(\mathcal{Z}_N)_{ij} := \mathbb{1}_{ij} + (\delta Z_{N(L)})_{ij} P_L + (\delta Z_{N(R)})_{ij} P_R , \quad (\text{A.51})$$

which are related by $Z_{N(L)} = Z_{N(R)}^*$. To verify this, note that

$$N_B^C = C \overline{N_B}^T = C \overline{Z_N^{1/2}}^T N = C (\gamma^0)^T \left(N^\dagger Z_N^{\dagger \frac{1}{2}} \right)^T = C \gamma^0 Z_N^{*\frac{1}{2}} (N^\dagger)^T . \quad (\text{A.52})$$

From $N_B^C = N_B$ we obtain $C \gamma^0 Z_N^{*\frac{1}{2}} = Z_N^{\frac{1}{2}} C \gamma^0$. Using $C \gamma^0 P_L = P_R C \gamma^0$ and the definition of equation (A.51), we obtain the desired relation. Note that we always choose the wavefunction renormalization constants to be Hermitian, which is possible because only the combination $(Z_\psi^{1/2})^\dagger Z_\psi^{1/2}$ can be determined from the two-point functions.

The counterterms for the vertices which are relevant for our calculations are defined by

$$\begin{aligned} \mathcal{C}_{\text{kin(F)}} &= \overline{\ell}_L^g (i\gamma^\mu D_\mu) (\delta Z_{\ell_L}^{(n)})_{gf} \ell_L^f + \overline{e}_R^g (i\gamma^\mu D_\mu) (\delta Z_{e_R}^{(n)})_{gf} e_R^f \\ &\quad + \overline{q}_L^g (i\gamma^\mu D_\mu) (\delta Z_{q_L}^{(n)})_{gf} q_L^f + \overline{u}_R^g (i\gamma^\mu D_\mu) (\delta Z_{u_R}^{(n)})_{gf} u_R^f \\ &\quad + \overline{d}_R^g (i\gamma^\mu D_\mu) (\delta Z_{d_R}^{(n)})_{gf} d_R^f \\ &\quad + \frac{1}{2} \overline{N}^j (i\gamma^\mu \partial_\mu) \left[(\delta Z_N^*)_{ji} P_L + (\delta Z_N)_{ji} P_R \right] N^i, \end{aligned} \quad (\text{A.53a})$$

$$\mathcal{C}_{\text{Mass}} = -\frac{1}{2} \overline{N}^j (M + \delta M)_{ji} N^i, \quad (\text{A.53b})$$

$$\begin{aligned} \mathcal{C}_{\text{Higgs}} &= \delta Z_\phi^{(n)} (D_\mu \phi)^\dagger (D^\mu \phi) - \delta \overline{m}^2 \phi^\dagger \phi - \frac{1}{4} \delta Z_\lambda^{(n)} \lambda (\phi^\dagger \phi)^2 \\ &\quad + \left[\frac{i}{2} (D_\mu \phi)^\dagger \left(\delta Z_{g_1}^{(n)} g_1 B^\mu + \delta Z_{g_2}^{(n)} g_2 \tau^i W^{i\mu} \right) \phi + \text{h.c.} \right], \end{aligned} \quad (\text{A.53c})$$

$$\begin{aligned} \mathcal{C}_{\text{Yuk}} &= -(Y_\nu \delta Z_{Y_\nu})_{jf} \overline{N}^j \tilde{\phi}^\dagger \ell_L^f - (Y_e \delta Z_{Y_e})_{gf} \overline{e}_R^g \phi^\dagger \ell_L^f \\ &\quad - (Y_u \delta Z_{Y_u})_{gf} \overline{u}_R^g \tilde{\phi}^\dagger q_L^f - (Y_d \delta Z_{Y_d})_{gf} \overline{d}_R^g \phi^\dagger q_L^f + \text{h.c.}, \end{aligned} \quad (\text{A.53d})$$

$$\mathcal{C}_\kappa = \frac{1}{4} \delta \kappa_{gf}^{(n)} \overline{\ell}_{Lc}^g \varepsilon_{cd} \phi_d \ell_{Lb}^f \varepsilon_{ba} \phi_a + \text{h.c.} \quad (\text{A.53e})$$

From these definitions, we obtain the following relations for the renormalized and the bare coupling constants and masses

$$Z_\phi^{(n)} m_B^2 = m^2 + \delta \overline{m}^2, \quad (\text{A.54a})$$

$$(Z_N^{T\frac{1}{2}} M_B Z_N^{\frac{1}{2}})^{(n)}_{ij} = (M + \delta M)_{ij}, \quad (\text{A.54b})$$

$$Z_\phi^{(n)} \lambda_B = \mu^\epsilon Z_\lambda \lambda, \quad (\text{A.54c})$$

$$(Z_{N(R)}^{\frac{1}{2}} Y_{\nu B} Z_\phi^{\frac{1}{2}} Z_{\ell_L}^{\frac{1}{2}})^{(n)}_{ig} = \mu^{\frac{\epsilon}{2}} (Y_\nu Z_{Y_\nu})_{ig}, \quad (\text{A.54d})$$

$$(Z_{eR}^{\frac{1}{2}} Y_{eB} Z_\phi^{\frac{1}{2}} Z_{\ell_L}^{\frac{1}{2}})^{(n)}_{fg} = \mu^{\frac{\epsilon}{2}} (Y_e Z_{Y_e})_{fg}, \quad (\text{A.54e})$$

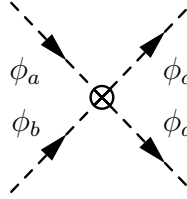
$$(Z_{uR}^{\frac{1}{2}} Y_{uB} Z_\phi^{\frac{1}{2}} Z_{q_L}^{\frac{1}{2}})^{(n)}_{fg} = \mu^{\frac{\epsilon}{2}} (Y_u Z_{Y_u})_{fg}, \quad (\text{A.54f})$$

$$(Z_{dR}^{\frac{1}{2}} Y_{dB} Z_\phi^{\frac{1}{2}} Z_{q_L}^{\frac{1}{2}})^{(n)}_{fg} = \mu^{\frac{\epsilon}{2}} (Y_d Z_{Y_d})_{fg}, \quad (\text{A.54g})$$

$$Z_{\ell_L}^{T\frac{1}{2}} Z_\phi^{\frac{1}{2}} \kappa_B Z_\phi^{\frac{1}{2}} Z_{\ell_L}^{\frac{1}{2}} = \mu^\epsilon (\kappa + \delta \kappa). \quad (\text{A.54h})$$

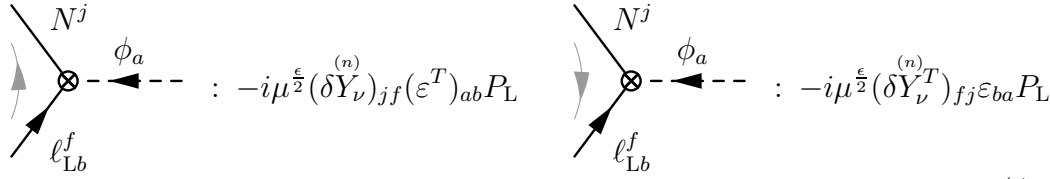
We have omitted the counterterms for the gauge sector, since we will not consider its renormalization in detail.

The counterterm for the Higgs self-interaction yields the rule

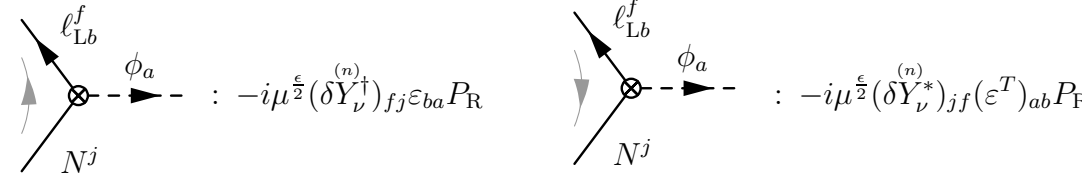


$$: -i\mu^\epsilon \delta\lambda \frac{1}{2}(\delta_{ca}\delta_{db} + \delta_{cb}\delta_{da}) . \quad (\text{A.57})$$

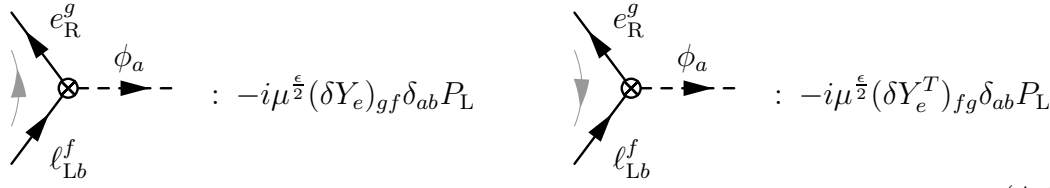
Finally, we give the Feynman rules for the counterterms corresponding to the Yukawa interactions, which involve the neutrino and the charged lepton Yukawa matrices.



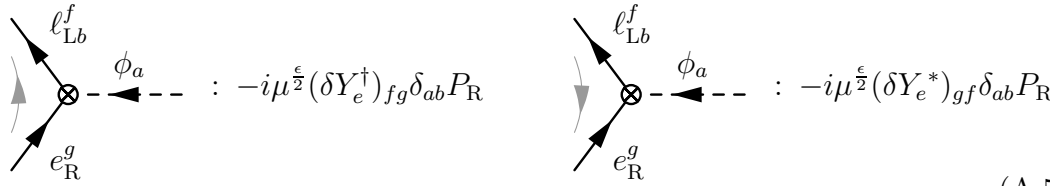
$$: -i\mu^{\frac{\epsilon}{2}}(\delta Y_\nu^{(n)})_{jf}(\varepsilon^T)_{ab}P_L \quad : -i\mu^{\frac{\epsilon}{2}}(\delta Y_\nu^{(n)T})_{ff}\varepsilon_{ba}P_L \quad (\text{A.58a})$$



$$: -i\mu^{\frac{\epsilon}{2}}(\delta Y_\nu^\dagger)_{ff}\varepsilon_{ba}P_R \quad : -i\mu^{\frac{\epsilon}{2}}(\delta Y_\nu^*)_{jf}(\varepsilon^T)_{ab}P_R \quad (\text{A.58b})$$



$$: -i\mu^{\frac{\epsilon}{2}}(\delta Y_e)_{fg}\delta_{ab}P_L \quad : -i\mu^{\frac{\epsilon}{2}}(\delta Y_e^T)_{fg}\delta_{ab}P_L \quad (\text{A.58c})$$



$$: -i\mu^{\frac{\epsilon}{2}}(\delta Y_e^\dagger)_{fg}\delta_{ab}P_R \quad : -i\mu^{\frac{\epsilon}{2}}(\delta Y_e^*)_{gf}\delta_{ab}P_R \quad (\text{A.58d})$$

A.3.2 Feynman Rules in Extended 2HDMs

We now summarize the Feynman rules for the Yukawa couplings of the charged leptons and the neutrinos as well as for the Higgs self-interactions in the classes of 2HDMs, defined in section 2.2.2. To specify the different models, we use the notation of tables 2.1 and 2.2 (page 36).

Yukawa Interactions

The rules for the Yukawa interactions depend on the specific 2HDM under consideration, which differ in the way the Higgses are coupled to the fermions. In our convention, the fields e_R^g always couple to the Higgs $\phi^{(1)}$.

$$\begin{aligned}
& \text{Diagram 1: } e_R^g \text{ and } \ell_{Lb}^f \text{ meet at a vertex, with } \phi_a^{(1)} \text{ line. Rule: } -i\mu^{\frac{\epsilon}{2}}(Y_e)_{gf}\delta_{ab}P_L \quad (\text{A.59a}) \\
& \text{Diagram 2: } e_R^g \text{ and } \ell_{Lb}^f \text{ meet at a vertex, with } \phi_a^{(1)} \text{ line. Rule: } -i\mu^{\frac{\epsilon}{2}}(Y_e^T)_{fg}\delta_{ab}P_L \quad (\text{A.59a}) \\
& \text{Diagram 3: } e_R^g \text{ and } \ell_{Lb}^f \text{ meet at a vertex, with } \phi_a^{(1)} \text{ line. Rule: } -i\mu^{\frac{\epsilon}{2}}(Y_e^\dagger)_{fg}\delta_{ab}P_R \quad (\text{A.59b}) \\
& \text{Diagram 4: } e_R^g \text{ and } \ell_{Lb}^f \text{ meet at a vertex, with } \phi_a^{(1)} \text{ line. Rule: } -i\mu^{\frac{\epsilon}{2}}(Y_e^*)_{gf}\delta_{ab}P_R \quad (\text{A.59b})
\end{aligned}$$

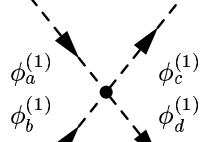
In the 2HDMs we consider in this work, the singlets N^i couple either to $\phi^{(1)}$ or $\phi^{(2)}$. In the Feynman rules, we use the variable $z_\nu^{(i)}$, defined analogous to $z_u^{(i)}$ and $z_d^{(i)}$ of table 2.2 for a specific model.

$$\begin{aligned}
& \text{Diagram 1: } N^j \text{ and } \ell_{Lb}^f \text{ meet at a vertex, with } \phi_a^{(i)} \text{ line. Rule: } -iz_\nu^{(i)}\mu^{\frac{\epsilon}{2}}(Y_\nu^{(n)})_{jf}(\varepsilon^T)_{ab}P_L \quad (\text{A.60a}) \\
& \text{Diagram 2: } N^j \text{ and } \ell_{Lb}^f \text{ meet at a vertex, with } \phi_a^{(i)} \text{ line. Rule: } -iz_\nu^{(i)}\mu^{\frac{\epsilon}{2}}(Y_\nu^{(n)T})_{jf}\varepsilon_{ba}P_L \quad (\text{A.60a})
\end{aligned}$$

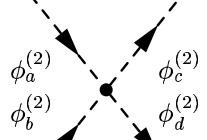
$$\begin{aligned}
& \text{Diagram 3: } N^j \text{ and } \ell_{Lb}^f \text{ meet at a vertex, with } \phi_a^{(i)} \text{ line. Rule: } -iz_\nu^{(i)}\mu^{\frac{\epsilon}{2}}(Y_\nu^{(n)\dagger})_{jf}\varepsilon_{ba}P_R \quad (\text{A.60b}) \\
& \text{Diagram 4: } N^j \text{ and } \ell_{Lb}^f \text{ meet at a vertex, with } \phi_a^{(i)} \text{ line. Rule: } -iz_\nu^{(i)}\mu^{\frac{\epsilon}{2}}(Y_\nu^{(n)*})_{jf}(\varepsilon^T)_{ab}P_R \quad (\text{A.60b})
\end{aligned}$$

The rules for the quarks can be given in a similar notation, using $z_u^{(i)}$ and $z_d^{(i)}$ to specify the couplings to the Higgs doublets.

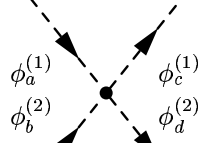
Feynman Rules for the Higgs Sector



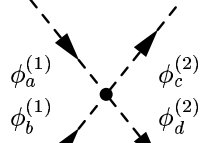
$$: -i\mu^\epsilon \lambda_1 \frac{1}{2} (\delta_{ac}\delta_{bd} + \delta_{ad}\delta_{bc}) \quad (\text{A.61a})$$



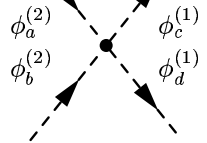
$$: -i\mu^\epsilon \lambda_2 \frac{1}{2} (\delta_{ac}\delta_{bd} + \delta_{ad}\delta_{bc}) \quad (\text{A.61b})$$



$$: -i\mu^\epsilon (\lambda_3 \delta_{ac}\delta_{bd} + \lambda_4 \delta_{ad}\delta_{bc}) \quad (\text{A.61c})$$



$$: -i\mu^\epsilon \lambda_5^* \frac{1}{2} (\delta_{ac}\delta_{bd} + \delta_{ad}\delta_{bc}) \quad (\text{A.61d})$$



$$: -i\mu^\epsilon \lambda_5 \frac{1}{2} (\delta_{ac}\delta_{bd} + \delta_{ad}\delta_{bc}) \quad (\text{A.61e})$$

A.3.3 Feynman Rules in the MSSM Extended by Heavy Singlets

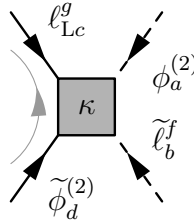
For the computation of the Feynman rules, we have to express the interaction Lagrangian in component fields. This has partly been done in section 2.3. We now consider the component field form of the interactions of the superpotential. They can be evaluated systematically using equation (2.52).

Rules from the Neutrino Mass Operator

The vertices in the component field formalism, which stem from the neutrino mass operator in superfield-notation, are derived from

$$-\frac{1}{2} \frac{\partial^2 \mathcal{W}_\kappa}{\partial \Phi_i \partial \Phi_j} \Big|_{\theta=0} \psi_i \psi_j, \quad \Phi_i \in \{\mathbb{h}_d^{(2)}, \mathbb{l}_c^g\}. \quad (\text{A.62})$$

In particular, (A.62) contains the dimension 5 neutrino mass operator present in the SM, which is given in equation (1.15), $\mathcal{L}_\kappa = \frac{1}{4} \kappa_{gf} \overline{\ell}_{Lc}^{Cg} \varepsilon^{cd} \phi_d^{(2)} \ell_{Lb}^f \varepsilon^{ba} \phi_a^{(2)} + \text{h.c.}$. Note that compared to the 2HDMs, in the MSSM there is only one such neutrino mass operator in the superpotential. In addition, we obtain further vertices from equation (2.47). Among them, there is the following vertex, which involves the superpartners $\tilde{\phi}_d^{(2)}$ and $\tilde{\ell}_b^f$ of the Higgs and the lepton doublets:



$$: i \mu^\epsilon \kappa_{gf} \frac{1}{2} (\varepsilon_{cd} \varepsilon_{ba} + \varepsilon_{ca} \varepsilon_{bd}) P_L. \quad (\text{A.63})$$

It is necessary for calculating the gaugino contributions to the vertex corrections. We will now consider the other interaction terms of the superpotential more systematically.

Systematic Computation of the Interaction Terms

To obtain the Feynman rules, we calculate the first derivatives w.r.t. the superfields:

$$\frac{\partial \mathcal{W}_R}{\partial \mathbb{v}^{Cj}} \Big|_{\theta=0} = M_{ji}^{(n)} \tilde{N}^i + (Y_\nu)_{jf} \phi_a^{(2)} (\varepsilon^T)^{ab} \tilde{\ell}_b^f, \quad (\text{A.64a})$$

$$\frac{\partial \mathcal{W}_R}{\partial \mathbb{e}^{Cg}} \Big|_{\theta=0} = (Y_e)_{gf} \phi_a^{(1)} \varepsilon^{ab} \tilde{\ell}_b^f, \quad (\text{A.64b})$$

$$\frac{\partial \mathcal{W}_R}{\partial \mathbb{l}_b^f} \Big|_{\theta=0} = (Y_e)_{gf} \tilde{e}^{Cg} \phi_a^{(1)} \varepsilon^{ab} + (Y_\nu)_{jf} \tilde{N}^{Cj} \phi_a^{(2)} (\varepsilon^T)^{ab}, \quad (\text{A.64c})$$

$$\left. \frac{\partial \mathcal{W}_R}{\partial h_a^{(1)}} \right|_{\theta=0} = m \varepsilon^{ab} \phi_b^{(2)} + (Y_e)_{gf} \tilde{e}^{Cg} \varepsilon^{ab} \tilde{\ell}_b^f + (Y_d)_{gf} \tilde{d}^{Cg} \varepsilon^{ab} \tilde{\ell}_b^f, \quad (\text{A.64d})$$

$$\left. \frac{\partial \mathcal{W}_R}{\partial h_a^{(2)}} \right|_{\theta=0} = m \phi_b^{(1)} \varepsilon^{ba} + (Y_\nu)_{jf} \tilde{N}^{Cj} (\varepsilon^T)^{ab} \tilde{\ell}_b^f + (Y_u)_{gf} \tilde{u}^{Cg} (\varepsilon^T)^{ab} \tilde{\ell}_b^f, \quad (\text{A.64e})$$

$$\left. \frac{\partial \mathcal{W}_R}{\partial u^{Cg}} \right|_{\theta=0} = (Y_u)_{gf} \phi_a^{(2)} (\varepsilon^T)^{ab} \tilde{q}_b^f, \quad (\text{A.64f})$$

$$\left. \frac{\partial \mathcal{W}_R}{\partial d^{Cg}} \right|_{\theta=0} = (Y_d)_{gf} \phi_a^{(1)} \varepsilon^{ab} \tilde{q}_b^f, \quad (\text{A.64g})$$

$$\left. \frac{\partial \mathcal{W}_R}{\partial q_b^f} \right|_{\theta=0} = (Y_d)_{gf} \tilde{d}^{Cg} \phi_a^{(1)} \varepsilon^{ab} + (Y_u)_{gf} \tilde{u}^{Cg} \phi_a^{(2)} (\varepsilon^T)^{ab}. \quad (\text{A.64h})$$

The second order derivatives of the superpotential w.r.t. the superfields can be read off table A.2.

	ν^{Cj}	e^{Cg}	\mathbb{J}_b^f	$h_a^{(1)}$	$h_a^{(2)}$
ν^{Cj}	$M_{ji}^{(n)}$	0	$(Y_\nu)_{jf} \phi_a^{(2)} (\varepsilon^T)^{ab}$	0	$(Y_\nu)_{jf} (\varepsilon^T)^{ab} \tilde{\ell}_b^f$
e^{Cg}	—	—	$(Y_e)_{gf} \phi_a^{(1)} \varepsilon^{ab}$	$(Y_e)_{gf} \varepsilon^{ab} \tilde{\ell}_b^f$	0
\mathbb{J}_b^f			—	$(Y_e)_{gf} \tilde{e}^{Cg} \varepsilon^{ab}$	$(Y_\nu)_{jf} \tilde{N}^{Cj} (\varepsilon^T)^{ab}$
$h_a^{(1)}$				—	$m \varepsilon^{ab}$
$h_a^{(2)}$					—

	u^{Cg}	d^{Cg}	\mathbb{Q}_b^f	$h_a^{(1)}$	$h_a^{(2)}$
u^{Cg}	—	0	$(Y_u)_{gf} \phi_a^{(2)} (\varepsilon^T)^{ab}$	0	$(Y_u)_{gf} (\varepsilon^T)^{ab} \tilde{q}_b^f$
d^{Cg}		—	$(Y_d)_{gf} \phi_a^{(1)} \varepsilon^{ab}$	$(Y_d)_{gf} \varepsilon^{ab} \tilde{q}_b^f$	0
q_b^f			—	$(Y_d)_{gf} \tilde{d}^{Cg} \varepsilon^{ab}$	$(Y_u)_{gf} \tilde{u}^{Cg} (\varepsilon^T)^{ab}$
$h_a^{(1)}$				—	$m \varepsilon^{ab}$
$h_a^{(2)}$					—

Table A.2: The $\theta = 0$ -components of the second order derivative of the superpotential. Note that the table is symmetric because of $\partial_i \partial_j \mathcal{W}_R = \partial_j \partial_i \mathcal{W}_R$.

The interaction terms in the component field formalism can now be obtained using equation (2.52).

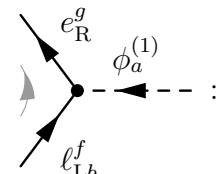
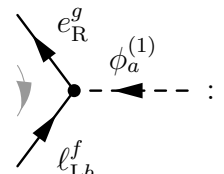
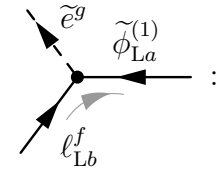
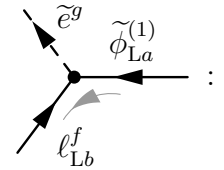
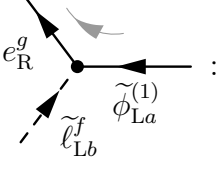
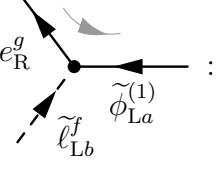
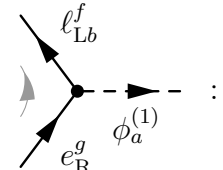
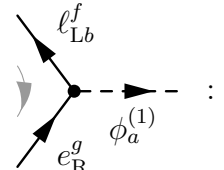
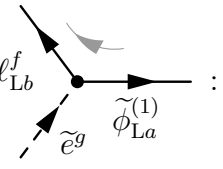
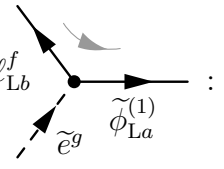
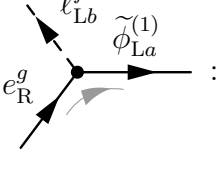
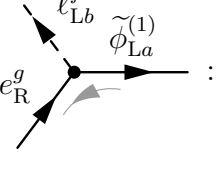
	
	
$-i\mu^{\frac{\epsilon}{2}}(Y_e)_{gf}\varepsilon_{ab}P_L$	$-i\mu^{\frac{\epsilon}{2}}(Y_e^T)_{fg}\varepsilon_{ba}^T P_L$
	
	
	
$-i\mu^{\frac{\epsilon}{2}}(Y_e^\dagger)_{fg}\varepsilon_{ba}^T P_R$	$-i\mu^{\frac{\epsilon}{2}}(Y_e^*)_{gf}\varepsilon_{ab} P_R$
	

Table A.3: Feynman rules for the Yukawa vertices containing Y_e in the MSSM. Similar Feynman rules can be derived for the down-type Yukawa interactions. Note that $\varepsilon_{ab}^T := (\varepsilon^T)_{ab}$.

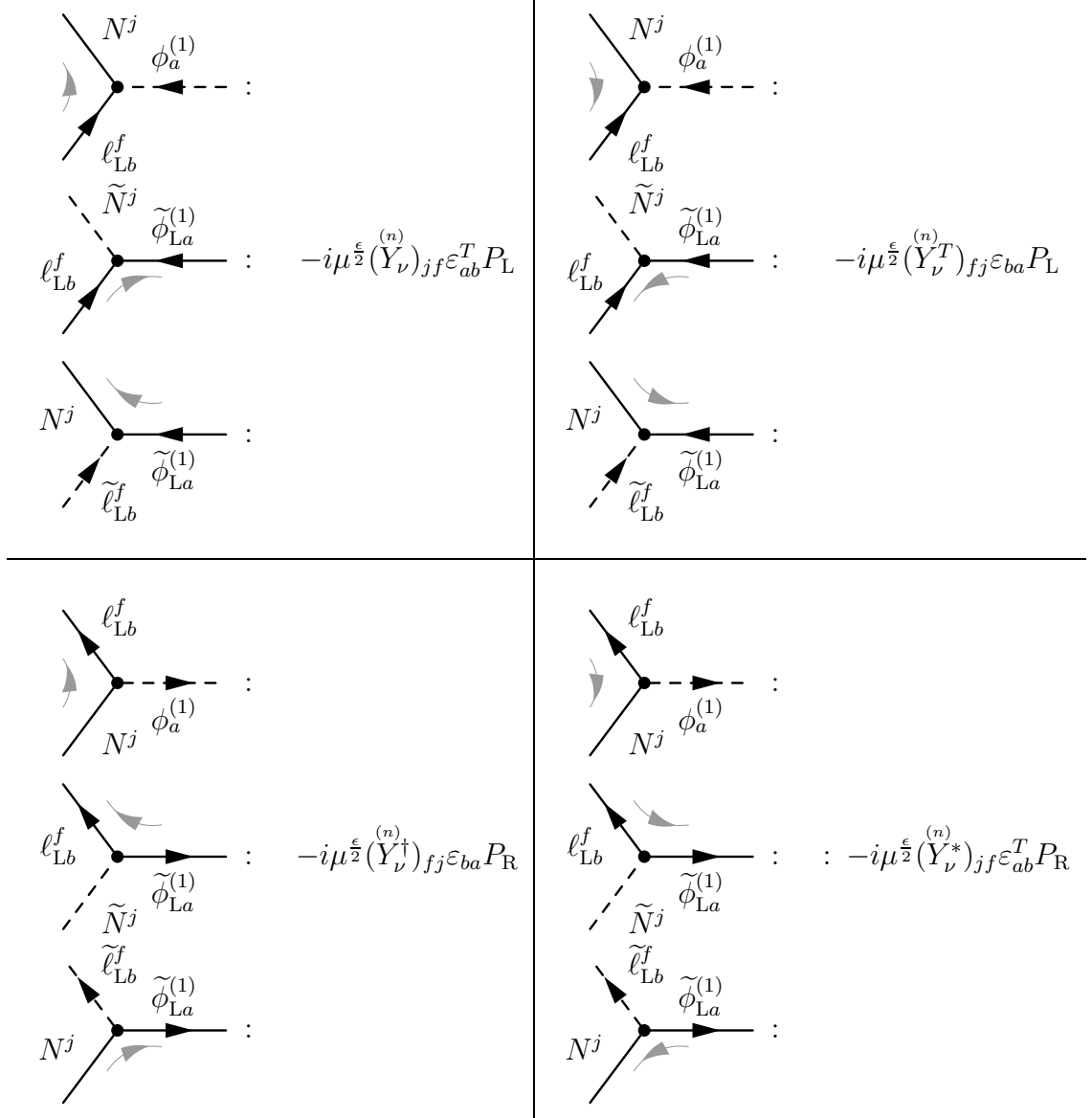


Table A.4: Feynman rules for the Yukawa vertices containing the neutrino Yukawa matrix in the MSSM extended by singlet Majorana fermions. The analogous Feynman rules can be derived for the up-type Yukawa interactions.

Gauge-Matter Interactions

In the used convention, we obtain the following Feynman rules for the coupling to the gauge bosons:

$$\begin{aligned}
 \text{Left diagram} & : -i\mu^{\frac{\epsilon}{2}} g_A \delta_{gf} (\mathbb{T}_A)_{ba} \gamma_\mu P_L \\
 \text{Right diagram} & : +i\mu^{\frac{\epsilon}{2}} g_A \delta_{gf} (\mathbb{T}_A^T)_{ab} \gamma_\mu P_R
 \end{aligned}
 \tag{A.65}$$

$$\begin{aligned}
 \text{Left diagram} & : -i\mu^{\frac{\epsilon}{2}} g_A (p_\mu + q_\mu) \mathbb{T}_A^{ba} \\
 \text{Right diagram} & : \frac{i}{2} \mu^\epsilon g_A g_B \eta_{\mu\nu} \{ \mathbb{T}_A, \mathbb{T}_B \}_{ba}
 \end{aligned}
 \tag{A.66}$$

$\{ \mathbb{T}^A, \mathbb{T}^B \} := \mathbb{T}^A \mathbb{T}^B + \mathbb{T}^B \mathbb{T}^A$ is the anti-commutator of the generators. Note that $\{ \mathbb{T}^A, \mathbb{T}^B \} = \delta^{AB}$ for $SU(N)$. Let λ^A be the superpartner of the gauge boson v^A . Then the gaugino-matter interactions have the following Feynman rules:

$$\begin{aligned}
 \text{Left diagram} & : -\sqrt{2} \mu^{\frac{\epsilon}{2}} g_A \mathbb{T}_A^{ab} \delta^{fg} P_L \\
 \text{Right diagram} & : -\sqrt{2} \mu^{\frac{\epsilon}{2}} g_A (\mathbb{T}_A^T)^{ba} \delta^{fg} P_L
 \end{aligned}
 \tag{A.67}$$

$$\begin{aligned}
 \text{Left diagram} & : \sqrt{2} \mu^{\frac{\epsilon}{2}} g_A \mathbb{T}_A^{ba} \delta^{fg} P_R \\
 \text{Right diagram} & : \sqrt{2} \mu^{\frac{\epsilon}{2}} g_A (\mathbb{T}_A^T)^{ab} \delta^{fg} P_R
 \end{aligned}
 \tag{A.68}$$

$\{ A, \psi \}$ can be replaced by any on-shell chiral multiplet of the theory.

A.4 Results for Relevant Vertex Corrections and Self-Energy Diagrams

A.4.1 Summary of Results in the SM

Diagram	Divergent Part
$i (\Sigma_\phi^e)_{ab}$	$\frac{i}{16\pi^2} 2 \text{Tr} (Y_e^\dagger Y_e) \delta_{ab} p^2 \frac{1}{\epsilon}$
$i (\Sigma_\phi^u)_{ab}$	$\frac{i}{16\pi^2} 6 \text{Tr} (Y_u^\dagger Y_u) \delta_{ab} p^2 \frac{1}{\epsilon}$
$i (\Sigma_\phi^d)_{ab}$	$\frac{i}{16\pi^2} 6 \text{Tr} (Y_d^\dagger Y_d) \delta_{ab} p^2 \frac{1}{\epsilon}$
$i (\Sigma_\phi^\lambda)_{ab}$	$\frac{i}{16\pi^2} 3 \lambda m^2 \frac{1}{\epsilon}$
$i (\Sigma_\phi^X)_{ab}$	0
$i (\Sigma_\phi^B)_{ab}$	$\frac{i}{16\pi^2} [2\xi_B(p^2 - m^2) - 6p^2] y_\phi^2 g_1^2 \delta_{ab} \frac{1}{\epsilon}$
$i (\Sigma_\phi^W)_{ab}$	$\frac{i}{16\pi^2} [2\xi_W(p^2 - m^2) - 6p^2] \frac{3}{4} g_2^2 \delta_{ab} \frac{1}{\epsilon}$

Table A.5: $1/\epsilon$ -poles of the self-energy diagrams for the Higgs doublet in the SM. The diagrams are shown in figure 2.3 on page 34. A quantity with a superscript W denotes the sum of the contribution from the three gauge bosons $W^i \in \{W^1, W^2, W^3\}$.

Diagram	Divergent Part
$i (\Sigma_{\ell_L}^e)^{gf}$	$\frac{i}{16\pi^2} (Y_e^\dagger Y_e)^{gf} \delta_{ab} \not{p} P_L \frac{1}{\epsilon}$
$i (\Sigma_{\ell_L}^B)_{ab}$	$\frac{i}{16\pi^2} 2 g_1^2 y_\ell^2 \xi_B \delta_{ab} \not{p} P_L \frac{1}{\epsilon}$
$i (\Sigma_{\ell_L}^W)_{ab}$	$\frac{i}{16\pi^2} 2 g_2^2 \frac{3}{4} \xi_W \delta_{ab} \not{p} P_L \frac{1}{\epsilon}$

Table A.6: Results for the $1/\epsilon$ -poles of the self-energy diagrams for the lepton doublets in the SM. The corresponding diagrams are shown in figure 2.2 on page 34.

Diagram	Divergent Part
$i \left(\Gamma_{\kappa}^{e(1)} \right)_{gf}^{abcd}$	$\frac{i}{16\pi^2} 2 (\kappa Y_e^\dagger Y_e)_{gf} \frac{1}{2} (\varepsilon_{cd}\varepsilon_{ba} + \varepsilon_{cb}\varepsilon_{da}) P_L \frac{1}{\epsilon}$
$i \left(\Gamma_{\kappa}^{e(2)} \right)_{gf}^{abcd}$	$\frac{i}{16\pi^2} 2 (\kappa Y_e^\dagger Y_e)_{gf} \frac{1}{2} (\varepsilon_{ca}\varepsilon_{bd} - \varepsilon_{cb}\varepsilon_{da}) P_L \frac{1}{\epsilon}$
$i \left(\Gamma_{\kappa}^{e(3)} \right)_{gf}^{abcd}$	$\frac{i}{16\pi^2} 2 (Y_e^T Y_e^* \kappa)_{gf} \frac{1}{2} (\varepsilon_{cd}\varepsilon_{ba} + \varepsilon_{cb}\varepsilon_{da}) P_L \frac{1}{\epsilon}$
$i \left(\Gamma_{\kappa}^{e(4)} \right)_{gf}^{abcd}$	$\frac{i}{16\pi^2} 2 (Y_e^T Y_e^* \kappa)_{gf} \frac{1}{2} (\varepsilon_{ca}\varepsilon_{bd} - \varepsilon_{cb}\varepsilon_{da}) P_L \frac{1}{\epsilon}$
$i \left(\Gamma_{\kappa}^{\lambda} \right)_{gf}^{abcd}$	$\frac{i}{16\pi^2} (-\lambda) \kappa_{gf} \frac{1}{2} (\varepsilon_{cd}\varepsilon_{ba} + \varepsilon_{ca}\varepsilon_{bd}) P_L \frac{1}{\epsilon}$
$i \left(\Gamma_{\kappa}^{B(1)} \right)_{gf}^{abcd}$	$\frac{i}{16\pi^2} \frac{1}{2} \xi_B g_1^2 \kappa_{gf} \frac{1}{2} (\varepsilon_{cd}\varepsilon_{ba} + \varepsilon_{ca}\varepsilon_{bd}) P_L \frac{1}{\epsilon}$
$i \left(\Gamma_{\kappa}^{B(2)} \right)_{gf}^{abcd}$	$\frac{i}{16\pi^2} \frac{1}{2} \xi_B g_1^2 \kappa_{gf} \frac{1}{2} (\varepsilon_{cd}\varepsilon_{ba} + \varepsilon_{ca}\varepsilon_{bd}) P_L \frac{1}{\epsilon}$
$i \left(\Gamma_{\kappa}^{B(3)} \right)_{gf}^{abcd}$	$\frac{i}{16\pi^2} \frac{1}{2} \xi_B g_1^2 \kappa_{gf} \frac{1}{2} (\varepsilon_{cd}\varepsilon_{ba} + \varepsilon_{ca}\varepsilon_{bd}) P_L \frac{1}{\epsilon}$
$i \left(\Gamma_{\kappa}^{B(4)} \right)_{gf}^{abcd}$	$\frac{i}{16\pi^2} \frac{1}{2} \xi_B g_1^2 \kappa_{gf} \frac{1}{2} (\varepsilon_{cd}\varepsilon_{ba} + \varepsilon_{ca}\varepsilon_{bd}) P_L \frac{1}{\epsilon}$
$i \left(\Gamma_{\kappa}^{B(5)} \right)_{gf}^{abcd}$	$\frac{i}{16\pi^2} \left(-\frac{1}{2}\right) \xi_B g_1^2 \kappa_{gf} \frac{1}{2} (\varepsilon_{cd}\varepsilon_{ba} + \varepsilon_{ca}\varepsilon_{bd}) P_L \frac{1}{\epsilon}$
$i \left(\Gamma_{\kappa}^{B(6)} \right)_{gf}^{abcd}$	$\frac{i}{16\pi^2} \left(-\frac{3}{2} - \frac{1}{2} \xi_B\right) g_1^2 \kappa_{gf} \frac{1}{2} (\varepsilon_{cd}\varepsilon_{ba} + \varepsilon_{ca}\varepsilon_{bd}) P_L \frac{1}{\epsilon}$
$i \left(\Gamma_{\kappa}^{W(1)} \right)_{gf}^{abcd}$	$\frac{i}{16\pi^2} \frac{1}{2} \xi_W g_2^2 \kappa_{gf} \frac{1}{2} (\varepsilon_{cd}\varepsilon_{ba} + 3\varepsilon_{ca}\varepsilon_{bd} - 2\varepsilon_{cb}\varepsilon_{da}) P_L \frac{1}{\epsilon}$
$i \left(\Gamma_{\kappa}^{W(2)} \right)_{gf}^{abcd}$	$\frac{i}{16\pi^2} \frac{1}{2} \xi_W g_2^2 \kappa_{gf} \frac{1}{2} (3\varepsilon_{cd}\varepsilon_{ba} + \varepsilon_{ca}\varepsilon_{bd} - 2\varepsilon_{cb}\varepsilon_{ad}) P_L \frac{1}{\epsilon}$
$i \left(\Gamma_{\kappa}^{W(3)} \right)_{gf}^{abcd}$	$\frac{i}{16\pi^2} \frac{1}{2} \xi_W g_2^2 \kappa_{gf} \frac{1}{2} (\varepsilon_{cd}\varepsilon_{ba} + 3\varepsilon_{ca}\varepsilon_{bd} - 2\varepsilon_{ad}\varepsilon_{bc}) P_L \frac{1}{\epsilon}$
$i \left(\Gamma_{\kappa}^{W(4)} \right)_{gf}^{abcd}$	$\frac{i}{16\pi^2} \frac{1}{2} \xi_W g_2^2 \kappa_{gf} \frac{1}{2} (3\varepsilon_{cd}\varepsilon_{ba} + \varepsilon_{ca}\varepsilon_{bd} - 2\varepsilon_{da}\varepsilon_{bc}) P_L \frac{1}{\epsilon}$
$i \left(\Gamma_{\kappa}^{W(5)} \right)_{gf}^{abcd}$	$\frac{i}{16\pi^2} \left(-\frac{1}{2}\right) \xi_W g_2^2 \kappa_{gf} \frac{1}{2} (\varepsilon_{cd}\varepsilon_{ba} + \varepsilon_{ca}\varepsilon_{bd}) P_L \frac{1}{\epsilon}$
$i \left(\Gamma_{\kappa}^{W(6)} \right)_{gf}^{abcd}$	$\frac{i}{16\pi^2} \left(-\frac{3}{2} - \frac{1}{2} \xi_W\right) g_2^2 \kappa_{gf} \frac{1}{2} (\varepsilon_{cd}\varepsilon_{ba} + \varepsilon_{ca}\varepsilon_{bd}) P_L \frac{1}{\epsilon}$

Table A.7: Summary of results for the $1/\epsilon$ -poles of the vertex corrections for κ in the SM. The corresponding diagrams are shown in figure 2.1 on page 31.

A.4.2 Summary of Results in the 2HDMs

We now summarize some results for the $1/\epsilon$ -poles of vertex corrections and self-energy diagrams which are relevant for the calculation of the β -functions for the neutrino mass operators in the 2HDMs classified in table 2.1 on page 36. Most of the calculations are similar to the ones in the SM and we use an analogous notation for the diagrams. The results for the self-energy diagrams of the lepton doublets in the 2HDMs are identical to the SM case (see table A.6).

Diagram	Divergent Part
$i \left(\Sigma_{\phi^{(1)}}^e \right)_{ab}$	$\frac{i}{16\pi^2} 2 \text{Tr} (Y_e^\dagger Y_e) \delta_{ab} p^2 \frac{1}{\epsilon}$
$i \left(\Sigma_{\phi^{(i)}}^u \right)_{ab}$	$\frac{i}{16\pi^2} 6 z_u^{(i)} \text{Tr} (Y_u^\dagger Y_u) \delta_{ab} p^2 \frac{1}{\epsilon}$
$i \left(\Sigma_{\phi^{(i)}}^d \right)_{ab}$	$\frac{i}{16\pi^2} 6 z_d^{(i)} \text{Tr} (Y_d^\dagger Y_d) \delta_{ab} p^2 \frac{1}{\epsilon}$
$i \left(\Sigma_{\phi^{(i)}}^B \right)_{ab}$	$\frac{i}{16\pi^2} [2\xi_B(p^2 - m_i^2) - 6p^2] y_\phi^2 g_1^2 \delta_{ab} \frac{1}{\epsilon}$
$i \left(\Sigma_{\phi^{(i)}}^W \right)_{ab}$	$\frac{i}{16\pi^2} [2\xi_W(p^2 - m_i^2) - 6p^2] \frac{3}{4} g_2^2 \delta_{ab} \frac{1}{\epsilon}$

Table A.8: Summary of results for the $1/\epsilon$ -poles of the self-energy diagrams, which contribute to the wavefunction renormalization of the Higgs doublets in 2HDMs. We use a notation analogous to the one for the diagrams in the SM (figure 2.3 on page 34). The constants $z_u^{(i)}$ and $z_d^{(i)}$ specify the couplings to the Higgs doublets and are given in table 2.2 for the models classified in table 2.1 (page 36).

Diagram	Divergent Part
$i \left(\Gamma_{\kappa^{(11)}}^{\lambda_1} \right)_{gf}^{abcd}$	$\frac{i}{16\pi^2} (-\lambda_1) \kappa_{gf}^{(11)} \frac{1}{2} (\varepsilon_{cd}\varepsilon_{ba} + \varepsilon_{ca}\varepsilon_{bd}) P_L \frac{1}{\epsilon}$
$i \left(\Gamma_{\kappa^{(22)}}^{\lambda_2} \right)_{gf}^{abcd}$	$\frac{i}{16\pi^2} (-\lambda_2) \kappa_{gf}^{(22)} \frac{1}{2} (\varepsilon_{cd}\varepsilon_{ba} + \varepsilon_{ca}\varepsilon_{bd}) P_L \frac{1}{\epsilon}$
$i \left(\Gamma_{\kappa^{(11)}}^{\lambda_5} \right)_{gf}^{abcd}$	$\frac{i}{16\pi^2} (-\lambda_5) \kappa_{gf}^{(11)} \frac{1}{2} (\varepsilon_{cd}\varepsilon_{ba} + \varepsilon_{ca}\varepsilon_{bd}) P_L \frac{1}{\epsilon}$
$i \left(\Gamma_{\kappa^{(22)}}^{\lambda_5^*} \right)_{gf}^{abcd}$	$\frac{i}{16\pi^2} (-\lambda_5^*) \kappa_{gf}^{(22)} \frac{1}{2} (\varepsilon_{cd}\varepsilon_{ba} + \varepsilon_{ca}\varepsilon_{bd}) P_L \frac{1}{\epsilon}$
$i \left(\Gamma_{\kappa^{(ii)}}^{e(1)} \right)_{gf}^{abcd}$	$\frac{i}{16\pi^2} 2 \left(\kappa^{(ii)} Y_e^\dagger Y_e \right)_{gf} \frac{1}{2} (\varepsilon_{cd}\varepsilon_{ba} + \varepsilon_{cb}\varepsilon_{da}) P_L \frac{1}{\epsilon}$
$i \left(\Gamma_{\kappa^{(ii)}}^{e(2)} \right)_{gf}^{abcd}$	$\frac{i}{16\pi^2} 2 \left(\kappa^{(ii)} Y_e^\dagger Y_e \right)_{gf} \frac{1}{2} (\varepsilon_{ca}\varepsilon_{bd} - \varepsilon_{cb}\varepsilon_{da}) P_L \frac{1}{\epsilon}$
$i \left(\Gamma_{\kappa^{(ii)}}^{e(3)} \right)_{gf}^{abcd}$	$\frac{i}{16\pi^2} 2 \left(Y_e^T Y_e^* \kappa^{(ii)} \right)_{gf} \frac{1}{2} (\varepsilon_{cd}\varepsilon_{ba} + \varepsilon_{cb}\varepsilon_{da}) P_L \frac{1}{\epsilon}$
$i \left(\Gamma_{\kappa^{(ii)}}^{e(4)} \right)_{gf}^{abcd}$	$\frac{i}{16\pi^2} 2 \left(Y_e^T Y_e^* \kappa^{(ii)} \right)_{gf} \frac{1}{2} (\varepsilon_{ca}\varepsilon_{bd} - \varepsilon_{cb}\varepsilon_{da}) P_L \frac{1}{\epsilon}$
$i \left(\Gamma_{\kappa^{(ii)}}^{B(n)} \right)_{gf}^{abcd}$	$\frac{i}{16\pi^2} \frac{1}{2} \xi_B g_1^2 \kappa_{gf}^{(ii)} \frac{1}{2} (\varepsilon_{cd}\varepsilon_{ba} + \varepsilon_{ca}\varepsilon_{bd}) P_L \frac{1}{\epsilon} \quad (n \in \{1, \dots, 4\})$
$i \left(\Gamma_{\kappa^{(ii)}}^{B(5)} \right)_{gf}^{abcd}$	$\frac{i}{16\pi^2} \left(-\frac{1}{2}\right) \xi_B g_1^2 \kappa_{gf}^{(ii)} \frac{1}{2} (\varepsilon_{cd}\varepsilon_{ba} + \varepsilon_{ca}\varepsilon_{bd}) P_L \frac{1}{\epsilon}$
$i \left(\Gamma_{\kappa^{(ii)}}^{B(6)} \right)_{gf}^{abcd}$	$\frac{i}{16\pi^2} \left(-\frac{3}{2} - \frac{1}{2} \xi_B\right) g_1^2 \kappa_{gf}^{(ii)} \frac{1}{2} (\varepsilon_{cd}\varepsilon_{ba} + \varepsilon_{ca}\varepsilon_{bd}) P_L \frac{1}{\epsilon}$
$i \left(\Gamma_{\kappa^{(ii)}}^{W(1)} \right)_{gf}^{abcd}$	$\frac{i}{16\pi^2} \frac{1}{2} \xi_W g_2^2 \kappa_{gf}^{(ii)} \frac{1}{2} (\varepsilon_{cd}\varepsilon_{ba} + 3\varepsilon_{ca}\varepsilon_{bd} - 2\varepsilon_{cb}\varepsilon_{da}) P_L \frac{1}{\epsilon}$
$i \left(\Gamma_{\kappa^{(ii)}}^{W(2)} \right)_{gf}^{abcd}$	$\frac{i}{16\pi^2} \frac{1}{2} \xi_W g_2^2 \kappa_{gf}^{(ii)} \frac{1}{2} (3\varepsilon_{cd}\varepsilon_{ba} + \varepsilon_{ca}\varepsilon_{bd} - 2\varepsilon_{cb}\varepsilon_{ad}) P_L \frac{1}{\epsilon}$
$i \left(\Gamma_{\kappa^{(ii)}}^{W(3)} \right)_{gf}^{abcd}$	$\frac{i}{16\pi^2} \frac{1}{2} \xi_W g_2^2 \kappa_{gf}^{(ii)} \frac{1}{2} (\varepsilon_{cd}\varepsilon_{ba} + 3\varepsilon_{ca}\varepsilon_{bd} - 2\varepsilon_{ad}\varepsilon_{bc}) P_L \frac{1}{\epsilon}$
$i \left(\Gamma_{\kappa^{(ii)}}^{W(4)} \right)_{gf}^{abcd}$	$\frac{i}{16\pi^2} \frac{1}{2} \xi_W g_2^2 \kappa_{gf}^{(ii)} \frac{1}{2} (3\varepsilon_{cd}\varepsilon_{ba} + \varepsilon_{ca}\varepsilon_{bd} - 2\varepsilon_{da}\varepsilon_{bc}) P_L \frac{1}{\epsilon}$
$i \left(\Gamma_{\kappa^{(ii)}}^{W(5)} \right)_{gf}^{abcd}$	$\frac{i}{16\pi^2} \left(-\frac{1}{2}\right) \xi_W g_2^2 \kappa_{gf}^{(ii)} \frac{1}{2} (\varepsilon_{cd}\varepsilon_{ba} + \varepsilon_{ca}\varepsilon_{bd}) P_L \frac{1}{\epsilon}$
$i \left(\Gamma_{\kappa^{(ii)}}^{W(6)} \right)_{gf}^{abcd}$	$\frac{i}{16\pi^2} \left(-\frac{3}{2} - \frac{1}{2} \xi_W\right) g_2^2 \kappa_{gf}^{(ii)} \frac{1}{2} (\varepsilon_{cd}\varepsilon_{ba} + \varepsilon_{ca}\varepsilon_{bd}) P_L \frac{1}{\epsilon}$

Table A.9: $1/\epsilon$ -poles of the vertex corrections for the two neutrino mass operators $\kappa^{(11)}$ and $\kappa^{(22)}$ in the 2HDMs, classified in table 2.1 on page 36. The diagrams proportional to the Higgs self-interactions are shown in figure 2.4 on page 38. The other diagrams are similar to the ones in the SM (figure 2.1 on page 31) and we use a notation analogous to the one defined there.

A.4.3 Summary of Results in the MSSM

Diagram	Divergent Part
$i \left(\Sigma_{\phi^{(2)}}^u \right)_{ab}$	$\frac{i}{16\pi^2} 6 \text{Tr} (Y_u^\dagger Y_u) \delta_{ab} p^2 \frac{1}{\epsilon}$
$i \left(\Sigma_{\phi^{(2)}}^B \right)_{ab}$	$\frac{i}{16\pi^2} [2 \xi_B (p^2 - m^2) - 6 p^2] y_\phi^2 g_1^2 \delta_{ab} \frac{1}{\epsilon}$
$i \left(\Sigma_{\phi^{(2)}}^{\lambda^0} \right)_{ab}$	$\frac{i}{16\pi^2} [-4 p^2] y_{\phi^{(2)}}^2 g_1^2 \delta_{ab} \frac{1}{\epsilon}$
$i \left(\Sigma_{\phi^{(2)}}^W \right)_{ab}$	$\frac{i}{16\pi^2} [2 \xi_W (p^2 - m^2) - 6 p^2] \frac{3}{4} g_2^2 \delta_{ab} \frac{1}{\epsilon}$
$i \left(\Sigma_{\phi^{(2)}}^{\Sigma \lambda^i} \right)_{ab}$	$\frac{i}{16\pi^2} [-4 p^2] \frac{3}{4} g_2^2 \delta_{ab} \frac{1}{\epsilon}$

Table A.10: Results for the $1/\epsilon$ -poles of the self-energy diagrams, which contribute to the wave-function renormalization of the Higgs doublet $\phi^{(2)}$ in the MSSM. The corresponding diagrams are shown in figure 2.7 on page 48. A quantity with a superscript W denotes the sum of the contribution from the gauge bosons $W^i \in \{W^1, W^2, W^3\}$ and a quantity with a superscript $\Sigma \lambda^i$ denotes the sum of the contribution from gauginos λ^i which are the superpartners of the three $SU(2)_L$ -gauge bosons.

Diagram	Divergent Part
$i \left(\Sigma_{\ell_L}^e \right)^{gf}_{ab}$	$\frac{i}{16\pi^2} (Y_e^\dagger Y_e)^{gf} \delta_{ab} \not{p} P_L \frac{1}{\epsilon}$
$i \left(\Sigma_{\ell_L}^{\tilde{e}} \right)^{gf}_{ab}$	$\frac{i}{16\pi^2} (Y_e^\dagger Y_e)^{gf} \delta_{ab} \not{p} P_L \frac{1}{\epsilon}$
$i \left(\Sigma_{\ell_L}^B \right)_{ab}$	$\frac{i}{16\pi^2} 2 g_1^2 y_\ell^2 \xi_B \delta_{ab} \not{p} P_L \frac{1}{\epsilon}$
$i \left(\Sigma_{\ell_L}^{\lambda^0} \right)_{ab}$	$\frac{i}{16\pi^2} 2 g_1^2 y_\ell^2 \delta_{ab} \not{p} P_L \frac{1}{\epsilon}$
$i \left(\Sigma_{\ell_L}^W \right)_{ab}$	$\frac{i}{16\pi^2} 2 g_2^2 \frac{3}{4} \xi_W \delta_{ab} \not{p} P_L \frac{1}{\epsilon}$
$i \left(\Sigma_{\ell_L}^{\Sigma \lambda^i} \right)_{ab}$	$\frac{i}{16\pi^2} 2 g_2^2 \frac{3}{4} \delta_{ab} \not{p} P_L \frac{1}{\epsilon}$

Table A.11: $1/\epsilon$ -poles of self-energy diagrams for the lepton doublets in the MSSM. The diagrams are shown in figure 2.6 on page 47.

Diagram	Divergent Part
$i \left(\Gamma_{\kappa}^{D(1)} \right)_{gf}^{abcd}$	$\frac{i}{16\pi^2} (-g_1^2) \kappa_{gf} \frac{1}{2} (\varepsilon_{cd}\varepsilon_{ba} + \varepsilon_{ca}\varepsilon_{bd}) P_L \frac{1}{\epsilon}$
$i \left(\Gamma_{\kappa}^{D(2)} \right)_{gf}^{abcd}$	$\frac{i}{16\pi^2} (-g_2^2) \kappa_{gf} \frac{1}{2} (\varepsilon_{cd}\varepsilon_{ba} + \varepsilon_{ca}\varepsilon_{bd}) P_L \frac{1}{\epsilon}$
$i \left(\Gamma_{\kappa}^{B(n)} \right)_{gf}^{abcd}$	$\frac{i}{16\pi^2} \frac{1}{2} \xi_B g_1^2 \kappa_{gf} \frac{1}{2} (\varepsilon_{cd}\varepsilon_{ba} + \varepsilon_{ca}\varepsilon_{bd}) P_L \frac{1}{\epsilon} \quad (n \in \{1, \dots, 4\})$
$i \left(\Gamma_{\kappa}^{B(5)} \right)_{gf}^{abcd}$	$\frac{i}{16\pi^2} (-\frac{1}{2}) \xi_B g_1^2 \kappa_{gf} \frac{1}{2} (\varepsilon_{cd}\varepsilon_{ba} + \varepsilon_{ca}\varepsilon_{bd}) P_L \frac{1}{\epsilon}$
$i \left(\Gamma_{\kappa}^{B(6)} \right)_{gf}^{abcd}$	$\frac{i}{16\pi^2} (-\frac{3}{2} - \frac{1}{2} \xi_B) g_1^2 \kappa_{gf} \frac{1}{2} (\varepsilon_{cd}\varepsilon_{ba} + \varepsilon_{ca}\varepsilon_{bd}) P_L \frac{1}{\epsilon}$
$i \left(\Gamma_{\kappa}^{W(1)} \right)_{gf}^{abcd}$	$\frac{i}{16\pi^2} \frac{1}{2} \xi_W g_2^2 \kappa_{gf} \frac{1}{2} (\varepsilon_{cd}\varepsilon_{ba} + 3\varepsilon_{ca}\varepsilon_{bd} - 2\varepsilon_{cb}\varepsilon_{da}) P_L \frac{1}{\epsilon}$
$i \left(\Gamma_{\kappa}^{W(2)} \right)_{gf}^{abcd}$	$\frac{i}{16\pi^2} \frac{1}{2} \xi_W g_2^2 \kappa_{gf} \frac{1}{2} (3\varepsilon_{cd}\varepsilon_{ba} + \varepsilon_{ca}\varepsilon_{bd} - 2\varepsilon_{cb}\varepsilon_{ad}) P_L \frac{1}{\epsilon}$
$i \left(\Gamma_{\kappa}^{W(3)} \right)_{gf}^{abcd}$	$\frac{i}{16\pi^2} \frac{1}{2} \xi_W g_2^2 \kappa_{gf} \frac{1}{2} (\varepsilon_{cd}\varepsilon_{ba} + 3\varepsilon_{ca}\varepsilon_{bd} - 2\varepsilon_{ad}\varepsilon_{bc}) P_L \frac{1}{\epsilon}$
$i \left(\Gamma_{\kappa}^{W(4)} \right)_{gf}^{abcd}$	$\frac{i}{16\pi^2} \frac{1}{2} \xi_W g_2^2 \kappa_{gf} \frac{1}{2} (3\varepsilon_{cd}\varepsilon_{ba} + \varepsilon_{ca}\varepsilon_{bd} - 2\varepsilon_{da}\varepsilon_{bc}) P_L \frac{1}{\epsilon}$
$i \left(\Gamma_{\kappa}^{W(5)} \right)_{gf}^{abcd}$	$\frac{i}{16\pi^2} (-\frac{1}{2}) \xi_W g_2^2 \kappa_{gf} \frac{1}{2} (\varepsilon_{cd}\varepsilon_{ba} + \varepsilon_{ca}\varepsilon_{bd}) P_L \frac{1}{\epsilon}$
$i \left(\Gamma_{\kappa}^{W(6)} \right)_{gf}^{abcd}$	$\frac{i}{16\pi^2} (-\frac{3}{2} - \frac{1}{2} \xi_W) g_2^2 \kappa_{gf} \frac{1}{2} (\varepsilon_{cd}\varepsilon_{ba} + \varepsilon_{ca}\varepsilon_{bd}) P_L \frac{1}{\epsilon}$
$i \left(\Gamma_{\kappa}^{\lambda^0(n)} \right)_{gf}^{abcd}$	$\frac{i}{16\pi^2} g_1^2 \kappa_{gf} \frac{1}{2} (\varepsilon_{cd}\varepsilon_{ba} + \varepsilon_{ca}\varepsilon_{bd}) P_L \frac{1}{\epsilon} \quad (n \in \{1, \dots, 4\})$
$i \left(\Gamma_{\kappa}^{\Sigma\lambda^i(1)} \right)_{gf}^{abcd}$	$\frac{i}{16\pi^2} g_2^2 \kappa_{gf} \frac{1}{2} (\varepsilon_{cd}\varepsilon_{ba} + 3\varepsilon_{ca}\varepsilon_{bd} - 2\varepsilon_{cb}\varepsilon_{da}) P_L \frac{1}{\epsilon}$
$i \left(\Gamma_{\kappa}^{\Sigma\lambda^i(2)} \right)_{gf}^{abcd}$	$\frac{i}{16\pi^2} g_2^2 \kappa_{gf} \frac{1}{2} (3\varepsilon_{cd}\varepsilon_{ba} + \varepsilon_{ca}\varepsilon_{bd} - 2\varepsilon_{cb}\varepsilon_{ad}) P_L \frac{1}{\epsilon}$
$i \left(\Gamma_{\kappa}^{\Sigma\lambda^i(3)} \right)_{gf}^{abcd}$	$\frac{i}{16\pi^2} g_2^2 \kappa_{gf} \frac{1}{2} (\varepsilon_{cd}\varepsilon_{ba} + 3\varepsilon_{ca}\varepsilon_{bd} - 2\varepsilon_{ad}\varepsilon_{bc}) P_L \frac{1}{\epsilon}$
$i \left(\Gamma_{\kappa}^{\Sigma\lambda^i(4)} \right)_{gf}^{abcd}$	$\frac{i}{16\pi^2} g_2^2 \kappa_{gf} \frac{1}{2} (3\varepsilon_{cd}\varepsilon_{ba} + \varepsilon_{ca}\varepsilon_{bd} - 2\varepsilon_{da}\varepsilon_{bc}) P_L \frac{1}{\epsilon}$

Table A.12: Results for the $1/\epsilon$ -poles of vertex corrections for κ in the MSSM, which are proportional to the gauge couplings. The sum of the $1/\epsilon$ -poles of the other vertex corrections vanishes due to the non-renormalization theorem. The corresponding diagrams are shown in figure 2.5 on page 45.

A.5 Summary of the RGEs for the Minimal See-Saw Scenarios

In order to calculate the RG evolution of the effective neutrino mass matrix, we have to solve the RGEs for all the parameters of the theory simultaneously. We therefore summarize the RGEs for the parameters in the minimal see-saw extensions of the SM, 2HDMs and the MSSM, using the notation defined in section 2.4. A superscript (n) denotes a quantity between the n th and the $(n+1)$ th mass threshold. The RGEs for the SM, 2HDM or MSSM can be recovered by setting the neutrino Yukawa coupling to zero. The RGEs for the gauge couplings are well known and are not affected by the additional singlets at 1-loop order. They are given by

$$16\pi^2 \beta_{g_A} = 16\pi^2 \mu \frac{dg_A}{d\mu} = b_A g_A^3, \quad (\text{A.69})$$

with $(b_{\text{SU}(3)_C}, b_{\text{SU}(2)_L}, b_{\text{U}(1)_Y}) = (-7, -\frac{19}{6}, \frac{41}{10})$ in the SM, $(-7, -3, \frac{21}{5})$ in the 2HDMs and $(-3, 1, \frac{33}{5})$ in the MSSM. For $\text{U}(1)_Y$, we use GUT charge normalization and denote the corresponding gauge coupling constant as g_1^{U} . The RGEs for the couplings in the SM and in the 2HDMs which have not been calculated explicitly in this thesis can be found in [119,120], except for the terms containing the neutrino Yukawa couplings.

A.5.1 The RGEs in the Extended SM

$$\begin{aligned} 16\pi^2 \beta_{\kappa}^{(n)} &= -\frac{3}{2} (Y_e^\dagger Y_e)^T \kappa^{(n)} - \frac{3}{2} \kappa^{(n)} (Y_e^\dagger Y_e) + \frac{1}{2} (Y_\nu^\dagger Y_\nu)^{T(n)} \kappa^{(n)} + \frac{1}{2} \kappa^{(n)} (Y_\nu^\dagger Y_\nu)^{(n)} \\ &\quad + 2 \text{Tr}(Y_e^\dagger Y_e) \kappa^{(n)} + 2 \text{Tr}(Y_\nu^\dagger Y_\nu) \kappa^{(n)} + 6 \text{Tr}(Y_u^\dagger Y_u) \kappa^{(n)} \\ &\quad + 6 \text{Tr}(Y_d^\dagger Y_d) \kappa^{(n)} - 3g_2^2 \kappa^{(n)} + \lambda \kappa^{(n)}, \end{aligned} \quad (\text{A.70a})$$

$$16\pi^2 \beta_M^{(n)} = (Y_\nu Y_\nu^\dagger)^{(n)} M + \dot{M} (Y_\nu Y_\nu^\dagger)^{(n)T}, \quad (\text{A.70b})$$

$$\begin{aligned} 16\pi^2 \beta_{Y_\nu}^{(n)} &= Y_\nu \left\{ \frac{3}{2} (Y_\nu^\dagger Y_\nu)^{(n)} - \frac{3}{2} (Y_e^\dagger Y_e) + \text{Tr}(Y_\nu^\dagger Y_\nu) + \text{Tr}(Y_e^\dagger Y_e) \right. \\ &\quad \left. + 3 \text{Tr}(Y_u^\dagger Y_u) + 3 \text{Tr}(Y_d^\dagger Y_d) - \frac{9}{20} (g_1^{\text{U}})^2 - \frac{9}{4} g_2^2 \right\}, \end{aligned} \quad (\text{A.70c})$$

$$\begin{aligned} 16\pi^2 \beta_{Y_e}^{(n)} &= Y_e \left\{ \frac{3}{2} Y_e^\dagger Y_e - \frac{3}{2} Y_\nu^\dagger Y_\nu - \frac{9}{4} (g_1^{\text{U}})^2 - \frac{9}{4} g_2^2 \right. \\ &\quad \left. + \text{Tr} \left[Y_e^\dagger Y_e + Y_\nu^\dagger Y_\nu + 3Y_d^\dagger Y_d + 3Y_u^\dagger Y_u \right] \right\}, \end{aligned} \quad (\text{A.70d})$$

$$16\pi^2 \beta_{Y_d}^{(n)} = Y_d \left\{ \frac{3}{2} Y_d^\dagger Y_d - \frac{3}{2} Y_u^\dagger Y_u - \frac{1}{4} (g_1^U)^2 - \frac{9}{4} g_2^2 - 8 g_3^2 \right. \\ \left. + \text{Tr} \left[Y_e^\dagger Y_e + \overset{(n)}{Y}_\nu^\dagger \overset{(n)}{Y}_\nu + 3 Y_d^\dagger Y_d + 3 Y_u^\dagger Y_u \right] \right\}, \quad (\text{A.70e})$$

$$16\pi^2 \beta_{Y_u}^{(n)} = Y_u \left\{ \frac{3}{2} Y_u^\dagger Y_u - \frac{3}{2} Y_d^\dagger Y_d - \frac{17}{20} (g_1^U)^2 - \frac{9}{4} g_2^2 - 8 g_3^2 \right. \\ \left. + \text{Tr} \left[Y_e^\dagger Y_e + \overset{(n)}{Y}_\nu^\dagger \overset{(n)}{Y}_\nu + 3 Y_d^\dagger Y_d + 3 Y_u^\dagger Y_u \right] \right\}, \quad (\text{A.70f})$$

$$16\pi^2 \beta_\lambda^{(n)} = 6 \lambda^2 - 3 \lambda \left(3 g_2^2 + \frac{3}{5} (g_1^U)^2 \right) + 3 g_2^4 + \frac{3}{2} \left(\frac{3}{5} (g_1^U)^2 + g_2^2 \right)^2 \\ + 4 \lambda \text{Tr} \left[Y_e^\dagger Y_e + \overset{(n)}{Y}_\nu^\dagger \overset{(n)}{Y}_\nu + 3 Y_d^\dagger Y_d + 3 Y_u^\dagger Y_u \right] \\ - 8 \text{Tr} \left[Y_e^\dagger Y_e Y_e^\dagger Y_e + \overset{(n)}{Y}_\nu^\dagger \overset{(n)}{Y}_\nu \overset{(n)}{Y}_\nu^\dagger \overset{(n)}{Y}_\nu + 3 Y_d^\dagger Y_d Y_d^\dagger Y_d + 3 Y_u^\dagger Y_u Y_u^\dagger Y_u \right]. \quad (\text{A.70g})$$

A.5.2 The RGEs in Extended 2HDMs

$$16\pi^2 \beta_{\kappa^{(ii)}}^{(n)} = \left(\frac{1}{2} - 2 \delta_{i1} \right) \left[\kappa^{(ii)} (Y_e^\dagger Y_e) + (Y_e^\dagger Y_e)^T \kappa^{(ii)} \right] + z_\nu^{(i)} 2 \text{Tr} \left(\overset{(n)}{Y}_\nu^\dagger \overset{(n)}{Y}_\nu \right) \\ + \left[\delta_{i1} 2 \text{Tr} (Y_e^\dagger Y_e) + z_u^{(i)} 6 \text{Tr} (Y_u^\dagger Y_u) + z_d^{(i)} 6 \text{Tr} (Y_d^\dagger Y_d) \right] \kappa^{(ii)} \\ + \lambda_i \kappa^{(ii)} + \delta_{i1} \lambda_5^* \kappa^{(22)} + \delta_{i2} \lambda_5 \kappa^{(11)} - 3 g_2^2 \kappa^{(ii)}, \quad (\text{A.71a})$$

$$16\pi^2 \beta_M^{(n)} = \left(\overset{(n)}{Y}_\nu \overset{(n)}{Y}_\nu^\dagger \right) \overset{(n)}{M} + \overset{(n)}{M} \left(\overset{(n)}{Y}_\nu \overset{(n)}{Y}_\nu^\dagger \right)^T, \quad (\text{A.71b})$$

$$16\pi^2 \beta_{Y_\nu}^{(n)} = \overset{(n)}{Y}_\nu \left\{ \frac{3}{2} \overset{(n)}{Y}_\nu^\dagger \overset{(n)}{Y}_\nu + \left(\frac{1}{2} - 2 z_\nu^{(1)} \right) \frac{3}{2} Y_e^\dagger Y_e - \frac{9}{20} (g_1^U)^2 - \frac{9}{4} g_2^2 \right. \\ \left. + \sum_{i=1}^2 z_\nu^{(i)} \text{Tr} \left[\delta_{i1} Y_e^\dagger Y_e + \overset{(n)}{Y}_\nu^\dagger \overset{(n)}{Y}_\nu + 3 z_d^{(i)} Y_d^\dagger Y_d + 3 z_u^{(i)} Y_u^\dagger Y_u \right] \right\}, \quad (\text{A.71c})$$

$$16\pi^2 \beta_{Y_e}^{(n)} = Y_e \left\{ \frac{3}{2} Y_e^\dagger Y_e + \left(\frac{1}{2} - 2 z_\nu^{(1)} \right) \overset{(n)}{Y}_\nu^\dagger \overset{(n)}{Y}_\nu - \frac{9}{4} (g_1^U)^2 - \frac{9}{4} g_2^2 \right. \\ \left. + \text{Tr} \left[Y_e^\dagger Y_e + z_\nu^{(1)} \overset{(n)}{Y}_\nu^\dagger \overset{(n)}{Y}_\nu + 3 z_d^{(1)} Y_d^\dagger Y_d + 3 z_u^{(1)} Y_u^\dagger Y_u \right] \right\}, \quad (\text{A.71d})$$

$$16\pi^2 \beta_{Y_d}^{(n)} = Y_d \left\{ \frac{3}{2} Y_d^\dagger Y_d + \left(\frac{1}{2} - 2 \sum_{i=1}^2 z_u^{(i)} z_d^{(i)} \right) Y_u^\dagger Y_u - \frac{1}{4} (g_1^U)^2 - \frac{9}{4} g_2^2 - 8 g_3^2 \right. \\ \left. + \sum_{i=1}^2 z_d^{(i)} \text{Tr} \left[\delta_{i1} Y_e^\dagger Y_e + z_\nu^{(i)} \overset{(n)}{Y}_\nu^\dagger \overset{(n)}{Y}_\nu + 3 Y_d^\dagger Y_d + 3 z_u^{(i)} Y_u^\dagger Y_u \right] \right\}, \quad (\text{A.71e})$$

$$\begin{aligned}
16\pi^2 \beta_{Y_u}^{(n)} &= Y_u \left\{ \frac{3}{2} Y_u^\dagger Y_u + \left(\frac{1}{2} - 2 \sum_{i=1}^2 z_u^{(i)} z_d^{(i)} \right) Y_d^\dagger Y_d - \frac{17}{20} (g_1^U)^2 - \frac{9}{4} g_2^2 - 8g_3^2 \right. \\
&\quad \left. + \sum_{i=1}^2 z_u^{(i)} \text{Tr} \left[\delta_{i1} Y_e^\dagger Y_e + z_\nu^{(i)} Y_\nu^{(n)\dagger} Y_\nu^{(n)} + 3z_d^{(i)} Y_d^\dagger Y_d + 3Y_u^\dagger Y_u \right] \right\}. \quad (\text{A.71f})
\end{aligned}$$

For the parameters of the Higgs interaction Lagrangian, the β -functions are

$$\begin{aligned}
16\pi^2 \beta_{\lambda_1}^{(n)} &= 6\lambda_1^2 + 8\lambda_3^2 + 6\lambda_3\lambda_4 + \lambda_5^2 - 3\lambda_1 \left(3g_2^2 + \frac{3}{5} (g_1^U)^2 \right) + 3g_2^4 \\
&\quad + \frac{3}{2} \left(\frac{3}{5} (g_1^U)^2 + g_2^2 \right)^2 + 4\lambda_1 \text{Tr} \left(Y_e^\dagger Y_e + z_\nu^{(1)} Y_\nu^{(n)\dagger} Y_\nu^{(n)} + 3z_d^{(1)} Y_d^\dagger Y_d \right. \\
&\quad \left. + 3z_u^{(1)} Y_u^\dagger Y_u \right) - 8 \text{Tr} \left(Y_e^\dagger Y_e Y_e^\dagger Y_e + z_\nu^{(1)} Y_\nu^{(n)\dagger} Y_\nu^{(n)} Y_\nu^{(n)\dagger} Y_\nu^{(n)} \right. \\
&\quad \left. + 3z_d^{(1)} Y_d^\dagger Y_d Y_d^\dagger Y_d + 3z_u^{(1)} Y_u^\dagger Y_u Y_u^\dagger Y_u \right), \quad (\text{A.72a})
\end{aligned}$$

$$\begin{aligned}
16\pi^2 \beta_{\lambda_2}^{(n)} &= 6\lambda_2^2 + 8\lambda_3^2 + 6\lambda_3\lambda_4 + \lambda_5^2 - 3\lambda_2 \left(3g_2^2 + \frac{3}{5} (g_1^U)^2 \right) + 3g_2^4 \\
&\quad + \frac{3}{2} \left(\frac{3}{5} (g_1^U)^2 + g_2^2 \right)^2 + 4\lambda_2 \text{Tr} \left(z_\nu^{(2)} Y_\nu^{(n)\dagger} Y_\nu^{(n)} + 3z_d^{(2)} Y_d^\dagger Y_d \right. \\
&\quad \left. + 3z_u^{(2)} Y_u^\dagger Y_u \right) - 8 \text{Tr} \left(z_\nu^{(2)} Y_\nu^{(n)\dagger} Y_\nu^{(n)} Y_\nu^{(n)\dagger} Y_\nu^{(n)} + 3z_d^{(2)} Y_d^\dagger Y_d Y_d^\dagger Y_d \right. \\
&\quad \left. + 3z_u^{(2)} Y_u^\dagger Y_u Y_u^\dagger Y_u \right), \quad (\text{A.72b})
\end{aligned}$$

$$\begin{aligned}
16\pi^2 \beta_{\lambda_3}^{(n)} &= (\lambda_1 + \lambda_2) (3\lambda_3 + \lambda_4) + 4\lambda_3^2 + 2\lambda_4^2 + \frac{1}{2} \lambda_5^2 - 3\lambda_3 \left(3g_2^2 + \frac{3}{5} (g_1^U)^2 \right) \\
&\quad + \frac{9}{4} g_2^4 + \frac{27}{100} (g_1^U)^4 - \frac{9}{10} (g_1^U)^2 g_2^2 \\
&\quad + 4\lambda_3 \text{Tr} \left(Y_e^\dagger Y_e + Y_\nu^{(n)\dagger} Y_\nu^{(n)} + 3Y_d^\dagger Y_d + 3Y_u^\dagger Y_u \right) \\
&\quad - 4 \text{Tr} \left(z_\nu^{(2)} Y_e^\dagger Y_e Y_\nu^{(n)\dagger} Y_\nu^{(n)} + 3 \left(z_d^{(1)} z_u^{(2)} + z_d^{(2)} z_u^{(1)} \right) Y_d^\dagger Y_d Y_u^\dagger Y_u \right), \quad (\text{A.72c})
\end{aligned}$$

$$\begin{aligned}
16\pi^2 \beta_{\lambda_4}^{(n)} &= 2(\lambda_1 + \lambda_2) \lambda_4 + 4(2\lambda_3 + \lambda_4) \lambda_4 + 8\lambda_5^2 - 3\lambda_4 \left(3g_2^2 + \frac{3}{5} (g_1^U)^2 \right) \\
&\quad + \frac{9}{5} (g_1^U)^2 g_2^2 + 4\lambda_4 \text{Tr} \left(Y_e^\dagger Y_e + Y_\nu^{(n)\dagger} Y_\nu^{(n)} + 3Y_d^\dagger Y_d + 3Y_u^\dagger Y_u \right) \\
&\quad + 4 \text{Tr} \left(z_\nu^{(2)} Y_e^\dagger Y_e Y_\nu^{(n)\dagger} Y_\nu^{(n)} + 3 \left(z_d^{(1)} z_u^{(2)} + z_d^{(2)} z_u^{(1)} \right) Y_d^\dagger Y_d Y_u^\dagger Y_u \right), \quad (\text{A.72d})
\end{aligned}$$

$$16\pi^2 \beta_{\lambda_5}^{(n)} = \lambda_5 \left[\lambda_1 + \lambda_2 + 8\lambda_3 + 12\lambda_4 - 6\left(\frac{3}{5}(g_1^U)^2 + 3g_2^2\right) + 2 \operatorname{Tr} \left(Y_e^\dagger Y_e + Y_\nu^\dagger Y_\nu + 3Y_d^\dagger Y_d + 3Y_u^\dagger Y_u \right) \right]. \quad (\text{A.72e})$$

A.5.3 The RGEs in the MSSM Extended by Heavy Singlets

We give the 2-loop RGEs for the quantities $Q \in \left\{ \kappa^{(n)}, M^{(n)}, Y_\nu^{(n)}, Y_d^{(n)}, Y_u^{(n)}, Y_e^{(n)} \right\}$ in the form

$$\mu \frac{dQ^{(n)}}{d\mu} = \beta_Q^{(n)(1)} + \beta_Q^{(n)(2)}. \quad (\text{A.73})$$

The 1-loop parts are given by

$$(4\pi)^2 \beta_{\kappa}^{(n)(1)} = (Y_e^\dagger Y_e)^T \kappa^{(n)} + \kappa^{(n)} (Y_e^\dagger Y_e) + (Y_\nu^\dagger Y_\nu)^T \kappa^{(n)} + \kappa^{(n)} (Y_\nu^\dagger Y_\nu) + 2 \operatorname{Tr} (Y_\nu^\dagger Y_\nu) \kappa^{(n)} + 6 \operatorname{Tr} (Y_u^\dagger Y_u) \kappa^{(n)} - \frac{6}{5} (g_1^U)^2 \kappa^{(n)} - 6g_2^2 \kappa^{(n)}, \quad (\text{A.74a})$$

$$(4\pi)^2 \beta_M^{(n)(1)} = 2 (Y_\nu Y_\nu^\dagger)^{(n)} M^{(n)} + 2 M^{(n)} (Y_\nu Y_\nu^\dagger)^{(n)T}, \quad (\text{A.74b})$$

$$(4\pi)^2 \beta_{Y_\nu}^{(n)(1)} = Y_\nu^{(n)} \left\{ 3 Y_\nu^\dagger Y_\nu + Y_e^\dagger Y_e + \operatorname{Tr} (Y_\nu^\dagger Y_\nu) + 3 \operatorname{Tr} (Y_u^\dagger Y_u) - \frac{3}{5} (g_1^U)^2 - 3g_2^2 \right\}, \quad (\text{A.74c})$$

$$(4\pi)^2 \beta_{Y_d}^{(n)(1)} = Y_d \left\{ 3 Y_d^\dagger Y_d + Y_u^\dagger Y_u + 3 \operatorname{Tr} (Y_d^\dagger Y_d) + \operatorname{Tr} (Y_e^\dagger Y_e) - \frac{7}{15} (g_1^U)^2 - 3g_2^2 - \frac{16}{3} g_3^2 \right\}, \quad (\text{A.74d})$$

$$(4\pi)^2 \beta_{Y_u}^{(n)(1)} = Y_u \left\{ Y_d^\dagger Y_d + 3 Y_u^\dagger Y_u + \operatorname{Tr} (Y_\nu^\dagger Y_\nu) + 3 \operatorname{Tr} (Y_u^\dagger Y_u) - \frac{13}{15} (g_1^U)^2 - 3g_2^2 - \frac{16}{3} g_3^2 \right\}, \quad (\text{A.74e})$$

$$(4\pi)^2 \beta_{Y_e}^{(n)(1)} = Y_e \left\{ 3 Y_e^\dagger Y_e + Y_\nu^\dagger Y_\nu + 3 \operatorname{Tr} (Y_d^\dagger Y_d) + \operatorname{Tr} (Y_e^\dagger Y_e) - \frac{9}{5} (g_1^U)^2 - 3g_2^2 \right\}. \quad (\text{A.74f})$$

The results for the 2-loop parts are [81]

$$\begin{aligned}
(4\pi)^4 \beta_\kappa^{(2)} = & \left[-6 \text{Tr} (Y_u^\dagger Y_d Y_d^\dagger Y_u) - 18 \text{Tr} (Y_u^\dagger Y_u Y_u^\dagger Y_u) - 2 \text{Tr} (Y_\nu^\dagger Y_e Y_e^\dagger Y_\nu) \right. \\
& - 6 \text{Tr} (Y_\nu^\dagger Y_\nu Y_\nu^\dagger Y_\nu) + \frac{8}{5} (g_1^U)^2 \text{Tr} (Y_u^\dagger Y_u) + 32 g_3^2 \text{Tr} (Y_u^\dagger Y_u) + \frac{207}{25} (g_1^U)^4 \\
& \left. + \frac{18}{5} (g_1^U)^2 g_2^2 + 15 g_2^4 \right] \kappa^{(n)} \\
& - \left[2 (Y_e^\dagger Y_e Y_e^\dagger Y_e)^T + 2 (Y_\nu^\dagger Y_\nu Y_\nu^\dagger Y_\nu)^T + \left(\text{Tr} (Y_\nu Y_\nu^\dagger) + 3 \text{Tr} (Y_u Y_u^\dagger) \right) (Y_\nu^\dagger Y_\nu)^T \right. \\
& \left. + \left(-\frac{6}{5} (g_1^U)^2 + \text{Tr} (Y_e Y_e^\dagger) + 3 \text{Tr} (Y_d Y_d^\dagger) \right) (Y_e^\dagger Y_e)^T \right] \kappa^{(n)} \\
& - \kappa^{(n)} \left[2 Y_e^\dagger Y_e Y_e^\dagger Y_e + 2 Y_\nu^\dagger Y_\nu Y_\nu^\dagger Y_\nu + \left(\text{Tr} (Y_\nu Y_\nu^\dagger) + 3 \text{Tr} (Y_u Y_u^\dagger) \right) Y_\nu^\dagger Y_\nu \right. \\
& \left. + \left(-\frac{6}{5} (g_1^U)^2 + \text{Tr} (Y_e Y_e^\dagger) + 3 \text{Tr} (Y_d Y_d^\dagger) \right) Y_e^\dagger Y_e \right], \tag{A.75a}
\end{aligned}$$

$$\begin{aligned}
(4\pi)^4 \beta_M^{(2)} = & M \left[-2 Y_\nu^* Y_e^T Y_e^* Y_\nu^T - 2 Y_\nu^* Y_\nu^T Y_\nu^* Y_\nu^T - 6 Y_\nu^* Y_\nu^T \text{Tr} (Y_u Y_u^\dagger) \right. \\
& \left. - 2 Y_\nu^* Y_\nu^T \text{Tr} (Y_\nu Y_\nu^\dagger) + \frac{6}{5} (g_1^U)^2 Y_\nu^* Y_\nu^T + 6 g_2^2 Y_\nu^* Y_\nu^T \right] \\
& + \left[-2 Y_\nu Y_e^\dagger Y_e Y_\nu^\dagger - 2 Y_\nu Y_\nu^\dagger Y_\nu Y_\nu^\dagger - 6 Y_\nu Y_\nu^\dagger \text{Tr} (Y_u Y_u^\dagger) - 2 Y_\nu Y_\nu^\dagger \text{Tr} (Y_\nu Y_\nu^\dagger) \right. \\
& \left. + \frac{6}{5} (g_1^U)^2 Y_\nu Y_\nu^\dagger + 6 g_2^2 Y_\nu Y_\nu^\dagger \right] M, \tag{A.75b}
\end{aligned}$$

$$\begin{aligned}
(4\pi)^4 \beta_{Y_\nu}^{(2)} = & Y_\nu \left\{ -2 Y_e^\dagger Y_e Y_e^\dagger Y_e - 2 Y_e^\dagger Y_e Y_\nu^\dagger Y_\nu - 4 Y_\nu^\dagger Y_\nu Y_\nu^\dagger Y_\nu \right. \\
& - 3 Y_e^\dagger Y_e \text{Tr} (Y_d Y_d^\dagger) - Y_e^\dagger Y_e \text{Tr} (Y_e Y_e^\dagger) - 3 Y_\nu^\dagger Y_\nu \text{Tr} (Y_\nu Y_\nu^\dagger) - 9 Y_\nu^\dagger Y_\nu \text{Tr} (Y_u Y_u^\dagger) \\
& - \text{Tr} (Y_\nu^\dagger Y_e Y_e^\dagger Y_\nu) - 3 \text{Tr} (Y_\nu^\dagger Y_\nu Y_\nu^\dagger Y_\nu) - 3 \text{Tr} (Y_u^\dagger Y_d Y_d^\dagger Y_u) - 9 \text{Tr} (Y_u^\dagger Y_u Y_u^\dagger Y_u) \\
& + \frac{6}{5} (g_1^U)^2 Y_e^\dagger Y_e + \frac{6}{5} (g_1^U)^2 Y_\nu^\dagger Y_\nu + 6 g_2^2 Y_\nu^\dagger Y_\nu + \frac{4}{5} (g_1^U)^2 \text{Tr} (Y_u^\dagger Y_u) \\
& \left. + 16 g_3^2 \text{Tr} (Y_u^\dagger Y_u) + \frac{207}{50} (g_1^U)^4 + \frac{9}{5} (g_1^U)^2 g_2^2 + \frac{15}{2} g_2^4 \right\}, \tag{A.75c}
\end{aligned}$$

$$\begin{aligned}
(4\pi)^4 \beta_{Y_d}^{(2)} = & Y_d \left\{ -4 Y_d^\dagger Y_d Y_d^\dagger Y_d - 2 Y_u^\dagger Y_u Y_d^\dagger Y_d - 2 Y_u^\dagger Y_u Y_u^\dagger Y_u - 9 \text{Tr} (Y_d^\dagger Y_d Y_d^\dagger Y_d) \right. \\
& \left. - 3 \text{Tr} (Y_d^\dagger Y_u Y_u^\dagger Y_d) - 3 \text{Tr} (Y_e^\dagger Y_e Y_e^\dagger Y_e) - \text{Tr} (Y_e^\dagger Y_\nu Y_\nu^\dagger Y_e) - 9 Y_d^\dagger Y_d \text{Tr} (Y_d Y_d^\dagger) \right\}
\end{aligned}$$

$$\begin{aligned}
 & -3 Y_d^\dagger Y_d \text{Tr}(Y_e Y_e^\dagger) - Y_u^\dagger Y_u \text{Tr}(Y_\nu^{(n)} Y_\nu^{(n)\dagger}) - 3 Y_u^\dagger Y_u \text{Tr}(Y_u Y_u^\dagger) + 6 g_2^2 Y_d^\dagger Y_d \\
 & + \frac{4}{5} (g_1^U)^2 Y_d^\dagger Y_d + \frac{4}{5} (g_1^U)^2 Y_u^\dagger Y_u - \frac{2}{5} (g_1^U)^2 \text{Tr}(Y_d^\dagger Y_d) + \frac{6}{5} (g_1^U)^2 \text{Tr}(Y_e^\dagger Y_e) \\
 & + 16 g_3^2 \text{Tr}(Y_d^\dagger Y_d) + \frac{287}{90} (g_1^U)^4 + (g_1^U)^2 g_2^2 + \frac{15}{2} g_2^4 + \frac{8}{9} (g_1^U)^2 g_3^2 \\
 & + 8 g_2^2 g_3^2 - \frac{16}{9} g_3^4 \left. \vphantom{\frac{4}{5}} \right\}, \tag{A.75d}
 \end{aligned}$$

$$\begin{aligned}
 (4\pi)^4 \beta_{Y_u}^{(n)(2)} &= Y_u \left\{ -2 Y_d^\dagger Y_d Y_d^\dagger Y_d - 2 Y_d^\dagger Y_d Y_u^\dagger Y_u - 4 Y_u^\dagger Y_u Y_u^\dagger Y_u - 3 Y_d^\dagger Y_d \text{Tr}(Y_d Y_d^\dagger) \right. \\
 & - Y_d^\dagger Y_d \text{Tr}(Y_e Y_e^\dagger) - 9 Y_u^\dagger Y_u \text{Tr}(Y_u Y_u^\dagger) - 9 Y_u^\dagger Y_u \text{Tr}(Y_u Y_u^\dagger) - 3 Y_u^\dagger Y_u \text{Tr}(Y_\nu^{(n)} Y_\nu^{(n)\dagger}) \\
 & - 3 \text{Tr}(Y_u^\dagger Y_d Y_d^\dagger Y_u) - 9 \text{Tr}(Y_u^\dagger Y_u Y_u^\dagger Y_u) - \text{Tr}(Y_\nu^{(n)\dagger} Y_e Y_e^\dagger Y_\nu^{(n)}) - 3 \text{Tr}(Y_\nu^{(n)\dagger} Y_\nu^{(n)} Y_\nu^{(n)\dagger} Y_\nu^{(n)}) \\
 & + \frac{2}{5} (g_1^U)^2 Y_d^\dagger Y_d + \frac{2}{5} (g_1^U)^2 Y_u^\dagger Y_u + 6 g_2^2 Y_u^\dagger Y_u + \frac{4}{5} (g_1^U)^2 \text{Tr}(Y_u^\dagger Y_u) \\
 & + 16 g_3^2 \text{Tr}(Y_u^\dagger Y_u) + \frac{2743}{450} (g_1^U)^4 + (g_1^U)^2 g_2^2 + \frac{15}{2} g_2^4 + \frac{136}{45} (g_1^U)^2 g_3^2 \\
 & \left. + 8 g_2^2 g_3^2 - \frac{16}{9} g_3^4 \right\}, \tag{A.75e}
 \end{aligned}$$

$$\begin{aligned}
 (4\pi)^4 \beta_{Y_e}^{(n)(2)} &= Y_e \left\{ -4 Y_e^\dagger Y_e Y_e^\dagger Y_e - 2 Y_\nu^{(n)\dagger} Y_\nu^{(n)} Y_e^\dagger Y_e - 2 Y_\nu^{(n)\dagger} Y_\nu^{(n)} Y_\nu^{(n)\dagger} Y_\nu^{(n)} - 9 Y_e^\dagger Y_e \text{Tr}(Y_d Y_d^\dagger) \right. \\
 & - 3 Y_e^\dagger Y_e \text{Tr}(Y_e Y_e^\dagger) - Y_\nu^{(n)\dagger} Y_\nu^{(n)} \text{Tr}(Y_\nu^{(n)} Y_\nu^{(n)\dagger}) - 3 Y_\nu^{(n)\dagger} Y_\nu^{(n)} \text{Tr}(Y_u Y_u^\dagger) - 9 \text{Tr}(Y_d^\dagger Y_d Y_d^\dagger Y_d) \\
 & - 3 \text{Tr}(Y_d^\dagger Y_u Y_u^\dagger Y_d) - 3 \text{Tr}(Y_e^\dagger Y_e Y_e^\dagger Y_e) - \text{Tr}(Y_e^\dagger Y_\nu^{(n)} Y_\nu^{(n)\dagger} Y_e) + \frac{6}{5} (g_1^U)^2 \text{Tr}(Y_e^\dagger Y_e) \\
 & + 6 g_2^2 Y_e^\dagger Y_e - \frac{2}{5} (g_1^U)^2 \text{Tr}(Y_d^\dagger Y_d) + 16 g_3^2 \text{Tr}(Y_d^\dagger Y_d) + \frac{27}{2} (g_1^U)^4 \\
 & \left. + \frac{9}{5} (g_1^U)^2 g_2^2 + \frac{15}{2} g_2^4 \right\}. \tag{A.75f}
 \end{aligned}$$

Acknowledgments

I would like to thank all the people who helped to make this work possible. I have enjoyed the many interesting discussions, the excellent working environment and the nice atmosphere at T30d. In particular, it is a pleasure to thank

- my supervisor Prof. Manfred Lindner for his support and advice during my time as a student and Ph.D. student.
- Jörn Kersten and Michael Ratz for perfect teamwork, proofreading of the manuscript and for being great colleagues.
- Prof. Evgeni Akhmedov, Prof. Andrzej Buras and Prof. Manuel Drees for interesting discussions and helpful answers to questions.

Last but not least, very special thanks to my parents for supporting me in every possible way and to my wife Sandra and my son Vincent for patience and support during the time when I finished this thesis.

Bibliography

- [1] For a review see for example: S. Bethke, *Determination of the QCD coupling α_s* , J. Phys. **G26** (2000), R27, hep-ex/0004021.
- [2] H. Georgi and S. L. Glashow, *Unity of all elementary particle forces*, Phys. Rev. Lett. **32** (1974), 438–441.
- [3] N. Cabibbo, L. Maiani, G. Parisi, and R. Petronzio, *Bounds on the fermions and Higgs boson masses in Grand Unified Theories*, Nucl. Phys. **B158** (1979), 295.
- [4] M. Lindner, *Implications of triviality for the Standard Model*, Zeit. Phys. **C31** (1986), 295.
- [5] J. C. Pati and A. Salam, *Lepton number as the fourth color*, Phys. Rev. **D10** (1974), 275–289.
- [6] R. N. Mohapatra and J. C. Pati, *A 'natural' left-right symmetry*, Phys. Rev. **D11** (1975), 2558.
- [7] G. Senjanović and R. N. Mohapatra, *Exact left-right symmetry and spontaneous violation of parity*, Phys. Rev. **D12** (1975), 1502.
- [8] J. C. Pati and A. Salam, *Unified lepton - hadron symmetry and a gauge theory of the basic interactions*, Phys. Rev. **D8** (1973), 1240.
- [9] H. Georgi, *Particles and fields* (edited by Carlson, C. E.), A.I.P., 1975, p. 575.
- [10] H. Fritzsch and P. Minkowski, *Unified interactions of leptons and hadrons*, Ann. Phys. **93** (1975), 193–266.
- [11] M. Fukugita and T. Yanagida, *Baryogenesis without grand unification*, Phys. Lett. **174B** (1986), 45.
- [12] KamLAND, K. Eguchi et al., *First results from KamLAND: Evidence for reactor anti-neutrino disappearance*, Phys. Rev. Lett. **90** (2003), 021802, hep-ex/0212021.

- [13] P. C. de Holanda and A. Y. Smirnov, *LMA MSW solution of the solar neutrino problem and first KamLAND results*, (2002), [hep-ph/0212270](#).
- [14] SNO, Q. R. Ahmad et al., *Direct evidence for neutrino flavor transformation from neutral-current interactions in the Sudbury Neutrino Observatory*, *Phys. Rev. Lett.* **89** (2002), 011301, [nucl-ex/0204008](#).
- [15] SuperKamiokande, T. Toshito, *Super-Kamiokande atmospheric neutrino results*, (2001), [hep-ex/0105023](#).
- [16] CHOOZ, M. Apollonio et al., *Limits on neutrino oscillations from the CHOOZ experiment*, *Phys. Lett.* **B466** (1999), 415–430, [hep-ex/9907037](#).
- [17] LSND, C. Athanassopoulos et al., *Evidence for $\nu_\mu \rightarrow \nu_e$ neutrino oscillations from LSND*, *Phys. Rev. Lett.* **81** (1998), 1774–1777, [nucl-ex/9709006](#).
- [18] M. Freund, *Messung der fundamentalen Neutrinoparameter mittels Long-Baseline-Oszillationsexperimenten an zukünftigen Neutrinofabriken*, Ph.D. thesis, T.U. München, 2002.
- [19] D. N. Spergel et al., *First year Wilkinson Microwave Anisotropy Probe (WMAP) observations: Determination of cosmological parameters*, (2003), [astro-ph/0302209](#).
- [20] H. V. Klapdor-Kleingrothaus et al., *Latest results from the Heidelberg-Moscow double-beta-decay experiment*, *Eur. Phys. J.* **A12** (2001), 147–154, [hep-ph/0103062](#).
- [21] 16EX Collaboration, C. E. Aalseth et al., *The IGEX Ge-76 neutrinoless double-beta decay experiment: Prospects for next generation experiments*, *Phys. Rev.* **D65** (2002), 092007, [hep-ex/0202026](#).
- [22] H. Fusaoka and Y. Koide, *Updated estimate of running quark masses*, *Phys. Rev.* **D57** (1998), 3986–4001, [hep-ph/9712201](#).
- [23] A. J. Buras, F. Parodi, and A. Stocchi, *The CKM matrix and the unitarity triangle: Another look*, *JHEP* **01** (2003), 029, [hep-ph/0207101](#).
- [24] R. N. Mohapatra and P. B. Pal, *Massive neutrinos in physics and astrophysics (second edition)*, *World Sci. Lect. Notes Phys.* **60** (1998), 1–397.
- [25] J. Erler and P. Langacker, *Electroweak model and constraints on new physics (rev.)*, *Phys. Rev.* **D66** (2002), 010001.
- [26] T. Yanagida, in *Proceedings of the Workshop on the Unified Theory and the Baryon Number in the Universe* (O. Sawada and A. Sugamoto, eds.), KEK, Tsukuba, Japan, 1979, p. 95.

-
- [27] S. L. Glashow, *The future of elementary particle physics*, in *Proceedings of the 1979 Cargèse Summer Institute on Quarks and Leptons* (M. Lévy, J.-L. Basdevant, D. Speiser, J. Weyers, R. Gastmans, and M. Jacob, eds.), Plenum Press, New York, 1980, pp. 687–713.
- [28] M. Gell-Mann, P. Ramond, and R. Slansky, *Complex spinors and unified theories*, in *Supergravity* (P. van Nieuwenhuizen and D. Z. Freedman, eds.), North Holland, Amsterdam, 1979, p. 315.
- [29] R. N. Mohapatra and G. Senjanović, *Neutrino mass and spontaneous parity violation*, Phys. Rev. Lett. **44** (1980), 912.
- [30] R. N. Mohapatra and G. Senjanović, *Neutrino masses and mixings in gauge models with spontaneous parity violation*, Phys. Rev. **D23** (1981), 165.
- [31] C. Wetterich, *Neutrino masses and the scale of $B-L$ violation*, Nucl. Phys. **B187** (1981), 343.
- [32] E. Ma and U. Sarkar, *Neutrino masses and leptogenesis with heavy Higgs triplets*, Phys. Rev. Lett. **80** (1998), 5716–5719, hep-ph/9802445.
- [33] A. Pich, *Effective field theory*, (1998), hep-ph/9806303.
- [34] A. Zee, *A theory of lepton number violation, neutrino Majorana mass, and oscillation*, Phys. Lett. **B93** (1980), 389.
- [35] E. Ma, *Pathways to naturally small neutrino masses*, Phys. Rev. Lett. **81** (1998), 1171–1174, hep-ph/9805219.
- [36] C. D. Froggatt and H. B. Nielsen, *Statistical analysis of quark and lepton masses*, Nucl. Phys. **B164** (1980), 114.
- [37] K. S. Babu and C. N. Leung, *Classification of effective neutrino mass operators*, Nucl. Phys. **B619** (2001), 667–689, hep-ph/0106054.
- [38] B. Brahmachari, E. Ma, and U. Sarkar, *Truly minimal left-right model of quark and lepton masses*, (2003), hep-ph/0301041.
- [39] N. G. Deshpande, J. F. Gunion, B. Kayser, and F. Olness, *Left-right symmetric electroweak models with triplet Higgs*, Phys. Rev. **D44** (1991), 837–858.
- [40] R. Slansky, *Group theory for unified model building*, Phys. Rept. **79** (1981), 1–128.
- [41] C. H. Albright and S. M. Barr, *Realization of the Large Mixing Angle solar neutrino solution in an $SO(10)$ supersymmetric grand unified model*, Phys. Rev. **D64** (2001), 073010, hep-ph/0104294.

- [42] K. S. Babu, J. C. Pati, and F. Wilczek, *Fermion masses, neutrino oscillations, and proton decay in the light of SuperKamiokande*, Nucl. Phys. **B566** (2000), 33–91, hep-ph/9812538.
- [43] J. C. Pati, *Leptogenesis within a predictive $G(224)/SO(10)$ framework*, (2002), hep-ph/0209160.
- [44] T. Blazek, S. Raby, and K. Tobe, *Neutrino oscillations in an $SO(10)$ SUSY GUT with $U(2) \times U(1)^n$ family symmetry*, Phys. Rev. **D62** (2000), 055001, hep-ph/9912482.
- [45] R. Kitano and Y. Mimura, *Large angle MSW solution in Grand Unified Theories with $SU(3) \times U(1)$ horizontal symmetry*, Phys. Rev. **D63** (2001), 016008, hep-ph/0008269.
- [46] G. G. Ross and L. Velasco-Sevilla, *Symmetries and fermion masses*, Nucl. Phys. **B653** (2003), 3–26, hep-ph/0208218.
- [47] T. Blazek, S. F. King, and J. K. Parry, *Global analysis of a supersymmetric Pati-Salam model*, JHEP **05** (2003), 016, hep-ph/0303192.
- [48] W. A. Bardeen, C. T. Hill, and M. Lindner, *Minimal dynamical symmetry breaking of the Standard Model*, Phys. Rev. **D41** (1990), 1647.
- [49] M. Lindner, *Top condensates as Higgs substitute*, Int. J. Mod. Phys. **A8** (1993), 2167–2240.
- [50] S. Antusch, J. Kersten, M. Lindner, and M. Ratz, *Dynamical electroweak symmetry breaking by a neutrino condensate*, Nucl. Phys. **B658** (2003), 203–216, hep-ph/0211385.
- [51] G. 't Hooft, *Dimensional regularization and the renormalization group*, Nucl. Phys. **B61** (1973), 455–468.
- [52] J. C. Collins, *Renormalization. An introduction to renormalization, the renormalization group, and the operator product expansion*, Cambridge, Uk: Univ. Pr. (1984) 380p.
- [53] G. 't Hooft, *Renormalization of massless Yang-Mills fields*, Nucl. Phys. **B33** (1971), 173–199.
- [54] G. 't Hooft, *Renormalizable Lagrangians for massive Yang-Mills fields*, Nucl. Phys. **B35** (1971), 167–188.
- [55] G. 't Hooft and M. J. G. Veltman, *Regularization and renormalization of gauge fields*, Nucl. Phys. **B44** (1972), 189–213.

-
- [56] T. Appelquist and J. Carazzone, *Infrared singularities and massive fields*, Phys. Rev. **D11** (1975), 2856.
- [57] S. Antusch, M. Drees, J. Kersten, M. Lindner, and M. Ratz, *Neutrino mass operator renormalization revisited*, Phys. Lett. **B519** (2001), 238–242, hep-ph/0108005.
- [58] P. H. Chankowski and Z. Pluciennik, *Renormalization group equations for seesaw neutrino masses*, Phys. Lett. **B316** (1993), 312–317, hep-ph/9306333.
- [59] K. S. Babu, C. N. Leung, and J. Pantaleone, *Renormalization of the neutrino mass operator*, Phys. Lett. **B319** (1993), 191–198, hep-ph/9309223.
- [60] R. Mertig, M. Böhm, and A. Denner, *FEYN CALC: Computer algebraic calculation of Feynman amplitudes*, Comput. Phys. Commun. **64** (1991), 345–359.
- [61] J. Kersten, *Renormalization group evolution of neutrino masses*, Diploma thesis, T.U. München, 2001.
- [62] P. H. Chankowski and P. Wasowicz, *Low energy threshold corrections to neutrino masses and mixing angles*, hep-ph/0110237 (2001).
- [63] S. Weinberg, *Gauge theory of CP violation*, Phys. Rev. Lett. **37** (1976), 657.
- [64] S. L. Glashow and S. Weinberg, *Natural conservation laws for neutral currents*, Phys. Rev. **D15** (1977), 1958.
- [65] E. A. Paschos, *Diagonal neutral currents*, Phys. Rev. **D15** (1977), 1966.
- [66] M. Ratz, *Running neutrino masses*, Ph.D. thesis, T.U. München, 2002.
- [67] S. Antusch, M. Drees, J. Kersten, M. Lindner, and M. Ratz, *Neutrino mass operator renormalization in Two Higgs Doublet Models and the MSSM*, hep-ph/0110366 (2001).
- [68] S. R. Coleman and J. Mandula, *All possible symmetries of the S matrix*, Phys. Rev. **159** (1967), 1251–1256.
- [69] R. Haag, J. T. Lopuszański, and M. Sohnius, *All possible generators of supersymmetries of the S matrix*, Nucl. Phys. **B88** (1975), 257.
- [70] J. Wess and J. Bagger, *Supersymmetry and supergravity*, Princeton, USA: Univ. Pr. (1992) 259 p.
- [71] I. L. Buchbinder and S. M. Kuzenko, *Ideas and methods of supersymmetry and supergravity: Or a walk through superspace*, Bristol, UK: IOP (1998) 656 p.

- [72] M. A. Diaz, J. C. Romao, and J. W. F. Valle, *Minimal supergravity with R-parity breaking*, Nucl. Phys. **B524** (1998), 23–40, [hep-ph/9706315](#).
- [73] A. Denner, H. Eck, O. Hahn, and J. Küblbeck, *Feynman rules for fermion number violating interactions*, Nucl. Phys. **B387** (1992), 467–484.
- [74] R. Delbourgo, *Superfield perturbation theory and renormalization*, Nuovo Cim. **A25** (1975), 646.
- [75] A. Salam and J. Strathdee, *Feynman rules for superfields*, Nucl. Phys. **B86** (1975), 142–152.
- [76] K. Fujikawa and W. Lang, *Perturbation calculations for the scalar multiplet in a superfield formulation*, Nucl. Phys. **B88** (1975), 61.
- [77] M. T. Grisaru, W. Siegel, and M. Roček, *Improved methods for supergraphs*, Nucl. Phys. **B159** (1979), 429.
- [78] J. Wess and B. Zumino, *A Lagrangian model invariant under supergauge transformations*, Phys. Lett. **B49** (1974), 52.
- [79] J. Iliopoulos and B. Zumino, *Broken supergauge symmetry and renormalization*, Nucl. Phys. **B76** (1974), 310.
- [80] S. Weinberg, *Non-renormalization theorems in non-renormalizable theories*, Phys. Rev. Lett. **80** (1998), 3702–3705, [hep-th/9803099](#).
- [81] S. Antusch and M. Ratz, *Supergraph techniques and two-loop β -functions for renormalizable and non-renormalizable operators*, JHEP **07** (2002), 059, [hep-ph/0203027](#).
- [82] P. West, *The Yukawa β -function in $N=1$ rigid supersymmetric theories*, Phys. Lett. **B137** (1984), 371.
- [83] W. Siegel, *Supersymmetric dimensional regularization via dimensional reduction*, Phys. Lett. **B84** (1979), 193.
- [84] W. A. Bardeen, A. J. Buras, D. W. Duke, and T. Muta, *Deep inelastic scattering beyond the leading order in asymptotically free gauge theories*, Phys. Rev. **D18** (1978), 3998.
- [85] S. Antusch, J. Kersten, M. Lindner, and M. Ratz, *Neutrino mass matrix running for non-degenerate see-saw scales*, Phys. Lett. **B538** (2002), 87–95, [hep-ph/0203233](#).

-
- [86] M. Tanimoto, *Renormalization effect on large neutrino flavor mixing in the Minimal Supersymmetric Standard Model*, Phys. Lett. **B360** (1995), 41–46, hep-ph/9508247.
- [87] J. R. Ellis and S. Lola, *Can neutrinos be degenerate in mass?*, Phys. Lett. **B458** (1999), 310–321, hep-ph/9904279.
- [88] J. A. Casas, J. R. Espinosa, A. Ibarra, and I. Navarro, *Naturalness of nearly degenerate neutrinos*, Nucl. Phys. **B556** (1999), 3–22, hep-ph/9904395.
- [89] J. A. Casas, J. R. Espinosa, A. Ibarra, and I. Navarro, *Nearly degenerate neutrinos, supersymmetry and radiative corrections*, Nucl. Phys. **B569** (2000), 82–106, hep-ph/9905381.
- [90] P. H. Chankowski, W. Krolikowski, and S. Pokorski, *Fixed points in the evolution of neutrino mixings*, Phys. Lett. **B473** (2000), 109, hep-ph/9910231.
- [91] J. A. Casas, J. R. Espinosa, A. Ibarra, and I. Navarro, *General RG equations for physical neutrino parameters and their phenomenological implications*, Nucl. Phys. **B573** (2000), 652, hep-ph/9910420.
- [92] K. R. S. Balaji, A. S. Dighe, R. N. Mohapatra, and M. K. Parida, *Radiative magnification of neutrino mixings and a natural explanation of the neutrino anomalies*, Phys. Lett. **B481** (2000), 33–38, hep-ph/0002177.
- [93] K. R. S. Balaji, A. S. Dighe, R. N. Mohapatra, and M. K. Parida, *Generation of large flavor mixing from radiative corrections*, Phys. Rev. Lett. **84** (2000), 5034–5037, hep-ph/0001310.
- [94] N. Haba, Y. Matsui, and N. Okamura, *The effects of Majorana phases in three-generation neutrinos*, Eur. Phys. J. **C17** (2000), 513–520, hep-ph/0005075.
- [95] T. Miura, E. Takasugi, and M. Yoshimura, *Quantum effects for the neutrino mixing matrix in the democratic-type model*, Prog. Theor. Phys. **104** (2000), 1173–1187, hep-ph/0007066.
- [96] P. H. Chankowski, A. Ioannisian, S. Pokorski, and J. W. F. Valle, *Neutrino unification*, Phys. Rev. Lett. **86** (2001), 3488–3491, hep-ph/0011150.
- [97] M.-C. Chen and K. T. Mahanthappa, *Implications of the renormalization group equations in three neutrino models with two-fold degeneracy*, Int. J. Mod. Phys. **A16** (2001), 3923–3930, hep-ph/0102215.
- [98] P. H. Chankowski and S. Pokorski, *Quantum corrections to neutrino masses and mixing angles*, Int. J. Mod. Phys. **A17** (2002), 575–614, hep-ph/0110249.

- [99] M. K. Parida, C. R. Das, and G. Rajasekaran, *Radiative stability of neutrino-mass textures*, (2002), [hep-ph/0203097](#).
- [100] G. Dutta, *Stable bimaximal neutrino mixing pattern*, (2002), [hep-ph/0203222](#).
- [101] T. Miura, T. Shindou, and E. Takasugi, *Exploring the neutrino mass matrix at M_R scale*, Phys. Rev. **D66** (2002), 093002, [hep-ph/0206207](#).
- [102] G. Bhattacharyya, A. Raychaudhuri, and A. Sil, *Can radiative magnification of mixing angles occur for two-zero neutrino mass matrix textures?*, (2002), [hep-ph/0211074](#).
- [103] A. S. Joshipura, S. D. Rindani, and N. N. Singh, *Predictive framework with a pair of degenerate neutrinos at a high scale*, Nucl. Phys. **B660** (2003), 362–372, [hep-ph/0211378](#).
- [104] A. S. Joshipura and S. D. Rindani, *Radiatively generated ν_e oscillations: General analysis, textures and models*, Phys. Rev. **D67** (2003), 073009, [hep-ph/0211404](#).
- [105] M. Frigerio and A. Y. Smirnov, *Radiative corrections to neutrino mass matrix in the Standard Model and beyond*, JHEP **02** (2003), 004, [hep-ph/0212263](#).
- [106] Z. Maki, M. Nakagawa, and S. Sakata, *Remarks on the unified model of elementary particles*, Prog. Theor. Phys. **28** (1962), 870.
- [107] K. S. Babu, *Renormalization-group analysis of the Kobayashi-Maskawa matrix*, Z. Phys. **C35** (1987), 69.
- [108] S. Antusch, J. Kersten, M. Lindner, and M. Ratz, *Running neutrino masses, mixings and CP phases: Analytical results and phenomenological consequences*, (2003), [hep-ph/0305273](#).
- [109] The LEP Electroweak Working Group, D. Abbaneo et al., *A combination of preliminary electroweak measurements and constraints on the Standard Model*, (2002), <http://lepewwg.web.cern.ch/LEPEWWG/>.
- [110] P. Huber, M. Lindner, T. Schwetz, and W. Winter, *Reactor neutrino experiments compared to superbeams*, (2003), [hep-ph/0303232](#).
- [111] P. Huber, M. Lindner, and W. Winter, *Synergies between the first-generation JHF-SK and NuMI superbeam experiments*, Nucl. Phys. **B654** (2003), 3–29, [hep-ph/0211300](#).
- [112] H. Minakata, H. Nunokawa, and S. Parke, *The complementarity of eastern and western hemisphere long-baseline neutrino oscillation experiments*, (2003), [hep-ph/0301210](#).

- [113] Y. Itow et al., *The JHF-Kamioka neutrino project*, (2001), hep-ex/0106019.
- [114] S. Antusch, J. Kersten, M. Lindner, and M. Ratz, *The LMA solution from bimaximal lepton mixing at the GUT scale by renormalization group running*, Phys. Lett. **B544** (2002), 1–10, hep-ph/0206078.
- [115] S. Antusch and M. Ratz, *Radiative generation of the LMA solution from small solar neutrino mixing at the GUT scale*, JHEP **11** (2002), 010, hep-ph/0208136.
- [116] C. Jarlskog, *Commutator of the quark mass matrices in the standard electroweak model and a measure of maximal CP violation*, Phys. Rev. Lett. **55** (1985), 1039.
- [117] G. Passarino and M. Veltman, *One loop corrections for $e^+ e^-$ annihilation into $\mu^+ \mu^-$ in the Weinberg model*, Nucl. Phys. **B160** (1979), 151.
- [118] A. Denner, *Techniques for calculation of electroweak radiative corrections at the one loop level and results for W physics at LEP200*, Fortschr. Phys. **41** (1993), 307–420.
- [119] C. T. Hill, C. N. Leung, and S. Rao, *Renormalization group fixed points and the Higgs boson spectrum*, Nucl. Phys. **B262** (1985), 517.
- [120] B. Grzadkowski and M. Lindner, *Nonlinear evolution of Yukawa couplings*, Phys. Lett. **B193** (1987), 71.